

*An Investigation into the Role of Morphology on the
Performance of Molecularly Imprinted Polymers.*



Submitted to Waterford Institute of Technology for the Degree of Doctor of
Philosophy
August 2008

By Niamh Holland,
Separation Science Research Group (SSRG),
Waterford Institute of Technology,
Waterford,
Ireland.

Under the supervision of
Dr. Helen Hughes, Dr. Peter Mc.Loughlin & Dr. Eleanor Owens.



Declaration

No element of this work presented, unless otherwise stated, has been presented for a degree at this or any other institution. The work described has been performed entirely by the author.

Signed: _____

Date: _____

Acknowledgments

Firstly I would like to thank my supervisors Dr. Helen Hughes, Dr. Peter McLoughlin and Dr. Eleanor Owens for giving me the chance to partake in this project. I would like to thank each of you for the time and patience you have invested in me. Your assistance, suggestions and words of support and encouragement are greatly appreciated.

Funding for this project was provided by the Council of Directors, under the Technology Sector, Strand 1 and by the European Unions INTERREG IIIA programme, which was gratefully acknowledged.

I would like to thank Dr. Patrick Duggan and Dr. June Frisby for their assistance and helpful input into this project. Thanks also to Dr. Jimmy Heiden-Dahlstrom of the Welsh School of Pharmacy, Cardiff, UK and Vince Lodge of the Tyndall National Institute, Cork for carrying out preliminary nitrogen sorption and SEM analyses, respectively.

Thanks to everyone in the Science Department, in particular all of my fellow postgraduates that I have encountered along the way. I hope that I have formed friendships that will last long into the future.

Finally, to my parents Bernard and Mary, my brother Richard and my dear friend Richard Cleary. I cannot even begin to express my sincere gratitude for all that you have done for me in so many different ways. You have been there for the ups and downs, the laughs and the plentiful tantrums. Thank you for putting up with me.

Publications

1. Thermal desorption characterisation of molecularly imprinted polymers. Part II: Use of direct probe GC-MS analysis to study crosslinking effects. N. Holland, P. Duggan, E. Owens, W. Cummins, J. Frisby, H. Hughes and P. McLoughlin. *Analytical and Bioanalytical Chemistry* (2008) 391:1245-1253.

Abstract

A detailed investigation into the role of polymer morphology on imprint medium performance has been carried out with a view to identifying the key physical parameters relating to affinity. A systematic and comprehensive study was carried out by synthesising a series of 2-aminopyridine (2-apy) imprinted polymers. The amount of crosslinking monomer (ethyleneglycol dimethacrylate, EGDMA) and the nature of functional monomer (methacrylic acid (MAA), 4-vinylpyridine (4-VP) and methyl methacrylate (MMA)) were all varied. The change in composition influenced polymer morphology, as shown by nitrogen sorption, SEM, particle size distribution and solvent swell studies. The polymers containing 4-VP were found to produce less porous materials than corresponding MAA counterparts. As a result, the free space within the network of the 4-VP polymers was reduced and so the diffusion of template into and out of the polymers was restricted. This was reflected in the affinity assessment of the polymers where the template, 2-apy, and two structural analogues, 3- and 4-aminopyridine (3- and 4-apy) displayed no affinity for the polymers in solvents with a range of polarities. The porosity of the MAA polymers decreased with decreasing EGDMA amount, but was greater than corresponding 4-VP counterparts. The flexibility of the polymers formed from lower amounts of EGDMA combined with the number of free carboxyl groups and the swelling effect of the solvents on the polymers resulted in an increase in affinity, which was both specific and non-specific in nature. A link between polymer composition and selectivity towards 3- and 4-apy was also identified, with the pKa of the binding analyte also contributing to the affinity.

The MAA polymers were comprehensively examined using the Langmuir (LI), Freundlich (FI) and Langmuir-Freundlich (L-FI) isotherms and using affinity distribution (AD) spectra. The L-FI was identified as the most appropriate model in analysing the binding behaviour of the polymers. A relationship between binding site number and strength and the morphology of the polymers was identified. This was the first report of the use of AD spectra generated from the L-FI binding parameters used as a methodology to display the sensitivity of binding site number and strength to changes in composition and morphology.

Thermal desorption GC-MS was identified as a powerful technique for the characterisation of molecularly imprinted polymers. Bleed composition analysis of the pre-treated polymers suggested that a fundamental difference in the degree of crosslinking between MIP and corresponding NIP polymers existed. The technique also correlated with the morphological assessment of the polymers, where the level of bleed and template removal from the 4-VP polymers was consistently less than corresponding MAA polymers. The affinity of the polymers was also determined and correlations with solution phase binding analysis were identified. The affinity of the MAA polymers increased with decreasing EGDMA amount, whilst the 4-VP polymers displayed limited affinity for the binding analyte (2-apy).

A second area of the research involved the preliminary investigation into the use of modified polyvinyl alcohol (PVA) for use as molecularly imprinted polymers. Photosensitivity was introduced into the PVA by reaction with chromophores containing an aldehyde functionality. Polymer solutions in the presence and absence of the template molecule (2-apy) were coated onto an ATR (attenuated total reflectance) crystal. The polymers were crosslinked via a UV initiated [2+2]-cycloaddition reaction. Subsequent analysis via ATR-FTIR spectroscopy, suggested that a minimum level of crosslinking was required to maintain the integrity and stability of the films. There was no evidence of template (2-apy) diffusion into the polymers formed with a higher level of crosslinking. This was due possibly to template surface binding or that the polymer was too flexible to facilitate pre-concentration within the sensing region.

Table of Contents

Chapter 1- Introduction	1
1.1. Polymers	2
1.2. Molecularly Imprinted Polymers	5
1.2.1. Introduction	5
1.3. Synthetic approaches to molecular imprinting	9
1.3.1. Covalent molecular imprinting	9
1.3.2. Non-covalent molecular imprinting	11
1.3.3. Semi-covalent molecular imprinting	15
1.4. Practical aspects of molecular imprinting	18
1.4.1. Template	18
1.4.1.1. Template requirements and its effect on the imprinting process	18
1.4.1.2. Examples of template molecules that have been imprinted	20
1.4.2. Functional monomer	23
1.4.2.1. Methods for the selection of an appropriate functional monomer	26
1.4.3. Crosslinking monomer	28
1.4.4. Solvent	31
1.4.5. Temperature of polymerisation	33
1.4.6. Initiation conditions	34
1.5. Polymerisation methods	36
1.5.1. Monolith synthesis	37
1.5.2. Bead polymerisation	37
1.5.3. Membrane and film imprinting	39
1.5.4. Combinatorial and computational imprinting	40
1.6. Polymer evaluation and characterisation	41
1.6.1. Template extraction	41
1.6.2. Binding site characterisation	42
1.6.3. Pore analysis	47
1.6.4. Differential Scanning Calorimetry	49
1.6.5. Fourier Transform Infra-Red (FTIR) analysis	50
1.6.6. Solid State Nuclear Magnetic Resonance Spectroscopy (NMR)	50

1.7. Applications of Molecularly Imprinted Polymers	51
1.7.1. Solid-Phase Extraction	51
1.7.1.1. Solid-Phase Microextraction	55
1.7.2. Stationary phases in chromatography	56
1.7.2.1. Liquid chromatography	56
1.7.2.2. Thin Layer Chromatography	58
1.7.2.3. Capillary Electrophoresis and Capillary Electrochromatography	59
1.7.3. Sensors	60
1.7.4. Drug delivery	60
1.7.5. Other uses of imprinted polymers	61
1.8. Photosensitive polymers	61
1.9. Poly(vinyl alcohol)	64
1.9.1. Properties of poly(vinyl alcohol)	65
1.10. Photosensitive poly(vinyl alcohol)	67
1.11. The potential for modified poly(vinyl alcohol) for use as molecularly imprinted polymers	70
1.12 Research aims	71
References	72
Chapter 2- Synthesis and physical characterisation of imprinted polymers	88
2.1. Introduction	89
2.2. Experimental	95
2.2.1. Materials, equipment and instrumentation	95
2.2.2. Polymer preparation	96
2.2.3. Template removal	97
2.2.4. Optical microscope and SEM analysis	98
2.2.5. Nitrogen sorption analysis	98
2.2.6. Particle size distribution analysis	100
2.2.7. Solvent swell ratio determination	101
2.3. Results and discussion	103
2.3.1. Template Removal	103
2.3.2. Optical microscope and SEM analysis	106
2.3.3. Nitrogen sorption analysis	109

2.3.3.1. Isotherm analysis	109
2.3.3.2. BET surface area analysis	113
2.3.3.3. Pore analysis	116
2.3.4. Particle size distribution	120
2.3.5. Solvent swell studies	126
2.4. Conclusions	128
References	130
Chapter 3-General assessment of polymer affinity	133
3.1. Introduction	134
3.2. Experimental	136
3.2.1. Materials, equipment and instrumentation	136
3.3. Results and discussion	138
3.3.1. Specificity of methacrylic acid polymers	138
3.3.2. Selectivity of methacrylic acid polymers	144
3.3.4. Specificity and selectivity of 4-vinylpyridine and 4-vinylpyridine-methyl methacrylate polymers	153
3.4. Conclusions	155
References	157
Chapter 4- A detailed examination of MAA-co-EGDMA binding characteristics using binding isotherms and affinity distribution spectra	159
4.1. Introduction	160
4.2. Experimental	163
4.2.1. Materials, equipment and instrumentation	163
4.3. Results and discussion	165
4.3.1. Experimental binding isotherm	165
4.3.2. The Langmuir, Freundlich and Langmuir Freundlich isotherms	168
4.3.2.1. LI results	171
4.3.2.2. FI results	171
4.3.2.3. L-FI results	172
4.3.3. Affinity distribution spectra	175

4.3.4. The effect of the template extraction procedure on binding characteristics	177
4.4. Conclusions	179
References	181
Chapter 5 - Characterisation of polymers using thermal desorption GC-MS	182
5.1. Introduction	183
5.2. Experimental	186
5.2.1. Materials and instrumentation	186
5.2.2. Thermal desorption analysis	186
5.3. Results and discussion	188
5.3.1. Mass spectra of polymer components	188
5.3.2. Polymer pre-treatment	189
5.3.2.1. Bleed composition analysis	189
5.3.2.2. Template removal	197
5.3.4. Examination of polymer specificity utilising thermal desorption studies	202
5.3.5. Comparison of binding results obtained using thermal desorption GC-MS and UV-based solution phase analysis	214
5.4. Conclusions	217
References	219
Chapter 6- Development of photosensitive PVA for use as Molecularly Imprinted Polymers	221
6.1. Introduction	222
6.2. Experimental	224
6.2.1. Materials, equipment and instrumentation	224
6.2.2. Preparation of photosensitive PVA	225
6.2.2.1. Synthesis of styrylpyridinium salt (4-SbQ)	225
6.2.2.2. Reaction of 4-SbQ and cinnamaldehyde with PVA and preparation of the imprinted polymers	226
6.2.3. ATR-FTIR analysis of the polymer films	227
6.3. Results and discussion	228
6.3.1. Initial investigations using PVA-4-SbQ	228

6.3.2. ATR-FTIR analysis	230
6.3.2.1. Water ingress	234
6.3.2.2. 2-aminopyridine reloading	236
6.4. Conclusions	239
References	241
Chapter 7- Conclusions and future work	242
7.1. Conclusions	243
7.2. Future work	250
References	254
Appendix	257

Chapter 1

Introduction

1.1. Polymers

Polymers are large high molecular weight molecules (macromolecules) which are comprised of smaller molecular weight units known as monomers. The monomers introduce functionality to the polymer, which in turn can influence the overall properties of the final polymer. Polymers are produced in biological systems and are essential for everyday life. Typical examples of biological polymers include DNA, proteins and polysaccharides [1]. These naturally occurring polymers are often referred to as biopolymers. Synthetic polymers on the other hand are formed because of a human controlled polymerisation process and include products such as paints, plastics and adhesives.

Polymers are grouped into three categories based on their architecture or the way in which the monomers are bonded together. These categories are:

- Linear-the polymer is formed from monomer units consisting of single, unbranched chains of atoms.
- Branched-these polymers have branches or side-chains that arise because of side reactions during the polymerisation process
- Network or crosslinked polymers- the polymer chains are joined together to form 3-dimensional networks.

Polymers can also be classified by their thermal behaviour, which is directly related to the polymer structure. Linear and branched polymers are also known as thermoplastics. At elevated temperatures they soften and flow as the individual polymer chains can slip past one each other [2]. The softened polymers can thus be shaped or moulded and will then harden on cooling. This process of heating and cooling can be repeated a number of times. These polymers are often referred to as plastics and they are sub-divided into amorphous and crystalline. Amorphous regions are simply regions in which the polymer chains are randomly ordered. Crystalline structures on the other hand, refer to a situation whereby the atoms or molecules are in a regular and ordered manner. Generally, most thermoplastics do not form perfect crystals upon cooling but instead are semi-crystalline and contain both crystalline and amorphous regions. Typical examples of thermoplastics are polypropylene, which has good thermal stability and can be used

for items requiring sterilization, and poly tetrafluorethylene which has superb chemical resistance, which in turn renders it useful for protective clothing and non-stick cookware [3].

Crosslinked polymers form very rigid and hard materials. The greater the degree of crosslinking the more rigid the polymer [2]. Such crosslinked polymers are called thermosets. Unlike thermoplastics, thermosets cannot be melted and re-moulded. The crosslinking reduces the mobility and flexibility of the polymer chains thus causing the polymer to be brittle. Bakelite is an example of a thermosetting polymer and is used, for example, in appliance handles [4].

Elastomers are crosslinked rubbery polymers that can be easily stretched to high extensions and rapidly recover to their original dimensions when the applied stress is released [2]. Elastomers are a form of crosslinked or networked polymers; however, the crosslink density is less in comparison to that of thermosets. The low level of crosslinks allows the polymer chains to become extended when force is applied but they do not permit the chains to flow or slip past one another, as in the case of thermoplastics. A prime example of an elastomer is polyethylene, which is used in household products, insulators, pipes and bottles [2].

There are two types of polymerisation reactions that can occur to form polymer networks. These are step growth (condensation) and chain growth (addition) polymerisations [5].

Step growth polymerisations involve organic reactions between the functional groups on a monomer or a group of monomers. There are two types of step growth polymers. The first is formed from a single monomer which contains two different functional groups, A and B, capable of reaction with one another. The second form of step growth polymerisation reaction is one which occurs between two different monomers, both having different functionality.

Chain growth polymers are formed by monomers that add on to the end of a growing chain. In contrast to step growth polymerisation, chain growth polymerisation proceeds

without the elimination of a by-product and the monomers consist of at least one double bond *e.g.* vinyl monomers. The polymerisation process consists of three distinct stages- 1) initiation, 2) propagation and 3) termination, Figure 1.1.

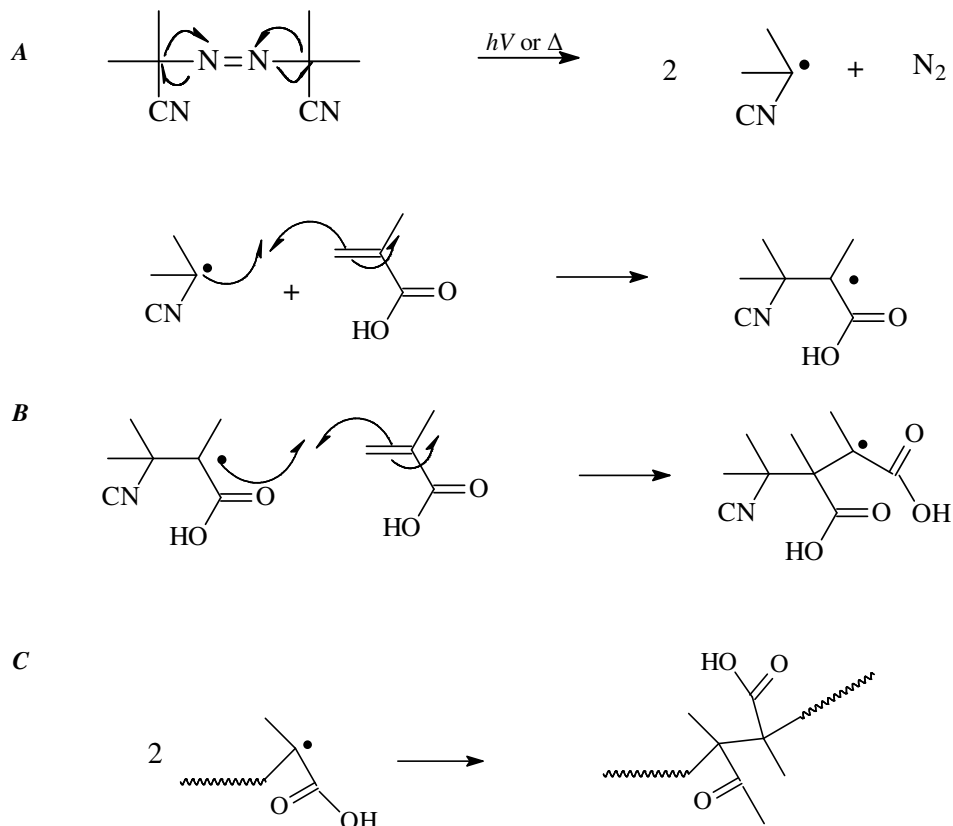


Figure 1.1. The stages of free radical initiation. A; free radical initiation of azobisisobutyronitrile (AIBN) with methacrylic acid (MAA) (both are commonly used in molecular imprinting), B; propagation, C; termination occurring by the combination of two radicals.

Initiation can be brought about through the formation of a free radical. An initiator decomposes to form a free radical upon addition of energy in the form of heat or light. A carbon-carbon double bond (or π -bond) within a vinyl monomer makes it susceptible to reaction with the unpaired electron of the radical, thus forming a new active centre at the end of the monomer. It also results in the formation of a new single bond (σ -bond) where the double bond once was.

This new active centre located at the end of the monomer is also very reactive and will begin to attack the double bond of a neighbouring monomer molecule, and thus the cycle continues. This sequence of events in which the polymer chain rapidly grows by the addition of monomer to the active centre is known as propagation. Propagation is ceased during the termination stage. This stage can occur by a number of mechanisms. The first involves the addition of two active centres, and is known as combination. The second mode of termination is known as disproportionation and occurs when a radical removes a hydrogen atom from a carbon adjacent to the radical producing a saturated and an unsaturated polymer.

Another method of termination called chain transfer can occur when the active centre is transferred to another molecule, for example oxygen (which can readily accept an electron from a radical). This step terminates one chain, but initiates another chain somewhere else along the length of the polymer [4]. It is for this reason that free radical polymerisations must be carried out in an inert environment. This is easily achieved by sparging the polymerisation mixture with nitrogen gas. Free radical initiation is not the only means by which chain polymerisations are initiated; anionic or cationic initiators may also be employed.

1.2. Molecularly Imprinted Polymers

1.2.1. Introduction

Molecular imprinting is a method by which highly selective recognition sites can be generated in a synthetic material, to yield Molecularly Imprinted Polymers (MIPs). MIPs, which are extensively cross-linked polymers, contain specific recognition sites with a pre-determined selectivity for a chosen analyte. The process of molecular imprinting is represented schematically in Figure 1.2.

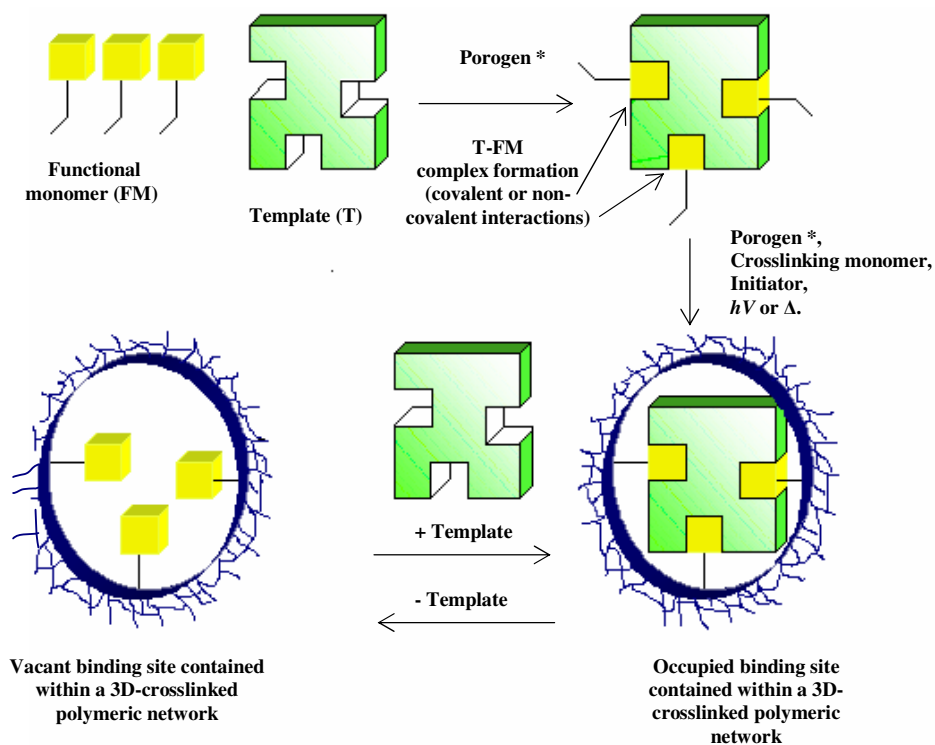


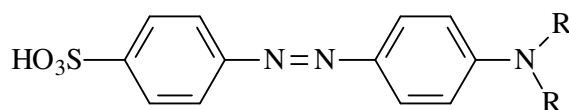
Figure 1.2. Schematic representation of molecular imprinting containing one type of functionality.

* In non-covalent molecular imprinting the porogen is typically added to facilitate T-FM complex formation, whereas in covalent imprinting the porogen is typically added after T-FM complex formation.

The template, which may be the target molecule, interacts with polymerisable functional monomers to form complexes. The mechanisms of interactions between both precursors are typically covalent or non-covalent. This template-monomer complex is then polymerised in the presence of a crosslinking monomer and a porogen (solvent) to hold the template within a rigid polymer matrix. Removal of the template leaves a vacant recognition site with high affinity for the target molecule. The shape and size of the imprint (or recognition/binding site) and the spatial arrangement of the functional groups are complementary to the structure of the template molecule.

Some of the greatest advantages of MIPs are their physical robustness, high strength, resistance to elevated temperatures and pressures, inertness to acids, bases, metal ions and organic solvents as well as the relatively low cost of preparation [6]. Such properties have enabled them to be used in a large number of applications, including solid phase extraction (SPE), liquid chromatography, sensors, catalysis and drug delivery systems [7-11]. The design of the selective cavities can be difficult and time consuming so when trying to imprint a new target molecule careful investigation of the complexation properties of the compounds involved is often required.

The concept of molecular imprinting can be traced back to 1940 [12] when Linus Pauling proposed that antibody formation took place in the presence of an antigen, which acted as a template for the antibody to form around. Pauling suggested that discrimination or selectivity arose due to differences in the structures of the antigens employed. In 1949 Dickey, who was inspired by Pauling's work, reported the polymerisation of silicates in the presence of a methyl orange based dye, Figure 1.3. [13]. After the removal of the dye, subsequent rebinding showed preference to the dye that was present during polymerisation.



R= methyl, ethyl, propyl and butyl.

Figure 1.3. Structure of methyl orange dyes imprinted in silica gels [14].

Following Dickey's initial work on silica gels, the imprinted phases found use in chromatographic separations [15].

It was not until 1972 that a team lead by Wulff reported the first examples of molecular imprinting in organic polymers [16]. Since then molecular imprinting has grown into a well-established research area, which is often referred to as Molecular Imprinting Technology (MIT). In recent years there has been an almost exponential growth in publications resulting from imprinted polymer research [17] (Figure 1.4).

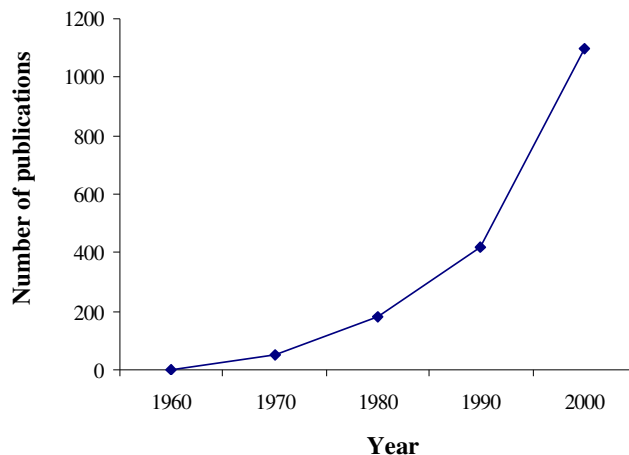


Figure 1.4. Graph demonstrating the number of publications in molecular imprinting since 1970 (adapted from reference [17]).

The growing interest in molecular imprinting has inevitably resulted in their use in commercial applications. MIP Technologies AB and Supelco (a division of Sigma-Aldrich) have entered a collaborative agreement for the production and supply of MIPs (SupelMIPs) for sample preparation, analytical and preparative applications [18]. SupelMIPs have been prepared for the detection of compounds which may be detrimental to human health, some of which include [18] beta antagonists (*e.g.* clenbuterol), antibiotics (*e.g.* chloramphenicol), amphetamine and other related drugs, and tobacco specific nitrosamines. The purification of a raw food product on a process scale has also been reported. Many of these examples are naturally found in complex matrices and so the use of highly selective imprinted polymers as pre-concentrating media affords an attractive alternative to conventional phases commonly employed in the past, such as C18 silica. Numerous examples of analyses using SulpeMIP cartridges have been published [19-26], and one of their main advantages is the lower levels of detection obtainable relative to conventional methods.

1.3. Synthetic approaches to molecular imprinting

Various strategies have been established for the generation of molecularly imprinted species. These strategies are based on the chemical functionality of the template molecule and of the functional monomer(s) employed in polymer formation. This section describes the various methods employed and the main factors to be considered when deciding on the desired technique.

1.3.1. Covalent molecular imprinting

Covalent molecular imprinting was pioneered by Wulff *et. al.* in the 1970s [16]. In covalent systems a template-monomer complex is formed through reversible covalent bonds in a chemical step that is independent of polymer formation *i.e.* the complex is formed in a pre-synthesis step. After polymerisation, cleavage of the template results in vacant binding sites, which contain the initial functionality that was chosen to form the pre-polymerisation template-monomer complexes. Subsequent rebinding of the template occurs through formation of the original covalent bonds.

A prime example of covalent imprinting involves the formation of boronic esters, for example by reaction of 4-phenylboronic acid (the functional monomer) with 4-nitrophenyl- α -D-mannopyranose (Figure 1.5.) [27,28]. The template and monomer were covalently bound through an ester linkage, which was formed by a condensation reaction. This template-monomer complex was polymerised in the presence of crosslinking monomer, and the complexes were thus incorporated into the polymer matrix. Template removal was achieved by mild hydrolysis to produce cavities that were capable of producing an exact-fit by reforming the same bonds, through a labile condensation process, that were present in the initial template-monomer complex. This process is illustrated in Figure 1.5. Template release and up-take was rapid enough for use in HPLC chiral stationary phases [27,28].

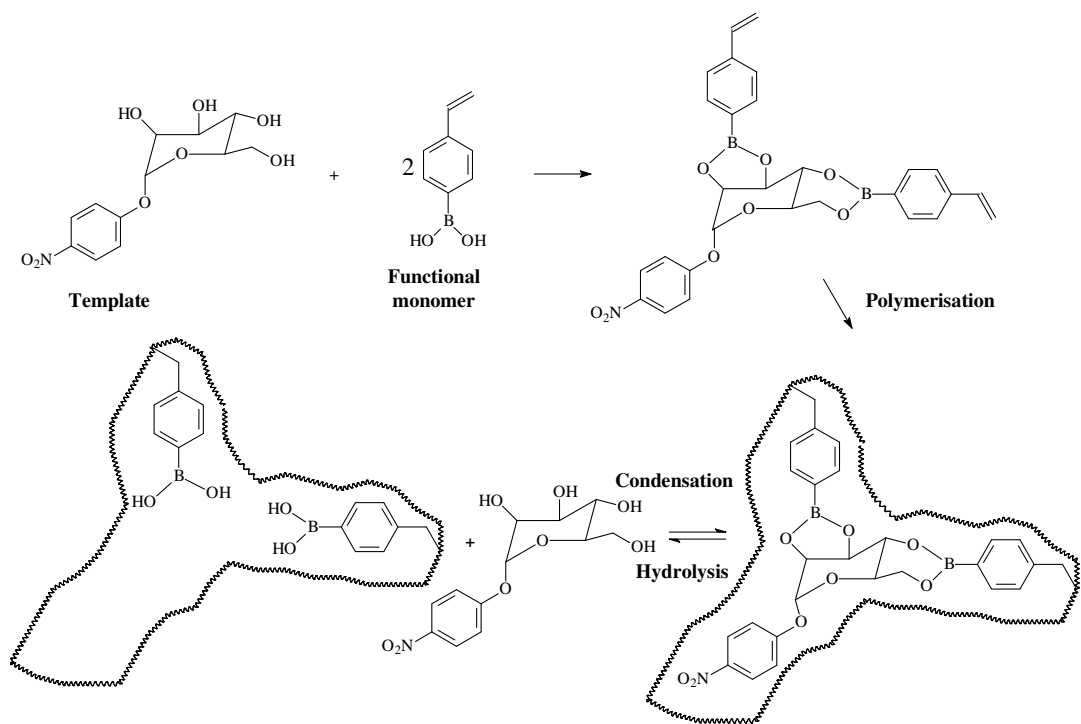


Figure 1.5. Covalent imprinting of 4-nitrophenyl- α -D-mannopyranose using 4-phenylboronate as the functional monomer [27].

The use of boronic ester formation has facilitated imprinting of template species such as glucose and fructose [29], sialic acid [30] and nucleotides [31]. Other examples of molecular imprinting which utilize covalent bonds include the formation of ketals [32] (diol plus a ketone), carboxylic esters [33] (carboxylic acid plus an alcohol) and Schiff-bases (aldehyde plus an amine) [34].

As the template and functional monomer are present in stoichiometric amounts, the functional monomer residues are incorporated fully within the polymer matrix and are found only in the binding cavities. The covalent bond also prevents dissociation of the template-monomer complex during polymerisation. As a result the degree of non-specific binding is reduced and there is generally a homogeneous distribution of binding site affinities, both of which are major advantages of this methodology. As template removal is facilitated through chemical cleavage of the covalent bond, there is little chance of template leaching under normal conditions of use.

There are limitations to this methodology as it is not always possible to find a system that can cleave and subsequently reform with relative ease, which can be a limiting factor for use in chromatography. Poor template recovery can also reduce the capacity of the polymer. The number of functional groups amenable to this method is limited, and thus covalent imprinting is not suitable for all template molecules. Another disadvantage is the pre-requisition for a synthesis stage for the reaction of template and monomer prior to polymerisation.

1.3.2. Non-covalent molecular imprinting

Non-covalent imprinting was developed by Mosbach and Arshady in 1981 [35]. In this strategy the interactions between the template and functional monomer are based on non-covalent associations, such as hydrogen bonding, ionic and π - π interactions (Figure 1.6.). The formation of a pre-polymerisation template-monomer complexes is carried out by simple dissolution in a solvent (or porogen) which is carefully chosen so as to maximise interactions. These interactions can be characterised by UV/ VIS spectroscopy [36,37], NMR titrations [38] or FTIR spectroscopy [39], fluorescence spectroscopy and isothermal Calorimetry (ITC) [40]. A crosslinker is then added and the polymerisation initiated. The polymer then forms around the template-monomer complexes and during polymerisation. The template is removed from the polymer *via* solvent extraction. The solvent is chosen so as to disrupt the non-covalent interactions that were present in the pre-polymerisation complexes. Subsequent template rebinding takes place through the formation of the same non-covalent interactions.

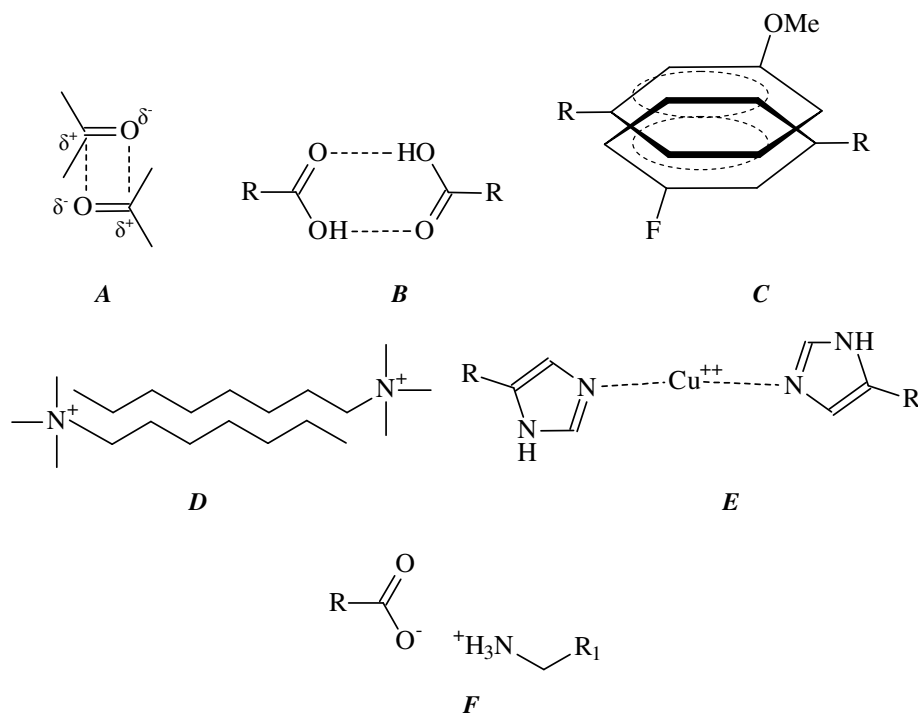


Figure 1.6. Examples of interactions found in non-covalent imprinting. A; electrostatic: dipole-dipole, B; hydrogen bonding, C; π - π stacking, D; van der Waals, E; coordination bond, F; electrostatic ion-ion [41].

Figure 1.7. represents the non-covalent imprinting of nicotine using methacrylic acid as the functional monomer [42]. In this particular example the imprinted polymers showed excellent recognition properties towards nicotine and were used as SPE phases for the clean up of nicotine (and related substances) from chewing gum.

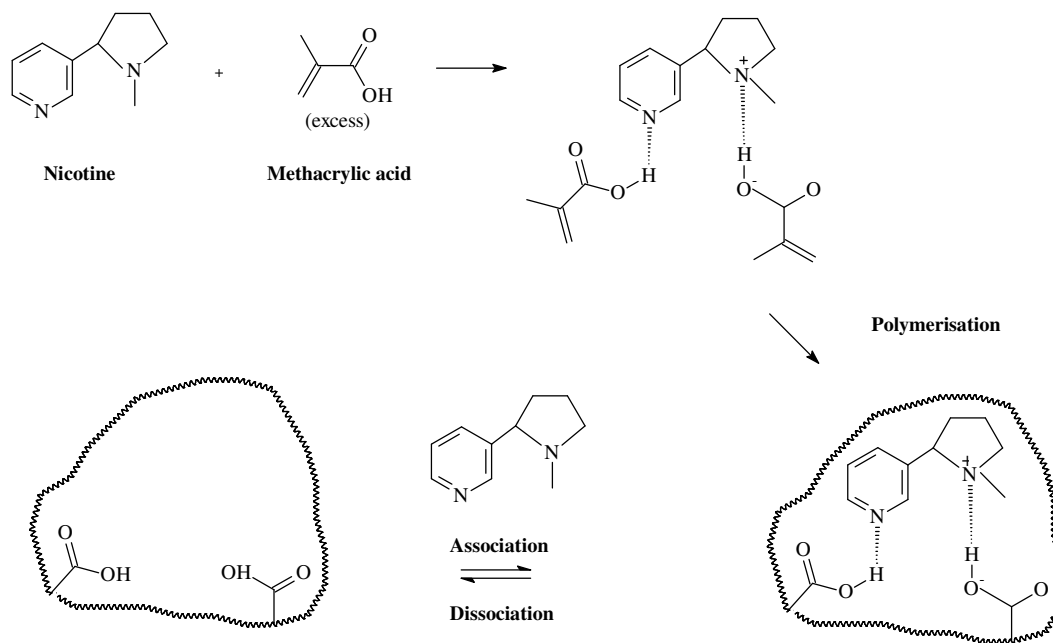


Figure 1.7. Non-covalent imprinting of nicotine using methacrylic acid as the functional monomer [42].

The non-covalent method is simpler than the covalent strategy as it does not require a pre-polymerisation synthesis stage between template and functional monomer. This combined with good template recovery means that the technique can be applied to a wider range of template molecules and subsequent applications. Hence it is the most widely reported method of molecular imprinting.

While the simplicity and the ease of preparation of the non-covalent methodology is advantageous, one of the major drawbacks is that the interactions may not be strong enough to maintain template-monomer complexes, therefore the formation of complex species is governed by equilibrium. An excess of functional monomer is usually added to the reaction mixture in order to complete template-monomer complexation and to maintain the complex stability under the polymerisation conditions. This non-stoichiometric nature results in the formation of a range of binding sites with varying affinities and selectivities, and the specific nature of the polymers is reduced. This can limit the extent to which imprinted polymers are used as chiral stationary phases in HPLC applications, as heterogeneity is a source of peak broadening and asymmetry [43,44]. The occurrence of binding site heterogeneity can be reduced by using covalent imprinting mechanisms or by using stoichiometric non-covalent imprinting. This latter

process involves the use of functional monomers that have high association constants ($> 900 \text{ M}^{-1}$), and thus are capable of interacting strongly, and to a high degree, with the template molecule. A prime example is the use of amidines as functional monomers for interaction with carboxylic acids [45,46].

Whitcombe *et al.* [47] utilised this strategy for imprinting ampicillin, Figure 1.8 A, (a derivative of penicillin). Ampicillin has an amino group and a carboxyl group available for interaction with appropriate functional monomers. The functional monomer shown in Figure 1.8. B was chosen to interact with the carboxyl groups, and was shown to have an association constant, K_{ass} , of $2.8 \times 10^2 \text{ M}^{-1}$ with the ampicillin salt (DMSO- d_6). Structure 1.8. C was used to form $n - \pi$ interactions with the amino group of ampicillin. Both functional monomers were used in a 1:1 stoichiometric ratio with the template (tetrabutylammonium salt of ampicillin) for polymer formation. Ampicillin was found to bind more strongly to MIP over NIP. The imprinted polymer also preferentially bound ampicillin over structurally related analogues.

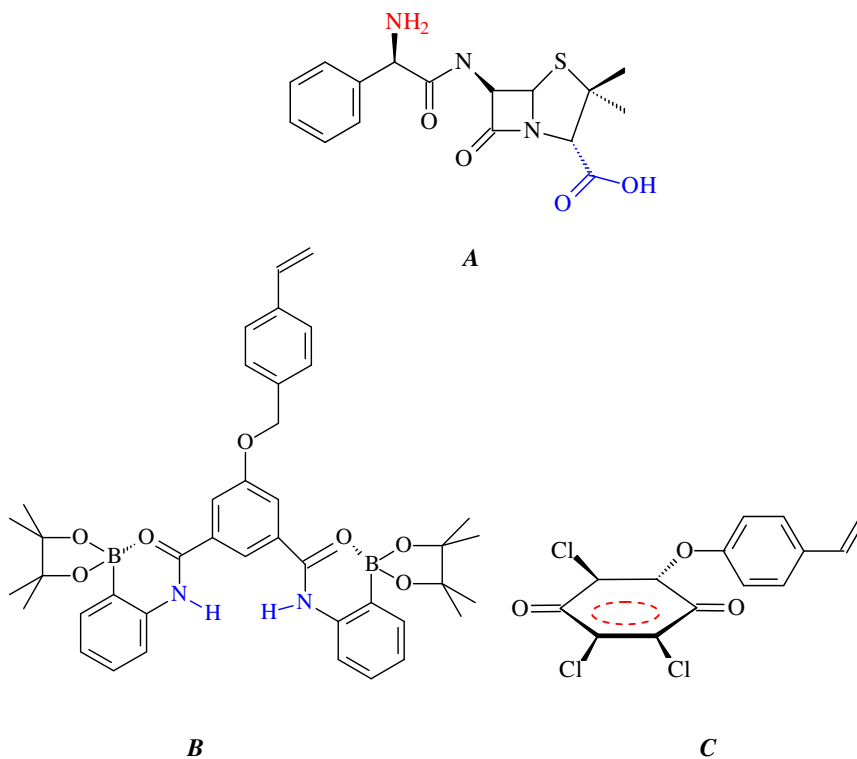


Figure 1.8. Example of precursors used in stoichiometric imprinting. *A*; ampicillin, *B*; and *C*; the functional monomers employed (adapted from reference [47]). Corresponding interacting functionalities are highlighted using the same colour.

1.3.3. Semi-covalent molecular imprinting

Both covalent and non-covalent imprinting strategies have their advantages and disadvantages. The semi-covalent approach combines both methodologies and this generic approach involves the initial covalent linkage of template and monomer in a stoichiometric manner, which prevents binding site heterogeneity. The covalent bond prevents dissociation during polymerisation. Following template removal, subsequent reloading is achieved by the rapid formation of non-covalent interactions.

The first reports of semi-covalent imprinting involved a direct covalent attachment of a structural analogue of a template to a polymerisable group *via* an ester linkage to prepare an imprinted site for *L-p*-aminophenylalanine ethyl ester [48]. Following polymerisation and hydrolysis to remove the structural analogue, two carboxyl groups remained within the polymer matrix which were capable of forming hydrogen bonds and ionic interactions with the amino group of the amino acid, Figure 1.9. Reverse enantioselectivity was observed with preferential separation of the D- isomer over the L-isomer.

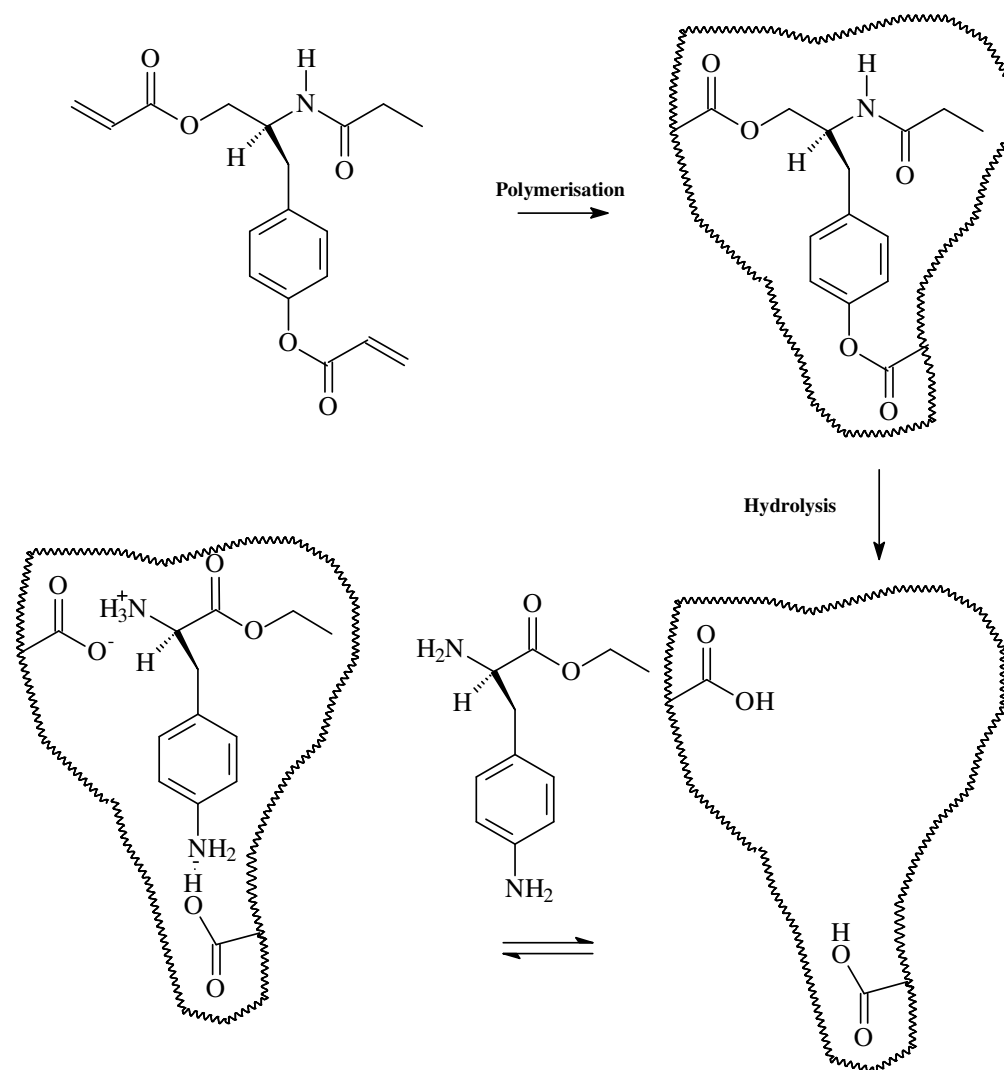


Figure 1.9. Polymerisation of N2-propionyl-O1-acryloyl-2-amino-3-(4-acryloyloxyphenyl)-1-propanol with divinylbenzene, followed by hydrolysis to leave an imprint cavity for L-p-aminophenylalanine ethyl ester [48].

This method proved problematic in terms of the steric requirements required for non-covalent interactions, in the rebinding stage. To overcome this problem, Whitcombe *et al.* introduced the concept of imprinting *via* a sacrificial spacer [49]. This methodology involves the use of a spacer group. This spacer group has the dual role of attaching the template to the functional monomer during polymer formation and acting as a spacer between the template and polymer-bound functionality to prevent steric crowding in the non-covalent rebinding step [50]. A prime example of this technique is illustrated in Figure 1.10. [49]. Cholesterol was covalently bonded to 4-vinylphenol *via* a carbonate linkage. After polymerisation with ethyleneglycol dimethacrylate (EGDMA), the

carbonate ester linkage was cleaved with the loss of carbon dioxide (CO₂). This resulted in the formation of phenolic residues within the binding site, which provided sufficient space to enable non-covalent interaction between the template and the hydroxyl residues, through the formation of hydrogen bonds. A more recent example of imprinting using carbonate as a sacrificial spacer group was reported by Pérez-Conde *et al.* [51] in the molecular imprinting of propazine. The imprinted polymers, once optimised, demonstrated the potential for use as solid-phase extraction media for the clean-up of triazines from soil and vegetable extracts.

Other sacrificial spacer groups that have been employed in the semi-covalent approach include salicylic acid [52] and silyl ether [53] groups.

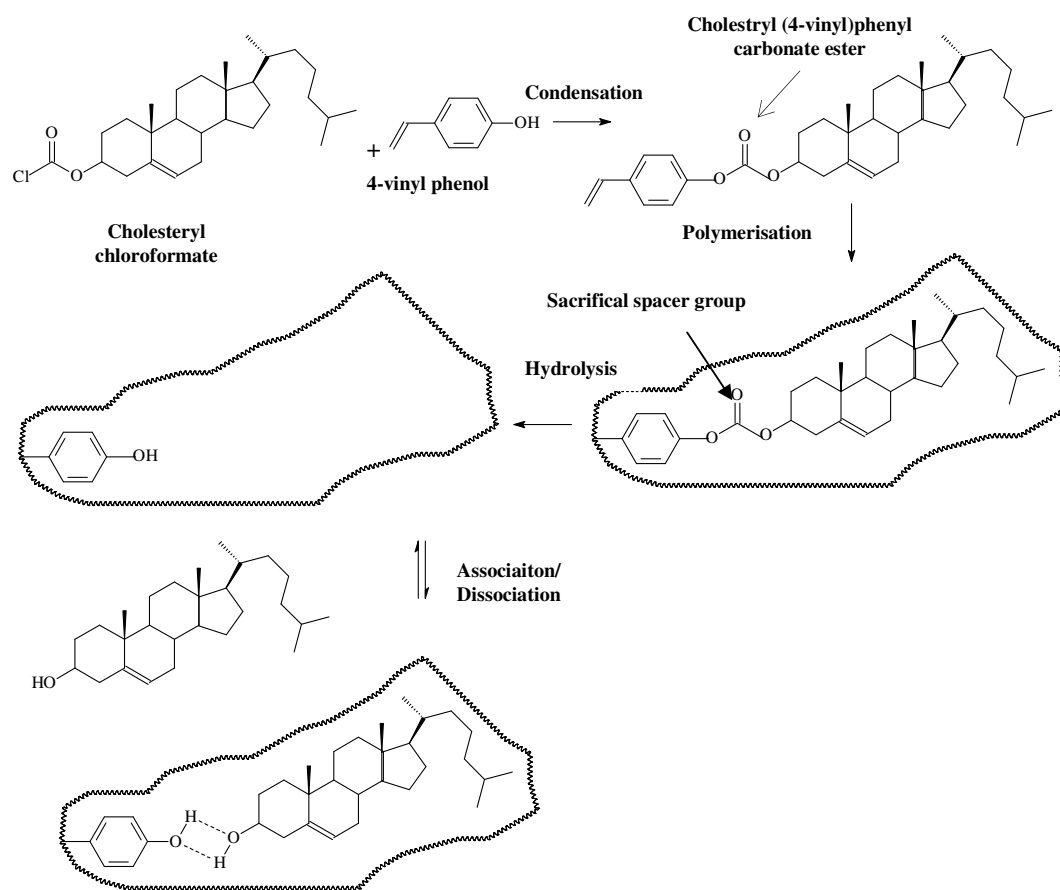


Figure 1.10. The sacrificial spacer approach to molecular imprinting utilising cholesteryl chloroformate as the template species [49].

1.4. Practical aspects of molecular imprinting

The recognition behaviour of imprinted polymers is determined by the preparation, and subsequently the final structure of the polymers. Ideally polymers should have a certain level of flexibility that facilitates template removal and subsequent rebinding, yet, it must also be rigid enough to retain the shape and integrity of the binding cavities so as to maximise polymer performance. The polymer must also possess a level of thermal and chemical stability to render them useful in their subsequent applications.

To achieve the most favourable chemical and physical properties required for a given imprinted system the components involved in polymer formation must be optimised. This can sometimes be difficult because of the number of variables involved, which include:

- Template
- Functional monomer
- Crosslinking monomer
- Solvent
- Temperature of polymerisation
- Initiation conditions

1.4.1. Template

1.4.1.1. Template requirements and its effect on the imprinting process

In all molecular imprinting processes the template is of critical importance in that it directs the organisation of the functional groups pendant to the functional monomers [54], to form template-monomer complexes. In theory, any molecule can be chosen as a template molecule, but, in practise this is not always the case. The most basic criterion for a template is that it contains functionality, which is complementary to that of the chosen functional monomer. This results in interactions between the template and functional monomer, which are *via* a covalent or non-covalent mechanism. The greater the number of interactions between both precursors, the greater the affinity and specificity of the resultant polymer [55,56]. Other factors which must be considered

include the solubility of the template in the presence of polymerisation components, and the template must also be stable at the chosen polymerisation conditions.

Removal of the template leaves binding sites with complementary shape, size and functionality to the template, within the matrix. As a result, the binding site is critical in the molecular recognition properties of the imprinted polymer. Various studies examining, in detail, the role of the template on polymer performance have been carried out. For example, in a cross selectivity study carried out by Cummins *et. al.* [57], the physical and chemical parameters of template species responsible for the binding interactions of the 2-aminopyridine substructure were investigated. It was concluded that a correlation between non-specific binding and template basicity and between non-specific binding and hydrophobicity existed. However, it was due to the competitive nature of basicity and hydrophobicity that no overall correlation existed between the two. It was also proposed that differences in cross-selectivity values could be attributed to the difference in shape and size of the binding species, which contributed to steric crowding in the proximity of the binding functionalities within the binding sites.

In a separate study on the effect of the template structure on molecular imprinting, Zhang *et. al.* [58] examined the role of intramolecular hydrogen bonds between the functional groups of various templates. Affinity was found to decrease for the templates that were capable of intramolecular hydrogen bond formation. The reason cited for this phenomenon is that intramolecular hydrogen bonds weaken the formation of template-monomer complexes, pre-polymerisation, which in turn reduced the number of high affinity binding sites.

Lanza *et. al.* [59] carried out an in-depth examination of the role of the template during polymerisation for a methacrylic acid-ethyleneglycol dimethacrylate (MAA-EGDMA) co-polymer tailored towards 9-ethyladenine, ametryn or tebutylazine. *In situ* ^1H NMR studies of the polymerisation of MIP and NIP materials indicated that template species decreased the rate of polymerisation. This was shown through plots of the integral areas of the vinyl protons of both MAA and EGDMA as a function of time for both imprinted and non-imprinted species. The addition of template at various time intervals after initiation resulted in the formation of binding sites with similar selectivity to those

formed in the presence of template throughout the entire polymerisation. The imprinting factor was found to decrease when addition occurred 60 min after initiation. The highly selective sites that were formed prior to 60 min were attributed to the sites being less embedded within the polymer and were therefore readily accessible. The final study reported by the group involved post-polymerisation treatment of the polymers by curing at temperatures up to and including 160 °C. Results indicated that an increase in selectivity was observed on the MIPs at temperatures up to 120 °C, while further increases in temperatures resulted in a loss of selectivity, due to the destruction of binding sites. As no change was observed on the non-imprinted polymer (NIP) (Figure 1.11) the phenomenon observed in the imprinted polymers was attributed solely to the presence of binding sites.

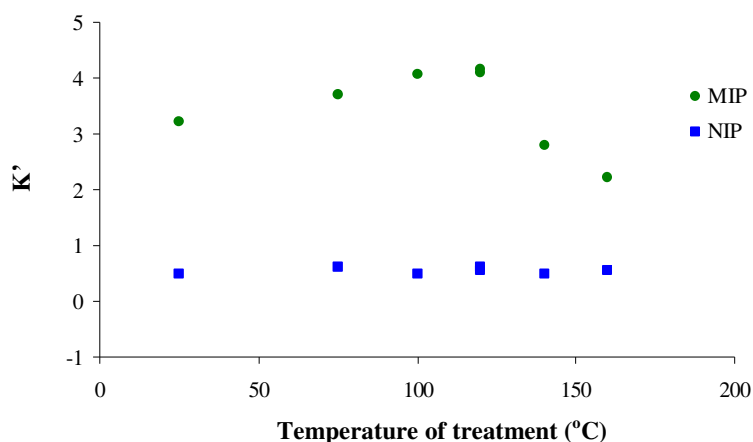


Figure 1.11. Capacity factors (K') for tebutylazine reloaded onto MIP and NIP polymers cured at different temperatures (adapted from reference [59]).

1.4.1.2. Examples of template molecules that have been imprinted

A diverse range of molecules have demonstrated their suitability to molecular imprinting. Table 1.1. lists some of the various categories (and specific examples) of templates that have been imprinted.

Table 1.1. Categories of template molecules (and specific examples) that have been utilised in molecular imprinting.

Category of template molecule	Specific examples	Reference
Amino acids	Phenylalanine anilide,	[60,61]
	Histidine.	[62]
Antibiotics	Trimethoprim,	[63]
	Penicillin,	[64]
	Norfloxacin.	[65]
Drugs	Propranolol,	[66]
	Paracetamol,	[67]
	Ibuprofen.	[68]
Narcotics	Cocaine	[69]
Pesticides/herbicides	2,4-dichlorophenoxyacetic acid,	[70]
	Carbaryl,	[71]
	Linuron & isoproturon.	[72]
Steroids	Cortisol,	[73]
	Testosterone.	[74]
Sugars	β -D-fructopyranose,	[29]
	Methyl- α -D-glucopyranoside-6-acrylate.	[75]

Molecular imprinting of small, low molecular weight molecules is generally successfully achieved through careful choice of polymeric components and optimisation of the imprinting procedure. For larger molecules imprinting success can often be more difficult to achieve, with size being one of the main limiting factors as it slows down or hinders diffusion within the polymer. Temperature can also be an issue for large biological templates. None the less, procedures have been developed for imprinting high molecular weight compounds. For example, proteins and peptides have been successfully imprinted using several different methods. The first method is called the epitope approach. This involves imprinting a small sequence of amino acids from the protein. When a protein containing this particular sequence is equilibrated with the imprinted polymer the entire protein can then bind (Figure 1.12.). A prime example of

imprinting *via* the epitope approach was presented by Rachkov and Minoura [76], who successfully synthesised an imprinted polymer selective towards oxytocin (protein) by imprinting a small three amino acid sequence of the same protein, utilising a non-covalent strategy.

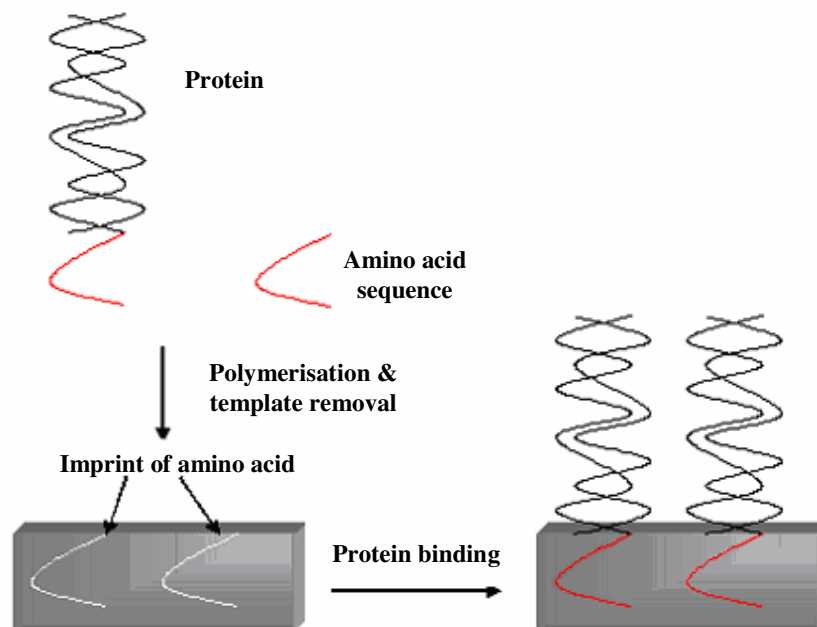


Figure 1.12. Schematic of epitope approach for the molecular imprinting of proteins (adapted from reference [77]).

A second approach involves surface imprinting. Sellergren *et. al.* used hierarchical imprinting to prepare methacrylate based mesoporous beads for chromatographic applications [78]. The method involved grafting the template precursors to the surface of a porous silica support. The pores were then filled with the polymerisation mixture (functional monomer, crosslinking monomer and initiator). After polymerisation the silica was dissolved to leave behind spherical imprinted beads which were subsequently used as stationary phases in liquid chromatography. Imprinted polymers exhibited clear selectivity for their template and structurally related analogues. The template molecule 9-ethyladenine (9EA) was retained approximately 3.5 times more on its MIP over its NIP, while triaminopyrimidine (TAP) was retained approximately 3.0 times more on its imprinted polymer. Free adenine was reloaded on to both 9EA and TAP imprinted polymers and it was retained to a higher degree on the latter polymer. This was

attributed largely to the orientation of the carboxyl groups in the imprinted site, *i.e.* the TAP polymer was more shape selective or less conformationally hindered towards free adenine than the 9EA imprinted polymer.

1.4.2. Functional monomer

Functional monomers are responsible for the binding interactions between the template and polymer matrix. It is clearly very important to match the functionality of the template with the functionality of the functional monomer in a complementary fashion in order to maximize complex formation. The functional monomer must also have a group that is capable of undergoing a polymerisation reaction thus facilitating the formation of the growing polymer.

In the covalent methodology, the functional monomer is reacted with the template species, in a step that is independent of the polymerisation reaction, to form template-monomer complexes that are linked *via* a covalent bond. As covalent linkages are employed, the functional monomer and template are used in stoichiometric ratios. Therefore, the formation of template-monomer complexes, which are central to the molecular recognition of imprinted polymers, is not governed by an equilibrium process. Classical methods of covalent imprinting involve a condensation reaction to form template-monomer complexes [50]. The structures of some common covalent functional monomers are shown in Figure 1.13.

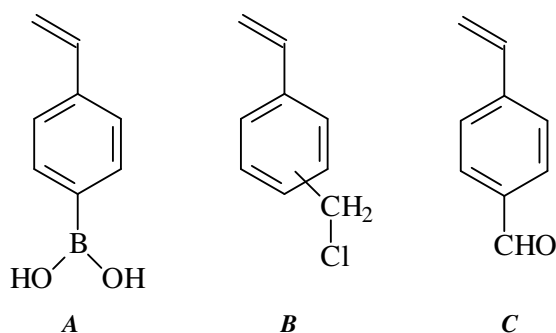


Figure 1.13. Examples of covalent functional monomers. *A*; 4- vinylphenylboronic acid [16], *B*; vinylbenzyl chloride [79], *C*; 4-vinylbenzaldehyde [80].

The formation of pre-polymerisation complexes in non-covalent imprinting is equilibrium based (governed by Le Chatelier's principle) and it is assumed that every individual complex results in the formation of one binding site. Therefore, by increasing the number of complexes in the system, and hence the number of resultant binding sites, it is assumed that the selectivity of the polymer is also increased. The pre-polymerisation complexes can be increased by increasing the concentration of functional monomer or template, or both. Too much monomer however, can result in a MIP containing highly non-specific binding sites with interacting groups present in undefined and random areas of polymer rather than well defined binding sites. Too little monomer can limit the capacity of the MIP, by creating inadequate MIP-template interactions [81]. An excess of template would increase the complex formation, but at and above a certain concentration, the template will no longer contribute to complex formation as all of the functional monomer is already complexed [82]. In general, an excess of functional monomer is used to promote maximum template complexation. As will be discussed in the following sections, other factors such as the amount of crosslinking monomer, the nature of the solvent and the temperature of polymerisation must also be taken into consideration.

In a study by Andersson *et. al.* [83], the effect of monomer: template ratio on the selectivity and retention of non-covalently imprinted nicotine (nic) polymers, using methacrylic acid as the functional monomer, was investigated. Results showed that the best selectivity ($K'_{\text{nic}}/K'_{\text{Bipy}}$) was obtained at a ratio of 4:1 functional monomer: template, Figure 1.14.

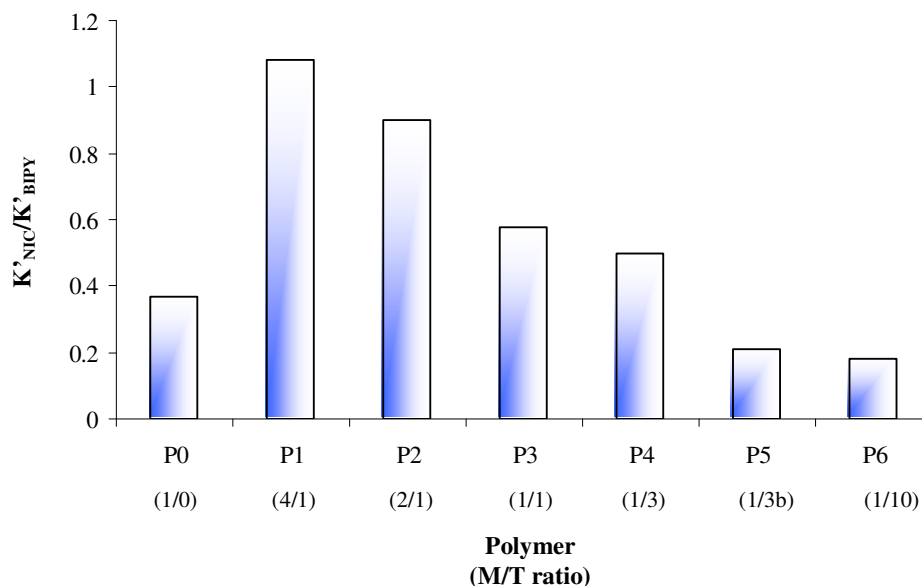


Figure 1.14. Selectivity values of nicotine relative to 4,4'-bipyridyl imprinted polymers with various monomer: template ratios. P5 was formed with acetic acid as well as methacrylic acid as the functional monomer (adapted from reference [83]).

It was proposed that the poor selectivity observed for the polymers formed with higher amounts of template was due to the formation of pre-polymerisation complexes with one point of interaction between the template and the functional monomer, thus, leading to the formation of low affinity binding sites. This was opposed to the two point interaction found when an excess of functional monomer was used. The excess functional monomer was thought to shift the equilibrium towards complex formation resulting in high affinity binding sites. However, as an excess of functional monomer contributes to non-specific binding the importance of optimisation of the polymerisation components is further highlighted.

Haupt *et al.* [84] also investigated the influence of the ratio of functional monomer to template on the performance of MIPs. Polymers were prepared using a monolith synthesis by varying the ratio of functional monomer to template. Results of binding the radioligand ^3H -theophylline indicated that an imprinting effect was observed when the polymer was formed with a ratio of functional monomer to template as high as 5000:1.

The functional monomer is chosen to compliment the functionality of the template species to be imprinted, for example a hydrogen -bond donor should be matched with a hydrogen -bond acceptor, or, strong basic templates should be imprinted using strong acidic functional monomers, and vice versa [85,86]. Figure 1.15. illustrates a selection of functional monomers employed in non-covalent strategies.

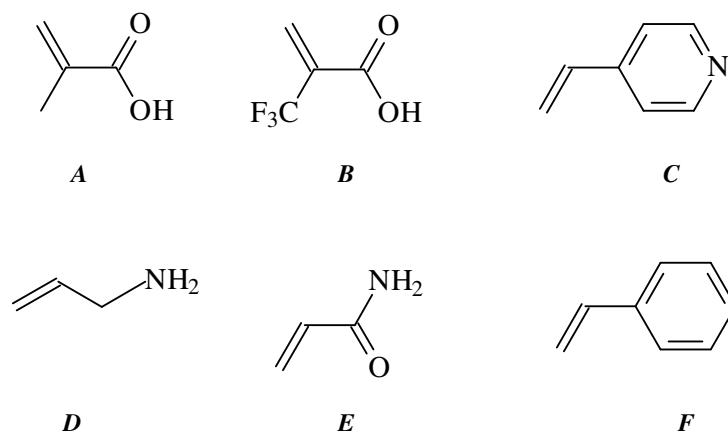


Figure 1.15. Commonly employed non-covalent functional monomers. A; methacrylic acid (acidic) [numerous references], B; trifluoromethylacrylic acid (acidic) [87], C; 4-vinylpyridine (basic) [88], D; allylamine (basic) [89], E; acrylamide (neutral) [90], F; styrene (neutral) [91].

Methacrylic acid, to date, is the most commonly employed functional monomer in non-covalent imprinting. It has the ability to act as a Lewis acid and a Lewis base with hydrogen donating or accepting functional groups in the template molecule [92]. Because of this it can be used to imprint a wide variety of template molecules.

1.4.2.1. Methods for the selection of an appropriate functional monomer

In covalent imprinting the suitability of a functional monomer is decided by the chemistry and reactivity of the functionality of both the template and the functional monomer. Through careful design of a synthetic procedure between both precursors, the resultant template-monomer complex can be characterised by conventional methods. The template-monomer interactions in non-covalent imprinting are generally based on weak intermolecular interactions, whose stabilisation is entirely dependant on the local

environment, such as the nature of the solvent and temperature, (which will be discussed later). Therefore, identification and characterisation of potential interactions is necessary to successfully produce imprinted polymers. The following describes the spectroscopic methods commonly used to establish the strength and stoichiometry of the potential interactions between functional monomers and templates. A combination of these methods are usually employed.

Nuclear Magnetic Resonance (NMR) spectroscopy (in particular ^1H NMR) has proved a useful tool in the characterisation of template-monomer interactions. Changes in the chemical shift values of the key entities of the template and monomer have been used to establish the stoichiometry of the complexes through the use of a Jobs plot [93,94] and/or the determination of the association constant of the complex [95]. Svenson *et. al.* carried out an extensive investigation of the interaction between (-)-nicotine and methacrylic acid [96]. Results indicated that at the concentrations used in molecular imprinting nicotine was capable of complexation with MAA. The strength of these interactions was dependant on the nature of the solvent. Template self-association was also found to take place. This phenomenon was found to exist during the polymerisation process, up to the gel formation stage.

UV/VIS spectroscopy has also been used for studying pre-polymerisation complexes. Svenson *et. al.* applied this methodology to study the nature of potential interactions between a dipeptide template (*N*-acetyl-L-phenylalaninyl-L-tryptophanyl methyl ester), methacrylic acid and two of its structural analogues, acetic acid and trifluoroacetic acid [36]. Analysis of the dissociation constants for template with each of the functional monomers indicated that trifluoroacetic acid had the lowest value. This implied that it was capable of forming stronger ion pairs than both methacrylic acid and acetic acid. Results correlated with earlier chromatographic studies where trifluoromethylacrylic acid polymers (an analogue of trifluoroacetic acid) displayed better selectivity for the herbicide prometryn in comparison to methacrylic acid polymers [97].

Fourier Transform Infra Red (FTIR) spectroscopy has shown to be useful in the identification of hydrogen bonding interactions. The formation of these interactions can be readily identifiable using FTIR since the stretching frequency of hydroxyl or amino

groups (hydrogen bond donors) and carbonyl groups (hydrogen bond acceptors) are displaced and an observable shift can be identified [39,98]. A recent study by Osmani *et al.* utilising this technique identified a two point cooperative interaction between 2-aminopyridine and the common functional monomer methacrylic acid [39]. Results were confirmed using ^1H NMR spectroscopy. The level of band shift observed in the IR spectra was found to be dependant on the pK_a of the binding analyte and a direct correlation to subsequent non-specific binding within the polymers (as presented in earlier studies within the group [57]) were identified.

1.4.3. Crosslinking monomer

The crosslinking monomer forms the bulk of the polymer around the pre-polymerisation complexes, thus “freezing” them in place within the polymer matrix. The degree of cross-linking dictates the rigidity of the MIP. A minimum amount of crosslinker is required to produce a rigid enough structure to maintain the shape of the binding sites, but at the same time keep it flexible enough so as not to hinder template removal. Apart from stabilising the binding sites, the crosslinking monomer provides mechanical stability to the polymers. It also influences the morphology of the polymer, *i.e.* if it is a gel type, macroporous or microgel powder. Imprinted polymers generally contain in excess of 80% crosslinking monomer [54].

In covalent imprinting the amount of crosslinking monomer has an inherent influence on the final polymer performance. Wulff *et al.* [99] demonstrated that the enantioselectivity of an imprinted polymer increases with increasing concentration of crosslinking monomer employed. The study investigated the effect of using three different crosslinking monomers on the selectivity of a phenyl- α -D-mannopyranoside covalently imprinted polymer, using 4-phenylboronic acid as the functional monomer, Figure 1.16.

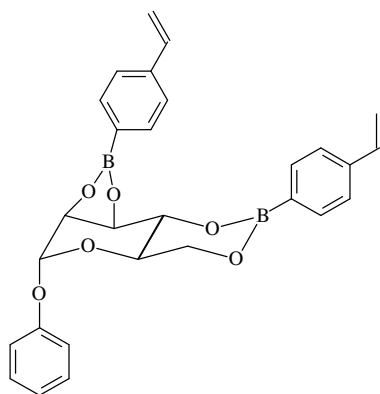


Figure 1.16. Phenyl- α -D-mannopyranoside derivatized with two 4-phenylboronic acid molecules [99].

The crosslinking monomers employed were ethylene glycol dimethacrylate (EGDMA), Butanediol dimethacrylate (BDMA) and 1,4-divinylbenzene (DVB), Figure 1.17. *A*, *B* and *C* respectively.

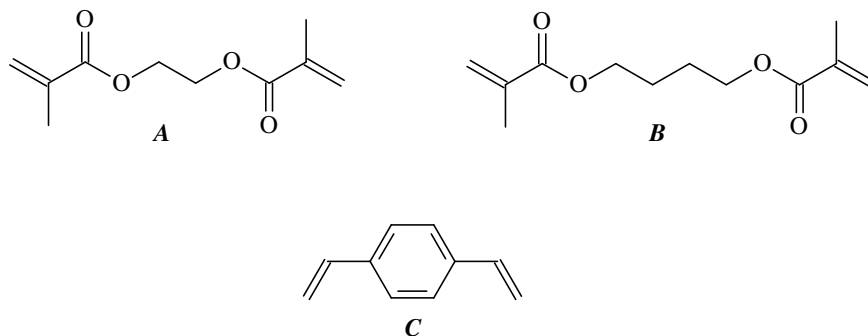


Figure 1.17. Functional monomers employed by Wulff *et al.* [99] in the covalent imprinting of phenyl- α -D-mannopyranoside. *A*; ethylene glycol dimethacrylate (EGDMA), *B*; butanediol dimethacrylate (BDMA), *C*; divinylbenzene (DVB).

A number of polymers were prepared by varying the concentration of crosslinking monomer in relation to the content of functional monomer. It was found that below 50 % crosslinking monomer enantioselectivity was low, but, that observed for EGDMA was slightly improved in comparison to DVB and BDMA (refer to Figure 1.18.). A further increase in crosslinker content to 95 % improved the enantioselectivity values obtained for all three crosslinkers. However the maximum selectivity obtained for BDMA was much lower than that obtained for EGDMA. This was attributed to the increased flexibility of the polymers prepared with BDMA due to its longer carbon chain length. The selectivity obtained for DVB was also less than EGDMA. Converse

to BDMA, this was attributed to the highly rigid matrix formed by DVB. From this it can be concluded that an optimum length and flexibility of the crosslinker is required.

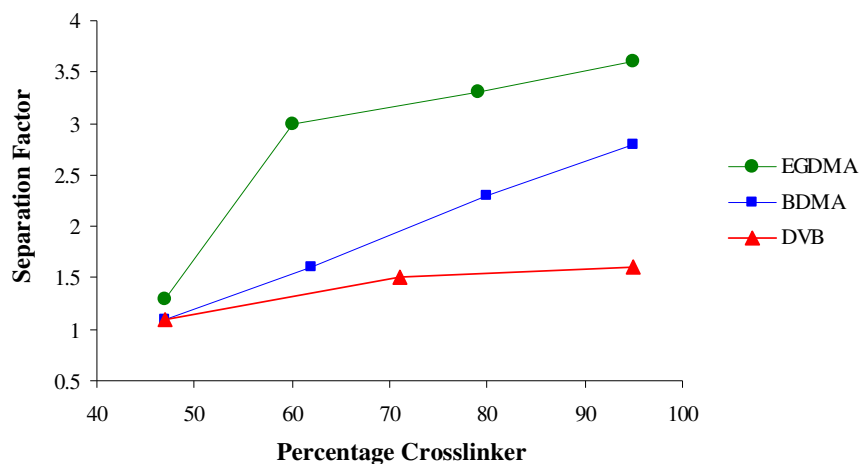


Figure 1.18. Selectivity versus amount of crosslinking monomer for covalently imprinted phenyl- α -D-mannopyranoside [82] (adapted from reference [99]).

Optimisation of the concentration of crosslinking monomer in non-covalent imprinting is complicated by a competing optimisation of monomer to template ratio [82]. Sellergren [100] proposed that the optimum ratio of functional monomer: template: crosslinking monomer is 4:1:20, for non-covalent imprinting. This was determined by assessing the enantioselectivity of a series of L-phenylalanine anilide imprinted polymers prepared with different concentrations of crosslinking monomer (EGDMA) to functional monomer (MAA). Results indicated that an increase in selectivity was observed with a 25 % mole ratio of MAA to EGDMA. As this concentration was increased further, selectivity was completely diminished. This observed effect was attributed to the presence of excess of functional monomer which increases the non-specific binding, which in turn lowers the overall selectivity of the MIP.

The use of a tri- functional crosslinker, trimethylolpropane trimethacrylate (TRIM), Figure 1.19., was investigated and it was found that polymers exhibited higher selectivity than those prepared with EGDMA [101,102]. This was most likely due to better quality, well defined binding sites due to the three crosslinking vinyl groups.

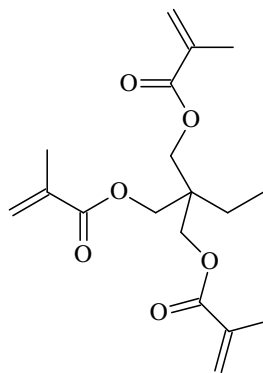


Figure 1.19. Trimethylolpropane trimethacrylate (TRIM) a trifunctional monomer.

Recently Spivak and Sibrian-Vazquez [103] have introduced the concept of using a single crosslinking monomer (OMNiMIPs- one monomer molecularly imprinted polymers) for molecular imprinting. A series of templates were imprinted using a crosslinking monomer, N,O-bismethacryloyl ethanolamine (NOBE), illustrated in Figure 1.20., which has the ability to interact non-covalently with the template species. Similar or improved enantioselective recognition was observed for the OMNiMIP system when compared to polymers prepared with methacrylic acid as the functional monomer and ethyleneglycol dimethacrylate as the crosslinking monomer. Another advantage of this system is that there was no need for additional functional monomer.

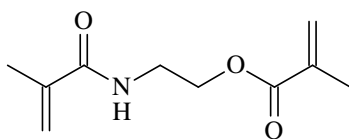


Figure 1.20. N,O-bismethacryloyl ethanolamine (NOBE) [103].

1.4.4. Solvent

The solvent serves to bring all the components of the polymerisation into one phase, *i.e.* template, functional monomer(s), cross-linker and initiator. Therefore a solvent that can easily dissolve all of the mentioned polymerisation components should be employed. The solvent also serves a second important function in that it is responsible for creating the pores in macroporous polymers. For this reason it is quite common to refer to the solvent as the "porogen". Porosity within the polymers originates from phase separation that occurs, during the polymerisation, between the solvent and the created polymer.

Polymers with low solubility for a given solvent phase separate early which results in larger pore sizes and a lower surface area, while those that have a higher solubility phase separate later and have a smaller pore distribution with larger surface areas [82].

Aside from solvating the polymerisation components and acting as a pore forming agent, the solvent must be carefully chosen in non-covalent imprinting so as to maximise monomer-template complex formation. The solvent must be chosen based on the type of interactions to be stabilised between monomer and template, as the polarity of the solvent dictates the formation or disruption of these interactions. Aprotic or less polar solvents allow the formation of polar hydrogen bonding interactions. In contrast, polar protic solvents, such as methanol and in some cases water, suppress the formation of hydrogen bonds but promote hydrophobic and ionic interactions between the template and the functional monomer [50]. As a result, the selectivity of the imprinted polymer is influenced by the nature of the solvent employed in the polymerisation stage. If water is used as the polymerisation medium then the solubility of the polymer components can be an issue. For example, ethyleneglycol dimethacrylate (EGDMA), trimethylolpropane trimethacrylate (TRIM) and other acrylic esters are insoluble in water and so alternatives such as acrylamides must be used [104].

Sellergren and Shea [105] performed a comprehensive study on the influence of the solvent on the enantioselectivity of a series of polymers non-covalently imprinted with L-phenylalanine analide, using methacrylic acid as the functional monomer. Selectivity was found to diminish with increasing solvent polarity, which indicated a marked dependency on the nature of solvent polarity.

In a study carried out by Ansell and Mosbach [106] the chromatographic performance of a number of polymers prepared in various porogens, using a suspension polymerisation method, were evaluated as stationary phases for chromatographic separations. The results obtained compounded those reported by Sellergren and Shea [105]. Less polar solvents provided the highest selectivity values, which was attributed to the stronger interactions between template and monomer in the non polar environment. As a result, specific recognition sites were formed, thus providing optimum selectivity.

It has been reported that optimum rebinding occurs when binding is assessed in the solvent that was used in the polymerisation stage. Shea *et. al.* [107] reported optimum chromatographic separation on a 9-ethyladenine imprinted polymer when the porogen was utilised as the mobile phase. Similarly, Yoskizako *et. al.* [108] reported greatest retention on ortho or paraxylene imprinted polymers for the solvent used during polymer formation.

Although the pore size of covalently imprinted polymers is affected by the choice of solvent, the selectivity is almost unaffected by the nature of the solvent employed and an optimum ratio of solvent to monomer of 1:1 has been suggested [28,109].

1.4.5. Temperature of polymerisation

In non-covalent imprinting the formation of template-monomer complexes is equilibrium based, and thus governed by thermodynamic factors [110]. Therefore, an increase in temperature can disrupt the formation of such interactions. Such a disruption leads to interactions that are less defined, which ultimately lowers the yield of binding sites.

It has been widely reported that the selectivity of polymers formed at lower temperatures is improved in comparison to those formed at higher temperatures. Sellergren [100,111] prepared a number of polymers *via* a non-covalent strategy, using L-phenylalanine anilide as the template molecule. The polymers were prepared at 40 and 60 °C, and the best enantioseparation was observed for the polymers prepared at the lower temperature. This result was ascribed to a higher degree of complex formation at lower temperatures. Similar effects on enantioseparation were reported by Mosbach *et. al* [112] whereby polymers prepared at 0 °C presented better enantioselectivity than polymers prepared at 40 or 60 °C.

Piletsky *et. al.* [113] carried out a detailed study on the effects of polymerisation temperature on the performance of (-)-ephedrine imprinted polymers, prepared in the temperature range -30 to 80 °C. HPLC analysis of the resultant polymers suggested that polymer affinity and selectivity was dependant on the polymerisation temperature. An

increase in capacity and separation factors was observed for those polymers prepared at lower temperatures.

While lower polymerisation temperatures favour the interactions between template and monomer, the polymerisation temperature can influence the polymer structure. Lu *et. al.* [114], through the preparation of a series of polymers formed at 10, 40 and 60 °C, found that the best selectivity was observed for polymers prepared at 40 °C. Further analysis demonstrated discrepancies in polymer morphology, depending on the polymerisation temperature. The various morphologies were attributed to various degrees of polymerisation, which was directly related to temperature. A key finding from this study suggested that there is trade-off between the extent of polymerisation and stabilisation of template- monomer interactions, and, that an optimum polymerisation temperature should be determined for every combination of template and monomer.

The stabilisation of template-monomer interactions is not vital when imprinting *via* a covalent strategy, as the monomer and template are joined covalently in a separate pre-polymerisation synthesis stage. Therefore, it is envisaged that polymerisation temperature is not an issue in covalent imprinting. However, Wulff and Haarer [115] demonstrated that covalently imprinted polymers prepared at lower temperatures exhibited better selectivity than those prepared at higher temperatures. This was attributed to the lower polymerisation temperatures which caused the polymerisation to proceed at a slow rate, which resulted in different morphologies (also suggested by Lu *et. al.* [114]) which effectively enhanced the kinetics of the up-take and release of template from the binding cavities.

1.4.6. Initiation conditions

In general, the most common method of initiation for the synthesis of imprinted polymers is *via* the formation of free radicals. Free radical polymerisations can be performed under mild reaction conditions (*e.g.* ambient temperatures and atmospheric pressures) in bulk or in solution, and are very tolerant of functional groups in the monomers and impurities in the system (*e.g.* water). It is for these reasons that free radical polymerisation is usually the method of choice for preparing molecularly

imprinted polymers [54,116]. The mechanism of free radical initiation has been described in section 1.1. and it essentially involves three distinct stages: 1) initiation, 2) propagation and 3) termination. Figure 1.21 illustrates typical examples of initiators employed in molecular imprinting.

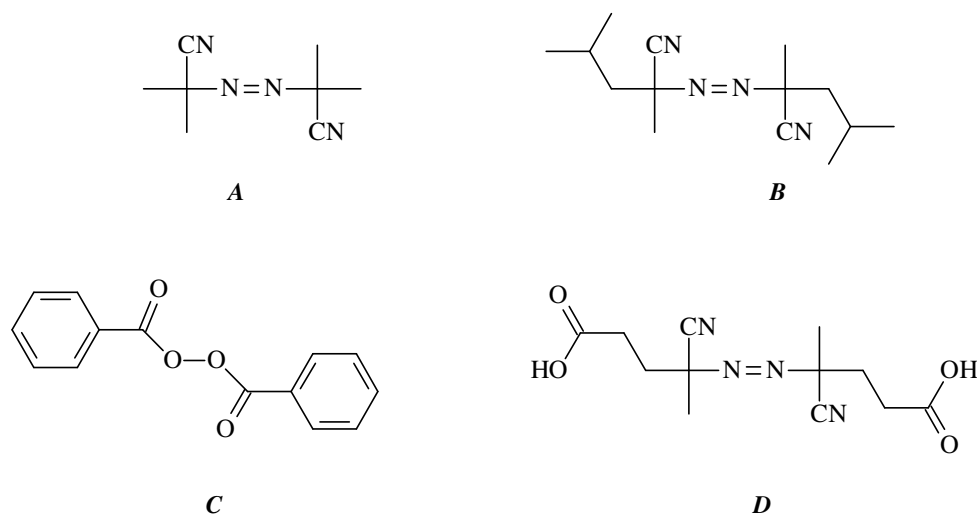


Figure 1.21. Typical examples of free radical initiators employed in molecular imprinting [54].

A; azobisisobutyronitrile (AIBN), B; azobisdimethylvaleronitrile (ABDV), C; benzylperoxide, D; 4,4'-azo(4-cyanovaleric acid).

In terms of molecular imprinting, free radical formation has generally been conducted thermally [117-120] or photolytically, for example utilising UV or visible light [64,121-123]. Sreenivasan [124,125] and Milojkovic *et. al.* [126] reported the use of γ -radiation as a source of free radical generation. A major advantage cited by both authors is that there is no need for additional initiator since the radiation provides a continuous source of radicals. Free radical generation is an exothermic process [50,127] and, with respect to thermal initiation, temperatures as high as 187 °C have been recorded in the centre of polymer monoliths when the initiation temperature was 80 °C [113]. This factor should be taken into consideration when imprinting *via* a non-covalent strategy as high temperatures can reduce the selectivity of the final polymers.

Mijangos *et. al.* highlighted the dependency of enantioseparation on the concentration of initiator and the length and temperature of polymerisation [128]. Higher concentrations lead to higher temperatures in the polymerisation mixture. This resulted in lower separation factors. The morphology of the polymers was also affected by initiator concentrations. It was proposed that higher amounts would increase the number of free radicals, which in turn would lead to a growing number of polymer nuclei and globules, which would however have a smaller size and a larger surface area, as confirmed by BET analysis. It was concluded from this comprehensive analysis that to achieve the best performance in enantioseparation, MIPs should be synthesised over a long period of time, at low temperatures with low concentrations of initiator.

If the use of a thermal initiator may potentially jeopardise the efficiency of the imprinting process, initiators with low activation energy should be employed, or, initiation should be activated photolytically, particularly if the template is thermolabile.

Recently Steinke [116] *et. al.* reported the use of a ring opening metathesis polymerisation for the generation of molecularly imprinted polymers. This method is reported to exhibit thermodynamic control over the polymerisation reaction, thus reducing binding site heterogeneity.

1.5. Polymerisation methods

Different uses and potential applications of imprinted polymers demand different properties from the polymers and as a result many different methods for the preparation of imprinted polymers have been developed. The main methods employed are monolith synthesis and bead polymerisation. A growing emergence is the formation of imprinted films or membranes as new separation techniques. Each of these procedures involves the control of different parameters during the synthesis to produce polymers with the desired properties. Also discussed is the preparation of imprinted polymers *via* combinatorial imprinting.

1.5.1. Monolith synthesis

Traditionally, the first polymerisation method employed to synthesise imprinted polymers was based on the formation of a monolith [129]. This method is simplistic as it involves the preparation of a mixture of the polymer components, which once initiated is left to polymerise to yield a polymer in the form of a bulk monolith. A major advantage is the absence of added substances, other than the polymer components. The formed monolith is ground and sieved and fractions of desired size are then collected.

The method, while apparently simplistic, has its disadvantages. The grinding and sieving process is laborious, and leads to a loss in yield; typically 30-50% of the polymer is retained. The grinding process forms particles of irregular shape and size, which is restrictive when the polymers are used for chromatographic applications. As there is a lack of control of the polymerisation process, in particular in the heat generated, the polymer forms with variations in structure which contribute to heterogeneity.

1.5.2. Bead polymerisation

As the synthesis of monoliths presents many limitations, numerous research groups in molecular imprinting technology have attempted the production of imprinted polymer beads. The process is generally carried out in a two phase system- typically an organic phase and an aqueous phase in the presence of a stabiliser. Advantages of bead formation include, a high yield of usable particles (with respect to monolith synthesis), control over particle shape and size, and uniformity of size, which enables ease of packing into columns with subsequent good flow properties for chromatographic applications [130,131].

The methods of polymerisation that are used to generate imprinted beads are:

- Precipitation polymerisation [132-137],
- Dispersion polymerisation [138-140],
- Suspension polymerisation [141-143],

- Core-shell emulsion polymerisation [141,144] and
- Multi-step swelling polymerisation [145,146].

Table 1.2. summarises each of the mentioned polymerisation techniques.

Table 1.2. Advantages and disadvantages of the various MIP polymerisation techniques [130,131,144,147].

MIP format	Advantages	Disadvantages
Monolith	Ease of polymerisation, no particular skills or sophisticated methods required.	Tedious procedure of grinding and sieving, high loss of yield, irregular particle size and shape, poor chromatographic performance.
Precipitation	High yields, no need for additional stabilizer.	High dilution factor, random aggregates produced.
Dispersion	Simple technique, spherical and near monodisperse beads.	Under developed in terms of molecular imprinting, stabilizer required.
Suspension- aqueous	Spherical beads, highly, scale up possible.	Incompatible with non-covalent systems, stabiliser required.
Suspension- perfluorocarbon	Spherical beads, does not interfere with non-covalent imprinting.	Cost of perfluorocarbon, specialist stabilisers required.
Core-shell emulsion	Monodisperse beads, surface imprinting.	Complex, can be irreproducible.
Multi-step swelling	Monodisperse beads, well developed method.	Complex, aqueous emulsions can limit use.

1.5.3. Membrane and film imprinting

A membrane is an interphase between two adjacent phases acting as a selective barrier, regulating the transport of substances between two the compartments [148]. Molecularly Imprinted Membranes (MIMs) is a relatively new field in the area of molecular imprinting and focuses on the separation of a mixture of molecules through membrane transport [149].

The methods by which MIMs are prepared are;

- Sequential approach [150],
- Simultaneous site and morphology approach [151] and
- Composite membranes [152].

The success of membranes in separation depends on the kinetics of diffusion which in turn is dependant on the pore size and the thickness of the membrane, with short and more direct paths leading to faster separation times. However, the function of a membrane also depends on its structural stability and integrity. Hence, limitations exist for reducing membrane thickness [153]. To achieve good performance, high permeability and selectivity are a pre-requisite.

An MIM is either composed of an imprinted polymer or contains an imprinted polymer, and so template binding can occur on or in the membrane or film. The mechanism of MIM separations has been described by Ulbricht [148,153] and is categorised into four main mechanisms, which are briefly discussed.

- Template binding is monitored directly, by techniques such as quartz crystal microbalance, UV or IR spectroscopy, or indirectly, based on competitive binding between the template and a template conjugate with a label (*e.g.* fluorescence).
- Template binding brings about local changes in the MIP binding site or in its immediate vicinity.
- Binding of the template brings about a change in the entire property of the entire MIP film, *e.g.* a change in permeability due to swelling.

- Template binding coupled with permeation selectivity, thus, enabling a membrane separation.

Examples of templates that have been utilised in MIM include caffeine [152], theophylline [154] and (s)-naproxen [155]. The technique has also been applied as a sensor for the detection of the biological analyte bilirubin [156] and for formaldehyde gas odour [157].

1.5.4. Combinatorial and computational imprinting

This method of polymer formation is related directly to the optimisation of polymer formulation. The technique generally involves the generation and screening of polymer libraries. This identifies the most suitable components and conditions for a particular imprint system.

Combinatorial synthesis is based on the preparation of a large number of compounds or materials in parallel, and the procedure employed for MIP analysis is essentially a scaled down version of the traditional monolithic approach [158]. The use of this method was first reported by Takeuchi *et. al.* who used a semi-automated procedure to prepare polymer libraries for the herbicides ametryn and atrazine [159]. Using a programmed liquid dispenser two functional monomers, methacrylic acid and trifluoromethacrylic acid, were added to 1.5 mL glass vials in different amounts. The template, crosslinking monomer and initiator, all dissolved in the porogen, were also dispensed into the vials which were then purged with nitrogen and subsequently polymerised. Instant first screening, which involved equilibration with acetonitrile, was used to facilitate template removal which enabled quantification of the remaining template retained within the polymer. Following a second thorough washing procedure regular screening was carried out to assess polymer affinity. This involved incubation with solutions of the original template species and analogous compounds. While this method was preliminary in terms of the variables studied, it was shown to be sufficient for the determination of optimal imprint formulations for the given systems.

Although combinatorial imprinting offers obvious advantages, the extrapolation of the obtained results has to be made with caution [160] as assessment is carried out on monolith polymers but in practice subsequent applications will be carried out in particulate format.

Computational imprinting involves the use of molecular modelling software to screen a virtual library of monomers and templates [160,161]. Chianella *et al.* used a computational approach for the design of a MIP specific for a cyanobacterial toxin microcystin-LR [162]. A virtual library of functional monomers was designed and screened against the template. The monomers that gave the highest binding energy were selected and used in a molecular dynamics process to investigate their interaction with the template, and the stoichiometric ratio determined was used in the preparation of a MIP using a monolith strategy. The rebinding analysis indicated that imprinted polymer had affinity and sensitivity comparable to those of polyclonal antibodies.

This method was used by Regan *et al.* who determined the binding energies for the interaction of caffeine and theophylline with the functional monomers methacrylic acid and 2- or 4-vinylpyridine [163].

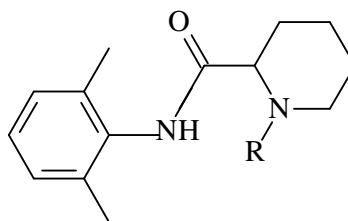
1.6. Polymer evaluation and characterisation

1.6.1. Template extraction

Template extraction is carried out on all imprinted polymers regardless of their method of preparation. When extracting the template molecule, 100 % removal is desired to maximise the capacity of the polymer. However, typically 1 % or higher of template remains embedded within the polymer despite extensive washing [164]. A reason which may be attributed to the incomplete removal of the template is that polymers may not be homogeneously crosslinked and may contain densely crosslinked regions thereby “trapping” the template within the polymer matrix. This residual template may leech out of the polymer inevitably leading to problems in the subsequent applications of the polymers, particularly in trace quantitative analytical applications. Such a problem was reported by Rashid *et al.* for the solid phase extraction (SPE) of tamoxifen using a tamoxifen imprinted polymer [165]. When low levels of tamoxifen were reloaded on to

the SPE cartridges 800 % tamoxifen recovery was reported. This was despite the suggestion that the initial washing of the polymer facilitated complete template removal.

As well as being time consuming, extensive solvent washing procedures can also be costly. To circumvent this problem of template leakage, imprinting structural analogues of the template has frequently been applied. The “surrogate” or “dummy” template must have structural features that are capable of forming imprints that are similar to that of the target molecule, and, because it is a different molecule, detection by an appropriate analytical technique is possible without interfering with the detection of the target. A typical example of this method of imprinting was reported by Andersson [166] who prepared an SPE sorbent selective to bupivacaine by imprinting its analogue pentylcaine (Figure 1.22.). The SPE phase was used for the pre-concentration of bupivacaine from human serum samples prior to analysis *via* gas chromatography, which was capable of clearly distinguishing bupivacaine from pentylcaine. This resulted in precise and accurate quantification of bupivacaine.



R = n-butyl; bupivacaine
R = n-pentyl; pentylcaine

Figure 1.22. Structures of pentylcaine (structural analogue used as the template) and bupivacaine (target molecule) used by Andersson [166].

1.6.2. Binding site characterisation

Imprinted polymers can be evaluated in terms of molecular recognition through simple batch binding experiments, direct chromatographic analysis, solid-phase extraction or membrane transport studies [167]. However, a factor that can complicate the evaluation, and potentially comprise the subsequent performance, of imprinted polymers is a phenomenon known as binding site heterogeneity. A heterogeneous system contains

binding sites of varying affinity and selectivity, as illustrated in Figure 1.23., and is more prevalent in non-covalent systems [44].

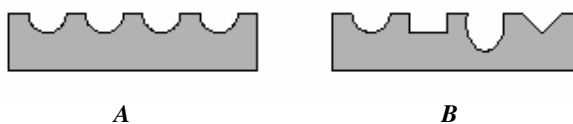


Figure 1.23. A; Homogeneous binding sites and B; heterogeneous binding sites (adapted from reference [44]).

The primary source of heterogeneity in non-covalent MIPs is the incomplete template-monomer complexation in the pre-polymerisation mixture [168]. The complexes are held together by relatively weak non-covalent interactions. As an excess of functional monomer is typically employed, which is used to promote maximum template complexation, most of the functional monomer remains un-associated in the pre-polymerisation mixture. This leads to the random integration of the functional monomer into the polymer matrix and produces a large population of low-affinity binding sites. Only a small fraction of functional monomer forms higher order complexes that on polymerisation yield the high affinity binding sites. This heterogeneous property can limit the use of MIPs, particularly in chromatographic applications where it can lead to poor resolution and peak asymmetry [43]. Heterogeneity can also cause cross-reactivity in sensors [122].

An accurate assessment of binding site affinity is depicted when an experimental binding isotherm is generated, typically through batch binding experiments or frontal chromatography, and a specific binding model is applied to the experimental isotherm [167,169]. Binding models can be categorised as discrete or continuous. Discrete models simplify a distribution into a finite number of binding sites, with each class having a different binding affinity [44]. This type of model accurately assesses the binding behaviour of homogenous systems, *i.e.* those systems having one or two types of binding sites. Continuous distribution models accurately model the binding behaviour of heterogeneous systems. Typical examples of binding models include Langmuir (LI) [126], Freundlich (FI) [94,168,170,171] and the Langmuir-Freundlich (L-FI) [172,173] isotherms.

The proposed broad affinity distribution of imprinted systems and the area which each of the mentioned binding models represents is illustrated in Figure 1.24. N is the number of binding sites and K is the binding energy.

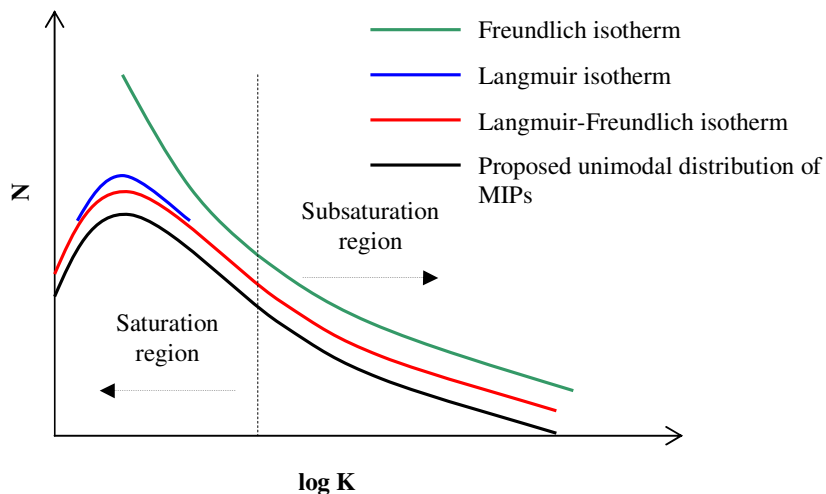


Figure 1.24. The proposed broad affinity distribution of imprinted systems and the area which each of the mentioned binding models represents (Note: this Figure combines numerous diagrams presented in reference [44]).

The LI is a discrete model which is used to assess a homogeneous surface [169]. It is expressed as:

$$B = \frac{N_t a F}{1 + a F} \quad \text{(Equation 1.1.)}$$

Where B is the concentration of substrate bound to the polymer, F is the concentration of free substrate in solution after equilibration, N_t is the total number of binding sites, a is related to the average binding affinity K_o via $K_o = a^{1/m}$, and m is the heterogeneity index with values of zero to one, with zero being heterogeneous and values approaching one indicating homogeneous systems. The LI has often been extended to a Bi-LI and has been plotted using Scatchard analysis. Until recently it has been the most common method for the assessment of MIPs. The assumptions made by LI are as follows [169]: 1) adsorption cannot take place beyond a monolayer and 2) all surface binding sites are equivalent, *i.e.* one class of binding sites, and can only recognise one template molecule.

The Freundlich Isotherm (FI) is a continuous distribution model that is deemed useful for assessing the heterogeneity of imprinted polymers, in particular non-covalent systems [172]. It expresses the relationship of B and F using a power function [172], as follows:

$$B = aF^m \quad \text{(Equation 1.2.)}$$

Where a is the Freundlich adsorption coefficient and is related to the average association constant (K_o) via $K_o = a^{1/m}$ [172] and m is the heterogeneity index with values of zero to one with zero being heterogeneous and values approaching one indicating homogeneous systems.

To determine the suitability of FI, the experimental binding isotherm is plotted in log B versus log F format to determine the appropriateness of FI in assessing the binding behaviour of the MIPs. If the data fits a straight line plot then the FI is deemed appropriate. The limitations of FI are that it is only accurate for a small region of the binding isotherm (in the low concentration subsaturation region). Application outside this region is said to yield inaccurate binding parameters [168]. It cannot be used at high concentrations as it cannot predict the monolayer saturation observed at those concentrations [169].

The hybrid L-FI expresses the relationship between B and F such that [172]

$$B = \frac{N_t a F^m}{1 + a F^m} \quad \text{(Equation 1.3.)}$$

N_t , a and m are fitting coefficients, where N_t is the total number of binding sites, a is related to the average association constant (K_o) via $K_o = a^{1/m}$, and, m is the heterogeneity index [172,174]. This model is particularly useful if binding is assessed in both the saturation and subsaturation regions as it can mathematically reduce to the FI at low concentrations and conversely it mathematically reduces to the LI at higher concentrations. This can lead to a more accurate assessment of MIPs due to the limitations encountered when using LI and FI individually. Unlike LI and FI, L-FI cannot be applied using linear regression analysis. Instead a curve fitting programme is required [167].

Shimizu *et. al.* carried out a comparative study examining the suitability and accuracy of LI, FI and L-FI in modelling the binding behaviour of a number of imprint systems [172]. Five MIPs, both covalent and non-covalent, were taken from the literature and the three mentioned models were applied to each system. Three of the systems had been assessed in the saturation and subsaturation concentration regions and when all three models were applied to each of the individual experimental isotherms, the L-FI was found to have a better fit than the LI or FI. This was further compounded by the improved linear regression (R^2) values of L-FI over LI and FI. A proposed explanation given by the authors for the good fit observed with L-FI is that it is a three parameter model as opposed to a two parameter LI or FI model. A more important, and probably more significant, reason is that the L-FI is physically more appropriate, given the proposed heterogeneity in MIPs. L-FI is capable of modelling the entire isotherm whereas LI and FI are limited to certain regions, as illustrated in Figure 1.24.

Affinity distribution (AD) plots can be generated from the binding parameters obtained from the binding models. AD spectra displaying the number of binding sites (N_i) having a particular association constant (K_i) can be plotted, for example, by substituting the Langmuir-Freundlich fitting parameters N_t , a and m into the following equation [172]:

$$N_i = N_t a m (1/K_i)^m x \frac{(1 + 2a(1/K_i)^m + a^2(1/K_i)^{2m} + 4a(1/K_i)^m m^2 - a^2(1/K_i)^{2m} m^2 - m^2)}{(1 + a(1/K_i)^m)^4}$$

(Equation 1.4.)

Where $\log K = \log \left(\frac{1}{\left(\frac{F}{1000} \right)} \right)$ and F is the concentration of free analyte in solution post-equilibrium.

AD plots are often referred to as site-energy distribution plots as the association constant is plotted in units of $\log K$ which renders it proportional to the binding energy, ΔG , of the imprinted polymer [44]. These plots can be more informative than the

information generated solely from the binding models. AD spectra are also particularly advantageous when comparing different polymeric media.

To reduce the occurrence of heterogeneity it is recommended that the polymerisation formulation and procedure be optimised, or alternatively, imprinted using a covalent procedure. However, as stated earlier not all templates are amenable to this method. Another emerging technique to circumvent the problem of heterogeneity is post-modification of polymers. An example of chemical modification, termed guest selective chemical modification, involves protecting a desired set of binding sites (typically high affinity sites) while the remaining undesired sites are modified [175]. The resultant polymer then contains high affinity binding sites.

Shimizu *et al.* successfully used this technique to improve the binding characteristics of an ethyl adenine-9-acetate (EA9A) selective polymer [176]. The low affinity binding sites were preferentially eliminated by esterification with diazomethane or phenyldiazomethane. Selectivity in the esterification reaction was achieved using a guest molecule as an *in situ* protecting group that preferentially shielded the high-affinity sites. The low-affinity sites were then exposed for reaction. Affinity distribution analysis suggested a higher percentage of high affinity binding sites when the polymers had been subjected to an esterification reaction.

While binding site distribution can be evaluated through the application of isotherms, the chemical and morphological structure of the polymer can be characterised by simple experimental procedures. However, because of the insoluble nature of polymers they are not amenable to characterisation in the solution state. They can however be sufficiently characterised in the solid state using conventional analytical methods [54].

1.6.3. Pore analysis

Pore and swelling analysis give an indication of the morphology of the imprinted polymer, which is typically carried out by solvent uptake analysis or porosimetry. An example of the latter is nitrogen sorption porosimetry. This involves a fixed mass of dry polymer being exposed to nitrogen at a series of fixed pressures. As the pressure

increases the gas condenses and fills the pores. By measuring the amount of gas adsorbed as a function of pressure, isotherms (Figure 1.25.) can be constructed from which information on the specific pore surface area ($\text{m}^2 \text{g}^{-1}$), specific pore volume (mL g^{-1}), average pore diameter and pore size distribution can be obtained [54,164].

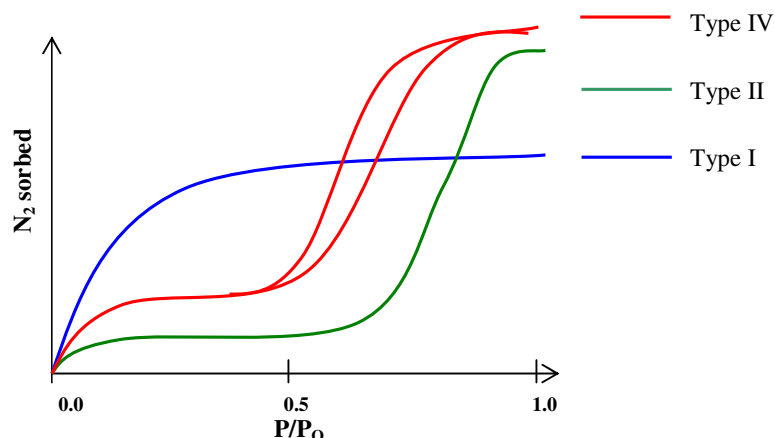


Figure 1.25. The types of isotherms that are generated for microporous (Type I), mesoporous (Type IV) and macroporous (Type II) polymers. P/P_0 is the relative pressure where P is the equilibrium pressure and P_0 is the saturation pressure (adapted from reference [177]).

The type of isotherm that is generated depends on the size of the pores. Materials with an average pore diameter $< 20 \text{ \AA}$ (microporous) adsorb *via* Type I isotherm, $20 - 500 \text{ \AA}$ (mesoporous) *via* Type IV and $> 500 \text{ \AA}$ (macroporous) *via* Type II [177]. The porosity of polymers (imprinted or otherwise) can be tailored by the concentration of crosslinking monomers, the amount and type of solvent and the method of polymerisation [178,179].

As the subsequent applications of imprinted polymers are generally carried out in a liquid medium, the effect of solvents on the morphology of the imprinted polymers should also be considered. The degree of swelling can give an indication of the extent of crosslinking [180]. Inverse size exclusion chromatography has been used to determine the pore structure in the swollen state [54,59].

1.6.4. Differential Scanning Calorimetry

Differential scanning calorimetry (DSC) is frequently employed to analyse the thermal stability of polymers, which in turn can provide information about physical properties such as glass transition temperature (T_g), crystallisation temperature (T_c), melt temperature (T_m), the degradation or decomposition temperature (T_D) and crosslink density.

DSC is based on heating (or cooling) a sample and a reference at a preset rate, while keeping their temperatures the same, and measuring the compensating heat flux that keeps the temperature of the sample within the limits of a predetermined programme [181]. The temperature difference is transformed into a differential heat flow rate, which is typically plotted against temperature (or time) to form a DSC curve (Figure 1.26.) [182].

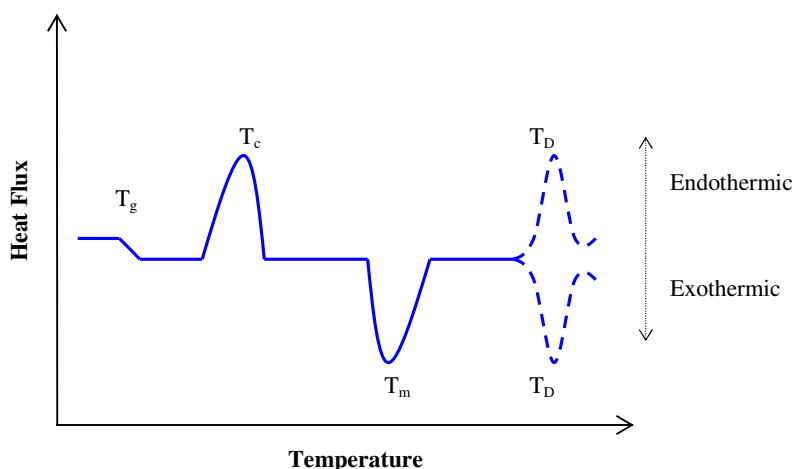


Figure 1.26. Example of a typical DSC isotherm (adapted from reference [183]).

DSC has the potential to identify physical differences between imprinted and non-imprinted polymers and differences pertaining from various polymerisation techniques.

1.6.5. Fourier Transform Infra-Red (FTIR) analysis

An FTIR spectrum of an imprinted polymer can be easily acquired through the preparation of a KBr disc or as a single bead or particle [54]. Analysis of distinct monomer bands to those of the polymer can give an indication of the extent of monomer incorporation into the polymer network. For example, methacrylic acid has distinct bands at 1638 cm^{-1} and 950 cm^{-1} which may be informative about the extent of un-reacted double bonds [164]. By use of this technique it is also possible to investigate the extent of non-covalent interactions, particularly hydrogen bonds, between the formed polymer and the template species.

Katz and Davis demonstrated how FTIR analysis could be used to show the binding capabilities of a sol-gel imprinted polymer whose functionality consisted of aminopropyl groups within the binding sites [184]. These groups were capable of amide bond formation with the reloaded analyte. This bond was confirmed by the appearance of a band at $1630\text{-}1665\text{ cm}^{-1}$ in the FTIR spectrum of the reloaded polymer.

1.6.6. Solid State Nuclear Magnetic Resonance Spectroscopy (NMR)

Solid state NMR enables the NMR spectra of insoluble polymers to be collected. ^{13}C -NMR has allowed the analysis of the different types of carbon atoms present in the polymer network. For example, it can be used for an estimation of un-reacted carbon-carbon double bonds remaining after polymerisation [164]. Shea and Sasaki [185] demonstrated the use of NMR for rebinding 1,3-diacetylbenzene to its imprinted polymer. The technique had the ability to monitor the ketal and ketone functionality of the polymer. NMR spectra were obtained at different time intervals, and analysis of the shifts indicative of rebinding indicated a time dependency on the degree of rebinding. A later study by Sasaki and Alam [186] further exemplified the use of NMR for characterisation and subsequent binding analysis on imprinted silica xerogels.

1.7. Applications of Molecularly Imprinted Polymers

Molecular imprinting has become an established technique for the preparation of polymeric materials with recognition properties for the template species. Due to the wide range of templates that are amenable to imprinting, a wide variety of polymers with different selectivities or recognition properties are obtainable. Because of the relatively low cost and ease of preparation, stability against high temperatures and pressures, chemical resistance to harsh environments, and the ability to act as synthetic biological receptors, imprinted polymers have found use in a wide variety of applications, some of which are described in the following sections. However, it is due to disadvantages such as binding site heterogeneity, template leeching and lower catalytic activity relative to biological counterparts [187] that their commercial application is not more widespread.

1.7.1. *Solid-Phase Extraction*

Prior to analysis, many organic and biological samples require pre-concentration (enrichment) or clean up (if it is in a complex matrix) which can be achieved by loading the analyte onto a solid phase. The analyte is retained on the solid phase where its elution is then facilitated by washing with an appropriate solvent. Imprinted polymers have high selectivities and affinities, and, as they can be tailored towards a particular analyte or class of compounds they are advantageous in terms of solid-phase extraction. It is due to the high selectivity that imprinted polymers potentially offer higher levels of clean-up or enrichment over conventional extraction materials that have been used in the past [188]. The feasibility of this approach has been described for several applications mainly bio-analysis, food analysis and environmental analysis. Table 1.3. lists some molecules to which molecularly imprinted solid phase extraction (MISPE) has been applied.

A disadvantage associated with using imprinted polymers as SPE media is that it is difficult to extract 100% of the template molecule following polymerisation. Typically, 1 % or higher remains within the polymer matrix. This can be problematic as the template can leach or “leak” from the polymer which can have a detrimental effect on

the accuracy of the subsequent SPE analysis. This problem can be overcome by imprinting a “dummy template” or a structural analogue of the analyte of interest, as described in section 1.6.1. Despite this potential drawback, MIP has great potential for commercial applications due to their low cost and speed of preparation, not to mention their excellent tailor made affinities.

Table 1.3. Examples of target molecules to which MISPE have been employed.

Analyte	Sample/Matrix	Reference
Clenbuterol	Calf urine	[19]
Bupivacaine	Human plasma	[166]
Phenytoin	Human plasma	[189]
Chlorotriazine	Environmental water samples	[190]
Phenoxy acids	Environmental water samples	[191]
Quercetin	Red wine	[192]
Triazines	River water sample	[193]
Tramadol	Human serum	[194]
Ibuprofen and naproxen	Human serum	[195]
Chloramphenicol	Milk	[196]
Ochratoxin A	Wheat	[197]
Dioxynivalenol	Wheat and pasta	[198]

Optimisation of the washing procedure is of utmost importance. The first step, termed conditioning, involves washing the MISPE with the loading solvent. This step activates the binding sites of the MIP, thus, maximising interactions with the target analyte in the sample [10]. In the next step the analyte is loaded on to the MISPE phase. The nature of the loading solvent is crucial in that it dictates the type and strength of interactions between the loaded analyte and the imprinted polymer. The nature of the solvent is dependent on the pre-polymerisation template-monomer interactions. If, for example, hydrogen bond formation is the predominant mechanism of interaction then loading is

generally carried out in a low-polarity solvent. This results in selective retention of the analyte while the sample matrix is not retained [199].

Complications can arise when the analyte is present in an aqueous medium, which is often the case for environmental and biological samples. The presence of water results in the analyte and other interfering compounds being non-selectively retained by hydrophobic interactions [10]. This problem can be minimised if a clean up step is employed prior to elution. For example, the MIP maybe washed with a low polarity organic solvent which suppresses the non-specific interactions without disrupting the specific interactions between the analyte and MIP [200]. Often, improved recognition is reported if the porogen is used in the clean up stage [190]. This is due to solvent memory effects. It should be remembered that if the analyte is loaded in an aqueous environment then the MISPE phase should be dried prior to the clean up stage due to potential immiscibility problems.

Finally analyte elution occurs by washing with an appropriate solvent that is capable of disrupting the interactions with the MIP. Low volumes of eluting solvent are required for high levels of enrichment. However, if the analyte displays a high affinity for the imprinted polymer low volumes are not always possible. To overcome this problem, low volumes of solvent containing a modifier (*e.g.* acetic acid) can instead be used.

MISPE applications can be used in an off-line or on-line mode. The former involves using analytical techniques (*i.e.* liquid or gas chromatography) to determine the analyte from the extract that has been collected after the elution stage (as described above). This procedure was used by Andersson *et al.* for the successful pre-concentration of sameridine from human plasma prior to analysis by gas chromatography [201]. Another example of off-line MISPE include the pre-concentration of Ni(II) ions from aqueous samples with subsequent detection by atomic absorption spectroscopy [202].

On-line MISPE predominately involves coupling a column packed with the imprinted polymer into the loop of the injection valve of a liquid chromatography (LC) system [203]. After pre-concentration and washing, the analytes are eluted with the mobile phase to an analytical column where separation occurs. The detector coupled to the LC

quantifies or identifies the analytes. As the entire sample passed through the MIP is eluted to the analytical column, a smaller sample volume is required [10]. Loss of analyte and risk of contamination are reduced [204] and this method is also useful for multianalyte determinations using imprinted polymers capable of recognising several structurally related compounds [203].

This on-line procedure has been used successfully for the determination of a mixture of triazine herbicides from an aqueous sample [205]. The triazines (simazine, atrazine, propazine and terbuthylazine) were selectively enriched using imprinted polymers as the recognition matrixes coupled to a C₁₈-SPE column (refer to Figure 1.27. for the schematic representation of the analytical system). The samples were loaded onto the C₁₈-SPE column. As they were added in an aqueous environment the hydrophobic components in the mixture were non-specifically retained. All retained species were eluted to the MIP column by switching the solvent to acetonitrile. The triazines were specifically retained on the imprinted polymer while the other sample components were eluted to the analytical column that was coupled to an HPLC system. Further solvent switching resulted in elution of the triazines to the HPLC system where they were subsequently identified. To determine the suitability of this procedure, samples were passed from the C₁₈-SPE straight to the analytical system (*i.e.* the MIP was bypassed). Resultant chromatograms contained a large amount of interfering compounds from the sample matrix (humic acid). This made analyte detection difficult or, depending on the analyte, impossible due to complete interference from the sample matrix. However, when the MIP was used, enrichment factors of up to 100 were recorded.

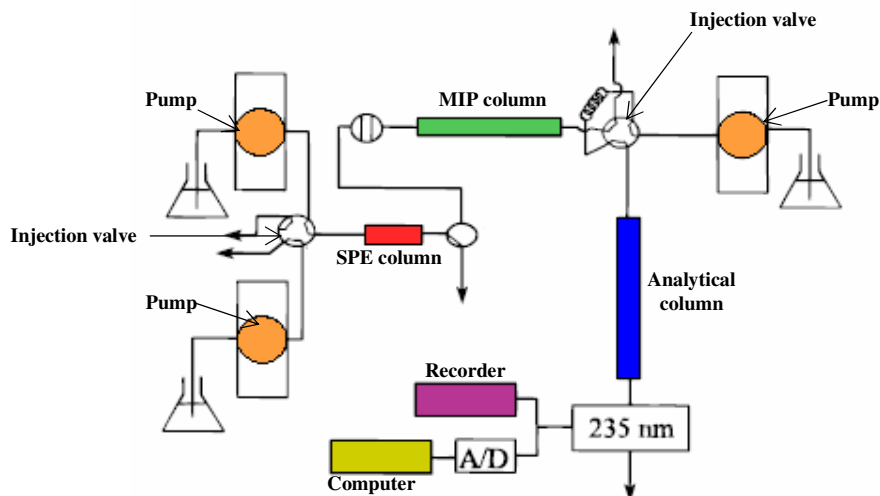


Figure 1.27. Schematic representation of an on-line SPE system for the enrichment of triazines (adapted from reference [205]).

In a more recent example of on-line MISPE, presented by Jiang *et. al.* [206], MIP microspheres selective to bisphenol A were packed into a column and attached directly to an HPLC system. This permitted direct injection, enrichment, separation and detection of bisphenol A from aqueous samples using only one column. An enrichment factor of 10,000 was reported from a 40 mL aqueous sample.

1.7.1.1. Solid-Phase Microextraction

Solid-phase microextraction (SPME) is a minaturised and solvent free sample preparation technique for chromatographic-spectrometric analysis by which the analytes are extracted from a gaseous or liquid sample by absorption in, or adsorption on, a thin layer polymer coating fixed to the solid surface of a fibre, inside an injection needle or inside a capillary [207]. Because of the success of MISPE, imprinted polymers offer great potential as SPME fibres.

The first reports of MIP-SPME were independently presented by Mullett [208] and Koster *et al.* [209]. Mullett immobilised a polymer, imprinted towards propranolol, inside a capillary tube. This automated on-line (coupled to a HPLC) procedure, which permitted the pre-concentration and separation of the template from biological fluids,

had increased sensitivity relative to traditional SPME coatings. Excellent method reproducibility (RSD < 5.0 %) and column reusability (> 500 injections) were observed over a fairly wide linear dynamic range (0.5-100 µg/mL) in serum samples. Koster coated a silica fibre with a poly(MAA-co-EGDMA) clenbuterol imprinted polymer. Selective extraction of bromobuterol from spiked human urine was demonstrated. Improved extraction selectivity of MIP over NIP was reported.

Hu *et al.* [210] recently prepared a MIP-SPME coating on the surface of silica fibres using prometryn as the template. To investigate the selectivity six trazines were reloaded and desorbed using the desorption chamber of a SPME-HPLC. The highest extraction efficiency was reported for the original template. The MIP fibre also had the ability to selectively extract the various structural analogues, the extent of which was found to be dependant on the shape of the analogue. While all reloaded analytes were retained to some degree on the MIP fibre, this was not the case for the NIP-fibre or for commercially available fibres, such as polyacrylate fibres. This finding further highlighted the suitability of imprinted polymers for use as SPME phases.

1.7.2. Stationary phases in chromatography

The use of MIPs as stationary phases for analytical chromatography and electrophoretic separations is one of the most studied applications of imprinted polymers, as is evident from analysis of the available literature. One of the major advantages of using this type of stationary phase is that the MIP can be prepared with a predetermined selectivity for the analyte of interest. The ability of MIPs to stereoselectively separate racemic mixtures in combination with their physical and chemical stability renders them attractive as separation materials for potential use in the pharmaceutical industry.

1.7.2.1. Liquid chromatography

Conventional non-imprinted column stationary phases have long been employed in HPLC for the separation of molecules. An advantage of using imprinted polymers over conventional stationary phases is the ability of the imprinted phase to selectively recognise a specific molecule. Chiral separation is facilitated by imprinting one

enantiomer of a drug compound. The polymer is then packed into a HPLC column, in bead form or as materials ground and sieved as a result of monolith formation. The imprinted enantiomer will then be preferentially retained over its non-imprinted counter part, thereby facilitating chiral separation.

An important application of MIPs is based on their ability to discriminate between the enantiomers of a drug solute containing one or more stereogenic centres. MIPs as chiral stationary phases (CSPs) for use in any separation technique possess predetermined three dimensional spatial cavities which have the ability to recognise one enantiomer over the other. Molecular imprinting has been used to generate CSPs for a wide variety of chiral compounds, including carbohydrates [211], amino acid derivatives [85] and drug compounds [212,213].

A study by Lu *et. al.* [214] attempted to investigate the mechanism of chiral recognition on imprinted polymers. The group successfully imprinted 4-L-phenylalanylaminopyridine (4-L-PheNHPy) using methacrylic acid (MAA) as the functional monomer (Figure 1.28). The polymer was packed into a HPLC column, and after optimisation of the HPLC method, it was found that the imprinted polymer could efficiently separate a racemic mixture of 4-L,D-PheNHPy, with elution of the D-enantiomer occurring first. The column was also used to separate analogue racemates such as 3-L,D-PheNHPy and 2-L,D-PheNHPy. These analogues were less retained and poorly resolved. The exact placement of functional groups inside the imprinting cavity of the imprinted polymer was proposed to be responsible for these results.

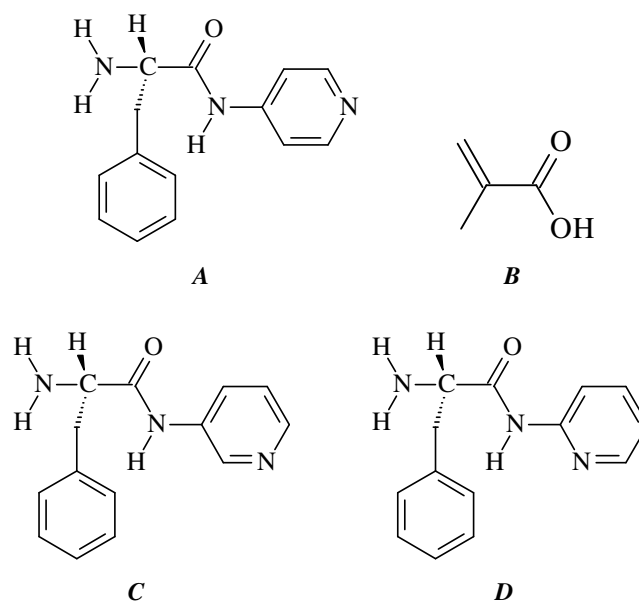


Figure 1.28. A; 4-L,-PheNHPy (template), B; methacrylic acid (functional monomer), C; 3-L,-PheNHPy (analogue) and D; 2-L,-PheNHPy(analogue) [214].

While numerous other examples of the use of imprinted polymers as stationary phases in liquid chromatography have been reported [102,215-218] the technique is not without its difficulties. Binding site heterogeneity and slow mass transfer leads to peak broadening [219], there is a risk of template leakage and the capacity of the polymers is often low. Traditionally MIPs were prepared in monolith format. As this inevitably results in irregular polymer particles that have polydisperse distributions, column packing can be irreproducible which results in poor column efficiency and high back pressures [220]. Molecular imprinting in bead format has been suggested to overcome these difficulties.

1.7.2.2. Thin Layer Chromatography

Polymers imprinted towards (-)-pseudoephedrine and (-)-norephedrine, using methacrylic acid or itaconic acid as the functional monomers, have been prepared for use as chiral stationary phases (CSPs) in thin layer chromatography (TLC) [221]. No enantiomeric resolution was observed for the (-)-pseudoephedrine polymer, itaconic

acid functional monomer, in the absence of acetic acid when acetonitrile was used as the mobile phase. This was in contrast to the same polymer prepared with methacrylic acid. The stronger retention displayed by itaconic acid was attributed to the two carboxyl groups available for binding, as opposed to only one for methacrylic acid. The imprinted polymers were also capable of separating chiral compounds of similar structure. Evidence of shape selectivity and the dependency of functional group spatial arrangement in the binding sites were demonstrated.

1.7.2.3. Capillary Electrophoresis and Capillary Electrochromatography

Electrophoresis is the migration of charged solutes in solvent under the influence of an electrical field. Nilsson *et. al.* [139] were the first to report the use of MIPs in capillary electrophoresis (CE) through the *in situ* imprinting of L-phenylalanine analide (L-PA), benzamidine (BAM) and pentamidine (PAM) directly in the capillaries that were used in the electrophoresis system. No enantiomeric separation was observed, which was ascribed to the low ratio of crosslinkers to monomers employed.

Lin *et. al.* [222] reported the first example of enantioseparation of a racemic mixture of L, D-phenylalanine analide using this technique. Resolution was examined as a function of polymer rigidity with optimum resolution occurring at 5:1 molar ratio of crosslinker: monomer.

A comprehensive review by Nilsson *et. al.* [223] describes in detail the techniques used for the formation of imprinted polymers for use in capillary electrophoresis and capillary electrochromatography (CEC), which include monolithic [224] and surface grafted [225]. Advantages of MIP-CEC include high selectivity, high resolution and fast analysis time [226]. The disadvantages are those associated with using MIPs in liquid chromatography and the preparation of suitable MIP columns can be more challenging than liquid chromatography equivalent applications [220]. None the less, a diverse range of molecules have been separated using this technique, including caffeine [227], amino acids [228], ephedrine [229] and propranolol [230].

1.7.3. Sensors

A chemical sensor is a device that recognises a specific target molecule in a complex matrix and generates an output signal, from a transducer, into a useful analytical signal. Hedborg *et. al.* [231] were the first to report the use of an L-phenylalanine analide molecularly imprinted polymer for use as a field sensor device. While the device displayed a regioselective effect, enantioselectivity was not achieved.

Since then there has been great interest in the generation of imprinted polymer sensor devices, and two principal types of MIP sensors have been developed; 1) affinity sensors and 2) receptor sensors [232]. In affinity sensors detection is based on the concentration of template bound to the MIP, which is immobilised on the surface of the detector. The second type of sensor is based on the ability of the MIP to change conformation upon binding with the template, leading to a change in a measurable property such as conductivity [233]. Alternatively, the sensor measures the ability of the functional monomer to change upon interaction with the template species. Examples of template species detected by MIP sensors include- atrazine [234], caffeine [235], cholesterol [236], carboxylic acids [237], 2,4-dichlorophenoxyacetic acid [238], sorbitol [239] and polyaromatic hydrocarbons (PAHs) [240].

Advantages of using MIPs as sensors include their high specificity and stability, which makes them promising alternatives to enzymes, antibodies and natural receptors used in sensor technology [232]. Some of the associated difficulties include integration of polymer with the transducer and difficulty in transforming the binding event into an electrical signal. A highly reproducible film is a requisite for application.

1.7.4. Drug delivery

The ability of MIPs to retain the template molecule with high affinity has led to their application as excipients for sustained drug delivery [241]. Allender *et. al.* [242] prepared an imprinted polymer for propranolol for use as a transdermal patch. Drug diffusion studies showed that the MIPs released the drug at a substantially lower rate than a non-imprinted counterpart. The lower diffusion from the MIP provided evidence

of how the specific binding could be used to control the drug release. Imprinted hydrogels have also been used for the ophthalmic delivery of timolol from soft contact lenses. Again, the imprinted polymers were found to have superior control of drug release relative to the NIPs [243].

The advantages of using MIPs as controlled drug release mechanisms have been identified. It has to be taken into account that the adaptability of molecular imprinting technology for drug delivery also requires the consideration of safety and toxicological concerns. The device is going to enter into contact with sensitive tissues; therefore, it should not be toxic, neither should its components, residual monomers, impurities or possible products of degradation [244].

1.7.5. Other uses of imprinted polymers

Other areas in which molecularly imprinted polymers have found use are listed as follows:

- Catalysis [17,245,246],
- By-product removal [247],
- Ligand-binding assays [248,249] and
- Metal ion separation [250].

While some of the areas mentioned may only be developed on a small, research scale, it is inevitable that in time, and with further optimisation, imprinted polymers will eventually play an integral role in the commercial chemical, pharmaceutical and analytical industries.

1.8. Photosensitive polymers

The functionality of polymers allow them to undergo various chemical reactions with chromophores to introduce photosensitivity to the polymers. The scope of application for these polymers is greatly widened as a result of chemical modification. Photosensitive polymers have found extensive use in photoimaging techniques such as

photography, printing and microlithography [251]. They have also found use in photofabricated products such as circuit boards and microelectronic chips [252].

Photosensitive polymers are mainly associated with the printing industry. However, photofabricated products are manufactured using the same concept of image transfer using a photoresist [251]. If a solution of photosensitive polymer is coated onto a substrate and exposed to radiation of an appropriate wavelength the physical properties of the polymer, namely solubility, are changed. The solubility change of a polymer in a solvent is as a result of irradiation through a pattern with transparent and opaque regions, which exposes certain areas of the polymer while masking others. The solvent is then used as a developer to wash away un-reacted polymer. Resists can work by a negative or positive mode of action. A schematic representation of negative and positive resists is shown, Figure 1.29. The radiation sources are generally electron beam, visible and UV light [253].

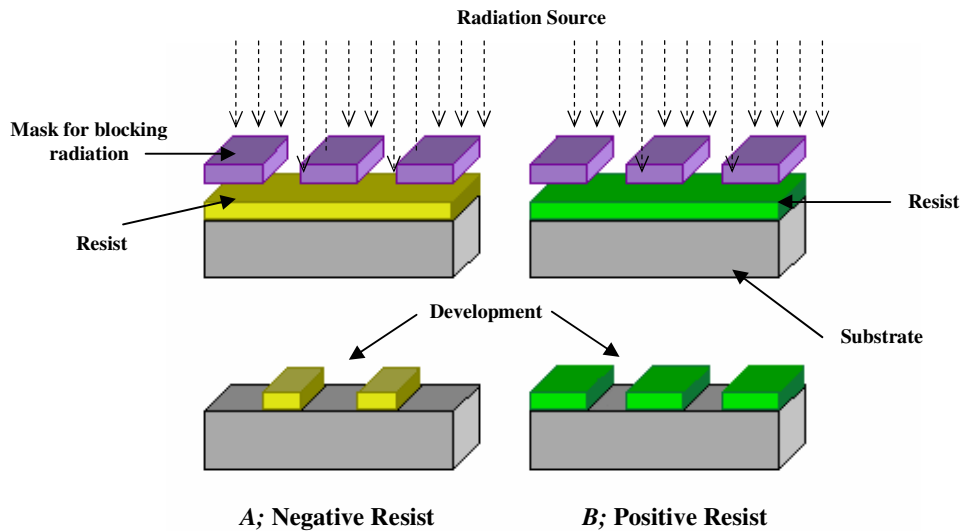


Figure 1.29. Schematic representation of A; negative resist and B; positive resist.

In negative resists, crosslinking occurs due to exposure to the radiation source, thus rendering the material less soluble in the developing solvent. The unexposed areas are un-crosslinked and are therefore washed away by the developer. In positive resists the exposure brings about an enhancement in solubility and it is the irradiated areas that are removed by the developer [251].

Negative resists result in insolubilisation through crosslink formation by a cycloaddition reaction *e.g.* α , β -unsaturated carbonyl groups, such as the cinnamoyl group [254-256] (Figure 1.30.), or through photoinitiated chain growth polymerisation [257] to name but two examples.

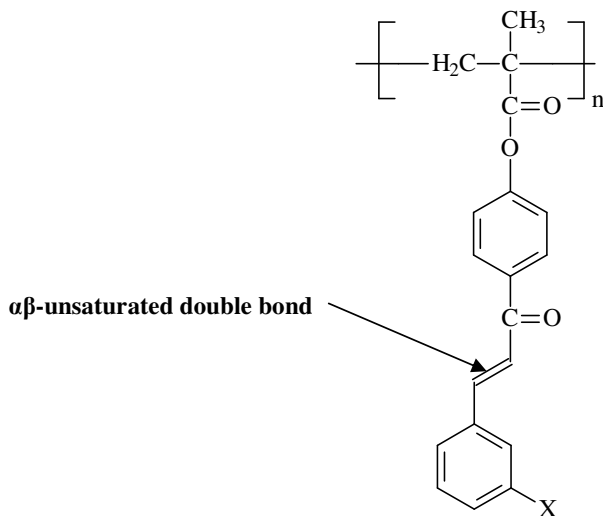


Figure 1.30. Negative working photoresist. The α,β -unsaturated double bond of the cinnamoyl group can undergo a photochemical [2+2]-cycloaddition reaction [255].

An example of a positive resist is the photochemical transformation of diazonaphthoquinones into indene carboxylic acids, Figure 1.31. The change in functionality as a result of the reaction increases the solubility of the exposed areas in the solvent used for development [258].

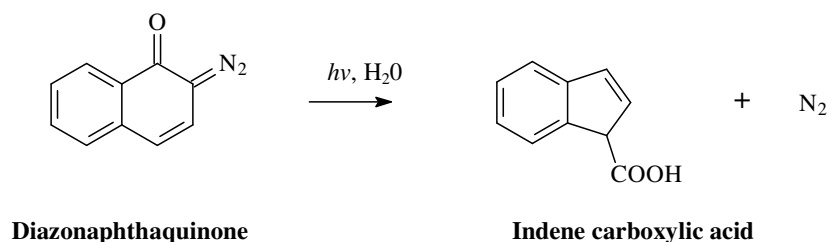


Figure 1.32. Positive working photoresist, photochemical transformation of diazonaphthoquinone to indene carboxylic acid [258].

Sensitizers can be added to the polymer mixture to speed up the rate of the photochemical reaction, or by increasing the photosensitivity. The sensitizer must be judiciously chosen so to match the spectral output of the radiation source. The

efficiency of energy transfer from sensitizer to the chromophore on the polymer can be maximised by adjustment of the concentration of sensitizer. The sensitizer must also be compatible with the polymer [251].

1.9. Poly(vinyl alcohol)

Poly(vinyl alcohol), PVA, is a water-soluble polyhydroxy resin. PVA is not synthesised from its monomer vinyl alcohol, as the monomer cannot be isolated because it tautomerises to acetaldehyde [259]. It is instead synthesised from vinyl acetate, which is polymerised, *via* free radical initiation, to form poly(vinyl acetate) (PVOAc). This polymer is then subjected to an alcoholysis reaction, typically in the presence of a base catalyst, to yield poly(vinyl alcohol) (Figure 1.33.)

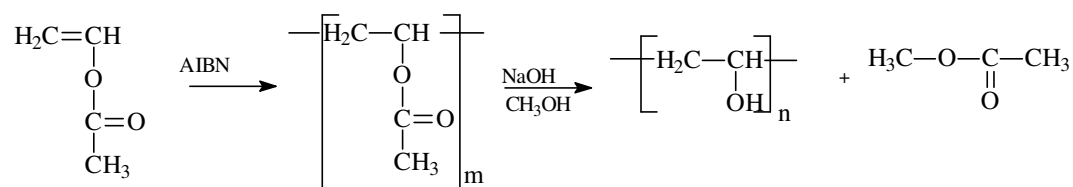


Figure 1.33. Preparation of PVA through the alcoholysis of PVOAc [260].

The hydrolysis reaction does not go to completion, and therefore PVA with varying degrees of hydrolysis are obtained. The grades are classified into partially hydrolysed, which contains 87-89 % hydroxyl groups, and fully hydrolysed which contains 98% hydroxyl groups, Figure 1.34.

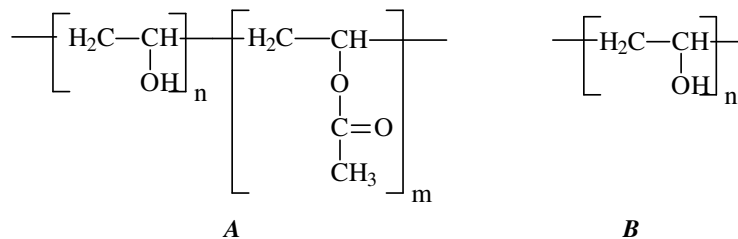


Figure 1.34. A; partially hydrolysed PVA and B; fully hydrolysed PVA.

1.9.1. Properties of poly(vinyl alcohol)

The physical properties of PVA are very much dependant on the degree of hydrolysis and the molecular weight of PVA [260]. Figure 1.35. shows that properties such as solubility, flexibility, viscosity and water resistance can be dictated by control of the degree of hydrolysis and molecular weight during the manufacture stage.

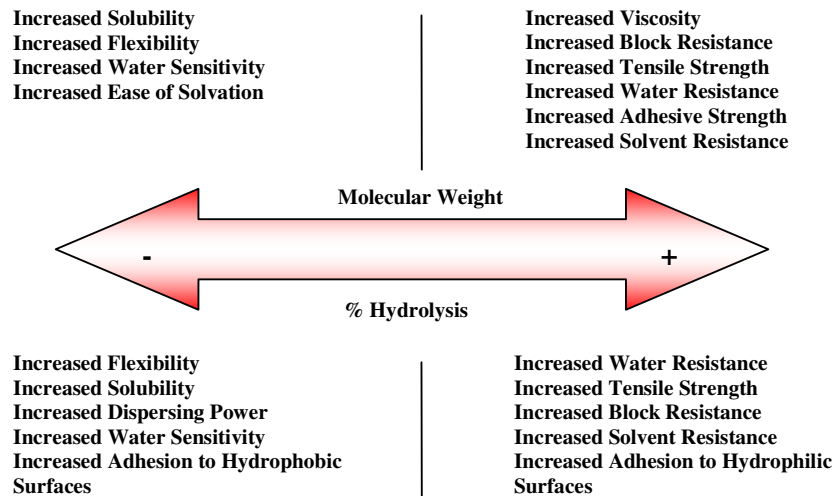


Figure 1.35. Properties of PVA (adapted from reference [261]).

PVA is not soluble in most common organic solvents *e.g.* methanol, benzene and acetone [260] and so water (and dimethyl sulphoxide) is the only practical solvent in which it is soluble. The ease of dissolution of PVA in water is dependant on its degree of hydrolysis. The hydroxyl groups on the PVA backbone can interact to form inter- or intramolecular hydrogen bonds, which impedes its solubility in water. The presence of residual hydrophobic acetate groups, found in partially hydrolysed PVA, weaken the hydrogen bonding interactions, thus increasing its water solubility. The dissolution of fully hydrolysed PVA into water requires the addition of heat (temperature of greater than 80 °C [262]) to the system to overcome the hydrogen bonding interactions. Partially hydrolysed grades can be dissolved at room temperature.

The viscosity of aqueous solutions of PVA is controlled by molecular weight and concentration. When preparing a solution of PVA the viscosity increases as the amount of PVA is added; gelation is eventually observed. Viscosity rather than solubility limits

the concentration of solutions. As the molecular weight of a polymer increases the solution viscosity of that polymer also increases. This is because the large molecular weight molecules swell, aggregate and intertwine with one another, which subsequently interferes with the flow of the solution [262]. The concentration limits for low, medium and high molecular weight PVA are approximately 30 wt %, 20 wt % and 15 wt %, respectively [260].

The hydroxyl groups pendant to the PVA backbone can undergo a number of chemical reactions to introduce different functionality to the PVA. One such reaction is an acid catalysed acetalisation reaction with aromatic or aliphatic aldehydes to form a six membered acetal ring. The acetal ring can form intramolecularly through adjacent hydroxyl groups on the 1,3-glycol unit, as shown in Figure 1.36 (A). There is also the possibility of intermolecular acetal formation through the hydroxyl groups of neighbouring molecules, 1.36 (B).

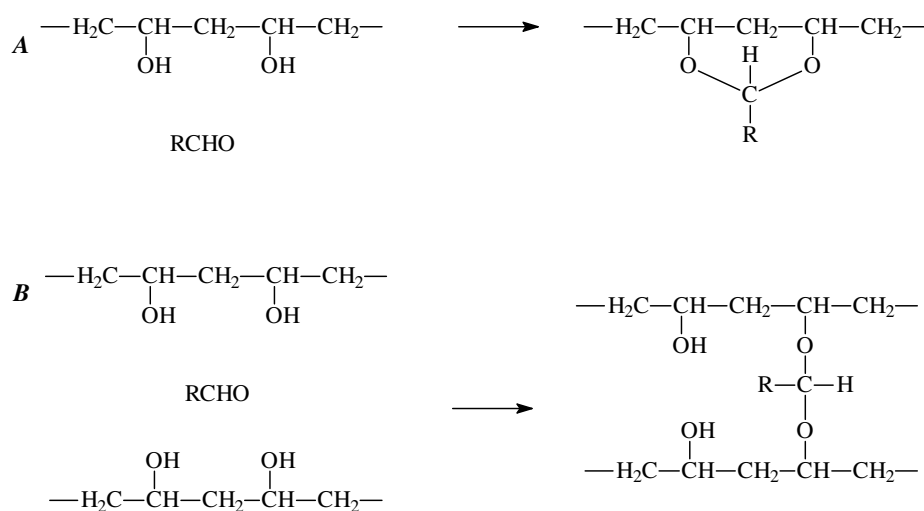


Figure 1.36. A; Intramolecular acetal formation and B; Intermolecular acetal formation [262].

It has been shown that the degree of acetalisation achieved is less than 100 % because of the presence of residual acetate groups and residual 1,2-glycol (1-2 %) units [263]. 1,2-glycol units are formed from head to head linkages of the propagating units during the polymerisation of vinyl acetate.

1.10. Photosensitive poly(vinyl alcohol)

PVA can be modified with a number of chromophores to render it photosensitive upon exposure to UV/ VIS light of an appropriate wavelength. Typical chromophores with which PVA has been derivatized with include:

- Cinnamate compounds *e.g.* reaction with cinnamoyl chloride to give polyvinyl cinnamate [264],
- Styrylpyridinium compounds [265],
- Conjugated heterocyclic compounds *e.g.* furan or thiophene compounds [266].

Poly(vinyl alcohol) can be esterified with cinnamate compounds to give the structure shown in Figure 1.37. This cinnamoylated PVA can undergo a [2+2]-cycloaddition reaction when it is irradiated with UV light of an appropriate wavelength, which renders the highly water soluble PVA less soluble. The reaction results in the formation of a substituted cyclobutane ring of the truxillic ester type [267]. The cinnamoyl groups can be appended to the PVA backbone *via* a simple esterification reaction, for example by reaction with cinnamoyl chloride [268,269].

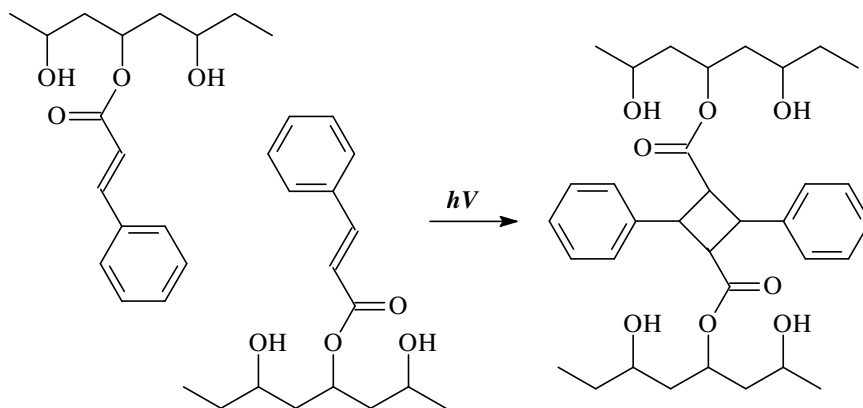


Figure 1.37. Photoinduced bimolecular crosslinking reaction of poly(vinyl cinnamate).

The cycloaddition reaction of the cinnamoyl groups [270] into a head to tail geometry, as shown in Figure 1.37, is proposed to form the pathway to the cycloaddition reaction. Reiser *et al.* [271] increased the sensitivity of poly(vinyl cinnamates) by using a mixture of electron donating and accepting substituents on the cinnamate groups. The increased

sensitivity, which was expressed in terms of the quantum yield of intermolecular crosslink formation, was shown to be directly proportional to the energy of electron donor-acceptor interaction, as measured by the difference in the Hammett σ -constants of the substituents. The increased sensitivity was attributed to increased reactant pre-ordering. This type of photosensitive system has found extensive use as negative resists [272].

The preparation of polyvinyl alcohol substituted with styrylpyridinium methosulphate salts, which are often abbreviated to SbQ (stilbazole (Sb) quaternized (Q)[273]), was first reported in 1980 [265]. Films of PVA when modified with styrylpyridinium salts, in particular 1-methyl-4-formylphenyl methosulphate (4-SbQ) (Figure 1.38), exhibit extremely high levels of photosensitivity and undergo a [2+2]-cycloaddition, even though the content of chromophore anchored to the polymer backbone is very low [265]. It has been suggested by Ichimura [274] that the remarkable photosensitivity of this type of polymeric system is due to the association or aggregation of the chromophores in the polymeric matrix leading to the enhanced photodimerization of the groups. When 4-SbQ is appended to PVA in an aqueous solution, at approximately 2 mole % 4-SbQ concentration, or the critical mole %, gelation of the solution occurs. This increase in viscosity is attributed to the association of the styrylpyridinium groups, causing the linear polymeric chains to interact, thereby increasing the viscosity [275].

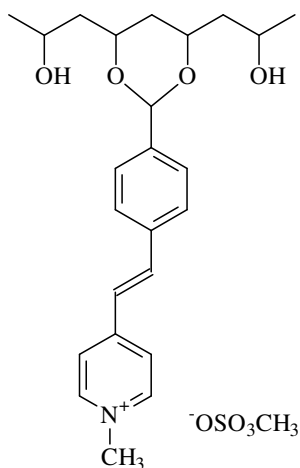


Figure 1.38. Poly(vinyl alcohol) modified with 4-SbQ [275-278].

A further investigation by Davidson *et. al.* [279] demonstrated a high degree of association of the styrylpyridinium groups in PVA-SbQ films, thus forming styrylpyridinium salt excimers, indicated by fluorescence emission bands. When the films were further irradiated, the emission bands reduced in intensity. It was thus concluded that the cycloaddition reaction occurs *via* an excimer intermediate.

PVA-SbQ systems have also found use as negative photoresists. The system affords more advantages over PVA modified with cinnamates or furan chromophores. One of the characteristic properties of PVA is its solubility in water. When PVA is subjected to an acetalisation reaction with styrylpyridinium groups, a remarkable level of photosensitivity is introduced, although the content of appended chromophore is very low [265]. Given that the bulk properties of PVA remain relatively unchanged when modified with such chromophores water is deemed the most appropriate solvent for use because of its availability, low cost and environment friendly nature.

2,5-furylene vinylene has also been appended to PVA to introduce photosensitivity (Figure 1.39.), with crosslinking occurring *via* a [2+2]-cycloaddition reaction [266]. The chromophore contains an aldehyde group which renders it suitable for reaction with the hydroxyl groups of PVA.

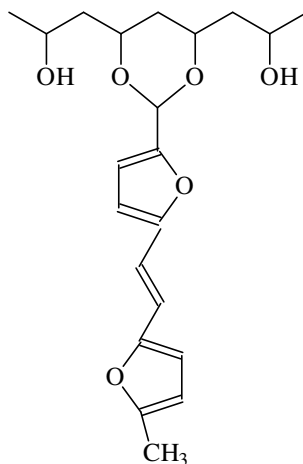


Figure 1.39. Poly(vinyl alcohol) modified with 2,5-furylene vinylene [266].

When cast as a film, the crosslinking reaction was followed *via* UV spectroscopy. Performance as a negative resist was comparable to commercial counterparts [280].

1.11. The potential for modified poly(vinyl alcohol) for use as MIPs

Due to its functionality PVA is amenable to numerous chemical reactions which alter its properties, thus broadening its subsequent use. For example, the styrylpyridinium salts mentioned above have been used as a biosensor for the detection of choline oxidase [281]. PVA hydrogels have also been used as drug delivery systems. Morimoto et. al. have used the hydrogels for the transrectal delivery of a drug used in the treatment of hypertension [282].

Modified PVA has been identified as a suitable candidate for use as imprinted polymeric media. Due to the highly specific nature of imprinted polymers, merging MIT (molecular imprinting technology) with modified PVA could potentially render the applications mentioned above more efficient.

Other advantages of modified PVA include;

- Excellent and reproducible film characteristics,
- Control over the extent of modification,
- Control over the extent of crosslinking and
- Not necessary for the crosslinking to occur in an inert atmosphere.

1.12 Research aims

- To synthesise a novel series of molecularly imprinted polymers selective to 2-aminopyridine by varying the amount of crosslinking monomer and the nature of the functional monomer employed.
- To carry out a detailed examination of the physical parameters of the polymers pertaining from the different polymer compositions.
- Investigation into the affinity and selectivity of the imprinted polymers and determination of the relationship of polymer response to the chemical properties of the binding analyte.
- To determine the sensitivity of polymer binding to the local chemical environment.
- To identify correlations in relation to polymer performance with the physical characteristics of the polymers.
- To carry out a novel and comprehensive examination of the binding characteristics of a poly(MAA-co-EGDMA) imprint system using binding isotherms and affinity distribution spectra, and to identify the most suitable isotherm for characterisation.
- To investigate the sensitivity of a novel thermal desorption GC-MS methodology for the characterisation of molecularly imprinted polymers, in terms of both bleed composition analysis and in affinity assessment, based on compositional changes.
- To validate the thermal desorption technique by identifying correlations with the results obtained from the physical analysis of the polymers and from the solution phase binding analysis.
- To carry out a preliminary investigation into the use of modified polyvinyl alcohol as a molecular imprinting strategy.

References

1. R. J. Young and P. A. Lovell, *Introduction to Polymer Science*, 2nd edition (Chapman and Hall, Cambridge, 1991).
2. P. Y. Bruice, *Organic Chemistry*, 3rd edition (Prentice Hall, 2001).
3. J. M. G. Cowie, *Polymers: Chemistry And Physics Of Modern Materials*, 1st edition (International textbook company limited, 1973).
4. H. Hart, D. J. Hart, and L. E. Craine, *Organic Chemistry A Short Course*, 9th edition (Houghton Mifflin Company, 1995).
5. M.P.Stevens and M.Alger, *Polymer Chemistry: An Introduction*, 2nd edition (Oxford University Inc., New York, 1990).
6. P. K. Owens, L. Karlson, E. S. M. Lutz, and L. I. Andersson, *Trends in Analytical Chemistry* **18**, 146-154 (1999).
7. M. Komiyama, T. Takeuchi, T. Mukawa, and H. Asanuma, *Molecular Imprinting: from fundamentals to applications*, (Wiley Inter Science, 2003).
8. H. Arnold and S. Vidyasankar, *Current Opinion in Biotechnology* **6**, 218-224 (1995).
9. L. Ye and K. Haupt, *Analytical and Bioanalytical Chemistry* **378**, 1887-1897 (2004).
10. C. He, Y. Long, J. Pan, K. Li, and F. Liu, *Journal of Biochemistry and Biophysics Methods* **70**, 133-150 (2007).
11. B. Sellergren and C. J. Allender, *Advanced Drug Delivery Reviews* **57**, 1733-1741 (2005).
12. L. Pauling , *Journal of the american chemical society* **62**, 2643-2657 (1940).
13. F. H. Dickey, *Proceedings of the National Academy of Sciences of the United States of America* **35**, 227-229 (1949).
14. H. S. Andersson and I. A. Nicholls, "A historical perspective of the development of molecular imprinting.," *Molecularly imprinted polymers: man-made mimics of antibodies and their applications in analytical chemistry*, B. Sellergren, ed., (Elsevier, Amsterdam, 2001), 1-19.
15. R. Curti and U. Colombo, *Journal of the American Chemical Society* **74**, 3961 (1952).
16. G. Wulff and A. Sarahan, *Angewandte Chemie-International Edition In English* **11**, 341 (1972).
17. C. Alexander, L. Davidson, and W. Hayes, *Tetrahedron* **59**, 2025-2057 (2003).

18. www.miptechnologies.com, (2008).
19. C. Berggren, A. Blomgren, A. Holmberg, F. Larsson, B. Sellergren, and K. Ensing, *Journal of Chromatography A* **975**, 157-164 (2002).
20. C. Widstrand, F. Larsson, M. Fiori, C. Civitareale, S. Mirante, and G. Brambilla, *Journal of Chromatography B* **804**, 85-92 (2004).
21. P. R. Kootstra, C. J. P. F. Kuijpers, K. L. Wubs, D. van Doorn, S. S. Sterk, L. A. van Ginkel, and R. W. Stephany, *Analytica Chimica Acta* **529**, 75-81 (2005).
22. N. Van Hoof, D. Courtheyn, J. P. Antignac, M. Van de Wiele, S. Poelmans, H. Noppe, and H. De Brabander, *Rapid Communications in Mass Spectrometry* **19**, 2801-2808 (2005).
23. M. Fiori, C. Civitareale, S. Mirante, E. Margo, and G. Brambilla, *Analytica Chimica Acta* **529**, 207-210 (2005).
24. Y. Xia, J. E. McGuffey, S. Bhattacharyya, B. Sellergren, E. Yilmaz, L. Wang, and J. T. Bernert, *Analytical Chemistry* **77**, 7639-7645 (2005).
25. B. Dirion, F. Lanza, B. Sellergren, C. Chassaing, R. Venn, and C. Berggren, *Chromatographia* **56**, 237-241 (2008).
26. C. Chassaing, J. Stokes, R. F. Venn, F. Lanza, A. Holmberg, and C. Berggren, *Journal of Chromatography B* **804**, 71-81 (2004).
27. G. Wulff, R. Vesper, R. Grobe-Einsler, and A. Sarhan, *Makromolekulare Chemie* **178**, 2799-2816 (1977).
28. G. Wulff and R. Vesper, *Journal of Chromatography* **167**, 171-186 (1978).
29. G. Wulff and S. Schauhoff, *Journal of Organic Chemistry* **56**, 395-400 (1991).
30. A. Kugimiya, J. Matsui, T. Takeuchi, K. Yano, H. Muguruma, A. V. Elgersma, and I. Karube, *Analytical Letters* **28**, 2317-2323 (1995).
31. N. Sallacan, M. Zaysts, T. Bourenko, A. B. Kharitonov, and I. Wullner, *Analytical Chemistry* **74**, 702-712 (2002).
32. K. J. Shea and T. K. Dougerty, *Journal of the American Chemical Society* **108**, 1091-1093 (1986).
33. K. J. Shea and E. A. Thompson, *Journal of Organic Chemistry* **43**, 4253-4255 (1978).
34. G. Wulff, B. Heide, and G. Helimer, *Journal of the American Chemical Society* **108**, 1089-1091 (1986).
35. K. Mosbach and R. Arshady, *Makromolekulare Chemie* **182**, 687-692 (1981).

36. J. Svenson, H. S. Andersson, S. A. Piletsky, and I. A. Nicholls, *Journal of Molecular Recognition* **11**, 83-86 (1998).
37. H. S. Andersson and I. A. Nicholls, *Bioorganic Chemistry* **25**, 203-211 (1997).
38. J. G. Karlsson, H. S. Andersson, B. Karlsson, and I. A. Nicholls, *Analyst* **129**, 456-462 (2004).
39. Q. Osmani, H. Hughes, K. Flavin, J. Hedin-Dahlstrom, C. J. Allender, J. Frisby, and P. McLoughlin, *Analytical and Bioanalytical Chemistry* **391**, 1229-1236 (2008).
40. C. Y. Hsu, H. Y. Lin, J. L. Thomes, and T. C. Chou, *Nanotechnology* **17**, S77-S83 (2006).
41. D. Spivak, "Selectivity in molecularly imprinted polymers," *Molecularly imprinted materials: science and technology*, Y. A. Ramstrom, ed., (Marcel Dekker, New York, 2005), 395-417.
42. A. Zander, P. Findlay, T. Renner, and B. Sellergren, *Analytical Chemistry* **70**, 3304-3314 (1998).
43. B. Sellergren and K. J. Shea, *Journal of Chromatography A* **690**, 29-39 (1995).
44. I. I. Umpleby, S. C. Baxter, A. M. Rampey, G. T. Rushton, Y. Chen, and K. D. Shimizu, *Journal of Chromatography B* **804**, 141-149 (2004).
45. G. Wulff and R. Schonfeld, *Advanced Materials* **10**, 957-959 (1998).
46. G. Wulff and K. Knorr, *Bioseparation* **10**, 257-276 (2002).
47. C. Lubke, M. Lubke, M. Whitcombe, and E. N. Vulfson, *Macromolecules* **33**, 5098-5105 (2000).
48. B. Sellergren and L. Andersson, *Journal of Organic Chemistry* **55**, 3381-3383 (1990).
49. M. Whitcombe, M. E. Rodriguez, E. N. Vulfson, and P. Villar, *Journal of the American Chemical Society* **117**, 7105-7111 (1995).
50. A. G. Mayes and M. J. Whitcombe, *Advanced Drug Delivery Reviews* **57**, 1742-1778 (2005).
51. C. Cacho, E. Turiel, A. Martin-Esteban, D. Ayala, and C. Perez-Conde, *Journal of Chromatography A* **1114**, 255-262 (2006).
52. M. Whitcombe, E. N. Vulfson, and M. Lubke, *Journal of the American Chemical Society* **120**, 13342-13348 (1998).
53. N. Kirsch, C. Alexander, S. Davies, and M. J. Whitcombe, *Analytica Chimica Acta* **504**, 63-71 (2004).

54. P. A. G. Cormack and A. Z. Elorza, *Journal of Chromatography B* **804**, 173-182 (2004).
55. B. Sellergren, *Trends in Analytical Chemistry* **18**, 164-174 (1999).
56. G. Wulff, *Angewandte Chemie- International Edition in English* **34**, 1812-1832 (1995).
57. W. Cummins, P. Duggan, and P. McLoughlin, *Biosensors and Bioelectronics* **22**, 372-380 (2006).
58. T. Zhang, F. Liu, W. Chen, J. Wang, and L. Kean, *Analytica Chimica Acta* **450**, 53-61 (2001).
59. F. Lanza, M. Ruther, A. J. Hall, C. Dauwe, and B. Sellergren, *Materials Research Society Symposium Proceedings* **723**, (2002).
60. B. Sellergren, M. Lepisto, and K. Mosbach, *Journal of the American Chemical Society* **110**, 5358-5384 (1988).
61. D. O'Shannessy, L. I. Andersson, and K. Mosbach, *Journal of Molecular Recognition* **2**, 1-5 (1981).
62. Z. Zhang, H. Liao, H. Li, L. Nie, and S. Yao, *Analytical Biochemistry* **336**, 108-116 (2005).
63. J. P. Lai, X. F. Cao, X. L. Wang, and X. W. He, *Analytical and Bioanalytical Chemistry* **372**, 391-396 (2002).
64. J. Cederfur, Y. Pei, M. Zihui, and M. Kemp, *Journal of Combinatorial Chemistry* **4**, 67-72 (2003).
65. Z. Xu, D. Kuang, L. Liu, and Q. Deng, *Journal of Pharmaceutical and Biomedical Analysis* **45**, 54-61 (2007).
66. H. Sanbe and J. Haginaka, *Analyst* **128**, 593-597 (2003).
67. L. Ozcan and Y. Sahin, *Sensors and Actuators B: Chemical* **127**, 362-369 (2007).
68. K. Farrington and F. Regan, *Biosensors and Bioelectronics* **22**, 1138-1146 (2007).
69. E. V. Piletska, M. Romero-Guerra, A. R. Guerreiro, K. Karim, A. P. F. Turner, and S. A. Piletsky, *Analytica Chimica Acta* **542**, 47-51 (2005).
70. K. Haupt, *Acs Symposium Series* **703**, 135-142 (1998).
71. J. Hantash, A. Bartlett, P. Oldfield, G. Denes, R. O'Rielly, and F. David, *Analytical and Bioanalytical Chemistry* **387**, 351-357 (2007).
72. F. G. Tamayo, J. L. Casillas, and A. Martin-Esteban, *Analytical and Bioanalytical Chemistry* **381**, 1234-1240 (2005).

73. C. Baggiani, G. Giraudi, F. Trotta, C. Giovannoli, and A. Vanni, *Talanta* **51**, 71-75 (2000).
74. K. Sreenivasan, *Journal of Applied Polymer Science* **68**, 1863-1866 (1998).
75. X. C. Lui and J. S. Dordick, *Journal of Polymer Science: Part A Polymer Chemistry* **37**, 1665-1671 (1999).
76. A. Rachkov and N. Minoura, *Journal of Chromatography A* **889**, 111-118 (2000).
77. D. S. Janiak and P. Kofinas, *Analytical and Bioanalytical Chemistry* **389**, 399-404 (2007).
78. M. M. Titirici, A. J. Hall, and B. Sellergren, *Chemical Matters* **14**, 21-23 (2002).
79. J. Damen and D. C. Neckers, *Tetrahedron Letters* **21**, 1913-1916 (1980).
80. G. Wulff, W. Best, and A. Akelah, *Reactive Polymers* **2**, 167-174 (1984).
81. M. Davies, V. De Biasi, and D. Perrett, *Analytica Chimica Acta* **504**, 7-14 (2004).
82. D. A. Spivak, *Advanced Drug Delivery Reviews* **57**, 1779-1794 (2005).
83. H. S. Andersson, J. G. Karlsson, S. A. Piletsky, A. C. Koch-Schmidt, K. Mosbach, and I. A. Nicholls, *Journal of Chromatography A* **848**, 39-49 (1999).
84. E. Yilmaz, K. Mosbach, and K. Haupt, *Analytical Communications* **36**, 167-170 (1999).
85. M. Kempe, L. Fischer, and K. Mosbach, *Journal of Molecular Recognition* **6**, 25-29 (1993).
86. O. Ramstrom, L. I. Andersson, and K. Mosbach, *Journal of Organic Chemistry* **58**, 7562-7564 (1993).
87. J. Matsui, O. Doblhoff-Dier, and T. Takeuchi, *Analytica Chimica Acta* **343**, 1-4 (1997).
88. M. Kempe and K. Mosbach, *Journal of Chromatography A* **664**, 276-279 (1994).
89. S. A. Piletsky, E. V. Piletskaya, K. Yano, A. Kugimiya, A. V. Elgersma, R. Levi, U. Kahlow, T. Takeuchi, and I. Karube, *Analytical Letters* **29**, 157-170 (1996).
90. O. Ramstrom and C. Yu, *Analytical Letters* **30**, 2123-2140 (1997).
91. M. Yoshikawa, J. Izumi, and T. Kitao, *Reactive and Functional Polymers* **42**, 93-102 (1999).
92. L.I. Andersson and K. Mosbach, *Journal of Chromatography* **516**, 313-322 (1990).

93. C. Alexander, H. S. Andersson, L. I. Andersson, R. J. Ansell, N. Kirsch, I. A. Nicholls, J. O. O'Mahony, and M. J. Whitcombe, *Journal of Molecular Recognition* **19**, 106-180 (2006).
94. H. Kim and D. A. Spivak, *Journal of the American Chemical Society* **125**, 11269-11275 (2003).
95. M. Whitcombe, L. Martin, and E. N. Vulfson, *Chromatographia* **47**, 457-464 (1998).
96. J. Svenson, J. G. Karlsson, and I. A. Nicholls, *Journal of Chromatography A* **1024**, 39-44 (2004).
97. J. Matsui, T. Takeuchi, and Y. Miyoshi, *Chemistry Letters* 1007-1008 (1995).
98. K. Karim, F. Breton, R. Rouillon, E. V. Piletska, A. Guerreiro, I. Chianella, and S. A. Piletsky, *Advanced Drug Delivery Reviews* **57**, 1795-1808 (2005).
99. G. Wulff, R. Kemmerer, J. Viatmeier, and H.-G. Poll, *Nouveau Journal De Chimie* **6**, 681-687 (1982).
100. B. Sellergren, *Makromolekular Chemistry* **190**, 2703-2711 (1989).
101. M. Kempe and K. Mosbach, *Tetrahedron Letters* **36**, 3563-3566 (1995).
102. M. Kempe, *Analytical Chemistry*. **68**, 1948-1953 (1996).
103. D. A. Spivak and M. Sibrian-Vazquez, *Journal of the American Chemical Society* **126**, 7827-7833 (2004).
104. O. Ramstrom, "Synthesis and selection of functional and structural monomers," *Molecularly imprinted materials: science and technology*, Y. A. Ramstrom, ed., (Marcel Dekker, New York, 2005), 181-224.
105. B. Sellergren and K. J. Shea, *Journal of Chromatography* **635**, 31-45 (1993).
106. R. J. Ansell and K. Mosbach, *Journal of Chromatography A* **787**, 55-66 (1997).
107. K. J. Shea, D. A. Spivak, and M. Gilmore, *Journal of the American Chemical Society* **119**, 4388-4392 (1997).
108. K. Yoshizako, K. Hosoya, Y. Iwakoshi, K. Kimata, and N. Tanaka, *Analytical Chemistry*. **70**, 386-389 (1998).
109. G. Wulff, H.-G. Poll, and M. Minarik, *Journal of Liquid Chromatography* **9**, 385-405 (1986).
110. I. Nicholls, K. Adbo, H. S. Andersson, P. O. Andersson, J. Ankarloo, J. Hedin-Dahlstrom, P. Jokela, J. G. Karlsson, L. Olofsson, and J. Rosengren, *Analytica Chimica Acta* **435**, 9-18 (2001).
111. B. Sellergren, *Chirality* **1**, 63-68 (1989).

112. D. O'Shannessy, B. Ekberg, and K. Mosbach, *Analytical Biochemistry* **177**, 144-149 (1989).
113. S. A. Piletsky, E. V. Piletska, K. Karim, K. Freebarin, C. Legge, and A. P. F. Turner, *Macromolecules* **35**, 7499-7504 (2002).
114. Y. Lu, C. Li, X. Wang, P. Sun, and X. Xing, *Journal of Chromatography B* **804**, 53-59 (2004).
115. G. Wulff and J. Haarer, *Makromolekular Chemistry* **192**, 1329-1338 (1991).
116. A. Patel, S. Fouace, and J. H. G. Steinke, *Analytica Chimica Acta* **504**, 53-62 (2004).
117. L. Piscopo, C. Prandi, M. Coppa, K. Sparnacci, M. Laus, A. Lagana, R. Curini, and G. D' Asconzo, *Macromolecular Chemistry and Physics* **203**, 1532-1538 (2002).
118. W. Chen, F. Liu, X. Zhang, K. A. Li, and S. Tong, *Talanta* **55**, 29-34 (2001).
119. Q. Fu, N. Zheng, Z. Y. Li, W. B. Chang, and Z. M. Wang, *Journal of Molecular Recognition* **14**, 151-156 (2001).
120. M. Knutsson, H. S. Andersson, and I. A. Nicholls, *Journal of Molecular Recognition* **2**, 87-90 (1998).
121. S. A. Piletsky, E. V. Piletska, K. Karim, C. Legge, A. P. F. Turner, and G. Foster, *Analytica Chimica Acta* **504**, 123-130 (2004).
122. C. J. Allender, K. R. Brian, and C. M. Heard, *Chirality* **9**, 233-237 (1997).
123. A. Ersoz, A. Denizli, I. Sener, A. Atilir, S. Diltemiz, and R. I. Say, *Separation and Purification Technology* **38**, 173-179 (2004).
124. K. Sreenivasan, *Polymer International* **42**, 172 (1997).
125. K. Sreenivasan, *Polymer Gels and Networks* **5**, 17-22 (1997).
126. S. S. Milojkovic, D. Kostoski, J. J. Comor, and J. M. Nedeljkovic, *Polymer* **38**, 2853-2855 (1997).
127. G. Moad and D. H. Solomon, *The chemistry of free radical polymerization.*, 1st edition (Elsevier Science Ltd, Bath, 1995).
128. I. Mijangos, F. Navarro-Villoslada, A. Guerreiro, E. Piletska, I. Chianella, K. Karim, A. Turner, and S. Piletsky, *Biosensors and Bioelectronics* **22**, 381-387 (2006).
129. A. G. Mayes and K. Mosbach, *Trends in Analytical Chemistry* **16**, 321-332 (1997).

130. A. G. Mayes, "Polymerisation techniques for the formation of imprinted beads," *Molecularly imprinted polymers: man-made mimics of antibodies and their applications in analytical chemistry*, B. Sellergren, ed., (Elsevier, Amsterdam, 2001), 305-324.
131. L. Ye and E. Yilmaz, "Molecularly imprinted polymer beads," *Molecularly imprinted materials: science and technology*, O. Ramstrom and M. Yan, eds., (Marcel Dekker, New York, 2005), 435-454.
132. L. Ye, P. Cormack, and K. Mosbach, *Analytical Chemistry*. **36**, 35-38 (1999).
133. L. Ye, R. Weiss, and K. Mosbach, *Macromolecules* **33**, 8239-8245 (2000).
134. L. Ye, P. Cormack, and K. Mosbach, *Analytica Chimica Acta* **435**, 187-196 (2001).
135. I. Sugurin, L. Ye, E. Yilmaz, A. Dzgoev, B. Danielsson, K. Mosbach, and K. Haupt, *Analyst* **125**, 13-16 (2000).
136. C. Cacho, E. Turiel, A. Martin-Esteban, C. Preze-Conde, and C. Camara, *Journal of Chromatography B* **802**, 347-353 (2004).
137. F. Wang, P. Cormack, D. Sherrington, and E. Khoshdel, *Pure and Applied Chemistry* **79**, 1505-1519 (2007).
138. B. Sellergren, *Journal of Chromatography A* **673**, 133-141 (1994).
139. K. Nilsson, J. Lindell, O. Norrlov, and B. Sellergren, *Journal of Chromatography A* **680**, 57-61 (1994).
140. B. Sellergren, *Analytical Chemistry*. **66**, 1578-1582 (1994).
141. N. Perez-Moral and A. G. Mayes, *Analytica Chimica Acta* **504**, 15-21 (2004).
142. M. Kempe and H. Kempe, *Macromolecular Rapid Communications* **25**, 315-320 (2004).
143. Y. Li, Q. Fu, Q. Zhang, and L. He, *Analytical Sciences* **22**, 1355-1360 (2006).
144. N. Perez-Moral and A. G. Mayes, *Bioseparation* **10**, 287-299 (2002).
145. K. Hosoya, K. Yoshizako, N. Tanaka, K. Kimata, T. Araki, and J. Haginaka, *Chemistry Letters* 1437-1438 (1994).
146. K. Hosoya, K. Yoshizako, Y. Shirasu, K. Kimata, K. Araki, N. Tanaka, and J. Haginaka, *Journal of Chromatography A* **728**, 139-147 (1996).
147. H. Yan and K. H. Row, *International Journal of Molecular Science* **7**, 155-178 (2006).
148. M. Ulbricht, *Polymer* **47**, 2217-2262 (2006).

149. M. Ulbricht, *Journal of Chromatography B* **804**, 113-125 (2004).
150. M. Lehmann, H. Brunner, and G. E. M. Tovar, *Desalination* **149**, 315 (2002).
151. M. Ramamoorthy and M. Ulbricht, *Journal of Membrane Science* **217**, 207-214 (2003).
152. J. M. Hong, P. E. Anderson, J. Qian, and C. R. Martin, *Chemical Matters*. **10**, 1029-1033 (1998).
153. M. Ulbricht, "Molecularly imprinted polymer film and membranes," *Molecularly imprinted materials: science and technology*, Y. A. Ramstrom, ed., (Marcel Dekker, New York, 2005), 455-490.
154. M. Yoshikawa, T. Ooi, and J. Izumi, *Journal of Applied Polymer Science* **72**, 493-499 (1999).
155. L. Donato, A. Figoli, and E. Drioli, *Journal of Pharmaceutical and Biomedical Analysis* **37**, 1003-1008 (2005).
156. A. H. Wu and M. J. Syu, *Biosensors and Bioelectronics* **21**, 2345-2353 (2006).
157. L. Feng, Y. Liu, X. Zhou, and J. Hu, *Journal of Colloid and Interface Science* **84**, 378-382 (2005).
158. F. Lanza and B. Sellergren, *Macromolecular Rapid Communications* **25**, 59-68 (2004).
159. T. Takeuchi, D. Fukuma, and J. Matsui, *Analytical Chemistry* **71**, 285-290 (1999).
160. F. G. Tamayo, E. Turiel, and A. Martin-Esteban, *Journal of Chromatography A* **1152**, 32-40 (2007).
161. D. Batra and K. J. Shea, *Current Opinion in Chemical Biology* **7**, 434-442 (2003).
162. I. Chianella, M. Lotierzo, S. A. Piletsky, I. E. Tothill, B. Chen, K. Karim, and A. P. F. Turner, *Analytical Chemistry* **74**, 1288-1293 (2002).
163. K. Farrington, E. Magner, and F. Regan, *Analytica Chimica Acta* **566**, 60-68 (2006).
164. B. Sellergren and A. Hall, "Fundamental aspects of the synthesis and characterisation of imprinted network polymers," *Molecularly imprinted polymers. Man-made mimics of antibodies and their applications in analytical chemistry.*, B. Sellergren, ed., (Elsevier, Amsterdam, 2001), 21-55.
165. B. A. Rashid, R. S. Briggs, J. N. Hay, and D. Stevenson, *Analytical Communications* **34**, 303-305 (1997).
166. L. I. Andersson, *Analyst* **125**, 1515-1517 (2000).

167. K. D. Shimizu, "Binding Isotherms," *Molecularly Imprinted Materials: Science and technology*, Y. A. Ramstrom, ed., (Marcel Dekker, New York, 2005), 419-434.
168. G. T. Rushton, C. L. Karns, and K. D. Shimizu, *Analytica Chimica Acta* **528**, 107-113 (2005).
169. J. A. Garcia-Calzon and M. E. Diaz-Garcia, *Sensors and Actuators B: Chemical* **123**, 1180-1194 (2006).
170. R. J. Umpleby, S. C. Baxter, M. Bode, J. Berch Jr., R. Shah, and K. D. Shimizu, *Analytica Chimica Acta* **435**, 35-47 (2001).
171. A. M. Rampey, R. J. Umpleby II, G. T. Rushton, J. Iseman, R. Shah, and K. D. Shimizu, *Analytical Chemistry*. **76**, 1123-1133 (2004).
172. R. J. Umpleby, S. C. Baxter, Y. Chen, R. Shah, and K. D. Shimizu, *Analytical Chemistry*. **73**, 4584-4591 (2001).
173. E. Turiel, C. Preze-Conde, and A. Martin-Esteban, *Analyst*. **128**, 137-141 (2003).
174. E. Corton, J. A. Garcia-Calzon, and M. E. Diaz-Garcia, *Journal of Non-Crystalline Solids* **353**, 974-980 (2007).
175. K. D. Shimizu, "Post modification of imprinted polymers," *Molecularly imprinted materials: science and technology*, Y. A. Ramstrom, ed., (Marcel Dekker, New York, 2005), 329-345.
176. R. J. Umpleby, G. T. Rushton, R. N. Shah, A. M. Rampey, J. Bradshaw, J. Berch, and K. D. Shimizu, *Macromolecules* **34**, 8116-8152 (2001).
177. S. Lowell, J. Shields, M. Thomas, and M. Thommes, *Characterization of Porous Solids and Powders: Surface Area, Pore Size and Density.*, (Kluwer Academic Publishers., Dordrecht, The Netherlands., 2004).
178. D. Sherrington, *Chemical Communications* 2275-2286 (1998).
179. A. Guyot, "Synthesis and structure of polymer supports," *Synthesis and separations using functional monomers*, D. Sherrington and P. Hodge, eds., (Wiley and Sons, 1988), 1-42.
180. H. Lange, *Colloid and Polymer Science* **264**, 488-493 (1986).
181. V. A. Bershtein and V. M. Egorov, *Differential Scanning Calorimetry of polymers*, 1st Edition (Ellis Horwood, Chichester, 1994).
182. G. W. H. Hohne, W. F. Hemminger, and H.-J. Flammersheim, *Differential scanning calorimetry*, 2nd edition (Springer, Berlin, 2003).
183. S. R. Sandler, W. Koro, J.-A. Bonested, and E. M. Pearce, *Polymer Synthesis and Characterization. A laboratory manual*, (Academic Press, San- Diego, 1998).

184. A. Katz and M. E. Davis, *Nature* **403**, 286-289 (2000).
185. K. J. Shea and D. Sasaki, *Journal of the American Chemical Society* **113**, 4109-4120 (1991).
186. D. Sasaki and T. Alam, *Chemical Matters*. **12**, 1400-1407 (2000).
187. J. O. Mahony, K. Nolan, M. R. Smyth, and B. Mizaikoff, *Analytica Chimica Acta* **534**, 31-39 (2005).
188. L. I. Andersson, "Solid Phase Extraction on Molecularly Imprinted Polymers-Requirements, Advancements and Future Work," *Molecular Imprinting of Polymers*, 2004).
189. A. Bereczki, A. Tolokan, G. Horvai, V. Horvath, F. Lanza, A. Hall, and B. Sellergren, *Journal of Chromatography A* **930**, 31-38 (2001).
190. I. Ferrer, F. Lanza, A. Tolokan, V. Horvath, B. Sellergren, G. Horvai, and D. Barcelo, *Analytical Chemistry*. **72**, 3934-3941 (2000).
191. C. Baggiani, C. Giovannoli, L. Anfossi, and C. Tozzi, *Journal of Chromatography A* **938**, 35-44 (2001).
192. A. Molinelli, R. Weiss, and B. Mizaikoff, *Journal of Agric. Food Chem.* **50**, 1804-1808 (2002).
193. R. Koeber, C. Fleischer, F. Lanza, B. Sellergren, K.-S. Boos, and D. Barcelo, *Analytical Chemistry*. **73**, 2437-2444 (2001).
194. K.-S. Boos and C. Fleischer, *Fresenius Journal of Analytical Chemistry* **371**, 16-20 (2001).
195. J. Haginaka and H. Sanbe, *Analytical Chemistry*. **72**, 5206-5210 (2000).
196. M. L. Mena, L. Agui, P. Martinez-Ruiz, P. Yanez-Sedeno, A. J. Reviejo, and J. M. Pingarron, *Analytical and Bioanalytical Chemistry* **376**, 18-25 (2003).
197. S. N. Zhou, E. P. C. Lai, and J. D. Miller, *Analytical and Bioanalytical Chemistry* **378**, 1903-1906 (2004).
198. M. Pascale, A. De Girolamo, A. Visconti, N. Magan, I. Chianella, E. V. Piletska, and S. A. Piletsky, *Analytica Chimica Acta* **609**, 131-138 (2008).
199. T. Pap, G. Horvai, A. Tolokan, and B. Sellergren, *Journal of Chromatography A* **973**, 1-12 (2002).
200. E. Caro, R. M. Marce, F. Borrull, P. A. G. Cormack, and D. C. Sherrington, *TrAC Trends in Analytical Chemistry* **25**, 143-154 (2006).
201. L. I. Andersson, A. Paprica, and T. Arvidsson, *Chromatographia* **46**, 57-62 (1997).

202. A. Ersoz, R. I. Say, and A. Denizli, *Analytica Chimica Acta* **502**, 91-97 (2004).
203. A. Martin-Esteban, *Fresenius Journal of Analytical Chemistry* **370**, 795-802 (2001).
204. F. Qiao, H. Sun, H. Yan, and K. H. Row, *Chromatographia* **64**, 625-634 (2006).
205. B. Bjarnason, L. Chimuka, and O. Ramstrom, *Analytical Chemistry* **71**, 2152-2156 (1999).
206. M. Jiang, J. Zhang, S. Mei, Y. Shi, L. Zou, Y. Zhu, and B. Lu, *Journal of Chromatography A* **1110**, 27-34 (2006).
207. F. Pragst, *Analytical and Bioanalytical Chemistry* **388**, 1393-1414 (2007).
208. W. M. Mullett, P. Martin, and J. Pawliszyn, *Analytical Chemistry* **73**, 2383-2389 (2001).
209. E. H. M. Koster, C. Crescenzi, W. den Hoedt, K. Ensing, and G. J. de Jong, *Analytical Chemistry* **73**, 3140-3145 (2001).
210. X. Hu, H. Hu, and G. Li, *Analytical Letters* **40**, 645-660 (2007).
211. A. G. Mayes, L. I. Andersson, and K. Mosbach, *Analytical Biochemistry* **222**, 483-488 (1994).
212. J. L. Suarez-Rodriguez and M. E. Diaz-Garcia, *Biosensors and Bioelectronics* **16**, 955-961 (2001).
213. N. Zheng, Y. Z. Li, W. B. Chang, Z. M. Wang, and T. J. Li, *Analytica Chimica Acta* **452**, 277-283 (2002).
214. Y. Lu, C. Li, H. Zhang, and X. Liu, *Analytica Chimica Acta* **489**, 33-43 (2003).
215. C. Hwang and W. Lee, *Journal of Chromatography B* **765**, 45-53 (2001).
216. O. Ramstrom, I. A. Nicholls, and K. Mosbach, *Tetrahedron: Asymmetry* **5**, 649-656 (1994).
217. G. Wulff and M. Minarik, *Journal of Liquid Chromatography* **13**, 2987-3000 (1990).
218. L. Fischer, R. Muller, B. Ekberg, and K. Mosbach, *Journal of the American Chemical Society* **113**, 9358-9360 (1991).
219. T. O'Brien, N. Snow, N. Gringberg, and L. Crocker, *Journal of Liquid Chromatography and Related Technology* **22**, 283-304 (1999).
220. N. M. Maier and W. Lindner, *Analytical and Bioanalytical Chemistry* **389**, 377-397 (2007).

221. R. Suedee, C. Songkram, A. Petmoreekul, S. Sangkunakup, S. Sankasa, and N. Kongyarit, *Journal of Pharmaceutical and Biomedical Analysis* **19**, 519-527 (1999).
222. J. Lin, T. Nakagama, K. Uchiyama, and T. Hobo, *Chromatographia* **43**, 583-589 (1996).
223. J. Nilsson, P. Spegel, and S. Nilsson, *Journal of Chromatography B* **804**, 3-12 (2004).
224. Andersson L.I., L. Schweitz, and S. Nilsson, *Analytical Chemistry*. **69**, 1179-1183 (1997).
225. O. Bruggemann, R. Freitag, M. Whitcombe, and E. N. Vulfson, *Journal of Chromatography A* **781**, 43-53 (1997).
226. A. Bossi, P. Righetti, and S. Nilsson, "Imprinted polymers in CE and CEC," *Molecular Imprinting of Polymers*, 2004).
227. L. S. Yan, Y. M. Wang, Z. H. Wang, and G. A. Luo, *Chemical Journal Of Chinese Universities-Chinese* **22**, 2008-2010 (2001).
228. J. M. Lin, T. Nakagama, K. Uchiyama, and T. Hobo, *Journal of Pharmaceutical and Biomedical Analysis* **15**, 1351-1358 (1997).
229. T. de Boer, R. Mol, R. A. de Zeeuw, G. J. de Jong, D. C. Sherrington, P. A. G. Cormack, and K. Ensing, *Electrophoresis* **23**, 1296-1300 (2002).
230. L. Schweitz, *Analytical Chemistry* **74**, 1192-1196 (2002).
231. E. Hedborg, F. Winquist, I. Lundstrom, L. I. Andersson, and K. Mosbach, *Sensors and Actuators A* **37-38**, 796-799 (1993).
232. S. A. Piletsky and A. Turner, "A New Generation of Chemical Sensors Based on MIPs," *Molecular Imprinting of Polymers*, 2004).
233. S. A. Piletsky, E. V. Piletska, T. Panasyuk, A. V. Elskaya, R. Levi, I. Karube, and G. Wulff, *Macromolecules* **31**, 2137-2140 (1998).
234. T. Sergeyeva, S. A. Piletsky, A. Brovko, E. Slinchenko, L. Sergeyeva, and A. El'Skaya, *Analytica Chimica Acta* **392**, 105-111 (1999).
235. T. Kobayaski, Y. Murawaki, P. Reddy, M. Abe, and N. Fujii, *Analytica Chimica Acta* **435**, 141-149 (2001).
236. S. A. Piletsky, E. V. Piletskaya, T. Sergeyeva, A. El'Skaya, and T. Panasyuk, *Sensors and Actuators B* **60**, 216-220 (1999).
237. H. Zhang, W. Verboom, and D. Reinhoudt, *Tetrahedron Letters* **42**, 4413-4416 (2001).

238. I. Surugui, B. Danielsson, L. Ye, K. Mosbach, and K. Haupt, *Analytical Chemistry*. **73**, 487-491 (2001).
239. L. Feng, Y. Liu, Y. Tan, and J. Hu, *Biosensors and Bioelectronics* **19**, 1513-1519 (2004).
240. F. Dickert and M. Tortschanoff, *Analytical Chemistry*. **71**, 4559-4563 (2006).
241. J. Z. Hilt and M. E. Byrne, *Advanced Drug Delivery Reviews* **56**, 1599-1620 (2004).
242. C. J. Allender, C. Richardson, B. Woodhouse, C. M. Heard, and K. R. Brian, *International Journal of Pharmaceuticals* **119**, 39-43 (2000).
243. H. Hiratani, A. Fujiwara, Y. Tamiya, Y. Mizutani, and C. Alvarez-Lorenzo, *Biomaterials* **26**, 1293-1298 (2005).
244. C. Alvarez- Lorenzo and A. Concheiro, *Journal of Chromatography B* **804**, 231-245 (2004).
245. A. Leonhardt and K. Mosbach, *Reactive Polymers* **6**, 285-290 (1987).
246. M. Whitcombe, E. N. Vulfsen, and C. Alexander, *Synlett* 911-923 (2000).
247. L. Ye, O. Ramstrom, and K. Mosbach, *Analytical Chemistry*. **70**, 2789-2795 (1998).
248. G. Vlatakis, L. I. Andersson, R. Muller, and K. Mosbach, *Nature* **361**, 645-647 (1993).
249. S. A. Piletsky, E. Terprtsching, Andersson H.S., I. A. Nicholls, and O. S. Wolfbeis, *Journal of Analytical Chemistry* **364**, 512-516 (1999).
250. P. K. Dhal and B. Arnold, *Macromolecules* **25**, 7051-7059 (1992).
251. *Encyclopedia of Chemical Technology Volume 17*, 3rd Edition (John Wiley and Sons, 1984).
252. *Concise Encyclopedia of Polymer Science and Engineering*, 1st edition J. Kroschwitz, ed., (Weiley, U.S.A., 1990).
253. K. W. Allen, E. S. Cockburn, R. S. Davidson, K. S. Tranter, and H. S. Zhang, *Pure and Applied Chemistry* **64**, 1225-1230 (1992).
254. A. Rehab, *European Polymer Journal* **34**, 1855 (1998).
255. R. Balaji, D. Grande, and S. Nanjundan, *Reactive and Functional Polymers* **56**, 45-57 (2003).
256. R. Balaji and S. Nanjundan, *Reactive and functional polymers* **49**, 77-86 (2001).

257. J. L. R. Williams, S. Y. Farid, J. C. Doty, R. C. Daly, D. P. Specht, R. Searle, D. G. Borden, H. J. Chang, and P. A. Martic, *Pure and Applied Chemistry* **49**, 523-538 (1977).
258. A. Reiser, *Photoreactive Polymers. The Science And Technology Of Resists*, (Weiley, New York, 1989).
259. C. M. Hassan and N. A. Peppas, *Advances in Polymer Science* **153**, 37-65 (2000).
260. *Encyclopedia Of Chemical Technology Volume 23*, 3rd Edition (John Weiley and Sons, 1984).
261. http://www.celanese.com/changes_poly_alcohol.bmp . 2006.
262. K. Toyoshima, "General Properties of Polyvinyl Alcohol in Relation to its Applications," *Properties and Applications of Polyvinyl Alcohol*, C. A. Finch, ed., (Weiley and Sons, Chichester, 1977), 17-65.
263. P. J. Flory, *Journal of the American Chemical Society* **61**, 1518 (1938).
264. B. Duncalf and A. S. Dunn, "Photosensitized Reactions of Polyvinyl Alcohol used in Printing Technology and Other Applications," *Properties and Applications of Polyvinyl Alcohol*, C. A. Finch, ed., (Weiley and Sons, Chichester, 1977), 461-490.
265. K. Ichimura and S. Watanabe, *Journal of Polymer Science: Polymer Letters Edition* **18**, 617 (1980).
266. S. W. Fang, J. H. Timpe, and A. Gandini, *Polymer* **43**, 3505-3510 (2002).
267. S. A. Zahir, G. E. Green, and B. P. Stark, *Journal of Macromolecular Sciences-Reviews Macromolecular Chemistry* **C21**, 187-273 (1982).
268. J. H. Liu, Y. C. Chung, and M. T. Lin, *Die Angewandte Makromolekular Chemie* **219**, 43-54 (1994).
269. F. Galindo and M. A. Miranda, *Journal of Photochemistry and Photobiology A: Chemistry* **113**, 155-161 (1998).
270. M. Tsuda, *Journal of Polymer Science Part A* **2**, 2907-2916 (1964).
271. A. Lin, C.-F. Chu, W.-Y. Haung, and A. Reiser, *Pure and Applied Chemistry* **64**, 1299-1303 (1992).
272. D. M. Haddleton, D. Creed, A. C. Griffin, C. E. Hoyle, and K. Venkataram, *Makromolekular Chemistry Rapid Communicaitons* **10**, 391-396 (1989).
273. K. Ichimura, *HCR Comprehensive review* **3**, 419-441 (1996).
274. K. Ichimura, *Makromolekular Chemistry* **188**, 2982 (1987).
275. E. S. Cockburn, R. S. Davidson, and J. E. Pratt, *Journal of Photochemistry and Photobiology A: Chemistry* **94**, 83-88 (1996).

276. K. Ichimura, *Journal of Polymer Science: Polymer Chemistry Edition*. **20**, 1411-1417 (1982).
277. K. Ichimura and T. Komatsu, *Journal of Polymer Science part A: Polymer Chemistry* **25**, 1475-1480 (1987).
278. K. Ichimura and S. Watanabe, *Journal of Polymer Science: Polymer Chemistry Edition* **20**, 1419-1432 (1982).
279. E. S. Cockburn, R. S. Davidson, S. A. Wilkinson, and J. Hamilton, *European Polymer Journal* **24**, 1015-1017 (1988).
280. Gandini, A., Waig Fang, S., Timpe, J. H., and Baumann, H. [6,270,938 B1]. 2001. US Patent.
281. B. Leca, R. M. Morelis, and P. R. Coulet, *Sensors and Actuators B* **26-27**, 436-439 (1995).
282. K. Morimoto, S. Fukanoki, K. Morisaka, S. H. Hyon, and Y. Ikada, *Chemical and Pharmaceutical Bulletins* **37**, 2491 (1989).

Chapter 2

Synthesis and physical characterisation of imprinted polymers

2.1 Introduction

The majority of molecularly imprinted polymers and other synthetic polymeric materials, used for example as supports for synthesis or catalysis [1], are formed based on crosslinked vinyl polymers. Imprinted polymers and to a certain extent the synthetic polymers mentioned above are generally insoluble materials whose subsequent use depends on their morphology in terms of the particle shape and size and the porous texture of the material. It is important to determine the morphology of imprinted polymers as it can effect their subsequent molecular recognition properties or their mode of application. For example, monolith formation which results in irregular shaped particles has limited use as chromatographic stationary phases.

The morphology of imprinted polymers can be tailored so as to improve its resulting performance. The use of polymerisation techniques such as suspension [2-4], precipitation [5-7], dispersion [8-10] and multi-step swelling [11,12] can provide better control over the shape, size and uniformity of the polymer particles, which renders them more appealing for use as stationary phases. Varying the different polymer components can play a role in the type of particles produced in the above polymerisation techniques. However, the resultant polymers are influenced more by the polymerisation technique as opposed to the polymer formulation.

The porosity and surface area of imprinted polymers are dictated by polymer composition. The porosity affects the rate of release of template from within the polymer matrix [13], which can have significant effects on the subsequent use and applications of the polymer. The solvent (porogen) in which the polymerisation is carried out imparts porosity to the polymers by phase separation between the solvent and the growing polymer. A diagram illustrating the formation of the porous structure is shown in Figure 2.1.

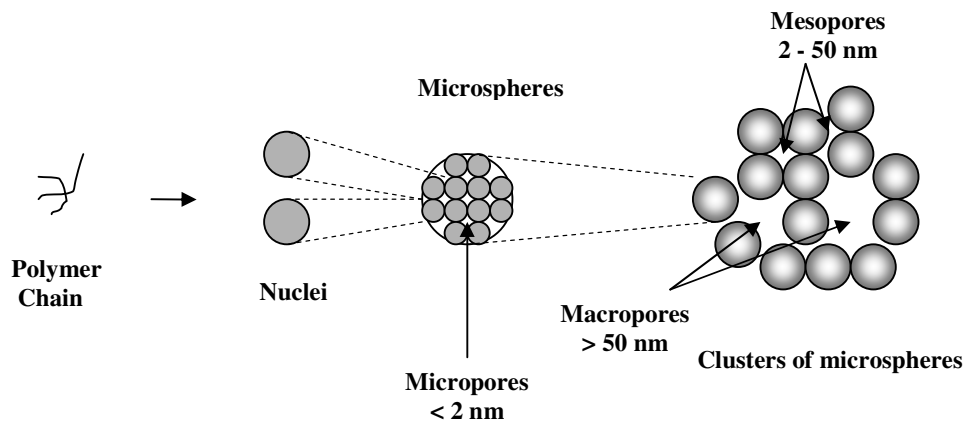


Figure 2.1 Formation of the porous structure in polymers (adapted from reference [14]).

The growing polymer chain forms nuclei, which aggregate to form microspheres. These microspheres then aggregate themselves to form clusters which make up the polymer particles [14]. The porosity is formed from the free voids among the aggregated microspheres or within the microspheres. The extent of separation is dictated by the solvating ability of the solvent. A good solvent will result in a uniform distribution of crosslinks whilst a poor solvent results in a heterogeneous distribution. The term porogen is only used for a particular polymer system if it forms pores, otherwise the term diluent is used [15]. Increasing the volume of porogen results in an increase in pore volume [16].

The functional monomer and crosslinking monomer can also affect the porosity of polymers [17]. There is a direct relationship between the solvent and the crosslink ratio, as shown in Figure 2.2.

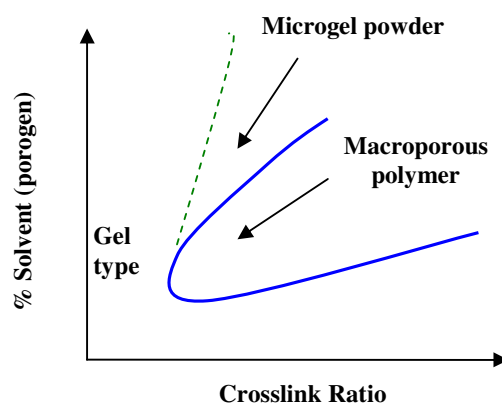


Figure 2.2. Polymer pseudo-phase diagram showing the relationship between the amount of solvent and crosslink ratio on the type of polymer obtained (adapted from reference [18]).

The crosslink ratio is the percentage of crosslinking monomer with respect to the total number of moles of monomers (including functional and crosslinking monomers) [16,18]. The nominal crosslink ratio does not give an actual value for the level of incorporation of monomers in a crosslinked polymer. It is useful for comparison of the theoretical degree of crosslinking for polymers with different monomer compositions. There is a minimum amount of both porogen and crosslinking monomer required to form a macroporous polymer (macroporous refers to polymers having a permanent porous structure and is not used here to classify the type of porosity).

Pores are classified by IUPAC according to their size, as follows [19];

- Macropores- pore width > 50 nm,
- Mesopores-pore width 2 – 50 nm,
- Micropores- pore width < 2 nm.

When investigating/altering the morphology for a given polymer system, it is important to consider the effect of varying each component on molecular recognition particularly in non-covalent imprinting where stabilisation of pre-polymerisation complexes is dependent on the local environment. The nature of the solvent is critical as it must be chosen so as to stabilise the interactions between the monomer and the template and should not be overlooked when establishing a good solvent for polymer porosity.

The crosslinking monomer forms the bulk of polymer matrix around the pre-polymerisation complexes during the polymerisation, hence forming the binding sites. The concentration of crosslinking monomer in an imprinted polymer is critical in that a minimum concentration is required to form a rigid polymer that will maintain the shape of the binding sites to produce a polymer with adequately positioned functionality [14]. On the other hand, the polymer must also be flexible enough to allow access to the binding sites to facilitate template removal and subsequent rebinding. Again, its effect on morphology must also be considered.

In the following study a series of polymers imprinted towards 2-aminopyridine (2-apy) have been synthesised by varying the type of functional monomer (methacrylic acid (MAA), 4-vinylpyridine (4-VP) and methyl methacrylate (MMA)) and the concentration of crosslinking monomer ethyleneglycol dimethacrylate (EGDMA).

The functional monomers were chosen as each had the potential to interact with the template and are commonly used in molecular imprinting. MAA has found extensive use as a functional monomer in molecular imprinting as it has the ability to act as a Lewis acid and a Lewis base with hydrogen donating or accepting functional groups in the template molecule [20], therefore rendering it a versatile monomer. It has previously been used for imprinting 2-apy (and structural analogues) at the commonly used ratio of 4:1:30 functional monomer: template: crosslinking monomer [21-24]. 4-VP is a basic monomer and has been used for imprinting templates using carboxyl groups [25-27], or using π - π interactions [28]. MMA has been used as a functional monomer, for example for the molecular imprinting of dimethoate where it was found to be superior to MAA and 4-VP [29].

Figure 2.3. illustrates the precursors used for polymer synthesis and the potential interacting functionalities between template and functional monomers are shown in matching colours. The potential for π - π interactions between the aromatic groups of 2-apy and 4-VP also existed.

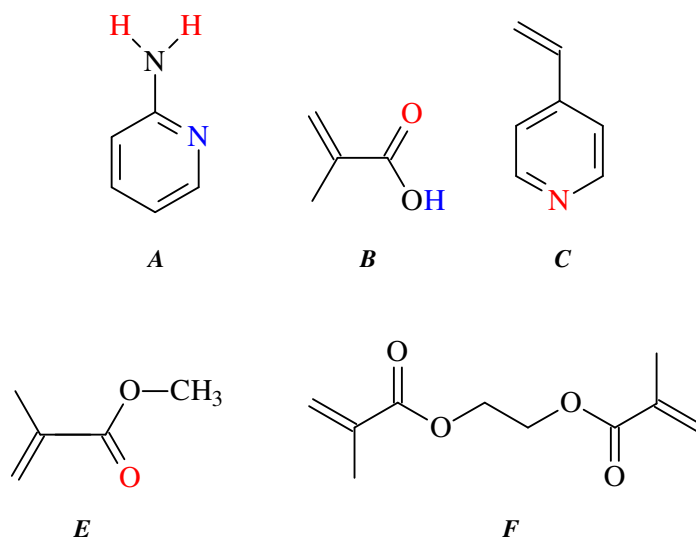


Figure 2.3. Structures of the components employed in polymer synthesis; *A*; 2-aminopyridine (template), *B*; methacrylic acid (functional monomer), *C*; 4-vinylpyridine (functional monomer), *D*; methyl methacrylate (functional monomer) and *E*; ethylene glycol dimethacrylate (crosslinking monomer).

2-apy was chosen as the template species as it is the building block for many pharmaceutical and active drug compounds, so the development of an efficient selective phase is desirable. An example of the use of the 2-apy substructure in the synthesis of pharmaceutical compounds is given in Figure 2.4., where it is a precursor used for the synthesis of an adenosine antagonist which can be used in the therapeutic and/or preventive treatment of disfunctions of the heart, kidney, respiratory system and can be used to inhibit the effect of adenosine in growing tumours [30].

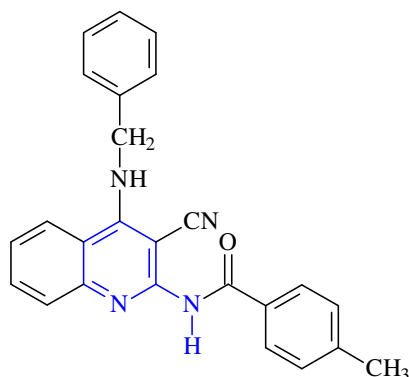


Figure 2.4. 3-methyl-N-(4-benzylamino-3-cyanoquinolin-2-yl) benzamide, which contains the 2-apy substructure, is used as an adenosine antagonist (adapted from reference [30]).

The aim of this study was to comprehensively examine the effect of polymer formulation on the physical properties of a novel series of imprinted polymers selective to 2-apy, using techniques such as nitrogen sorption porosimetry, solvent swelling, SEM and particle size analysis. The effect of the physical nature of the polymers on subsequent molecular recognition will be carried out in the subsequent chapters of work.

2.2. Experimental

2.2.1. Materials, equipment and instrumentation

Table 2.1. The materials used.

Reagent	Supplier	Assay
Methacrylic acid	Sigma-Aldrich (Ireland)	99 %
4-Vinylpyridine	Sigma-Aldrich (Ireland)	98 %
Methyl methacrylate	Sigma-Aldrich (Ireland)	99 %
Ethyleneglycol dimethacrylate	Sigma-Aldrich (Ireland)	98 %
1,1-Azo bis(cyclohexanecarbonitrile)	Sigma-Aldrich (Ireland)	98 %
Chloroform	Lennox (Ireland)	99.0-99.4 %
2-Aminopyridine	Sigma -Aldrich (Ireland)	99+%
Methanol	Lennox (Ireland)	99.8 %
Acetone	Lennox (Ireland)	99 %
Acetic acid (glacial)	Sigma-Aldrich (Ireland)	100 %
Molecular sieves	Sigma-Aldrich (Ireland)	3Å 3.2 mm

Equipment and instrumentation

- Thermal water bath: Memmert – Lennox Laboratory Supplies.
- Endicott test sieves: 25 and 75µm- Lennox Laboratory Supplies.
- UV/Vis spectrometer: Cary 100- Varian, JVA Ireland Ltd.
- Particle size analyser: Mastersizer 2000 coupled with Hydro 2000S, Malvern Instruments Particular Sciences.
- Nitrogen sorption porosimeter: Gemini VI, Micrometrics, Particular Sciences.
- Microscope: Olympus CH20
- Scanning Electron Microscope (SEM): Hitachi S4000 SEM System and Sputter Coater Unit PS3 Agar Aids for Electron Microscopy.
- Vortex: Disruptor Gene, Scientific Industries.
- Desktop Centrifuge, Sigma.

2.2.2. Polymer preparation

Polymers were prepared using a method described by Cummins *et. al.* [24]. A summary of the various polymer compositions is given in Table 2.2. A typical formulation was carried out as follows: in a 30 mL glass vial, 94 mg (1 mmol) of 2-apy and 4.5 mmol of functional monomer were dissolved in 12.5 mL of chloroform (which had been stored over molecular sieves, pore size 3 Å). The concentration of EGDMA required was then added with 65 mg (0.26 mmol) of azo bis (cyclohexanecarbonitrile) (ACCN). The vials were stoppered and crimp sealed. Each polymer solution was then purged with nitrogen for 5 min, followed by sonication for 10 min. The pre-polymer mixtures were placed in a stationary water bath at 65 °C for 24 h. For each of the imprinted polymers a corresponding reference polymer was prepared in the absence of 2-apy. Imprinted and non-imprinted polymers containing 40 and 10 mmol EGDMA were also prepared in the absence of functional monomer. The 10 mmol polymers were scaled up during synthesis to increase the yields.

Table 2.2. Summary of polymer compositions.

2-apy (mmol)	MAA, 4-VP or 4-VP* and MMA* (mmol)	EGDMA (mmol)	CHCl₃ (mL)	ACCN (mmol)
1	4.5	40	12.5	0.26
1	4.5	30	12.5	0.26
1	4.5	20	12.5	0.26
1	4.5	10	12.5	0.26

* 4.5 mmol of both 4-VP and MMA were used

The various polymer compositions are expressed as the nominal crosslink ratio in Table 2.3.

Table 2.3. Polymer compositions expressed as nominal crosslink ratio.

EGDMA (mmol)	Nominal crosslink ratio (mol %)*	Nominal crosslink ratio (mol %)**	Nominal crosslink ratio (mol %)***
40	89.9	81.6	100
30	86.9	76.9	100
20	81.6	68.9	100
10	68.6	52.6	100

* For MAA and 4-VP polymers.

** For 4-VP-MMA polymers.

*** For polymers formed in the absence of functional monomer.

Note; the polymers will commonly be referred to using the functional monomer abbreviation and the number of mmol of EGDMA in the particular composition, for example, MAA 10 mmol EGDMA refers to the MAA polymer formed using 10 mmol of EGDMA. The polymers formed in the absence of functional monomer will be referred to in legends, etc, as no FM. The 4-VP and MAA polymers are technically copolymers because of the presence of EGDMA and the 4-VP-MMA polymers are termonomers. However, for the purposes of comparing different functional monomers the 4-VP-MMA will commonly be referred to as a co-monomer system.

2.2.3. Template removal

The bulk monoliths were ground and wet sieved, using acetone. Fractions ranging from 25-75 μm diameter were collected, using Endicott test sieves. Particles < 25 μm were retained for use in Chapter 5.

Template was removed from polymers (particles 25-75 μm) by agitation in hot 10 % acetic acid acidified methanol, for 15 min. Particles were collected by filtration and washed with a further 50 mL of hot acidified methanol, followed by successive washing

with hot methanol to not only facilitate 2-apy removal, but also to remove acetic acid. Washing continued until 2-apy and acetic acid could no longer be detected by UV/VIS spectroscopic analysis of the filtrate stream. To ensure complete removal of residual acetic acid, polymers were suspended in hot methanol, collected by Buchner filtration, and again washed with hot methanol. Polymers were oven dried at 80 °C to a constant mass.

2-apy was removed from 4-VP and 4-VP-MMA polymers by extraction in 50 % acetic acid acidified methanol using a Soxhlet apparatus for 3 h intervals, until it could no longer be detected by UV/VIS spectroscopy. Acetic acid was removed as described for MAA polymers. All NIP species were treated in an identical manner.

2.2.4. Optical microscope and SEM analysis

Images of the polymers were obtained using an Olympus CH20 microscope fitted with a camera, at magnification 10X. The images were captured using Scope photo software. For SEM analysis the polymer samples were attached to 10 mm diameter metal mounts using carbon tape and sputter coated with gold under vacuum in an argon atmosphere. The coated samples were then analysed using SEM with a voltage of 20 kV. The surface of the polymer samples were then scanned at the desired magnification to study the morphology of the beads and particles.

2.2.5. Nitrogen sorption analysis

Approximately 15 mg of polymer (adsorbent) was weighed into an analysis sample tube. The sample was first prepared by degassing using a constant flow of nitrogen whilst at the same time volatile components were removed by exposing the sample to 120 °C for 2 h. The mass of the sample was then determined post-preparation, and this value was entered into the sample log information. All analyses were carried out using filler rods, and, as the height of the rods had to be equivalent in the sample and reference tubes, glass beads were added to the sample tube to ensure equal height.

The prepared sample, and reference tube, were attached to the appropriate sample port, evacuated (at 50 mmHg min⁻¹ for 6 min) and cooled to a cryogenic temperature (boiling point of liquid nitrogen, 77 K) by raising a Dewar containing liquid nitrogen, thus immersing both tubes. The free space, which is the volume of the sample tube that is not occupied by the sample, was measured by dosing helium into both sample and reference tubes. The system was then evacuated and the analysis started by dosing volumes of nitrogen gas (the adsorptive) into the sample, after which the pressure was equilibrated and the volume of gas sorbed was determined.

Adsorption analysis followed by desorption, in the relative pressure (P/P_o) range 0.01-0.99 (where P is the equilibrium pressure and P_o is the nitrogen saturation pressure at 77 K), was carried out on the polymer samples to generate a 109 point sorption isotherm. P_o was measured after each data point.

The surface area of the polymers was derived from the adsorption isotherm, in the P/P_o range < 0.3 for a six point plot, using Brunauer, Emmett and Teller (BET) analysis [19,31-33]. The BET equation is usually applied in its linear form (Equation 2.1.)

$$\frac{P}{n^a \cdot (P_o / P)} = \frac{1}{n_m^a \cdot C} + \frac{(C-1)P}{n^a \cdot C P_o} \quad \text{(Equation 2.1.)}$$

Where: n^a is the amount adsorbed at the relative pressure P/P_o ,

n_m^a is the monolayer capacity,

C is a constant dependent on the shape of the isotherm.

A plot of $\frac{P}{[n^a (P_o / P) - 1]}$ versus P/P_o (BET plot) gives a linear relationship at $P/P_o <$

3 to give n_m^a from which the surface area is subsequently determined using Equation 2.2.

$$a_s = n_m^a \cdot L \cdot a_m \quad \text{(Equation 2.2.)}$$

Where: a_s is the surface area,

L is Avogadro constant,

a_m is the molecular cross-sectional area of the adsorptive (nitrogen).

Pore analysis on the adsorption branch of the isotherm was carried out using the Barrett, Joyner and Halden (BJH) method [34]. Pore radii at each P/P_0 point was determined using the Kelvin equation (Equation 2.3.), which was corrected for multilayer adsorption using the Halsey thickness equation (Equation 2.4.) Differential pore volumes were generated by plotting dV/dD versus D (V is the pore volume and D is the pore diameter) [35].

$$r^k = \frac{2\sigma^{lg}v^l}{RT \ln(P_o / p)} \quad \text{(Equation 2.3.)}$$

Where [19]; r^k is the Kelvin radius,

σ^{lg} is the surface tension of the liquid condensate,

v^l is the molar volume of the liquid condensate.

The Halsey thickness equation, which corrects for multilayer adsorption is given in Equation 2.4.

$$t = 3.55 \left[\frac{-5.00}{\ln(P/P_o)} \right]^{1/3} \quad \text{(Equation 2.4.)}$$

Where [32]; t is the thickness of the adsorbed liquid monolayer (monolayer coverage is an assumption),

3.45 and 5.00 are empirical values.

The instrument was calibrated with a carbon black reference standard prior to use and was frequently monitored for potential errors by performing a blank test tube analysis.

2.2.6. Particle size distribution analysis

Approximately 30 mg of the polymer particles were suspended in excess methanol *via* sonication for 5 min. The sample was then added to the dispersant chamber, which contained methanol, until laser obscuration was within the pre-defined limits (between 5 and 12 %). The sample was circulated around the system at a speed of 2100 rpm. 1000 measurement snaps per second were taken over a measurement time of 6 s. The average

of three measurements was reported by the software for each analysis and each polymer sample was analysed in triplicate. Result calculation was carried out using the general purpose model in the range 0.02 – 2000 μm . The results were expressed as $D(v, 0.1)$, $D(v, 0.5)$ and $D(v, 0.9)$. $D(v, 0.5)$ represents the size in microns below which 50 % of the particles are smaller and above which 50 % are larger. $D(v, 0.1)$ represents the size below which 10 % of the sample lies and $D(v, 0.9)$ represents is the size of particles below which 90 % of the sample lies.

To ensure accurate results using this technique it is imperative that a good sample background is obtained. Factors such as dirty cell windows can lead to a poor background as a result of light scattering from the contaminant. To ensure confidence in the results obtained, the system was extensively washed with water and methanol between each sample analysis. Prior to analysis the instrument was calibrated with 1 and 9 μm diameter NIST traceable latex standards, the results of which were within specification.

2.2.7. Solvent swell ratio determination

Solvent swell ratio was determined in chloroform, acetonitrile and methanol based on a method described by Mashelkar *et al.* [36]. 50 mg of polymer was weighed into an Eppendorf tube and 1 mL of the appropriate solvent (acetonitrile and methanol) was added. The tubes were sealed and the sample mixed using a vortex. Samples were equilibrated in Stuart Scientific Orbital were weighed. Due to the density of chloroform (1.484 g cm^{-3}), which inhibited centrifuging, the swelling effect of chloroform on the polymers was determined by adding 100 μL increments of chloroform to the polymers until saturation was achieved. The chloroform was left to equilibrate with the polymers for 1 h between each addition. The swelling ratio (Sr) was calculated using Equation 2.5. [37], based on the volume of the dry polymer Incubator S150 for 24 h at 250 rpm after which they were centrifuged (Desktop Centrifuge, Sigma) for 5 min at 13500 rpm. The excess solvent was removed and the samples and the volume of the wet polymer.

$$\text{Swelling ratio (Sr)} = \frac{\text{volume of wet polymer}}{\text{volume of dry polymer}} \quad \text{(Equation 2.5.)}$$

The bulk density was used for the determination of polymer volume, and was determined by obtaining the mass of polymer which was added to the graduation mark of a 1 mL volumetric flask. The bulk density measurements include the voids occupied by pores and interparticle spaces, and, is not a measurement of the true density, which omits these gaps. Given that the polymers were used in a non-compacted form *i.e.* the interparticle spaces were not removed bulk density was sufficient for density determination.

2.3. Results and discussion

2.3.1. Template Removal

Template removal, for all the polymers, was first attempted by suspension in 10 % acetic acid acidified methanol. The acid was employed as it has previously been shown to compete with MAA for the formation of hydrogen bonds [38]. Methanol was also capable of acting in a similar manner.

Although some of the template was lost during the sieving process, a substantial amount of template was displaced by the acidified methanol, for MAA polymers. Figure 2.5. illustrates the extraction profile for 2-apy removed from MAA imprinted polymer prepared with 10 mmol of EGDMA. As the concentration of EGDMA in the MAA polymers decreased the amount of 2-apy displaced increased, thus indicating that the polymers formed with a lower concentration of crosslinker yielded flexible polymers that did not retain the template to the same degree as the polymers prepared with a higher concentration of EGDMA.

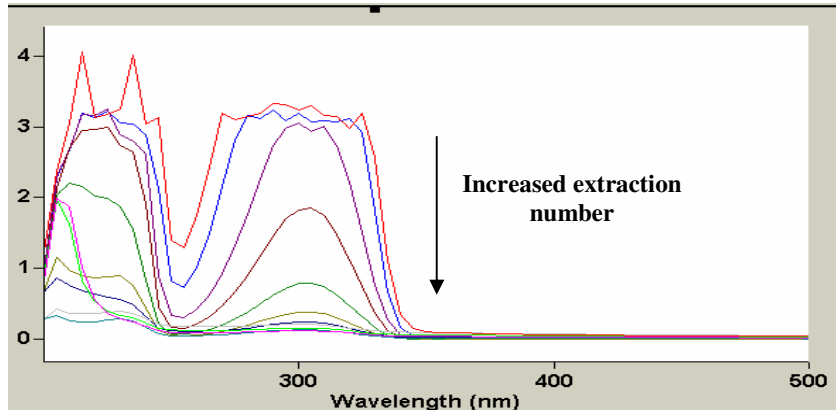


Figure 2.5. 2-apy extraction profile obtained by suspension in 10 % acetic acid acidified methanol for MAA-EGDMA (10mmol) imprinted polymer.

While suspension in 10 % acetic acid acidified methanol was sufficient for 2-apy extraction for the MAA polymers, it did not however displace 2-apy to the same degree from the 4-VP and 4-VP-MMA polymers. Figure 2.6. shows a typical extraction profile obtained for 4-VP polymers formed with 10 mmol EGDMA.

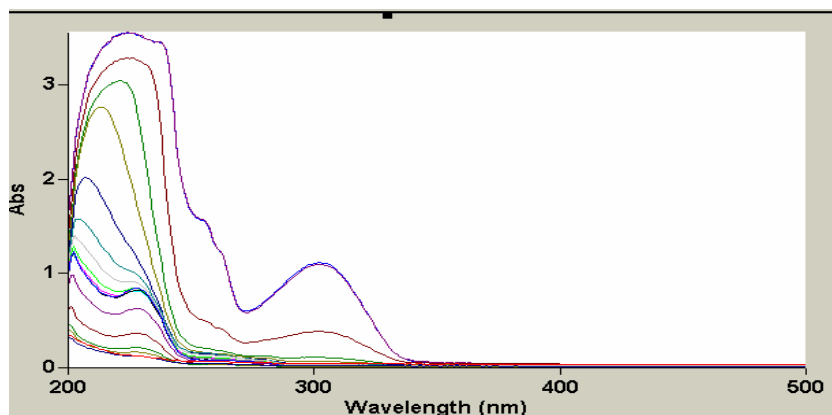


Figure 2.6. 2-apy extraction profile obtained by suspension in 10 % acetic acid acidified methanol for 4-VP-EGDMA (10mmol) imprinted polymer.

The profiles illustrated in Figures 2.5 and 2.6. were generated by suspending 0.5 g of each of the polymers in equal volumes of acidic methanol, followed by successive washing with methanol, also equal volumes, until a flat baseline was achieved.

As the absorbance values for 2-apy displaced from 4-VP and the co-monomer system were less than for MAA polymers, an alternative template removal procedure was attempted by extraction in 50 % acetic acid acidified methanol using a Soxhlet apparatus, for three hour intervals, until 2-apy could no longer be detected by UV/VIS spectroscopy. This alternative, and more rigorous, procedure did displace 2-apy, from the polymeric systems, however, removal was not to the same degree as that from MAA polymers. It is suggested that the template was irreversibly bound within these polymers. Potential variations in polymer morphology between the different monomeric systems must also be considered as a reason for this phenomenon.

Although the amount of template removed from the polymers could not be quantified, it was apparent that the amount displaced from the 4-VP-MMA polymers was less than that displaced from the MAA polymers, but was greater than template removal from the 4-VP polymers. This suggested that the different monomeric systems produced polymers with varying flexibility, rigidity and overall different morphologies, which was examined through further experimental analysis. Storing the 4-VP containing polymers in chloroform for 1 week resulted in minimal template removal. If π - π interactions were the predominant interaction mechanisms in the 4-VP polymers it was

expected that the ability of the template to form H-bonds with the methanol and acetic acid during template removal would overcome these interactions, and template removal would be achieved. As this did not occur, it is suggested that morphological differences in the polymers between MAA and 4-VP existed.

Template removal from the polymers formed with no functional monomer was initially carried out by suspension in 10 % in acetic acid acidified methanol. 2-apy was not found to be present in the washings (Figure 2.7). This suggests that the template may have been removed during the grinding and sieving process, which was carried out in acetone. It should also be considered that when higher amounts of EGDMA were used in polymer formulation, the mole ratio of functional monomer to EGDMA decreased, and the resultant polymers that formed were more rigid. Lower amounts of crosslinking monomer, and hence higher mole ratios of functional monomer to EGDMA, produced more flexible polymers. Therefore, with the addition of no functional monomer it might be expected that polymers with a higher crosslink density would form, and that the template may be irreversibly retained within the polymer matrix (Refer to Table 2.3. for nominal crosslink ratio values).

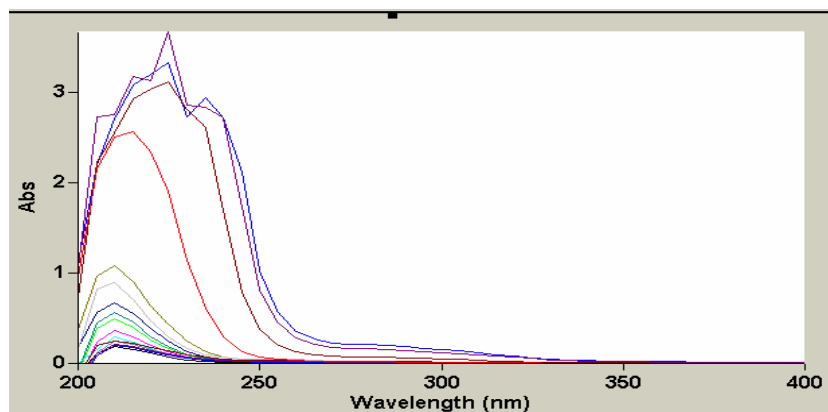


Figure 2.7. Extraction profile obtained by suspension in 10 % acetic acid acidified methanol for imprinted polymer formed from 10 mmol EGDMA but in the absence of functional monomer.

During the assessment of polymer affinity (Section 3.3.) there was evidence of bleed from the polymers formed with no functional monomers. As a result the polymers were subjected to extraction in acetic acid acidified methanol using a Soxhlet apparatus. After this extraction procedure the polymers were stored in chloroform for 1 week, isolated by

filtration and washed with chloroform. Analysis of the chloroform filtrate suggested that all bleed components had been removed. However, subsequent analysis of the affinity showed that this was not the case.

2.3.2. Optical microscope and SEM analysis

The images obtained using the optical microscope showed that overall the particles were irregular in shape. As monolith synthesis was the method employed, this was expected. It is due to this irregular shape that polymers formed by this method find limited use in subsequent applications, particularly in chromatography. Within each functional monomer system as the concentration of EGDMA in the polymer formulation was reduced, the overall shape of the particles changed, and the size decreased with decreasing EGDMA concentration. The images for the 40 and 10 mmol MIPs formed using MAA and 4-VP as the functional monomers are shown in Figure 2.8.

After the grinding and sieving process the polymers formed from 40 mmol EGDMA (MAA) resulted in particles that were more crystalline in structure, albeit irregular in shape, whilst those formed from 10 mmol were fine, less crystalline and tended to form aggregates (an aggregate is an assemblage of particles which are loosely coherent [19]). The 10 mmol 4-VP polymer while smaller than corresponding 40 mmol 4-VP, it was also crystalline which was in contrast to the MAA polymer. The 10 mmol co-monomer system was also similar to that seen for the 4-VP polymer.

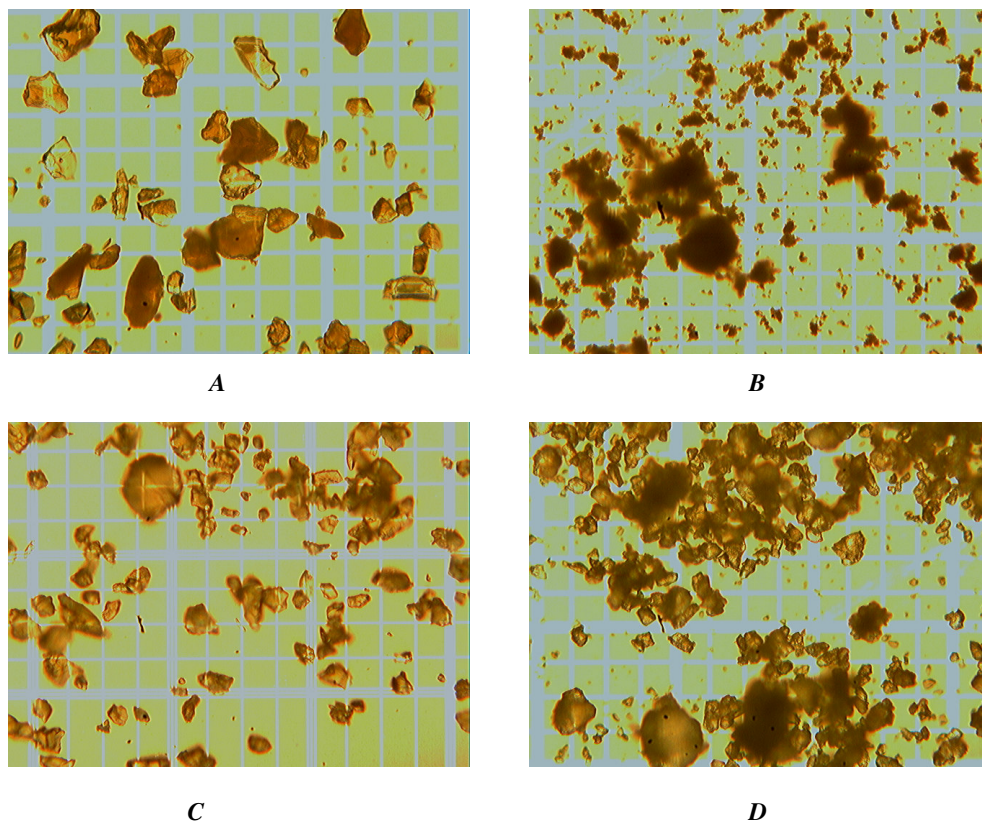


Figure 2.8. Optical microscope images of *A*; 40 mmol MAA MIP, *B*; 10 mmol MAA MIP, *C*; 40 mmol 4-VP MIP, *D*; 10 mmol 4-VP MIP.

The SEM image of the 10 mmol MAA MIP shows that it consisted of what appeared to be aggregates (Figure 2.9.). The 40 mmol polymer contained larger irregular shaped particles having a relatively smooth surface.

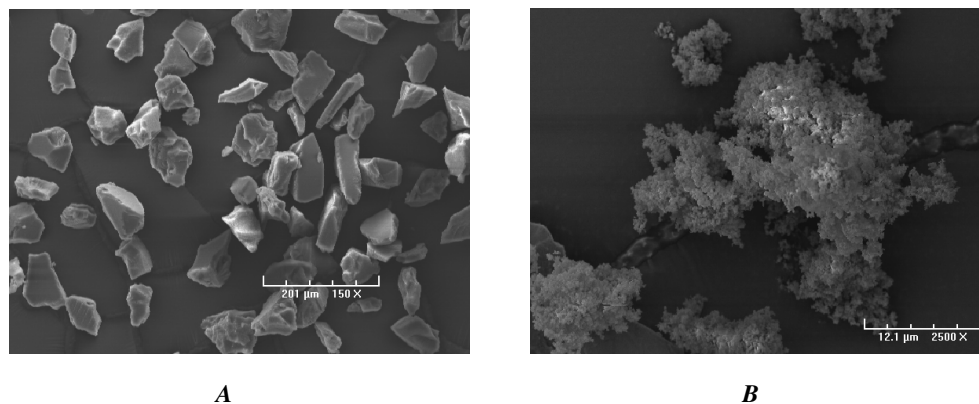


Figure 2.9. SEM images of *A*; 40 mmol MIP (magnification 150 X) and *B*; 10 mmol MIP (magnification 2500 X), both formed using MAA as the functional monomer.

The corresponding 10 mmol polymers for the 4-VP and the 4-VP-MMA had a distinctly different morphology to the MAA polymers, Figure 2.10. The 40 mmol polymers had irregular shape particles similar to those observed with MAA. The 10 mmol 4-VP containing polymers appeared to form agglomerates, which are defined as an assemblage of particles rigidly joined together [19].

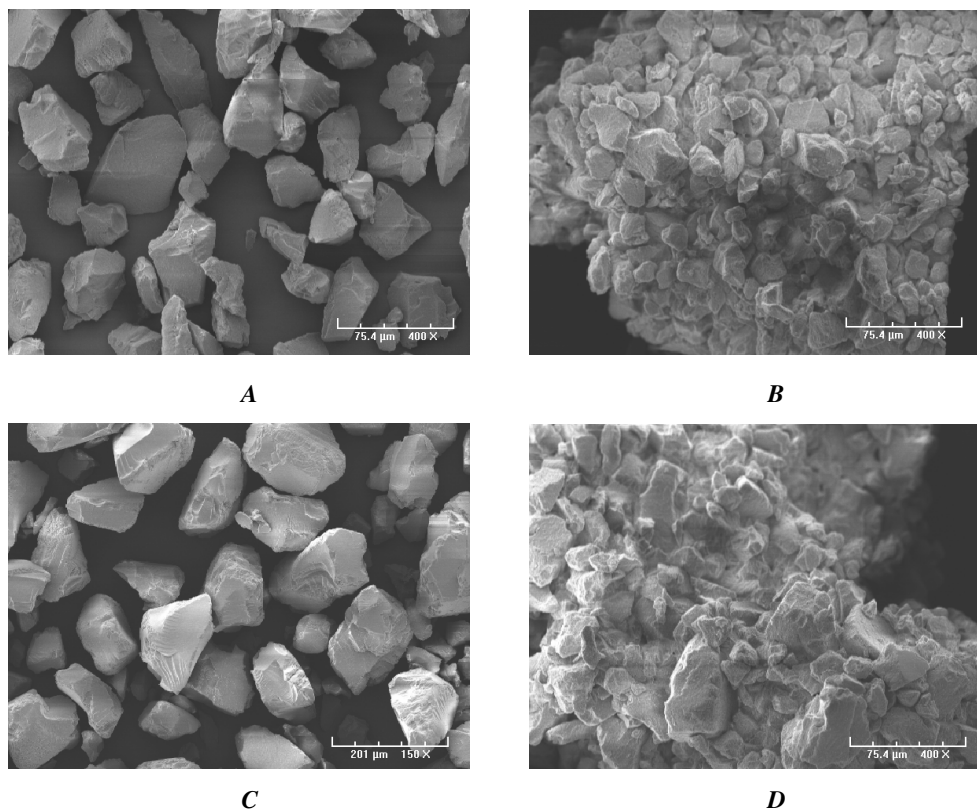


Figure 2.10. SEM images of A; 40 mmol MIP 4-VP (magnification 400 X), B; 10 mmol MIP 4-VP (magnification 400 X), C; 40 mmol MIP 4-VP-MMA (magnification 150 X) and D; 10 mmol MIP 4-VP-MMA (magnification 400 X).

When going from 40 to 10 mmol EGDMA in the polymer composition the nominal crosslink ratio decreased, whilst the % of solvent in the formulation increased. It has been proposed through the use of a pseudo phase diagram that such a combination results in a tendency for gel-type polymers to form as opposed to macroporous polymers [16,18]. The monoliths for the 10 mmol polymers all had a gel like texture presumably due to the low degrees of crosslinking or polymerisation and were physically less demanding to grind than those formed with higher amounts of EGDMA. It should be noted that gel-type polymers are very lightly crosslinked (typically 5 % of a divinyl monomer) and do not have a permanent pore structure in the dry state [39]. Thus,

the polymers under study in this instance do not directly fall into the category of gel polymers but instead are said to be tending towards gel-type. The different morphologies obtained for the 10 mmol polymers may have been due to different degrees of solubility between the growing polymer and the porogen (chloroform) which may have resulted in different rates of phase separation, ultimately affecting the morphology and textural properties of the monoliths, which in turn affected the resultant particles obtained from the grinding and sieving process.

2.3.3. Nitrogen sorption analysis

2.3.3.1. Isotherm analysis

Sorption isotherms, of which there are six types classified by IUPAC [19], can be used to gain information on porosity. The most commonly encountered isotherms are;

- Type I- materials having extremely small pores,
- Type II- non-porous or macroporous materials,
- Type IV- mesoporous materials. These isotherms contain characteristic hysteresis loops which arise from different adsorption/desorption mechanisms.

During adsorption the pores fill from the walls inwards towards a central core of decreasing diameter [1]. During desorption, the evaporation starts from the pore ends at the menisci receding inwards. This results in different adsorption/desorption mechanisms which leads to a hysteresis loop in the resultant isotherm. Different pore sizes and shapes as well as the interconnectivity of the porous network contribute to different hysteresis types. The overlay of the 40 and 10 mmol EGDMA MIP isotherms (quantity sorbed $\text{cm}^{-3} \text{g}^{-1}$ STP (Standard Temperature and Pressure) versus relative pressure) for MAA are shown in Figure 2.11

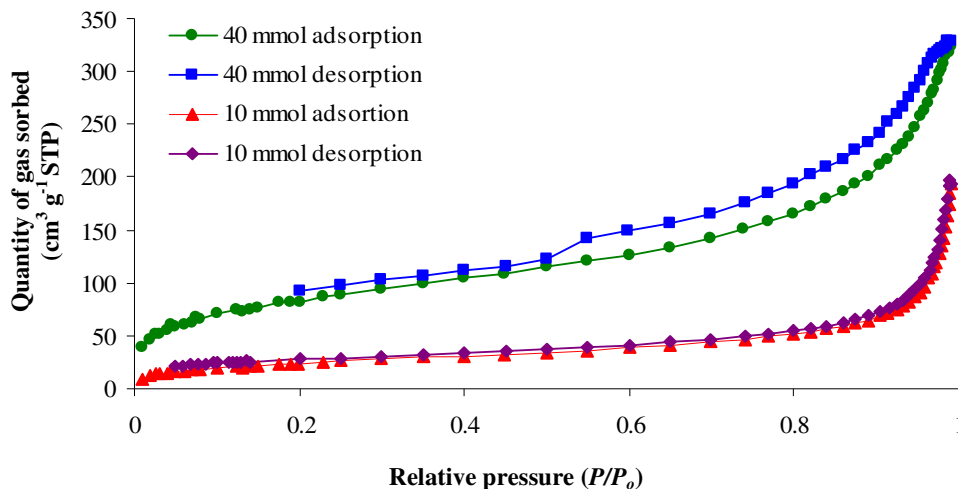


Figure 2.11. Sorption isotherms for 40 and 10 mmol MAA imprinted polymers.

The 40 mmol polymers, both MIP and NIP (NIP isotherms not shown), produced Type IV isotherms, consistent with mesoporous structures, with type H3 or H4 hysteresis. The 10 mmol polymers produced isotherms similar to a Type II isotherm which is indicative of non-porous or macroporous materials. The adsorption and desorption mechanisms were similar which is usually indicative of larger pores [40]. Non closure of the loop, which was observed for all isotherms, implies incomplete removal of adsorbate from narrow pores [19].

The maximum amount of gas sorbed on the 10 mmol polymers is less than that sorbed for the 40 mmol polymers. As the mass of both polymers that were weighed for analysis were similar (to within ± 0.3 mg in this case) the larger quantity of gas sorbed on the 40 mmol polymer can be attributed to its higher surface area. Table 2.4. shows the quantity of gas sorbed at P/P_0 0.99 for the analysed polymers.

Table 2.4. The quantity of gas sorbed (n^a) at P/P_o 0.99. Data is based on the average value from duplicate analysis.

Polymer	n^a ($\text{cm}^3 \text{g}^{-1}$ STP)	
	MIP	NIP
40 mmol MAA	315.4 (+/- 10.1)	400.0 (+/- 3.7)
10 mmol MAA	203.2 (+/- 14.6)	150.4 (+/- 20.7)
40 mmol MIP 4-VP	146.3 (+/- 6.9)	105.1 (+/- 7.5)
10 mmol MIP 4-VP	8.2 (+/- 0.9)	8.8 (+/- 0.5)
40 mmol MIP 4-VP-MMA	73.4 (+/- 4.3)	146.3 (+/- 8.6)
10 mmol MIP 4-VP-MMA	7.7 (+/- 2.5)	75.1 (+/- 0.4)
40 mmol MIP no FM	258.9 (+/- 11.0)	255.2 (+/- 6.2)
10 mmol MIP no FM	284.3 (+/- 1.6)	255.3 (+/- 6.3)

The isotherms for the 4-VP 40 and 10 mmol MIPs are shown in Fig 2.12. The 40 mmol polymer was also Type IV with hysteresis type H2 which suggests that the presence of “ink bottle” pores [19,40]. The 10 mmol MIP (and NIP) displayed some negative values for the quantity of gas sorbed up to P/P_o 0.2 in the adsorption region of the isotherm. It should be noted that this phenomenon, which was also observed for the 10 mmol MIP and NIP for the co-monomer system, was repeated on a different instrument (Nova, Quantachrome carried out at the Welsh School of Pharmacy, University of Cardiff, Cardiff, UK), using approximately 120 mg of the polymer samples, carried out by a different operator and the results were the same.

The 40 mmol 4-VP-MMA imprinted polymer (Figure 2.13.) displayed a hysteresis loop similar to that of the 4-VP 40 mmol MIP. The difference between the hysteresis loop and the adsorption branch of the isotherm was slightly greater than that seen for the 4-VP polymer, indicating a different desorption mechanism due to different pore sizes.

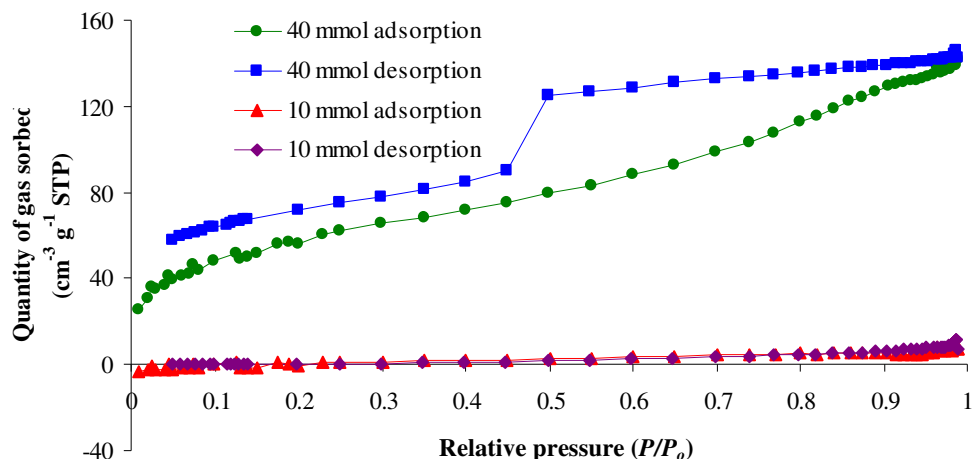


Figure 2.12. Sorption isotherms for 40 and 10 mmol 4-VP imprinted polymers.

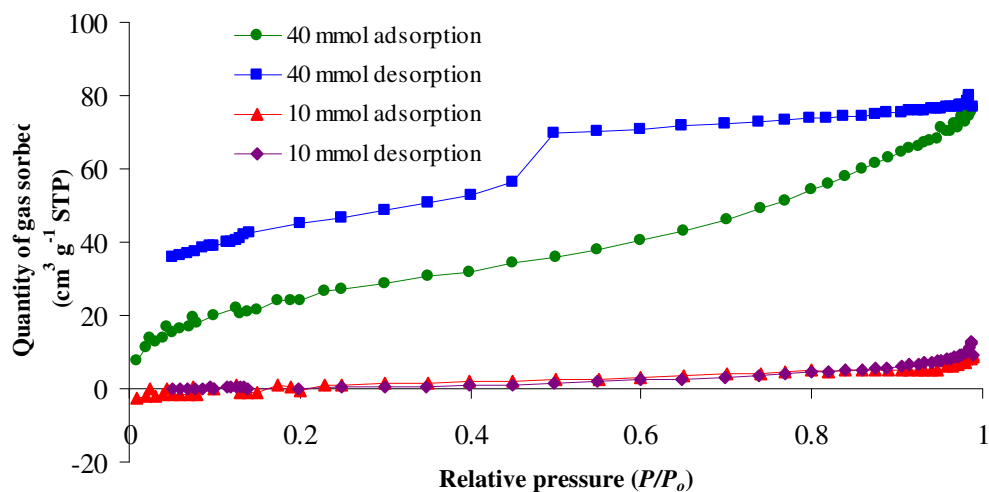


Figure 2.13. Sorption isotherms for 40 and 10 mmol 4-VP-MMA imprinted polymers.

The polymers formed with no functional monomer also displayed Type IV isotherms, suggesting that the polymers were mesoporous in nature. Both the 40 and the 10 mmol imprinted polymers (Figure 2.14.) exhibited isotherms that were similar in shape, which implied that their porous structures were closely related.

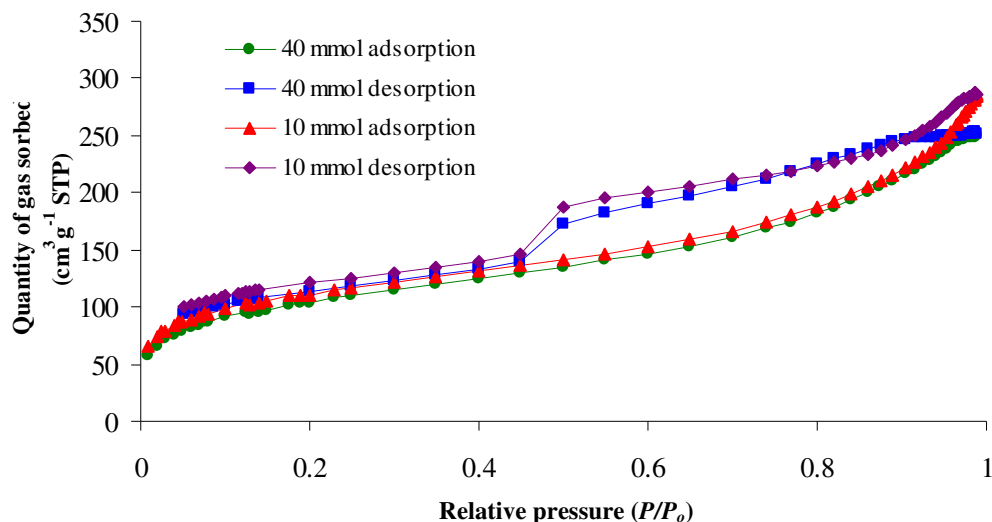


Figure 2.14. Sorption isotherms for 40 and 10 mmol imprinted polymers formed in the absence of functional monomer.

2.3.3.2. BET surface area analysis

A six point BET plot was generated for all polymers in the relative pressure region P/P_0 0.05 – 0.3 in order to determine the surface area of the polymers. Figure 2.15. illustrates an example of a BET plot for the MAA 40 mmol MIP polymer. A summary of the surface areas are given in Table 2.5.

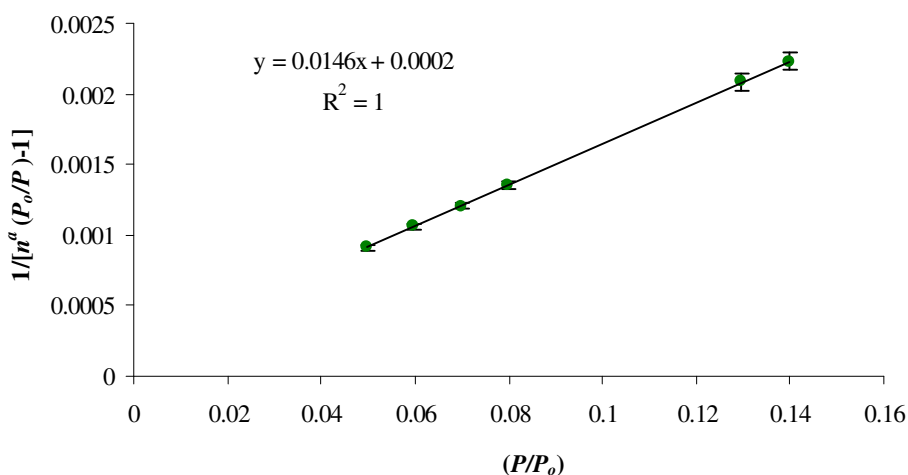


Figure 2.15. BET plot for MAA imprinted polymer formed with 40 mmol EGDMA. Data is based on the average value for duplicate analysis.

Table 2.5. BET surface area. Data is based on the average value for duplicate analysis.

Polymer	BET surface area (m²g⁻¹)	C	N (cm³ g⁻¹ STP)	R²
40 mmol MIP MAA	293.9 (+/- 9.9)	81.0 (+/- 7.2)	67.5 (+/- 2.3)	0.9999
10 mmol MIP MAA	93.1 (+/- 11.8)	58.9 (+/- 1.9)	21.4 (+/- 2.7)	0.9999
40 mmol NIP MAA	347.2 (+/- 2.5)	91.4 (+/- 0.6)	79.4 (+/- 0.6)	0.9998
10 mmol NIP MAA	67.1 (+/- 0.6)	36.6 (+/- 1.3)	15.4 (+/- 0.2)	0.9999
40 mmol MIP 4-VP	221.1 (+/- 25.3)	77.1 (+/- 5.9)	51.0 (+/- 5.8)	0.9999
10 mmol MIP 4-VP	N/D	N/D	N/D	N/D
40 mmol NIP 4-VP	131.5 (+/- 4.2)	55.8 (+/- 1.9)	30.2 (+/- 1.0)	0.9999
10 mmol NIP 4-VP	N/D	N/D	N/D	N/D
40 mmol MIP 4-VP-MMA	83.5 (+/- 6.4)	45.1 (+/- 5.6)	19.2 (+/- 1.5)	0.9994
10 mmol MIP 4-VP-MMA	N/D	N/D	N/D	N/D
40 mmol NIP 4-VP-MMA	239.8 (+/- 22.1)	78.1 (+/- 1.1)	55.1 (+/- 5.1)	0.9999
10 mmol NIP 4-VP-MMA	N/D	N/D	N/D	N/D
40 mmol MIP no FM	387.9 (+/- 16.2)	126.8 (+/- 2.1)	89.1 (+/- 3.7)	0.9999
10 mmol MIP no FM	400.4 (+/- 0.2)	159.3 (+/- 3.9)	92.0 (+/- 0.1)	0.9999
40 mmol NIP no FM	410.4 (+/- 1.2)	124.9 (+/- 4.4)	94.3 (+/- 0.3)	0.9999
10 mmol NIP no FM	399.4 (+/- 8.7)	169.2 (+/- 15.7)	91.8 (+/- 2.0)	0.9999

N/D = not determined.

C is a constant derived from the linear plot and it is exponentially related to the enthalpy of adsorption of the first layer [1].

N is the quantity of gas sorbed.

A correlation between the surface areas and the total quantity of gas sorbed (Table 2.4.) was identified; high surface areas were accompanied by larger volumes of gas sorbed. For the 10 mmol polymers formed using 4-VP and 4-VP-MMA as the functional monomers, the total quantity of gas sorbed was very low implying low surface areas and that the polymers did not retain porosity in the dry state. For materials with low surface areas it is recommended that an adsorptive such as krypton or xenon at liquid nitrogen temperature be used for analysis [19]. Thus, the method of nitrogen sorption utilised in this study is deemed inappropriate for the 10 mmol EGDMA polymers containing 4-VP.

With the exception of the polymers formed in the absence of functional monomer, the polymers containing 40 mmol EGDMA had a larger surface area than corresponding 10 mmol polymers. This is in agreement with previous studies where surface areas have been shown to decrease with decreasing crosslink ratios [17]. Higher surface areas are indicative of phase separation occurring at later stages of the polymerisation and the formed polymers are accompanied with smaller pore size distributions [39]. This may be due to the high levels of crosslinker which is responsible for interbonding of the growing agglomerates.

The amount of initiator in the polymer formulations remained constant as the concentration of crosslinker was reduced. Therefore, there was a larger number of free radicals available for a lower number of double bonds in the case of the 10 mmol polymers. The polymerisation reaction may then possibly proceed at a faster rate which would result in phase separation earlier, which is typically accompanied by a lower surface area.

There was no overall correlation identified between MIPs and NIPs. For the MAA polymers the NIPs had lower surface areas than MIPs for both the 40 and 10 mmol compositions. The same was true for the 40 mmol 4-VP polymers. The 40 mmol co-monomer MIP had a very low surface area in respect to the 40 mmol MAA and 4-VP while the NIP was substantially higher.

The surface areas for the 40 mmol 4-VP containing MIPs and NIPs were lower than those for the corresponding MAA polymers. They were however larger than those

measured for the 10 mmol MAA polymers. This would imply that they had pore properties in between those of the 40 and 10 mmol polymers. As the isotherms were classified differently, analysis of the pore data should be considered before reaching any conclusions.

The polymers formed in the absence of functional monomer had large surface areas. The high C values approaching 200 indicated the presence of a large amount of micropores, which would have contributed to the large surface areas. Statistically the difference between each composition was relatively small, regardless of the amount of crosslinking monomer. Similar results were reported where polymers formed as a monolith had higher surface areas when EGDMA was used independent of a functional monomer (methyl methacrylate in this case) [17].

2.3.3.3. Pore analysis

The data derived from the BJH analysis was corrected for multilayer adsorption using the Halsey thickness equation. The cumulative pore surface area, cumulative volume of pores and the average pore diameter are shown in Tables 2.6. The average pore diameter was calculated from Equation 2.6. [41].

$$\text{Average pore diameter} = 4 \times \frac{(\text{pore volume})}{(\text{pore surface area})} \quad \text{(Equation 2.6.)}$$

As to whether or not the adsorption or desorption branch is used is dependant on the hysteresis loop due to potential pore blocking effects [1]. For hysteresis of Type H2, the pore data must be derived from the adsorption region of the isotherm as the desorption region can lead to large inaccuracies. As the hysteresis loops did not close for any of the polymers under examination, the adsorption isotherms was chosen for analysis (the results are shown in Table 2.6.) It is interesting to note that the 10 mmol 4-VP and 4-VP-MMA polymers gave very low porosity features. However, as they were deemed unsuitable for analysis *via* this method their derived pore data will not be discussed further.

Table 2.6. BJH adsorption data obtained for pores between 2 and 300 nm using the Halsey thickness equation. Data is based on the average value for duplicate analysis.

Polymer	Cumulative surface area of pores (cm ³ g ⁻¹)		Cumulative volume of pores (cm ³ g ⁻¹)		Average pore diameter (nm)	
	MIP	NIP	MIP	NIP	MIP	NIP
40 mmol MAA	260.9 (+/-20.4)	289.6 (+/- 4.6)	0.481 (+/- 0.025)	0.606 (+/- 0.005)	7.4 (+/- 0.2)	8.4 (+/- 0.2)
10 mmol MAA	92.4 (+/- 14.5)	64.6 (+/- 4.9)	0.313 (+/- 0.022)	0.225 (+/- 0.022)	13.6 (+/- 1.2)	14.0 (+/- 2.4)
40 mmol 4-VP	204.8 (+/- 2.7)	142.4 (+/- 13.2)	0.233 (+/- 0.012)	0.174 (+/- 0.012)	4.6 (+/- 0.2)	4.9 (+/- 0.2)
10 mmol 4-VP	6.3 (+/- 1.1)	7.6 (+/- 1.2)	0.012 (+/- 0.001)	0.014 (+/- 0.001)	8.0 (+/- 2.1)	7.5 (+/- 0.7)
40 mmol 4-VP-MMA	67.1 (+/- 15.8)	206.0 (+/- 10.6)	0.103 (+/- 0.005)	0.218 (+/- 0.010)	6.3 (+/- 1.8)	4.2 (+/- 0.1)
10 mmol 4-VP-MMA	6.5 (+/- 1.3)	7.0 (+/- 0.1)	0.012 (+/- 0.004)	0.015 (+/- 0.001)	7.4 (+/- 0.9)	8.7 (+/- 0.3)
40 mmol no FM	271.0 (+/- 12.8)	286.7 (+/- 3.6)	0.359 (+/- 0.016)	0.382 (+/- 0.002)	5.3 (+/- 0.0)	5.3 (+/- 0.1)
10 mmol no FM	256.7 (+/- 2.1)	255.6 (+/- 9.4)	0.386 (+/- 0.001)	0.341 (+/- 0.011)	6.0 (+/- 0.1)	5.4 (+/- 0.0)

The average diameter for all polymers falls in the mesoporous region. The cumulative volume of pores for the 40 mmol 4-VP and 4-VP-MMA polymers were approximately half (or less) for corresponding MAA polymers. The average pore diameter was also less. The values were also smaller than the 10 mmol MAA polymers suggesting that overall they were less porous. The 10 mmol MAA polymers were less porous than corresponding 40 mmol polymers but they had a larger average pore diameter. This was potentially due to the higher percentage of porogen in the 10 mmol formulation which caused phase separation to occur quickly resulting in lower surface areas and a higher average pore diameter [18], or it may have been due to an increased polymerisation rate.

The polymers formed in the absence of functional monomer had similar pore properties regardless of the amount of crosslinking monomer used. They had similar cumulative pore areas to the 40 mmol MAA polymers, but the cumulative volume of pores was less, suggesting overall lower pore sizes.

The differential pore volume distributions for the 40 and 10 mmol MAA polymers are shown Figures 2.16. and 2.17., respectively.

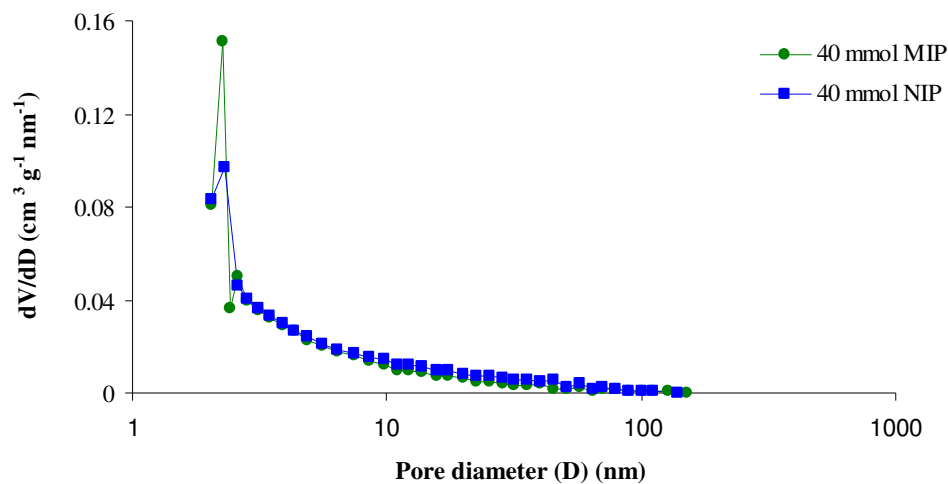


Figure 2.16. Pore volume distribution curves for 40 mmol MAA MIP and NIP

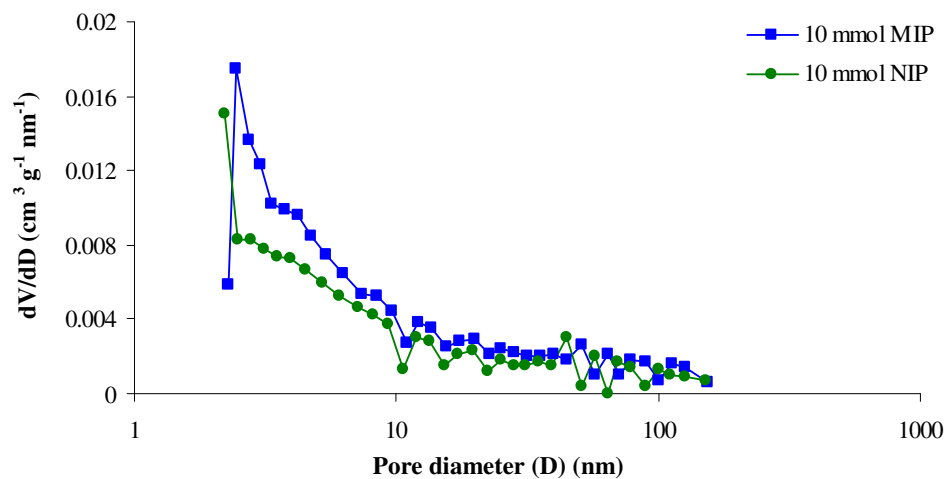


Figure 2.17. Pore volume distribution curves for 10 mmol MAA MIP and NIP.

The peak at approximately 3.5 nm was seen for all polymers and it has been suggested elsewhere that it is due to the presence of solvent molecules during the polymerisation [35]. The 40 mmol MAA polymers have a distribution that gradually tails off as it approaches the macroporous region. It reaches zero at approximately 50 nm (note the x-axis is in logarithmic scale). The 10 mmol polymers have a broader and less homogeneous distribution which spans into the low macroporous region, which was in line with the sorption isotherm. Overall both compositions are said to have a broad distribution.

Figure 2.18. shows the distribution curves for the 40 mmol MIPs for 4-VP and 4-VP-MMA. All polymers fall within the lower limits for mesoporosity. The distributions for the 4-VP containing polymers drops off gradually until approximately 15 nm. Overall they have a relatively narrow pore volume distribution. The polymers formed in the absence of functional monomer also had narrow distributions which reached zero at approximately 20-25 nm. The distributions for the polymers formed in the absence of functional monomer were more homogeneous than those displayed in Figure 2.18.

The 40 mmol 4-VP polymers had a distribution that was slightly more heterogeneous than the corresponding MAA polymers. The distribution for the MAA polymers was wider as it tailed off at approximately 50 nm, whilst the 4-VP polymer tailed off at approximately 15 nm.

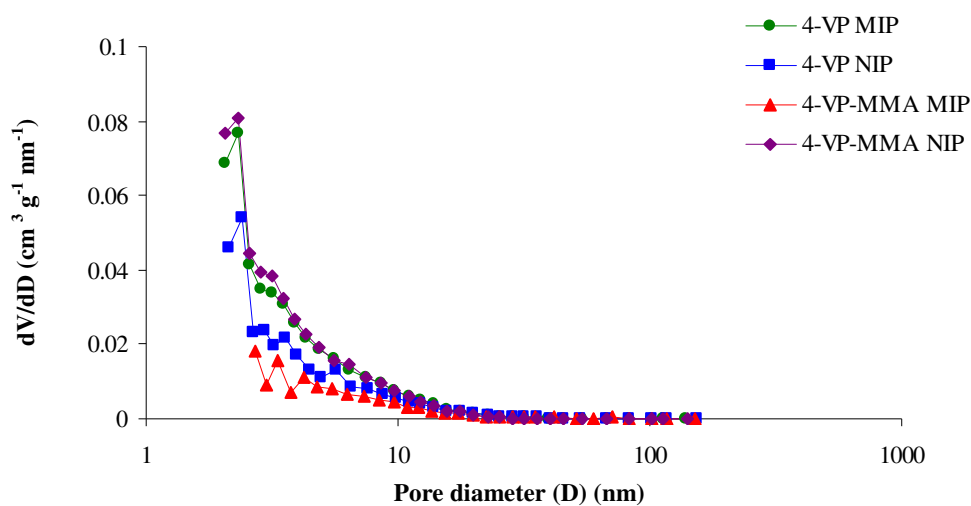


Figure 2.18. Pore volume distribution curves for 40 mmol 4-VP and 4-VP-MMA polymers.

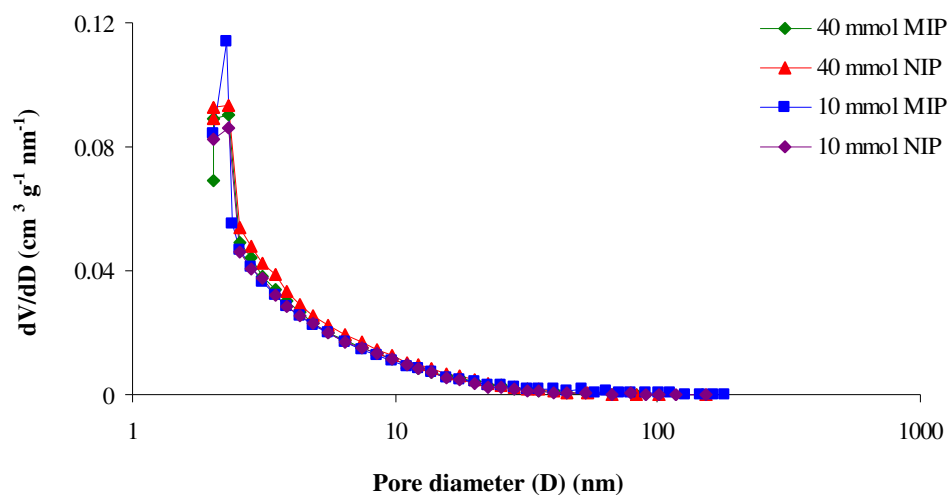


Figure 2.19. Pore volume distribution curves for 40 mmol and 10 mmol polymers formed in the absence of functional monomer.

2.3.4. Particle size distribution

Measurement of particle size distribution was carried out based on a laser diffraction technique. It is based on the principle that particles passing through a laser will scatter light at an angle that is inversely proportional to the particle size. The Mie theory, which predicts the light scattering of a particle of known size, was applied to the measured scattering pattern to generate a predicted scattering pattern or model. For the Mie theory to be accurate it requires that the refractive index of the material is known. The Mastersizer 2000 uses the Mie theory in reverse *i.e.* it knows the light scattering pattern generated for a given sample (measured), and if the refractive index of the material is known it calculates the particle size. A predictive model is generated in this manner and a comparison of fit is then made between the predicted model and the measured data. The weighted residual value is a measurement of goodness of fit; the lower the residual the better the fit. Typically this value should be less than 1 %.

As the refractive index was not known for the samples under study, the default value was edited post-measurement to improve the fit to the predicted model as illustrated in Figures 2.20 and 2.21. As the refractive index was not determined accurately for each

polymer sample, the results quoted are approximate values as opposed to absolute values.

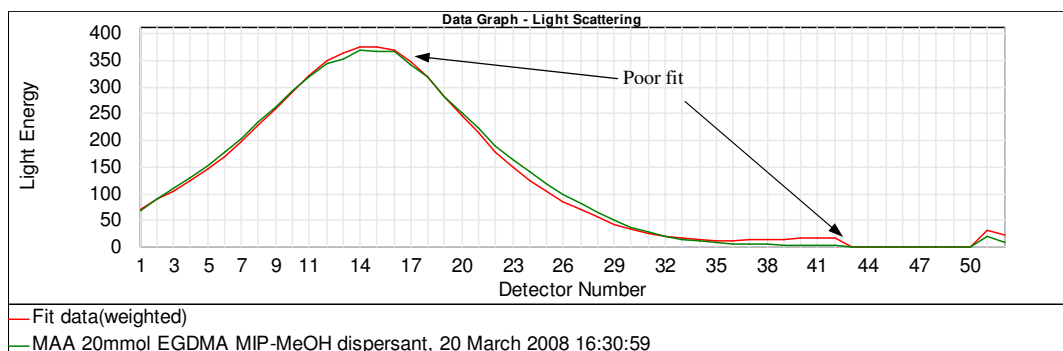


Figure 2.20. Example of a poor fit to the predicted model using the default refractive index value.

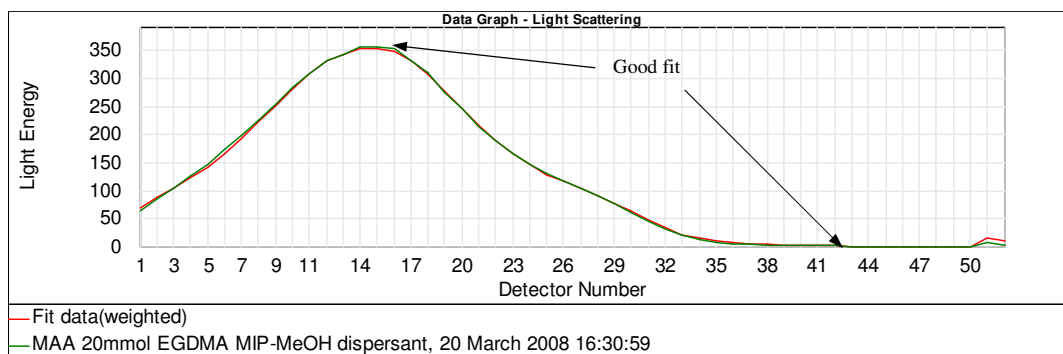


Figure 2.21. Example of a good fit to the predicted model using an adjusted refractive index value (same measurement as shown in Figure 2.20).

The polymers were synthesised as monoliths and were subsequently ground and sieved and the 25- 75 μm fractions were used for analysis. Figure 2.22. illustrates the particle size distribution results obtained for the MAA imprinted polymers

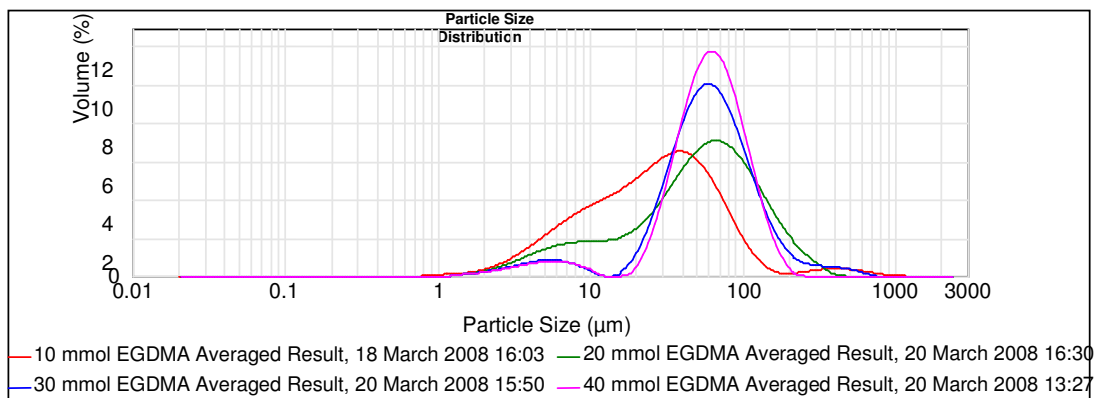


Figure 2.22. The particle size distributions obtained for MAA imprinted polymers (25- 75 µm fractions).

Analysis of the distributions showed a decrease in the particle size with decreasing EGDMA amount, which correlated with the images obtained by the SEM. An interesting feature from Figure 2.22. is that the distributions encompassed particles that were both greater and less than 25 – 75 µm (the particles which were collected and analysed), which was consistent with the SEM images. The presence of the larger particles can be attributed to the swelling effect of methanol on the polymers. As the distributions above were representative of particles swollen in methanol, it can be concluded that overall the 10 mmol composition contained particles of smaller sizes.

Table 2.7 lists the D (v, 0.1), D (v, 0.5) and D (v, 0.9) percentile values for the MAA polymers.

Table 2.7. D (v, 0.1), (v, 0.5) and (v, 0.9) values for MAA polymers, 25 – 75 μm, determined in methanol. Data is based on the average value for triplicate analysis.

	D (v, 0.1) μm	D (v, 0.5) μm	D (v, 0.9) μm
40 mmol MIP	25.2 (+/- 0.9)	53.3 (+/- 1.1)	102.8 (+/- 4.9)
40 mmol NIP	17.4 (+/- 2.1)	48.5 (+/- 3.1)	96.5 (+/- 10.7)
30 mmol MIP	23.1 (+/- 1.3)	54.4 (+/- 3.8)	119.9 (+/-18.5)
20 mmol MIP	7.4 (+/- 0.6)	46.2 (+/- 3.2)	115.23 (+/- 15.3)
10 mmol MIP	4.2 (+/- 0.1)	18.4 (+/- 4.6)	54.3 (+/- 12.0)
10 mmol NIP	5.9 (+/- 0.2)	25.1 (+/- 1.5)	60.1 (+/- 3.3)

The D (v, 0.1) and D (v, 0.5) values decreased with decreasing EGDMA amount (true for MIP and NIP polymers). This trend is illustrated in Figure 2.23. In general, NIP values were smaller than MIPs with the exception of the D (v, 0.9) for the 10 mmol composition. For the D (v, 0.9) is the value at which 90 % of the polymer is below that size and so the result are less significant.

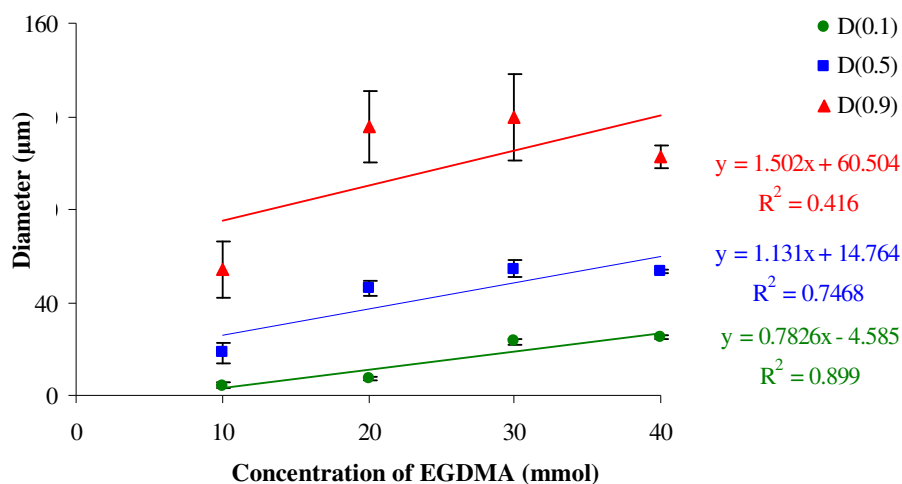


Figure 2.23. Plot of percentile values for MAA imprinted polymers formed from 40 -10 mmol EGDMA. Data is based on the average value for triplicate analysis.

Table 2.8. lists the percentile values for the 4-VP and 4-VP-MMA monomeric systems.

Table 2.8. D (v, 0.1), (v, 0.5) and (v, 0.9) values for 4-VP and 4-VP-MMA polymers, 25 – 75 μm , determined in methanol. Data is based on the average value for triplicate analysis.

	D (v, 0.1) μm	D (v, 0.5) μm	D (v, 0.9) μm
4-VP polymers			
40 mmol MIP	21.0 (+/- 1.0)	51.5 (+/- 0.5)	100.8 (+/- 6.7)
40 mmol NIP	21.3 (+/- 0.7)	52.7 (+/- 0.2)	104.8 (+/- 1.7)
10 mmol MIP	16.6 (+/- 0.5)	43.5 (+/- 0.5)	100.6 (+/- 2.1)
10 mmol NIP	7.7 (+/- 0.5)	37.1 (+/- 1.2)	75.6 (+/- 1.4)
4-VP-MMA polymers			
40 mmol MIP	21.2 (+/- 1.1)	49.5 (+/- 0.7)	104.9 (+/- 0.8)
40 mmol NIP	25.9 (+/- 1.2)	56.0 (+/- 2.6)	119.5 (+/- 13.5)
10 mmol MIP	13.9 (+/- 0.9)	41.3 (+/- 1.3)	83.5 (+/- 6.7)
10 mmol NIP	7.3 (+/- 0.2)	35.9 (+/- 0.4)	71.4 (+/- 0.7)

All percentile values decreased with decreasing EGDMA amounts. Between each monomeric composition, in general the 40 mmol composition percentile values were similar. The 10 mmol compositions did, however, deviate more, as shown in Figure 2.24 and 2.25. This then suggests at 10 mmol EGDMA, MAA MIPs resulted in particles with an overall smaller size distribution. The SEM images of the 10 mmol 4-VP containing polymers showed agglomerates of particles which appear to have dispersed in the methanol for the particle size measurements.

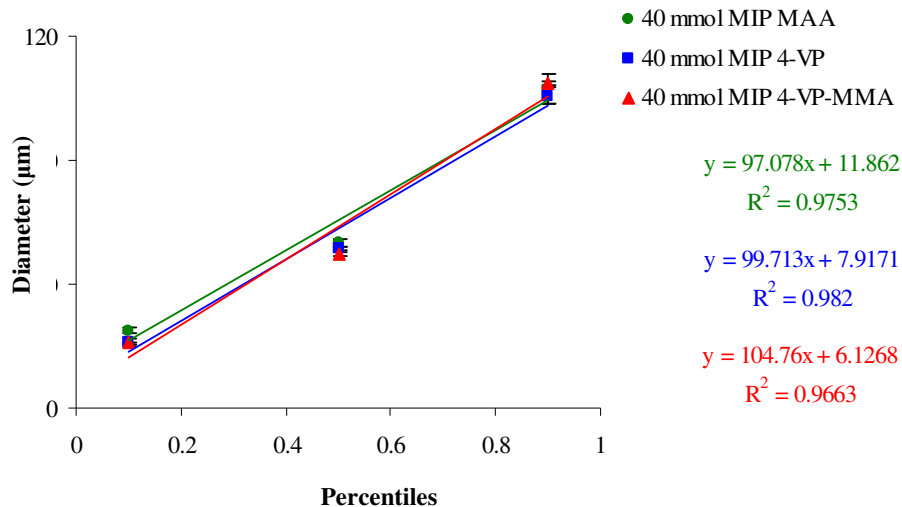


Figure 2.24. Particle diameter (μm) versus percentile values for 40 mmol imprinted polymers for each monomeric system. Data is based on the average value for triplicate analysis.

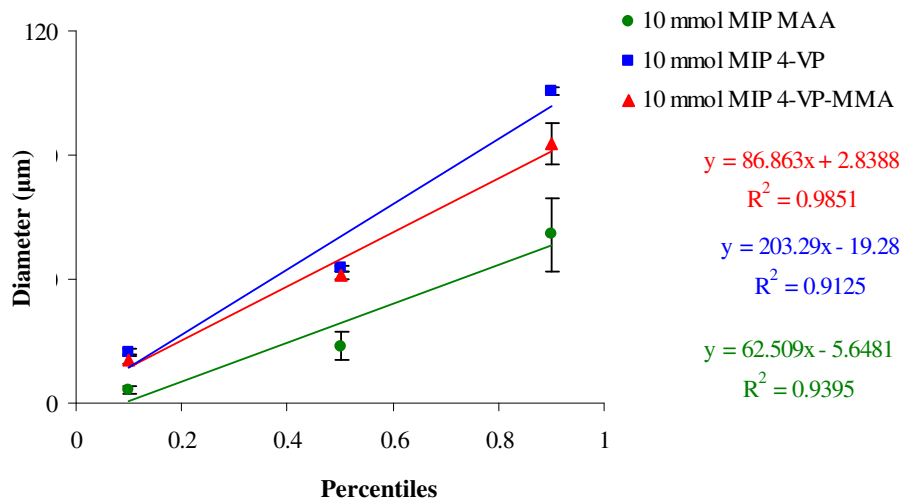


Figure 2.25. Particle diameter (μm) versus percentile values for 10 mmol imprinted polymers for each monomeric system. Data is based on the average value for triplicate analysis.

2.3.5. Solvent swell studies

As imprinted polymers are typically used in solvents, the swelling behaviour of the polymers was determined in chloroform, acetonitrile and methanol and the results are listed in Table 2.9.

Table 2.9. Swell ratio (Sr) for each of the polymers in chloroform, acetonitrile and methanol. Data is based on the average value for triplicate analysis.

Chloroform						
EGDMA (mmol)	MAA		4-VP		4-VP-MMA	
	MIP	NIP	MIP	NIP	MIP	NIP
40	8.7 (+/- 0.5)	8.4 (+/- 0.3)	6.8 (+/- 0.1)	6.7 (+/- 0.1)	4.3 (+/- 0.8)	4.4 (+/- 0.3)
30	8.7 (+/- 0.8)	9.5 (+/- 0.2)	8.2 (+/- 0.5)	7.1 (+/- 1.7)	7.1 (+/- 0.8)	6.5 (+/- 1.3)
20	12.4 (+/- 0.3)	12.4 (+/- 0.1)	10.9 (+/- 0.5)	10.9 (+/- 0.4)	8.2 (+/- 1.6)	6.7 (+/- 1.0)
10	20.4 (+/- 0.9)	19.7 (+/- 0.5)	14.1 (+/- 1.19)	13.0 (+/- 0.4)	14.6 (0.7)	13.4 (+/- 0.4)
Acetonitrile						
EGDMA (mmol)	MAA		4-VP		4-VP-MMA	
	MIP	NIP	MIP	NIP	MIP	NIP
40	4.3 (+/- 0.5)	4.4 (+/- 0.2)	3.4 (+/- 0.1)	3.4 (+/- 0.2)	3.4 (+/- 0.2)	3.2 (+/- 0.1)
30	4.4 (+/- 0.1)	5.0 (+/- 0.2)	3.8 (+/- 0.2)	3.9 (+/- 0.2)	4.8 (+/- 0.2)	3.9 (+/- 0.2)
20	5.9 (+/- 0.3)	6.2 (+/- 0.3)	4.7 (+/- 0.5)	4.9 (+/- 0.4)	4.7 (+/- 0.1)	4.9 (+/- 0.2)
10	11.1 (+/- 0.1)	9.4 (+/- 0.5)	8.6 (+/- 2.5)	5.6 (+/- 0.1)	6.8 (+/- 0.7)	6.1 (+/- 0.2)
Methanol						
EGDMA (mmol)	MAA		4-VP		4-VP-MMA	
	MIP	NIP	MIP	NIP	MIP	NIP
40	4.1 (+/- 0.3)	4.5 (+/- 0.1)	3.6 (+/- 0.4)	3.6 (+/- 0.3)	3.5 (+/- 0.1)	3.2 (+/- 0.1)
30	4.8 (+/- 0.2)	5.1 (+/- 0.1)	3.8 (+/- 0.1)	4.1 (+/- 0.2)	4.1 (+/- 0.1)	3.9 (+/- 0.7)
20	6.5 (+/- 0.2)	6.7 (+/- 0.1)	4.9 (+/- 0.1)	4.5 (+/- 0.7)	4.8 (+/- 0.2)	5.1 (+/- 0.1)
10	9.4 (+/- 0.2)	11.4 (+/- 0.2)	8.7 (+/- 0.9)	6.7 (+/- 0.2)	6.8 (+/- 0.3)	6.4 (+/- 0.1)

Chloroform swelled the polymers to a larger extent than acetonitrile or methanol. This was expected as chloroform was the porogen and would be expected to fill the pores in accordance with polymerisation conditions. The swelling was more pronounced for the MAA polymers particularly at the lower concentrations of EGDMA, as shown in Figure 2.26

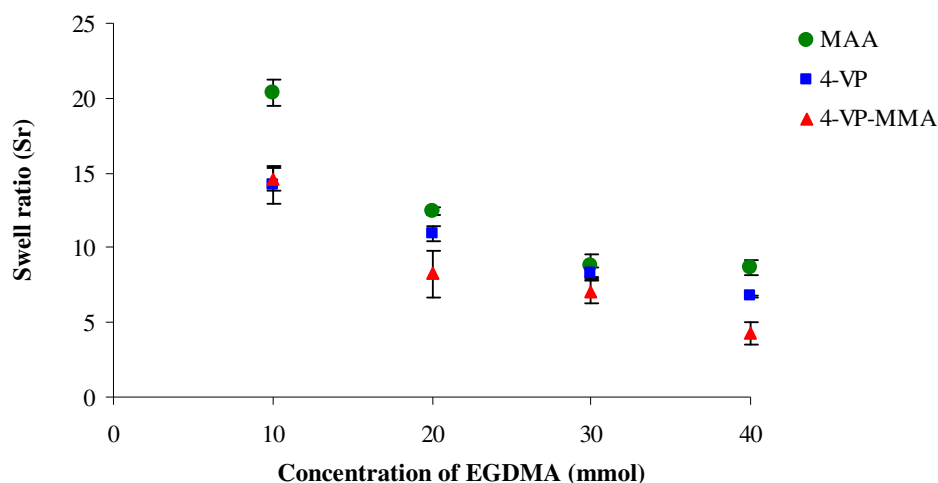


Figure 2.26. Swell ratio in chloroform for imprinted polymers. Data is based on the average value for triplicate analysis.

The polymers with higher surface areas had lower swell ratios. This was consistent with previous studies [36,42]. Higher swelling would be expected with lower crosslink ratios. Although the cumulative volume of pores was less for the polymers formed from lower amounts of EDGMA, the greater flexibility allowed greater solvent ingress to the pores. Thus, more of the pores may have been filled possibly causing greater expansion of the pores and the surrounding polymer network. The broader distribution of pore sizes for the 10 mmol MAA polymers must also be considered

2.4. Conclusions

A series of polymers with a range of physical properties were successfully synthesised by varying the amount of crosslinking monomer and the type of functional monomer employed. The polymers synthesised using 4-VP as the functional monomer formed different physical structures to those using MAA as the functional monomer. This suggests that different polymer forming processes occurred depending on the nature of the functional monomer. 4-VP which is more basic than MAA may have had a higher affinity for the porogen, chloroform, which is relatively non-polar (dielectric constant of 5). As a result phase separation of the growing polymer may have occurred at a later stage resulting in a higher conversion of monomers to polymer.

The pore volume for the 40 mmol 4-VP polymers was lower than MAA polymers. A higher rate of polymerisation could have resulted in this phenomenon, whereby the forming nuclei and growing microspheres agglomerated and fused at a quicker rate, resulting in a higher degree of polymerisation.

Reducing the amount of crosslinking monomer in the formulation resulted in a lower specific surface area for the polymers, as was determined for the MAA polymers. This could be attributed to an increased polymerisation rate as a result of a larger number of free radicals or to a higher level of porogen. The 10 mmol MAA MIP also had a smaller cumulative surface area of pores and a smaller cumulative volume of pores than the corresponding 40 mmol polymer. Therefore, the large degree of template removal may not be attributed solely to porosity, but to a potentially lower level of crosslinking and/or degree of polymerisation. The pore data was determined in the dry state and as the swelling studies suggested, the porosity may be different in the swollen state, and so the effect of methanol on the porous structure in the swollen state and its subsequent effect on the level of template removal must also be considered.

The template removal from the 10 mmol 4-VP polymers was minimal. A lower porosity and surface area was suggested for these polymers. This combined with a higher level of crosslinking relative to the MAA polymers (as indicated by the swell studies), may have contributed to the low levels of template removal.

In summary, the different polymeric structures obtained are attributed to the following:

- The amount of crosslinking monomer affected the interbonding between the polymer aggregates. Lower amounts of crosslinking monomer, combined with the higher levels of solvent (for the 10 mmol compositions) would have reduced coalescence of the growing aggregates relative to the 40 mmol polymers causing phase separation to occur quickly. This then would explain the wider pore distribution, lower surface area and higher solvent swelling.
- The solubility differences between the growing polymer and the mixture of unreacted monomer and solvent. Higher solubility differences would cause phase separation to occur sooner and would result in larger pore sizes.
- Increased polymerisation rates, due to the reactivity of the monomers and the number of free radicals in the system.

Overall the 4-VP polymers appear to have a more dense structure which can be attributed to closer packing of the polymer chains. This is based on the lower pore volumes, and ultimately free space within the polymer network, relative to corresponding MAA polymers. The physical characteristics which were determined in this chapter of work will be subsequently linked to the performance of the polymers in the following chapters.

References

1. Y. deMiguel, T. Rohr, and D. Sherrington, "Structure, morphology, physical formats and characterisation of polymer supports," *Polymeric materials in organic synthesis and catalysis*, M. R. Buchmeiser, ed., (Wiley-VCH, Weinheim, 2003), 1-52.
2. M. Kempe and H. Kempe, *Macromolecular Rapid Communications* **25**, 315-320 (2004).
3. N. Perez-Moral and A. G. Mayes, *Analytica Chimica Acta* **504**, 15-21 (2004).
4. Y. Li, Q. Fu, Q. Zhang, and L. He, *Analytical Sciences* **22**, 1355-1360 (2006).
5. L. Ye, P. Cormack, and K. Mosbach, *Analytical Chemistry*. **36**, 35-38 (1999).
6. L. Ye, R. Weiss, and K. Mosbach, *Macromolecules* **33**, 8239-8245 (2000).
7. L. Ye, P. Cormack, and K. Mosbach, *Analytica Chimica Acta* **435**, 187-196 (2001).
8. B. Sellergren, *Journal of Chromatography A* **673**, 133-141 (1994).
9. K. Nilsson, J. Lindell, O. Norrlov, and B. Sellergren, *Journal of Chromatography A* **680**, 57-61 (1994).
10. B. Sellergren, *Analytical Chemistry* **66**, 1578-1582 (1994).
11. K. Hosoya, K. Yoshizako, N. Tanaka, K. Kimata, T. Araki, and J. Haginaka, *Chemistry Letters* 1437-1438 (1994).
12. K. Hosoya, K. Yoshizako, Y. Shirasu, K. Kimata, K. Araki, N. Tanaka, and J. Haginaka, *Journal of Chromatography A* **728**, 139-147 (1996).
13. M. Komiyama, T. Takeuchi, T. Mukawa, and H. Asanuma, *Molecular Imprinting: from fundamentals to applications*, (Wiley Inter Science, 2003).
14. D. A. Spivak, *Advanced Drug Delivery Reviews* **57**, 1779-1794 (2005).
15. B. Sellergren and A. Hall, "Fundamental aspects of the synthesis and characterisation of imprinted network polymers," *Molecularly imprinted polymers. Man-made mimics of antibodies and their applications in analytical chemistry.*, B. Sellergren, ed., (Elsevier, Amsterdam, 2001), 21-55.
16. P. A. G. Cormack and A. Z. Elorza, *Journal of Chromatography B* **804**, 173-182 (2004).
17. B. P. Santora, M. R. Gange, K. G. Moloy, and N. S. Radu, *Macromolecules* **34**, 658-661 (2001).
18. D. Sherrington, *Chemical Communications* 2275-2286 (1998).
19. K. S. W. Sing, *Pure and Applied Chemistry* **54**, 2201-2218 (1982).

20. L.I. Andersson and K. Mosbach, *Journal of Chromatography* **516**, 313-322 (1990).
21. Z. Jie and H. Xiwen, *Analytica Chimica Acta* **381**, 85-91 (1999).
22. W. M. Mullett, M. F. Dirie, E. P. C. Lai, H. Guo, and X. He, *Analytica Chimica Acta* **414**, 123-131 (2000).
23. W. Cummins, P. Duggan, and P. McLoughlin, *Analytica Chimica Acta* **542**, 52-60 (2005).
24. W. Cummins, P. Duggan, and P. McLoughlin, *Biosensors and Bioelectronics* **22**, 372-380 (2006).
25. M. Kempe and K. Mosbach, *Journal of Chromatography A* **664**, 276-279 (1994).
26. M. Kempe, L. Fischer, and K. Mosbach, *Journal of Molecular Recognition* **6**, 25-29 (1993).
27. K. Haupt, A. Dzgoev, and K. Mosbach, *Analytical Chemistry* **70**, 628-631 (1998).
28. M. Jonatta, R. Weiss, B. Mizaikoff, O. Bruggemann, L. Ye, and K. Mosbach, *International Journal of Environmental Analytical Chemistry*. **80**, 75-86 (2001).
29. Y. Lv, Z. Lin, W. Feng, X. Zhou, and T. Tan, *Biochemical Engineering Journal* **36**, 221-229 (2007).
30. Arányi, P., Balázs, L., Balogh, M., Bata, I., Bátori, S., Nagy, L. T., Tímári, G., Boér, K., Finance, O., Kapui, Z., Mikus, E., Szamosvölgyi, Z., Szeleczky, G., and Urbán-szabó, K. Aminoquinoline and aminopyridine derivatives and their use as adenosine A3 ligands. 10/478721[US 6,969,723 B2]. 2005. United States.
31. S. Brunauer, P. H. Emmett, and E. Teller, *Journal of the American Chemical Society* **60**, 309-319 (1938).
32. P. A. Webb and C. Orr, *Analytical Methods in Fine Particle Technology*, 1st edition (Micromeritics Instrument Corp., 1997).
33. S. Lowell, J. Shields, M. Thomas, and M. Thommes, *Characterization of Porous Solids and Powders: Surface Area, Pore Size and Density.*, (Kluwer Academic Publishers., Dordrecht, The Netherlands., 2004).
34. E. P. Barrett, L. Joyner, and P. P. Halenda, *Journal of the American Chemical Society* **73**, 373-380 (1951).
35. J. L. Urraca, M. C. Carbajo, M. J. Torralvo, J. Gonzalez-Vazque, G. Orellana, and M. C. Moreno-Bondi, *Biosensors and Bioelectronics* **24**, 155-161 (2008).
36. V. P. Joshi, M. G. Kulkarni, and R. A. Mashelkar, *Journal of Chromatography A* **849**, 319-330 (1999).

37. S. A. Piletsky, E. V. Piletska, A. Guerreiro, I. Chianella, K. Karim, and A. P. F. Turner, *Macromolecules* **37**, 5018-5022 (2004).
38. J. Svenson, H. S. Andersson, S. A. Piletsky, and I. A. Nicholls, *Journal of Molecular Recognition* **11**, 83-86 (1998).
39. A. Guyot, "Synthesis and structure of polymer supports," *Synthesis and separations using functional monomers*, D. Sherrington and P. Hodge, eds., (Wiley and Sons, 1988), 1-42.
40. M. Thommes, "Physical adsorption characterization of ordered and amorphous mesoporous materials," *Nonporous materials-science and engineering*, G. Q. Lu and X. S. Zhao, eds., (Imperial college press, London, 2004), 317-364.
41. B. Sellergren and K. J. Shea, *Journal of Chromatography* **635**, 31-45 (1993).
42. Y. Lu, C. Li, X. Wang, P. Sun, and X. Xing, *Journal of Chromatography B* **804**, 53-59 (2004).

Chapter 3

General assessment of polymer affinity and specificity

3.1. Introduction

In recent years the interest in molecular imprinting has grown rapidly, and has seen a diverse range of template molecules attempted to be imprinted. This growing interest has been accompanied with a strive to merge what is now termed Molecular Imprinting Technology (MIT) with traditional or conventional selective phases, such as chromatographic stationary phases [1,2], sensors [3,4] and ligand binding assays [5].

To achieve maximum output, it is undoubtedly essential to have knowledge of the underlying factors pertaining to polymer performance and it is advised that each new polymerisation protocol be optimised. For example, the template, which is of critical importance to molecular imprinting, and the role it plays in the imprinting process has been extensively examined. Spivak demonstrated that shape selectivity exists in non-covalently imprinted polymers [6]. Twelve secondary amines with different sized side chains were imprinted, and enantioselectivity evaluated by HPLC for each amine on each imprinted polymer. Steric hinderance played a role in the obtained separation factors in cases where a molecules structure was too big to fit into an imprinted site formed from a smaller template molecule. In other words an “optimal spatial fit” existed which maximised the binding interactions.

Spectroscopic studies (UV, NMR and FTIR) on pre-polymerisation mixtures have been widely used in an attempt to determine an optimum ratio of template to functional monomer for imprinting a specific template [7-10]. This can result in maximum polymer performance in subsequent applications. While the effect of polymer composition has been examined in the past, the precise role of the physical nature of the final imprinted polymers on their chemical performance (in terms of affinity) is often overlooked.

In Chapter 2 a series of polymers tailored towards 2-aminopyridine (2-apy) were synthesised and a concise examination of the effect of composition on the physical nature of the polymers was carried out. The amount of crosslinking monomer combined with the type of functional monomer was found to produce polymers with different morphological properties. Based on those findings, the focus of this section of work was

to systematically examine the effect of polymer morphology on subsequent polymer affinity. This permitted examination of the critical parameters responsible for optimisation of a 2-apy selective phase. To achieve a better understanding of the interactions between the template and polymer within these systems the selectivity towards structural analogues and its sensitivity to the local chemical environment were also examined.

Although 2-apy has previously been imprinted using a methacrylic acid-co-ethyleneglycol dimethacrylate (MAA-co-EGDMA) matrix [11-13], and, the role of the 2-apy substructure on affinity and selectivity differences has been comprehensively examined [14], a detailed examination of affinity changes resulting from morphological variations has not previously been presented

3.2. Experimental

3.2.1. Materials, equipment and instrumentation

Materials

The polymers that were synthesised and subjected to template extraction as described in Sections 2.2.2. and 2.3.3. were used for this study with the addition of the following materials;

Table 3.1. The materials used.

Reagent	Supplier	Assay
2-Aminopyridine	Sigma-Aldrich (Ireland)	99 +%
3-Aminopyridine	Sigma-Aldrich (Ireland)	99 %
4-Aminopyridine	Sigma-Aldrich (Ireland)	99 +%
Chloroform	Lennox (Ireland)	99.0-99.4 %
Methanol	Lennox (Ireland)	99.8 %
Acetonitrile	Lennox (Ireland)	99.9 %
Molecular sieves	Sigma-Aldrich (Ireland)	3A 3.2 mm

Equipment and instrumentation

- Stuart scientific orbital incubator S150
- Sterile syringes: Omnifix ® Braun- Lennox Laboratory Supplies
- Syringe nylon filters: 0.4 µm, 13 mm diameter- Antech Technologies Ltd
- UV/Vis spectrometer: Cary 100- Varian (JVA Ireland Ltd)

3.2.2. Assessment of polymer affinity and specificity

Separate 50 mg quantities of MIP species and their corresponding reference polymers were weighed into 10 mL volumetric flasks (*). Five mL of 0.2 mM of binding species (2-, 3- or 4-apy, see Figure 3.1.) in chloroform, acetonitrile or methanol were separately added to the polymers. Flasks were stoppered and equilibrated in a Stuart Scientific Orbital Incubator S150 at 25 °C for 16 h. Polymer solutions were then filtered using Omnifix 10 mL syringes fitted with OEM syringe nylon filters (0.45 µm). The quantity

of reloaded binding substrate bound to the polymer, B (see Equation 3.1), was determined by UV/VIS spectroscopic analysis of the post equilibrium solution at the pre-determined wavelength (approximately $\lambda_{\text{abs}} \approx 290$ nm for 2- and 3-apy and $\lambda_{\text{abs}} \approx 240$ nm for 4-apy depending on the solvent). The average values of triplicate independent results were obtained.

$$B = T - F \quad \text{(Equation 3.1.)}$$

Where B = amount of substrate bound to the polymer,
 T = the initial amount of substrate added to the polymer,
 F = the amount of free substrate in solution after equilibration.

The imprinting factor, IF which expresses the relationship between specific and non-specific binding, was calculated as follows [15]:

$$IF = B_{\text{MIP}} / B_{\text{NIP}} \quad \text{(Equation 3.2.)}$$

Where B is the amount of substrate bound to the polymer (as determined from equation 3.1). By determining the IF for polymers information on the affinity of the polymers is generated.

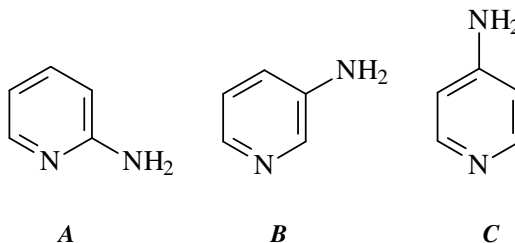


Figure 3.1. Structures of A; 2-apy, B; 3-apy, C; 4-apy.

* Affinity was determined for all polymers with the exception of those formed in the absence of functional monomer as the amount of analyte bound, B , could not be determined due to high levels of bleed from the polymers.

3.3. Results and discussion

3.3.1. Specificity of methacrylic acid polymers

To determine the success of the imprinting process and to examine the relationship between polymer morphology and affinity (and its subsequent dependence on solvent polarity), a general assessment of polymer affinity was carried out by reloading 0.2 mM 2-apy in chloroform, acetonitrile and methanol onto the polymers. This concentration was chosen as it had previously been used for the assessment of 2-apy and other template molecules containing the 2-apy sub-structure that were all imprinted using an MAA-co-EGDMA polymeric phase [14], and it corresponded to 12 % reloading of the theoretical number of binding sites.

Analysis of the binding results obtained (Figure 3.2.) shows that the binding affinity of the polymers towards 2-apy in the various solvents decreased in the order of chloroform < acetonitrile < methanol. In all cases, MIPs demonstrated a higher affinity for 2-apy over their corresponding NIP polymers, *i.e.* an imprinting effect was observed.

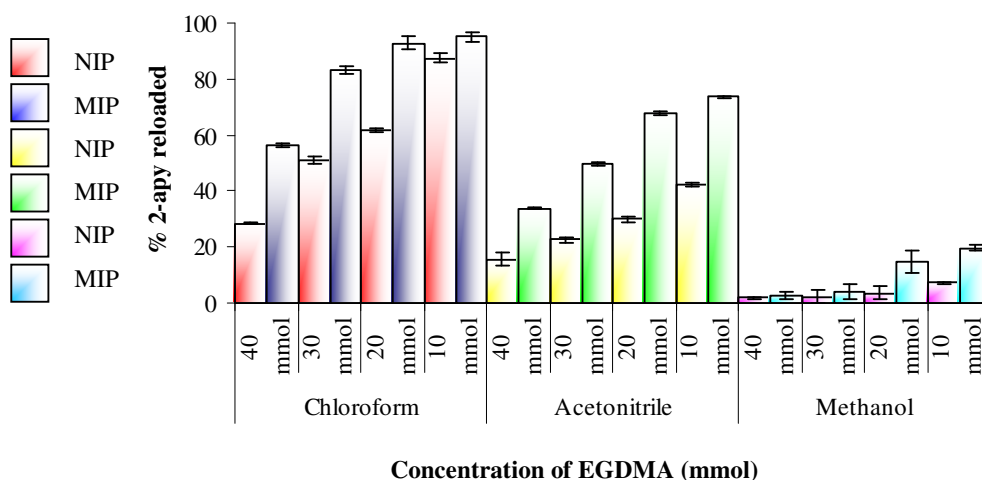


Figure 3.2. Binding results obtained for reloading 2-apy in chloroform, acetonitrile and methanol onto 2-apy imprinted polymers (methacrylic acid as the functional monomer). Errors are based on +/- 1 standard deviation for triplicate analysis.

It has been suggested [10-14] that the mechanism for interactions between 2-apy and methacrylic acid (MAA) is predominately based on polar co-operative hydrogen bonding interactions, with the amino group acting as a proton donator and the pyridyl nitrogen acting as a proton acceptor (Refer to Figure 2.3.). Therefore, non-polar solvents such as chloroform would not compete with the monomer for hydrogen bonding with the template. A more polar solvent, on the other hand, would be expected to disrupt these interactions and reduce the degree of binding. The polarity of the solvents, in terms of dielectric constant, ϵ , and the hydrogen bonding capability, HBC, of the solvents are listed in Table 3.2. The HBC is expressed as a hydrogen bond term (δ_h) and also as a measure of the hydrogen bond capacity (H bond) [16,17].

Table 3.2. The polarity (ϵ) and hydrogen binding capability (HBC) of the solvents employed in polymer reloading [16,17].

Solvent	Dielectric constant E	HBC	
		(δ_h)	H bond
Chloroform	4.8	5.7	Poor
Acetonitrile	36.2	6.1	Poor
Methanol	35	29.3	Strong

As acetonitrile is slightly more polar than methanol, the lower capacity observed in methanol (Figure 3.2) can be attributed to the hydrogen bonding capability of the solvent as oppose to the polarity. Chloroform is the least polar of the solvents and is also least capable of forming hydrogen bonds. Therefore, it is expected that the highest capacity was displayed when reloading was carried out in it.

It has been suggested by Spivak that the optimum chromatographic performance of an imprinted polymer is obtained using a mobile phase similar to that of the porogen [18]. It was proposed that this was due to the position of the functional groups of the binding sites which were locked into position during polymer formation, and were swelled to different degrees in different solvents during subsequent polymer analysis. This in turn resulted in differences in the shape and distance of the functional groups (or the fidelity of the sites), and that the porogen swelled the polymers so as to mimic the interactions

pre-and during polymerisation. This may also be a contributing factor to the results shown in Figure 3.2. as chloroform was the porogen employed in polymer synthesis. The study by Spivak also demonstrated by synthesising the same polymer using different porogens that the effect of solvent, or porogen, swell on the fidelity of the sites was more significant than the polarity of the solvents when assessing the chromatographic retention behaviour of the polymers.

Although the degree of swell for the polymers varied for each of the solvents depending on the composition, each corresponding MIP and NIP polymer displayed similar swell ratios (Section 2.3.5.). Therefore, the increased binding of MIP over NIP can be attributed to the presence of specific binding sites. Figure 3.3. shows the relationship between the percentage reloading and swell ratio, both in chloroform, for MIP and corresponding NIP species. As the swelling ratio for the 40 and 30 mmol polymers was similar, the increased binding of the 30 mmol composition can be attributed to a more flexible polymer and a greater number of free carboxyl groups relative to the 40 mmol composition.

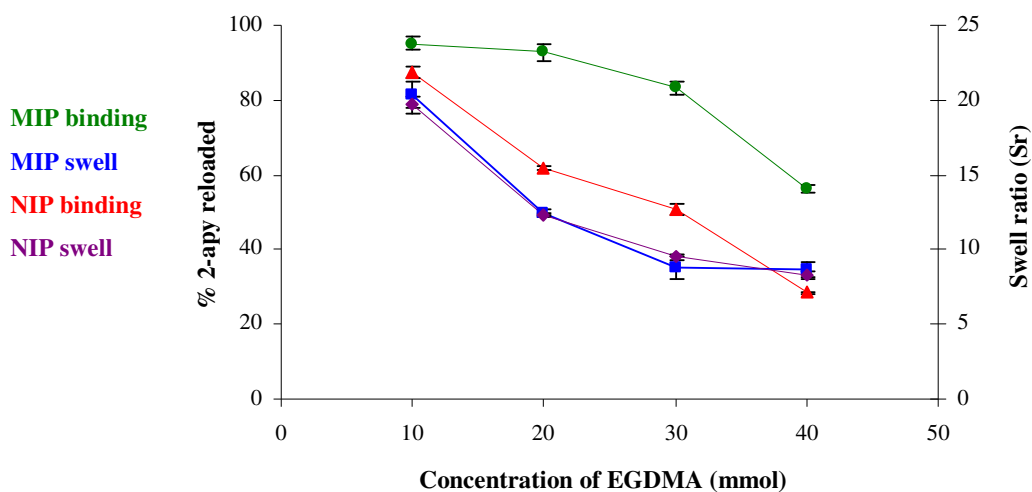


Figure 3.3. The relationship between 2-apy binding and the swell ratio in chloroform for MIP and corresponding NIP polymers.

The relationship between the affinity and the cumulative volume of pores for the 40 and 10 mmol MIPs and NIPs are illustrated in Figure 3.4. There is an inverse relationship between the cumulative volume of pores and the affinity. Increased affinity is observed

with decreased pore volume. Therefore, it is suggested that the increased affinity is due to the flexibility of the polymers in chloroform.

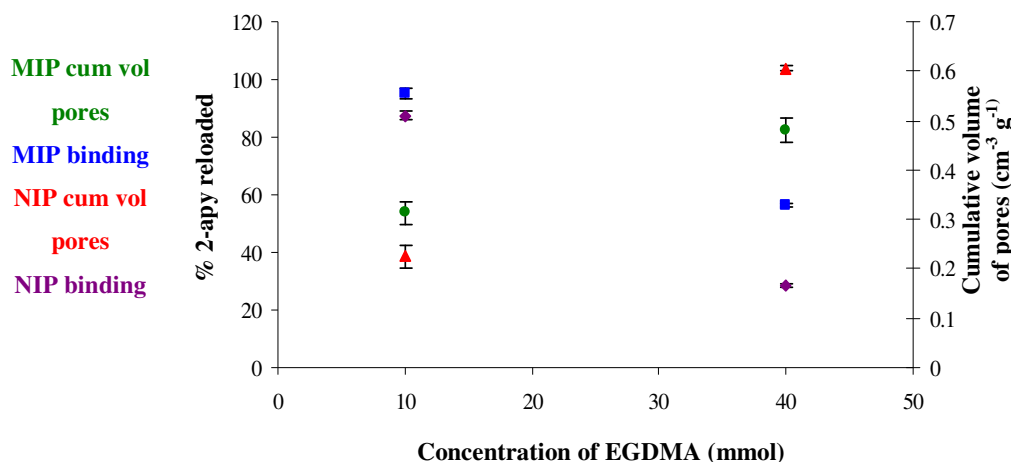


Figure 3.4. The relationship between 2-apy binding and the cumulative volumes of pores (cum vol pore) in chloroform for 40 and 10 mmol MIPs and NIPs.

A higher degree of non-specific binding was encountered in chloroform. Analysis of the binding characteristics in acetonitrile and methanol showed a disruptive effect in both specific and non-specific binding, as both had the ability to compete with MAA for the formation of hydrogen bonds with 2-apy. The effect of solvent swell (Refer to Section 2.3.5.) on the physical structure of the polymers should also be considered when comparing affinity in the three solvents, as increased solvent ingress may have resulted in increased site accessibility. While the binding capacity of the polymers was found to increase as the concentration of crosslinking monomer decreased, chloroform exhibited the most dramatic effect on polymer specificity. The observed reduction in specificity can be attributed to a combination of the porosity characteristics, increased polymer flexibility (which may have resulted in poor binding site integrity) and the effect of solvent swell, as previously discussed in Chapter 2.

Another parameter in terms of the physical differences of the polymers which must be considered when examining polymer affinity is the average particle size distribution. The average particle diameter was found to decrease with decreasing EGDMA concentrations (40 mmol MIP \approx 53 μ m, 10 mmol MIP \approx 18 μ m). Therefore, those polymers formed from lower amounts of EGDMA had a larger surface area available

for analyte binding (per 50 mg of polymer- the quantity used for affinity assessment), which may also have contributed to the affinity shown in Figure 3.2. The differences in particle size distributions were confirmed by using a particle size analyser (Section 2.3.4.) and also by obtaining SEM images of the polymers (Section 2.3.2.).

The capacity of the polymers increased as the concentration of crosslinking monomer decreased. However specificity also decreased. The higher degree of non-specific binding may be attributed to one of two reasons. Firstly, varying the concentration of crosslinker while maintaining a fixed concentration of functional monomer yielded a series of polymers whereby the mole ratio of MAA to EGDMA changed. It is presumed that polymers formed from a lower amount of EGDMA had a large proportion of functional monomer that may not have been directly or fully incorporated into the crosslinked polymer network. As a result, the extra functionality increased the degree of non-specific binding. The flexible nature of the polymer matrix allowed access to the available functionality not incorporated into the polymer network. Secondly, as the concentration of crosslinking monomer present in the pre-polymerisation mixture decreased, the polymer that was formed may not have been heavily crosslinked, thus forming a polymer that was so flexible binding sites were easily accessible. Alternatively, the low concentrations may not have been sufficient to “freeze” pre-polymerisation complexes in place during the polymerisation reaction, and thus potential binding sites may have been destroyed, or sites with a range of affinities and integrities may have formed; also adding to the non-specific nature of the polymers.

The percentage of initiator in the final polymer composition increased as the concentration of EGDMA was reduced. It was demonstrated by Piletsky *et al.* [19] that increasing the concentration of initiator in a polymerisation mixture can have detrimental effects on the molecular recognition properties of the resultant polymer due to excess heat generated from the additional initiator. The increased temperature would disrupt the monomer-template interactions during the polymerisation. This is also thought to be contributing factor to the loss of specificity observed in the 10 mmol polymers, albeit minor in comparison to the degree of crosslinking.

When analysing polymer specificity in terms of the imprinting factor, IF (Table 3.3.), it is apparent that the polymers, in general, displayed the best IF values when binding was assessed in acetonitrile. While the overall polymer capacity was reduced in acetonitrile, the improved IF values suggested that acetonitrile competed with non-specific binding to a larger degree than specific binding within imprinted sites, relative to chloroform.

Table 3.3. IF (or specificity factors) obtained for reloading 2-apy in chloroform, acetonitrile and methanol onto 2-apy imprinted polymers (MAA as the functional monomer). Errors are based on +/- 1 standard deviation for triplicate analysis.

EGDMA (mmoles)	CHCl₃	ACN	MeOH
40	1.97 (+/- 0.05)	2.14 (+/- 0.32)	1.61 (+/- 0.17)
30	1.64 (+/- 0.08)	2.21 (+/- 0.14)	1.91 (+/- 0.95)
20	1.50 (+/- 0.05)	2.27 (+/- 0.08)	4.12 (+/- 1.09)
10	1.09 (+/- 0.03)	1.75 (+/- 0.08)	2.75 (+/- 0.42)

In acetonitrile the IF values remained constant, within experimental error, as the concentration of crosslinking monomer decreased from 40 to 20 mmol. This result contrasted with that of chloroform, where the IF decreased as the concentration of EGDMA decreased. The trend observed in chloroform was expected as a reduction in EGDMA would result in a decrease in discrimination between MIP and NIP. The effect of acetonitrile on the swelling properties of the polymers, as shown in Section 2.3.5., suggested that it was unable to swell the pores to the same extent as chloroform, thereby retaining the shape and integrity of the binding cavities. This trend then accounts for the IF results obtained in acetonitrile. The decrease in specificity observed with 10 mmol EGDMA may be ascribed to the flexible nature and increased porosity, which may have permitted intrinsic access to the polymer network. The IF obtained for 10 mmol EGDMA (1.75, +/- 0.08) in acetonitrile was between that obtained for 40 and 30 mmol EGDMA (1.97, +/- 0.05, and 1.64, +/- 0.08, respectively) when binding was assessed in chloroform. This result also emphasised the point that although polymers prepared from 10 mmol EGDMA had a different morphology and flexibility to those polymers prepared from 40 or 30 mmol crosslinker, the solvent played a critical role on the

swelling properties of the polymer. This in turn may have had a dramatic effect on the integrity of the binding sites and ultimately the polymer performance.

In methanol the IF increased with decreasing EGDMA concentration (40-20 mmol). Binding onto the polymers formed from 20 mmol EGDMA produced the highest IF value (4.12, +/- 1.09) for all of the solvents employed. As methanol is capable of forming strong hydrogen bonds (Refer to Table 3.2.) this result was unexpected. However, it does suggest that methanol has the ability to disrupt non-specific binding to a higher degree than specific binding in such MAA polymers. The lower binding capacity may also be linked to the lower swelling capability of methanol. While binding in a certain solvent for a particular polymer composition may produce the highest specificity, it may not be the optimum condition as the overall capacity values must also be considered.

3.3.2. Selectivity of methacrylic acid polymers

Selectivity of 2-apy imprinted polymers was assessed by reloading two structural analogues, 3- and 4-apy. As these three compounds are isomers, their structures differ only in the position of the substituted amine group relative to the pyridine nitrogen. The effect of solvent HBC on selectivity was also investigated by reloading in chloroform, acetonitrile and methanol. Figures 3.5 and 3.6. illustrate the binding results obtained.

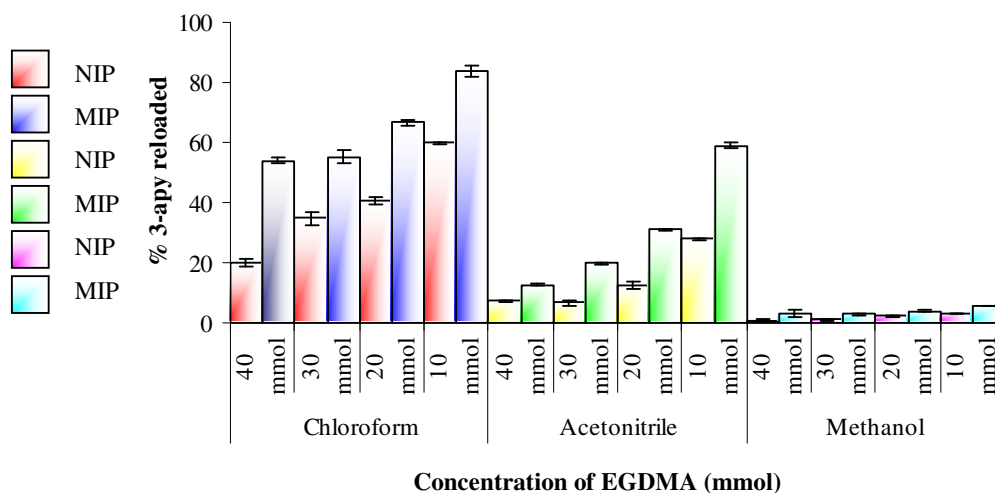


Figure 3.5. Binding results obtained for reloading 3-apy and chloroform, acetonitrile and methanol onto 2-apy imprinted polymers (MAA as the functional monomer). Errors are based on +/- 1 standard deviation for triplicate analysis.

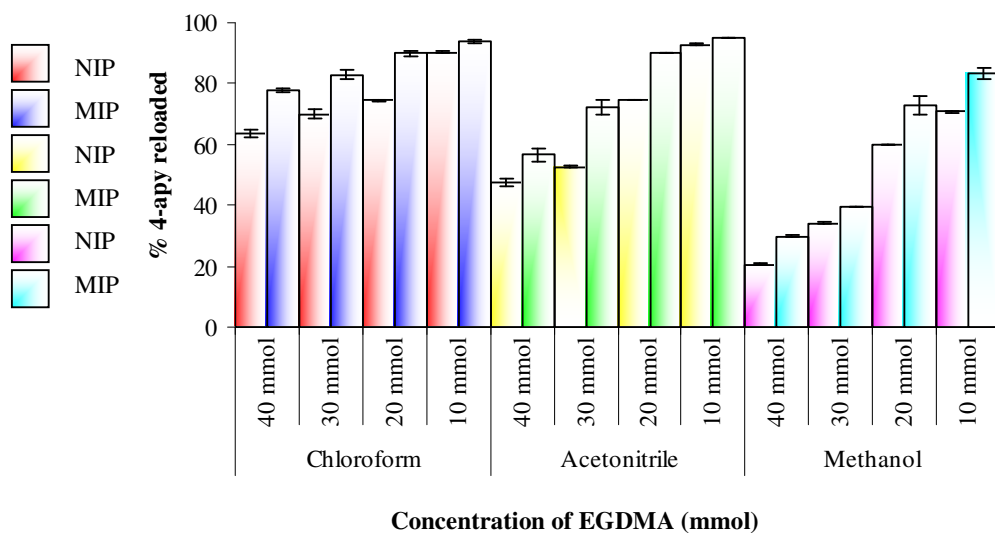
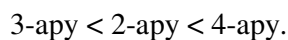


Figure 3.6. Binding results obtained for reloading 4-apy and chloroform, acetonitrile and methanol onto 2-apy imprinted polymers (MAA as the functional monomer). Errors are based on +/- 1 standard deviation for triplicate analysis.

A general trend that is apparent for binding of the three isomers is that the binding or affinity of the polymers towards the ligands increased in the order of:



As with specificity, polymer selectivity was influenced by composition, morphology, solvent nature and solvent swell. However, another parameter that must be considered is the pK_a of the binding analyte. The difference in binding characteristics can be attributed to the difference in basicity of the three isomers, which can be explained by their resonance structures, Figure 3.7 [12]. The resonance structures show the importance of where the negative charge lies in each isomer with respect to the pyridine nitrogen. The negative charge delocalises to the pyridine nitrogen within 2- and 4-apy, but in 3-apy it delocalises to a carbon atom. Nitrogen is more capable of facilitating this excess charge than carbon, and therefore, 4-apy is more basic than 2-apy which is more basic than 3-apy. As the basicity, or pK_a values increase, the strength of ionic interactions between the carboxyl groups of the functional monomer and the pyridine nitrogen of the isomer also increases.

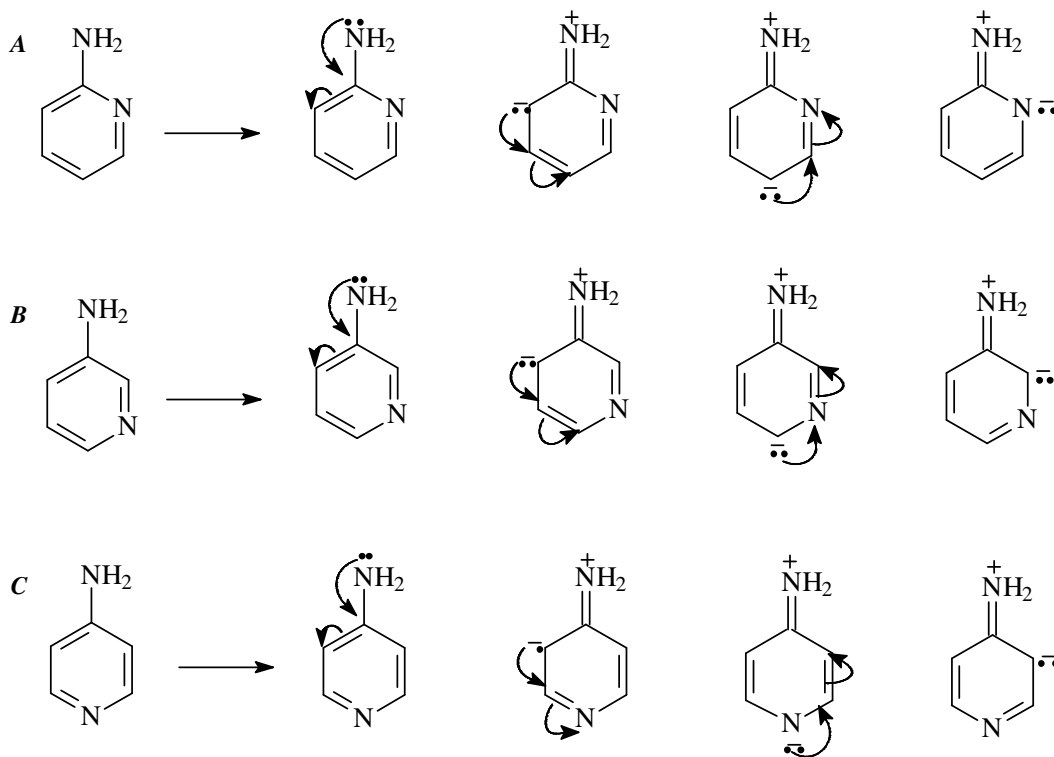


Figure 3.7. Resonance structures of A; 2-apy, B; 3-apy and C; 4-apy.

The non-specific binding data in chloroform, acetonitrile and methanol is presented in Table 3.4. Plots of pK_a values for 2-, 3- and 4-apy versus non-specific binding for the various polymer compositions, when binding was assessed in chloroform, acetonitrile and methanol are shown in Figures 3.8., 3.9. and 3.10. Examination of the non-specific binding allowed for an assessment of the relationship between the chemical properties of the binding ligand to that of the actual physical nature of the polymers arising from the differences in initial polymer composition.

Table 3.4. Non-specific binding values (% analyte bound) obtained for reloading 3-, 2- and 4-apy in chloroform, acetonitrile and methanol onto 2-apy imprinted polymers (MAA as the functional monomer). Data based on average values for triplicate analysis.

EGDMA (mmoles)	3-apy (pK_a 6.16)			2-apy (pK_a 6.72)			4-apy (pK_a 9.13)		
	CHCl ₃	ACN	MeOH	CHCl ₃	ACN	MeOH	CHCl ₃	ACN	MeOH
40	20.1	7.2	0.9	28.5	15.7	1.7	63.8	47.5	20.5
30	34.7	6.8	1.0	50.7	22.5	2.2	69.9	52.7	34.2
20	40.6	12.4	2.2	61.8	29.9	3.6	74.4	74.6	59.8
10	59.7	28.1	3.0	87.5	42.1	7.1	90.4	92.9	70.8

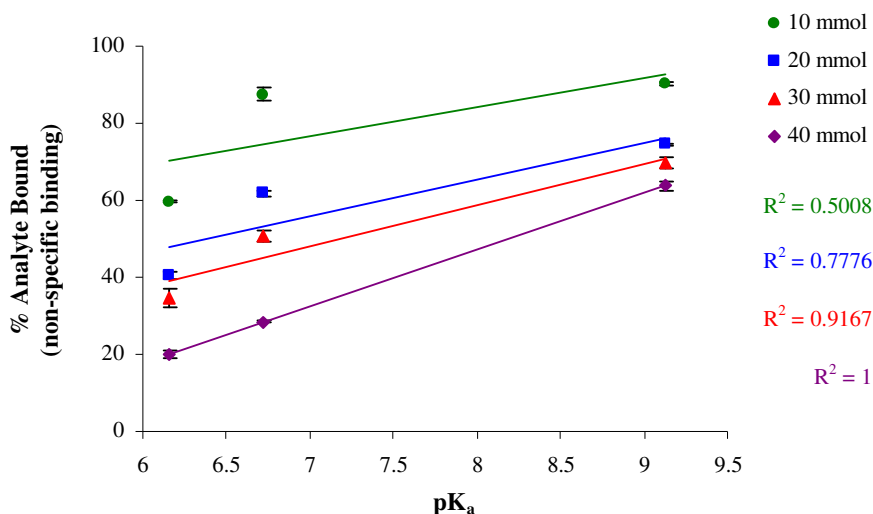


Figure 3.8. pK_a versus non-specific binding in chloroform for non-imprinted polymers (MAA as the functional monomer) prepared with different concentrations of EGDMA (40-10 mmol). Errors are based on +/-1 standard deviation for triplicate analysis.

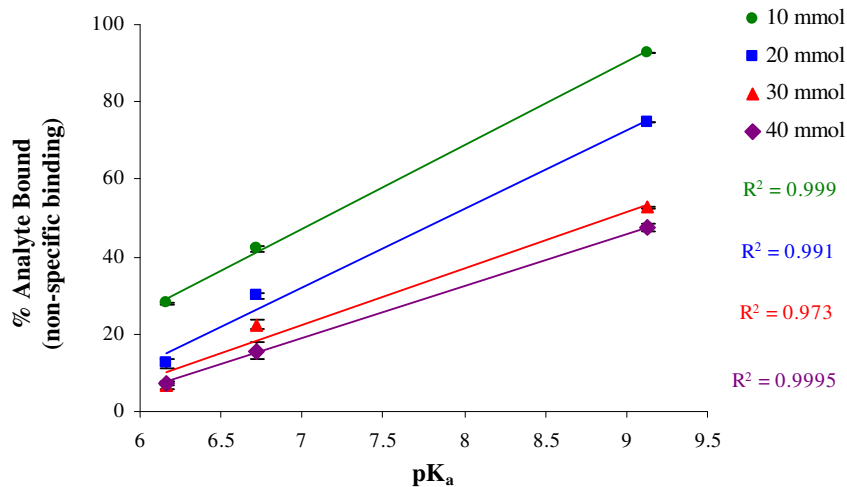


Figure 3.9. pK_a versus non-specific binding in acetonitrile for non-imprinted polymers (MAA as the functional monomer) prepared with different concentrations of EGDMA (40-10 mmol). Errors are based on ± 1 standard deviation for triplicate analysis.

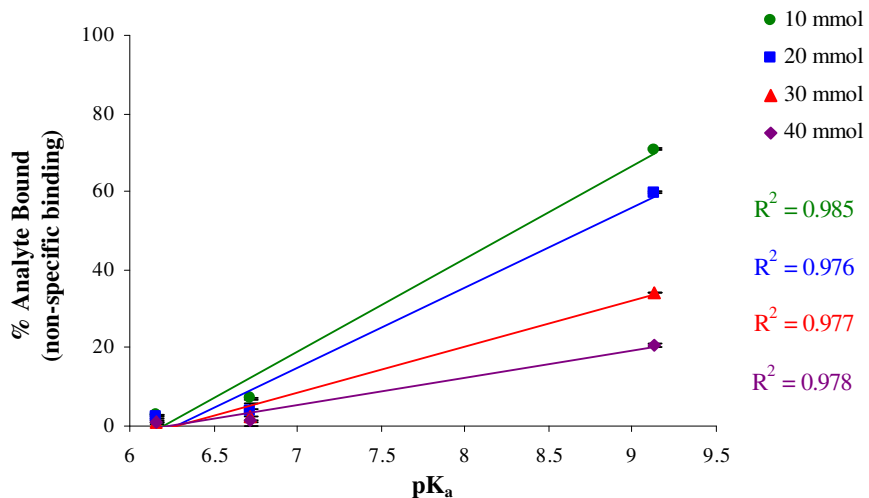


Figure 3.10. pK_a versus non-specific binding in methanol for non-imprinted polymers (MAA as the functional monomer) prepared with different concentrations of EGDMA (40-10 mmol). Errors are based on ± 1 standard deviation for triplicate analysis.

3-apy had the lowest pK_a value, 6.16. As a result it was unable to bind to the acidic moiety of the functional group to the same degree as 2-apy (6.72) or 4-apy (pK_a 9.13),

thereby reducing the capacity. As the hydrogen bonding capability of the binding solvent increased, the degree of binding decreased. In general, binding of 2-apy and 3-apy was much less in methanol than in chloroform and acetonitrile. However, 4-apy due to its higher basicity had the ability to form stronger ionic interactions with the COOH groups of the polymer. The HBC of the methanol was insufficient to overcome the strength of the interactions between 4-apy and the carboxyl residues of the polymeric matrix, hence the high degree of binding.

Overall it can be deduced from Figures 3.8.- 3.10 that in general a linear correlation between non-specific binding due to pK_a was observed for the polymers. This correlation was most pronounced for the rigid polymers, and it diminished with decreasing EGDMA amounts. The linear relationship was also affected by the nature of the reloading solvent and was found to be more sensitive in chloroform which had a lower hydrogen bonding capability and had a higher swelling effect on the polymers. The linear correlation observed in chloroform decreased with decreasing EGDMA amounts.

Cummins *et. al.* [13] analysed a 2-apy imprinted polymer (formed using a ratio of MAA to EGDMA of 4:30) by packing it into a solid-phase extraction cartridge (SPE). 4-apy in chloroform or acetonitrile was reloaded onto two separate cartridges and was subsequently eluted under vacuum using 3 mL aliquots of the reloading solvent, which was analysed by UV/VIS spectroscopy. In chloroform 3.6 % was eluted from the imprinted polymers by extraction 20 while 0.8 % was eluted in acetonitrile. This compared with 52.5 % and 84.4 % for elution of 2-apy in chloroform and acetonitrile, respectively. Following the first 20 extractions in the mentioned solvents the remainder of the extractions were carried out in methanol which eventually facilitated the removal of 4-apy from the polymers. 100 % 4-apy removal was not achieved. The findings reported by Cummins are similar to those mentioned here. However, the data presented in this instance demonstrates the significance of the physical (morphology) properties of the polymers and the impact exhibited by the nature of the solvent used.

The binding for 2- and 4-apy onto the 40 and 10 mmol imprinted polymers in chloroform is seen in Table 3.5.

Table 3.5. The percentage of 2- and 4-apy reloaded in chloroform onto 40 and 10 mmol imprinted polymers (MAA as the functional monomer).

EGDMA	2-apy (% reloaded)	4-apy (% reloaded)
40 mmol	56.3 (+/- 0.8)	77.9 (+/- 0.7)
10 mmol	94.8 (+/- 1.8)	93.7 (+/- 0.5)

At the 40 mmol concentration, binding due to the cooperative two point interaction between analyte and methacrylic acid (MAA) was eclipsed by pK_a . In other words the functionality within the binding cavity was in the correct spatial arrangement for 2-apy as opposed to 4-apy, Figure 3.11. Thus, the higher degree of binding observed for 4-apy can be attributed to its pK_a value as opposed to the small degree of steric hindrance proposed in Figure 3.11.

This trend diminished for the 10 mmol composition where the binding of 2- and 4- apy were the same within experimental error. This may have been due to a reduction in binding site integrity or fidelity due to insufficient crosslinker to maintain the 2-apy-MAA complexes in the pre- and early polymerisation stages.

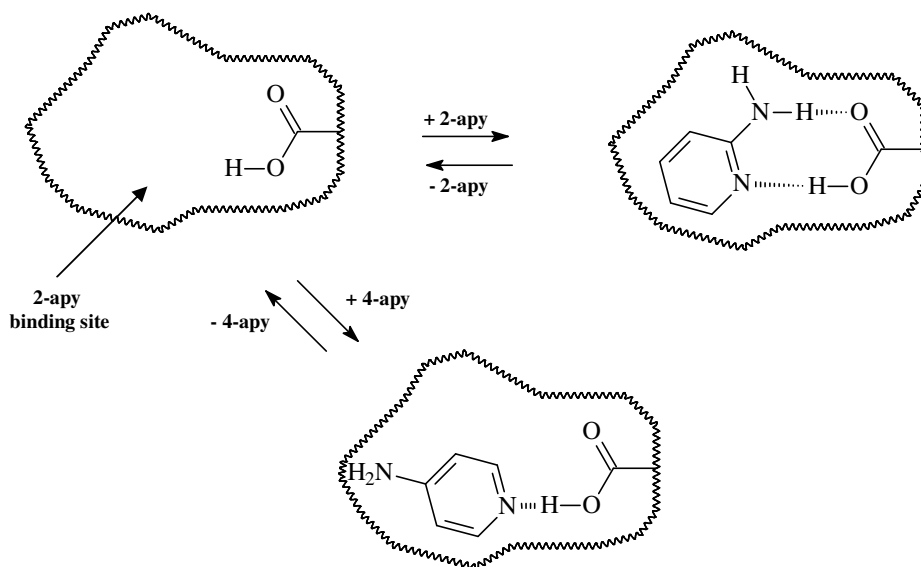


Figure 3.11. The two point cooperative hydrogen bonding interaction between 2-apy and MAA and the fit of 4-apy into the 2-apy binding cavity.

By preparing polymers with reduced concentrations of crosslinking monomer while maintaining a fixed concentration of functional monomer, the percentage of the final polymer that can be attributed to functional monomer increases. While a critical concentration of crosslinker is required to maintain the fidelity of the binding sites, too much functional monomer present in the polymer matrix can lead to an increase in the non-specific binding. Figures 3.12., 3.13. and 3.14. represent the non-specific binding for the various polymer compositions that can be attributed to the increased concentration of carboxyl groups within the various polymers.

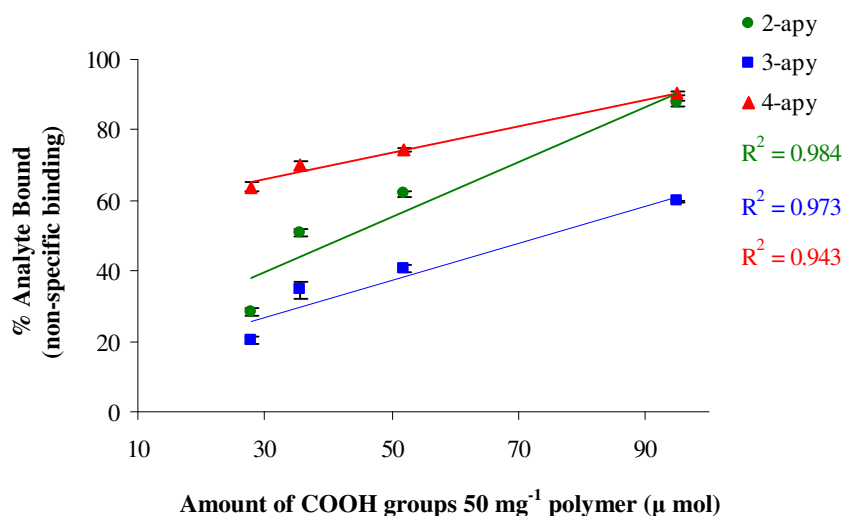


Figure 3.12. Amount of carboxyl groups (COOH) versus non-specific binding in chloroform for non- imprinted polymers (MAA as the functional monomer) prepared with different concentrations of EGDMA (40-10 mmol). Errors are based on +/- 1 standard deviation for triplicate analysis.

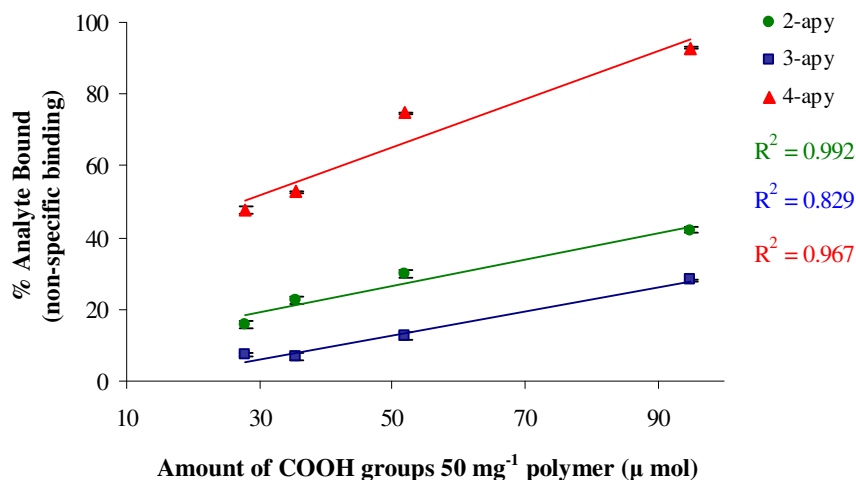


Figure 3.13. Amount of carboxyl groups (COOH) versus non-specific binding in acetonitrile for non- imprinted polymers (MAA as the functional monomer) prepared with different concentrations of EGDMA (40-10 mmol). Errors are based on +/- 1 standard deviation for triplicate analysis.

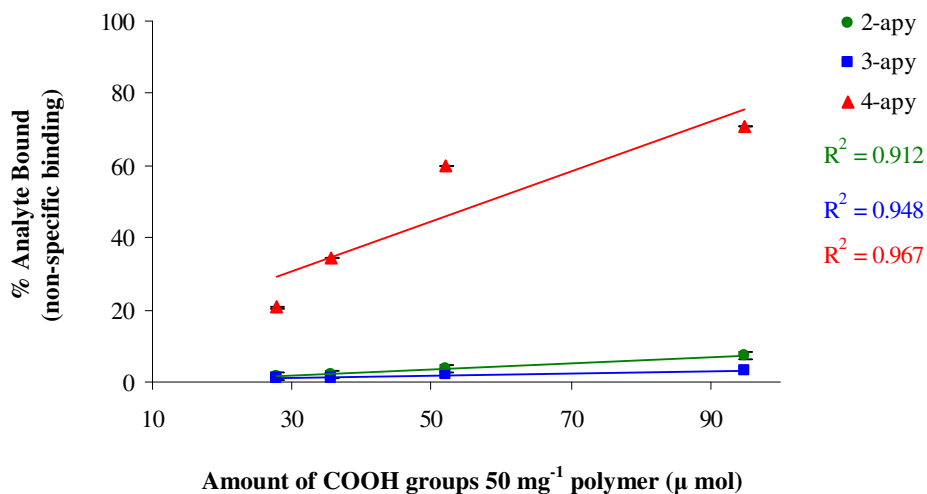


Figure 3.14. Amount of carboxyl groups (COOH) versus non-specific binding for non- imprinted polymers (MAA as the functional monomer) in methanol prepared with different concentrations of EGDMA (40-10 mmol). Errors are based on +/- 1 standard deviation for triplicate analysis.

In all solvents 4-apy interacted significantly stronger with the polymer than 2- or 3-apy. As mentioned this was attributed to the high pK_a value of 4-apy. As the concentration of

COOH groups per 50 mg of polymer increased there was a positive, relatively linear, increase in non-specific binding for all analytes in all of the solvents. In methanol, the 4-apy capacity was less than that in acetonitrile and chloroform. For the other two isomers binding in methanol was significantly less relative to 4-apy. This can be attributed to stronger ionic interactions between 4-apy and the carboxyl residues, and, it highlights the strength of these interactions relative to those formed between methanol and 4-apy.

In chloroform, Figure 3.12., the difference in the degree of non-specific binding for 2-, 3- and 4-apy decreased as the concentration of COOH groups increased. For example, at 28 μmol of COOH per 50 mg of polymer the difference between non-specific binding for 2- and 4-apy is 35.3 % but at 95 μmol of COOH per 50 mg the difference is reduced to 2.9 %. The difference between 3- and 4-apy at 95 μmol of COOH per 50 mg is 30.7 %. The disparity in non-specific binding can be attributed to the pK_a values of the isomers as discussed earlier. But, given that the difference in binding between 2- and 4-apy and 3- and 4-apy in acetonitrile and methanol (2- and 4-apy 50.8 %, 3- and 4-apy 64.8 % in acetonitrile, 2- and 4-apy 63.7 %, 3- and 4-apy 67.8 % in methanol) at 95 μmol of COOH per 50 mg are less than for chloroform the result is mainly due to the effect of solvent swelling on the polymer, with basicity playing a minor role.

3.3.4. Specificity and selectivity of 4-vinylpyridine and 4-vinylpyridine-methyl methacrylate polymers

2-apy has been successfully imprinted using methacrylic acid (MAA) as the functional monomer [11-14]. The effect of the nature of functional monomer combined with the polymer flexibility and rigidity on the imprinting effect of 2-apy was also examined. 4-VP was used as the functional monomer. A co-monomer system of 4-VP-MMA was also investigated. 4-VP was chosen as the functional monomer for imprinting 2-apy as it had potential for interaction with 2-apy as depicted in Figure 2.4. The effect of various polymer compositions on affinity was also investigated.

Specificity and selectivity was carried out as described for MAA polymers. In contrast to MAA polymers, 4-VP or 4-VP-MMA polymers demonstrated no affinity or

selectivity towards 2-, 3- and 4-apy. This was regardless of the method of template extraction. It is suggested that the template was irreversibly retained within the polymer matrix as minimum template removal, with respect to MAA polymers, was achieved. No re-binding was observed from either extraction technique which suggests that 2-apy was not imprinted, despite the potential for interactions.

The differences in the morphology of the polymers as shown in Chapter 2 must also be considered. Overall, the 4-VP polymers were found to be less porous than MAA polymers, which would have prevented ingress into the polymeric matrix. Polymer swelling was also slightly greater for MAA polymers indicating a different crosslinked structure.

Reloading in chloroform, acetonitrile or methanol did not promote binding between 2-apy and the imprinted species. As chloroform was the porogenic solvent employed in polymer formation, some degree of binding was expected. However, this was not the case. Had the interactions been π - π in nature some binding would have been expected in methanol. Some degree of non-specific binding on the NIPs would also be expected.

Decreasing the concentration of EGDMA did not increase the affinity of the polymers towards the template species, as was seen for MAA polymers. However, as opposed to the MAA polymers, the 4-VP polymers formed with 10 mmol MAA were suggested as being very non-porous, and so analyte ingress would have been reduced. If the number of free pyridine rings available for binding increased with decreasing EGDMA, as was suggested for the carboxyl groups of the MAA polymers, a level of binding might have been expected. A degree of affinity for one of the three loaded analytes in one of the solvent would have been expected. Thus, the morphology of the polymers is attributed to the results obtained. The co-monomer system also displayed no affinity for 2-apy, despite the potential for interaction with MMA. Possible interactions between 4-VP and MMA in the pre-polymerisation mixture may have resulted in its functionality being unavailable for subsequent interaction with 2-apy during the reloading.

3.4. Conclusions

The main aim of this study was to identify correlations between the physical properties, obtained in Chapter 2, and the performance of the polymers, as described in the above sections. 2-apy was successfully imprinted using MAA as the functional monomer. A series of polymers of various flexibility and rigidity were formed by varying the concentration of crosslinking monomer. The affinity varied depending on the solvent polarity. This was because of the polar two point cooperative hydrogen bonding interactions between 2-apy and MAA. As the ratio of MAA to EGDMA increased (by reducing the amount of EGDMA in the pre-polymerisation mixture) the overall binding to the polymers increased. A combination of the following factors were attributed to this phenomenon;

- Morphology differences (in terms of specific surface area, average pore diameter and cumulative volume of pores). There was an inverse relationship between cumulative pore volume and affinity of the polymers
- Different rigidity and flexibility-expressed in terms of the swelling effects of the solvents on the polymers. Increased binding site access was associated with increased flexibility. The inverse relationship mentioned above was attributed to flexibility of the polymers in the solvents.
- The average particle size distribution. Smaller particle diameters were found to exist in those polymers formed from lower amounts of EGDMA. As a fixed mass of polymer was used for re-binding a larger surface area was available for binding in the polymers formed from lower amounts of EGDMA.
- The number of free carboxyl groups increased as the percentage of EGDMA in the polymer composition decreased. Therefore, there was more functionality available for binding with 2-apy, per fixed mass of polymer.

The imprinting factors in chloroform were found to decrease with decreasing EGDMA. This suggested a loss in specificity of the polymers, due to the points mentioned above.

As imprinting factors were overall improved in acetonitrile relative to chloroform it highlights the effect of solvent polarity and swell on the binding performances of the polymers. It is therefore suggested that with lower amounts of EGDMA reloading in the porogen, chloroform, may result in a loss of binding site integrity.

The trends observed with increasing analyte pK_a were expected as increased pK_a resulted in an increase in strength in ionic interactions with MAA. An interesting result was that binding to the 40 mmol MIP for 4-apy was higher relative to 2-apy (the imprint molecule). This difference in binding decreased with decreasing EGDMA, with binding at the 10 mmol composition being essentially equal. This result is significant as it suggests a loss of binding site integrity being the dominant factor for the binding observed at 10 mmol EGDMA as opposed to increased pK_a , as seen at the 40 mmol composition.

Analysis of slope values for the plots of pK_a versus non-specific binding for all the compositions in the three solvents showed that in chloroform the rigid polymer were more sensitive to changes in pK_a . The combined physical parameters and the effect of solvent swell on the polymers formed with lower amounts of EGDMA reduced the response to differences in pK_a .

Results for 4-vinylpyridine suggest that 2-apy, although irreversibly retained within the 4-VP polymers is not imprinted. But, given the potential for definite non-covalent interactions between template and functional monomer(s) it is proposed that the results obtained were due to the morphology characteristics as determined in Chapter 2.

References

1. Y. Lu, C. Li, H. Zhang, and X. Liu, *Analytica Chimica Acta* **489**, 33-43 (2003).
2. L. Fischer, R. Muller, B. Ekberg, and K. Mosbach, *Journal of the American Chemical Society* **113**, 9358-9360 (1991).
3. E. Hedborg, F. Winqvist, I. Lundstrom, L. I. Andersson, and K. Mosbach, *Sensors and Actuators A* **37-38**, 796-799 (1993).
4. S. A. Piletsky and A. Turner, "A New Generation of Chemical Sensors Based on MIPs," *Molecular Imprinting of Polymers*, 2004).
5. G. Vlatakis, L. I. Andersson, R. Muller, and K. Mosbach, *Nature* **361**, 645-647 (1993).
6. D. Spivak, R. Simon, and J. Campbell, *Analytica Chimica Acta* **504**, 23-30 (2004).
7. H. Kim and D. A. Spivak, *Journal of the American Chemical Society* **125**, 11269-11275 (2003).
8. M. Whitcombe, L. Martin, and E. N. Vulfson, *Chromatographia* **47**, 457-464 (1998).
9. K. Karim, F. Breton, R. Rouillon, E. V. Piletska, A. Guerreiro, I. Chianella, and S. A. Piletsky, *Advanced Drug Delivery Reviews* **57**, 1795-1808 (2005).
10. Q. Osmani, H. Hughes, K. Flavin, J. Hedin-Dahlstrom, C. J. Allender, J. Frisby, and P. McLoughlin, *Analytical and Bioanalytical Chemistry* **391**, 1229-1236 (2008).
11. Z. Jie and H. Xiwen, *Analytica Chimica Acta* **381**, 85-91 (1999).
12. W. M. Mullett, M. F. Dirie, E. P. C. Lai, H. Guo, and X. He, *Analytica Chimica Acta* **414**, 123-131 (2000).
13. W. Cummins, P. Duggan, and P. McLoughlin, *Analytica Chimica Acta* **542**, 52-60 (2005).
14. W. Cummins, P. Duggan, and P. McLoughlin, *Biosensors and Bioelectronics* **22**, 372-380 (2006).
15. T. Pap and G. Horvai, *Journal of Chromatography A* **1034**, 99-107 (2004).
16. J. Brandrup and E. H. Immergut, *Polymer Handbook*, 3rd edition (Wiley, New York, 1989).
17. B. Sellergren and K. J. Shea, *Journal of Chromatography* **635**, 31-45 (1993).
18. K. J. Shea, D. A. Spivak, and M. Gilmore, *Journal of the American Chemical Society* **119**, 4388-4392 (1997).

19. I. Mijangos, F. Navarro-Villoslada, A. Guerreiro, E. Piletska, I. Chianella, K. Karim, A. Turner, and S. Piletsky, *Biosensors and Bioelectronics* **22**, 381-387 (2006).

Chapter 4

A detailed examination of the methacrylic acid-co-ethyleneglycol dimethacrylate (MAA-co-EGDMA) binding characteristics using binding isotherms and affinity distribution spectra

4.1. Introduction

A typical schematic diagram of molecular imprinting (Figure 1.2.), which is commonly found in the literature, suggests an ideal fit of the template within the binding sites of imprinted polymers, and that all sites possess an identical or similar affinity for a given template molecule. However, in non-covalent imprinting this is typically not the case and imprinted polymers contain a wide distribution of binding sites with various affinities for the template molecule.

This heterogeneous nature can complicate the binding behaviour of MIPs, particularly when comparing different imprint systems. The phenomenon is particularly troublesome when applying MIPs to various analytical applications and thus it can be a limiting factor for commercial usage. Sellergren and Shea demonstrated how the origins of peak asymmetry for the enantiomeric separation of D- and L- phenylalanine analide (D, L-PA) on a L-PA imprinted polymer was due to the heterogeneous nature of the binding sites [1]. Allender *et. al.* [2] demonstrated, by use of Scatchard plots ($[\text{Bound ligand}]/[\text{Free ligand}]$ versus $[\text{Bound ligand}]$), that the cross reactivity observed for a series of Boc-D,L-amino acid imprinted polymers was also attributed to the heterogeneous nature of the imprinted polymers.

The origins of heterogeneity are said to arise from the following:

- Polymer formation is typically carried out *via* a free radical process. This is a random mechanism and can result in regions that have different crosslink densities *i.e.* the polymer is amorphous. Consequently, binding sites of different types and integrities are formed [3].
- Incomplete template-monomer (T-M) pre-polymerisation complex formation. The excess amounts of functional monomer that is generally used in non-covalent imprinting (see section 1.4.2.) may result in a variety of T-M structures with different association constants [4]. Non-associated functional monomer can be randomly incorporated into the polymer, also contributing to non-specific binding.
- Clusters of templates imprinted within a binding site as opposed to imprinting a single template molecule [5].

- Template solvent extraction can result in shrinkage of the binding sites [6], thus resulting in a range of association constants

The first record of heterogeneity in imprinted polymers was reported by Wulff *et al.* in 1977 for the separation of the 4-nitrophenyl- α -D,L-mannopyranoside racemate [7]. The separation factor was found to increase with decreasing sample load, indicating the presence of highly specific binding sites. Only in recent years have attempts been made to characterise the binding properties and to assess the heterogeneous nature of imprinted polymers. Typically an experimental binding isotherm is generated for the imprinted polymers and it is then possible to estimate the binding behaviour of the system by fitting the experimental isotherm to various mathematical models, for example Langmuir (LI), Freundlich (FI) and the hybrid Langmuir-Freundlich (L-FI) isotherms. Each of these models has their advantages and disadvantages, as discussed in section 1.6.2.

Haupt *et al.* used the LI to determine the affinity of a series of theophylline imprinted polymers [8]. An assumption using this method was that one type or class of binding sites existed. However, it did allow for a direct comparison of the binding behaviour of the imprinted polymers to be made. The LI has often been extended to a Bi-LI and has been plotted using Scatchard analysis. Until recently it has been the most common method for the assessment of MIPs. However, because of its limitations, including the assumption that binding occurs at either high or low affinity binding sites as opposed to a range of affinities of binding sites, a recent trend has been to use a variety of binding isotherms in polymer assessment.

Shimizu *et al.* applied a FI to a series of twelve different polymers taken from the literature [9]. The chosen polymers represented a diverse range of polymerisation conditions, template molecules and functional monomers. The respective experimental isotherms also contained a reasonable number of data points (at least seven points). Of the twelve systems, eleven displayed a good fit (based on regression, or R^2 , values) to the FI. The limitations cited by the authors was that deviation from FI occurred at high analyte concentrations (refer to Figure 1.24).

A combination of both LI and FI has been shown to accurately characterise the binding behaviour of a series of polymers with respect to the individual models [10]. This is due to the reduced accuracy of the individual models which is dependant on the analytical window or concentration range in which the analysis is being carried out (refer to Section 1.6.2.).

Based on the affinity and specificity results obtained in Chapter 3, the objective of the study presented in this chapter was to examine in more detail the role of polymer morphology on the binding behaviour of imprinted polymers. To comprehensively assess the binding behaviour, LI, FI and L-FI were used to examine changes in relation to initial polymer composition, and the most suitable model identified. It was envisaged that the amount of crosslinking monomer used in polymer formulation would influence not only the stabilisation of T-M complexes, but also effect the integrity and access to resultant binding sites, all of which have been said to influence binding site heterogeneity.

Affinity distribution (AD) spectra plotting the number of binding sites with respect to association constant, were generated from L-FI binding parameters in an attempt to further highlight potential differences between the different imprint systems. Such a comprehensive analysis of the role of polymer composition of polymer affinity has not previously been presented using combination of L-FI and affinity distribution spectra as the method of analysis.

The examination of polymer affinity is described for the polymers formed using methacrylic acid (MAA) as the functional monomer as initial investigations into polymer binding indicated that MAA polymers displayed the best affinity for the template species. The parameters to be determined from the various isotherms are,

- m , which is a measure of the heterogeneity, with values approaching one indicating a homogeneous system,
- N_t , a quantitative measure of the number of binding sites in the polymer,
- K_o , the average association constant of the binding sites.

4.2. Experimental

4.2.1. Materials, equipment and instrumentation

Materials

The polymers that were synthesised using methacrylic acid (MAA) as the functional monomer and subjected to template extraction as described in Sections 2.2.2. and 2.3.3. were used for this study with the addition of the following materials:

Table 4.1. The materials used.

Reagent	Supplier	Assay
2-Aminopyridine	Sigma-Aldrich (Ireland)	99 +%
Chloroform	Lennox (Ireland)	99.0-99.4 %
Molecular sieves	Sigma-Aldrich (Ireland)	3A 3.2 mm

Equipment and instrumentation

- Stuart scientific orbital incubator S150
- Sterile syringes: Omnifix ® Braun- Lennox Laboratory Supplies
- Syringe nylon filters: 0.4 µm, 13 mm diameter- Antech Technologies Ltd
- UV/Vis spectrometer: UV-2401PC Shimadzu (JVA Ireland Ltd)

4.2.2. Experimental Binding Isotherm

5 mL of 0.025 mM – 4 mM of 2-aminopyridine (2-apy) in chloroform was added to 50 mg quantities of the polymers. The equilibration period and determination of quantity bound was carried out as described in Section 3.2.2. Appropriate dilutions were carried out prior to analysis for the higher concentration analyte solutions, post-equilibrium. Experimental binding isotherms were generated by plotting B versus F (as determined from Equation 3.1.). The experimental isotherm was fit to LI, FI and L-FI (Equations 4.1, 4.2 and 4.3. respectively). Affinity distribution spectra were generated by fitting the L-FI binding parameters into Equation 4.4.

- **Langmuir isotherm (LI)**

$$B = \frac{N_t a F}{1 + a F} \quad \text{(Equation 4.1.)}$$

- **Freundlich isotherm (FI)**

$$B = a F^m \quad \text{(Equation 4.2.)}$$

- **Langmuir-Freundlich isotherm (L-FI)**

$$B = \frac{N_t a F^m}{1 + a F^m} \quad \text{(Equation 4.3.)}$$

- **Affinity distribution equation for the L-FI**

$$N_i = N_t a m (1/K_i)^m \times \frac{(1 + 2a(1/K_i)^m + a^2(1/K_i)^{2m} + 4a(1/K_i)^m m^2 - a^2(1/K_i)^{2m} m^2 - m^2)}{(1 + a(1/K_i)^m)^4} \quad \text{(Equation 4.4.)}$$

Where

- B = amount of substrate bound to the polymer,
- F = the amount of free substrate after equilibration,
- N_t = the total number of binding sites,
- a = is related to the average binding affinity K_o via $K_o = a^{1/m}$,
- m = the heterogeneity index,

$$\log K = \log \left(\frac{1}{\left(\frac{F}{1000} \right)} \right)$$

For a detailed explanation on the binding models mentioned above refer to Section 1.6.2.

4.3. Results and discussion

4.3.1. Experimental binding isotherm

Ten different solutions of 2-apy in chloroform, in the concentration range of 0.025 mM to 4.0 mM, were reloaded onto the imprinted and non-imprinted polymers for all EGDMA compositions (the actual concentrations equilibrated with 50 mg of polymer ranged from 0.125 $\mu\text{mol } 5\text{mL}^{-1}$ to 20 $\mu\text{mol } 5\text{mL}^{-1}$). It was envisaged that the wide concentration range used would be sufficient to cover the binding behaviour in both the saturation and sub-saturation zones of the proposed model which is used to describe MIP binding (refer to Section 1.6.2 and Figure 1.24).

Analysis of the post equilibrium solutions at the lower concentrations (0.025 – 0.1 mM) indicated leeching, or bleed, due to potential un-reacted monomer components back into the liquid phase, which prevented the assessment of analyte binding at those particular concentrations. The amount of leeching or bleed was higher for NIP materials, indicating that polymerisation had not proceeded to the same extent as corresponding imprinted polymers. The bleed was also higher for those polymers formed with higher amounts of EGDMA. This suggested that polymers formed with lower amounts were more flexible which facilitated more efficient washing during the template removal stage. Table 4.2. indicates whether bleed occurred at the mentioned concentrations for the various polymers.

Table 4.2. Outline of polymer bleed and the associated analyte concentrations.

Solution Concentration	40 mmol EGDMA		30 mmol EGDMA		20 mmol EGDMA		10 mmol EGDMA	
	MIP	NIP	MIP	NIP	MIP	NIP	MIP	NIP
0.025 mM	yes	yes	yes	yes	no	yes	no	no
0.05 mM	no	yes	no	yes	no	no	no	no
0.068 mM	no	yes	no	yes	no	no	no	no
0.1 mM	no	yes	no	yes	no	no	no	no

Due to this bleed, a new batch of 30 mmol EGDMA MIP and NIP were synthesised and subjected to extraction in 10 % acetic acid acidified methanol for 24 h followed by two

4 h intervals in methanol. For clarification purposes, the 30 mmol EGDMA polymers that had been subjected to the different extraction procedures will be referred to as described in Table 4.3.

Table 4.3. Verification of the methods by which the 30 mmol EGDMA polymers were extracted.

Polymer	Extraction Method
30 mmol MIP 1	1 *
30 mmol NIP 1	1
30 mmol MIP 2	2 **
30 mmol NIP 2	2

* Extraction method 1: suspension in 10 % acetic acid acidified methanol followed by washing with hot methanol.

** Extraction method 2: extraction in 10 % acetic acid acidified methanol for 24 h followed by two 4 h extractions in methanol using a Soxhlet apparatus.

Experimental binding isotherms were generated by plotting the amount of analyte bound to the polymer, B (μmol of substrate per gram of polymer, $\mu\text{mol g}^{-1}$), versus the free analyte remaining in solution, F (mM). Figure 4.1. illustrates the binding isotherms generated for the imprinted polymers (extracted *via* method 1).

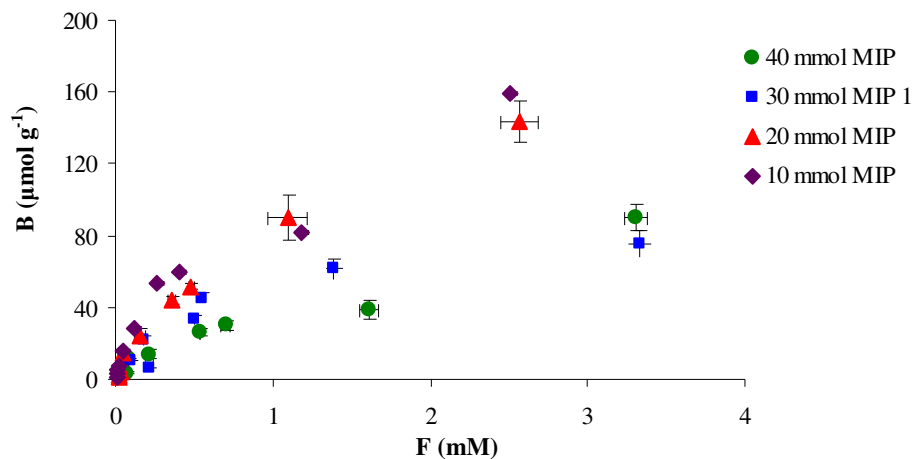


Figure 4.1. Experimental isotherms generated for imprinted polymers (extracted *via* method 1) by reloading 0.025-4.0 mM solutions of 2-apy in chloroform. Data is based on the average value for triplicate analysis.

As the concentration of crosslinking monomer decreased the capacity of the polymers was found to increase. This trend was expected because of the variations in surface area, porosity, particle size distribution and the number of free COOH groups within the differing polymer compositions. While there was a substantial difference in capacity between the 40 and 10 mmol polymers at $T = 400 \mu\text{mol g}^{-1}$ of polymer (concentration of analyte solution was $20 \mu\text{mol 5mL}^{-1}$, see Equation 3.1. for definition of T), differentiation between 10 and 20 mmol and between 30 and 40 mmol at $T = 400 \mu\text{mol g}^{-1}$ of polymer diminished within experimental error *i.e.* there is a non-statistical difference. This trend is illustrated in Figure 4.2. As chloroform was the reloading solvent used a correlation can also be made between the high degree of binding observed with decreasing EGDMA concentration and the solvent swell results (discussed in Section 2.3.5.) *i.e.* the higher affinity may be attributed to the combined flexibility and swelling property of the polymers in chloroform. Analysis of 30 mmol MIP 1 and 2 indicated that at $T = 400 \mu\text{mol g}^{-1}$ polymer capacity decreased slightly when the polymer was subject to extraction using a Soxhlet apparatus as opposed to extraction using only method 1.

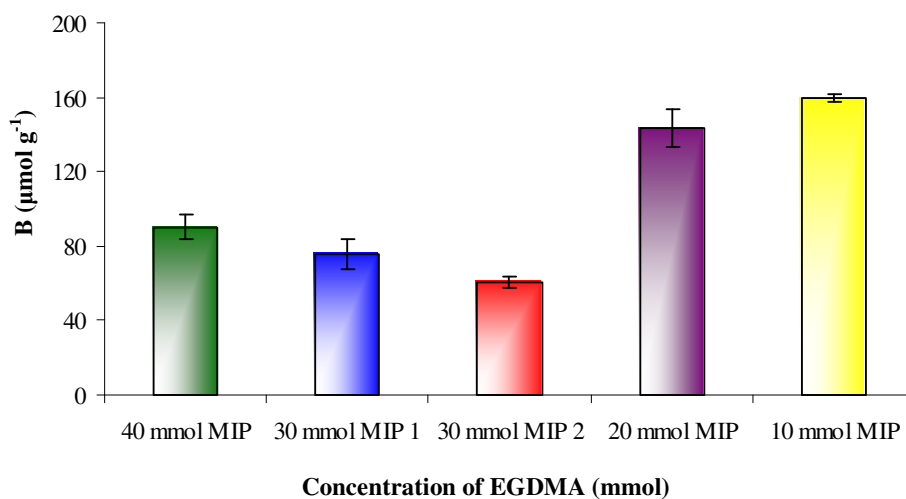


Figure 4.2. Capacity of the imprinted polymers at $T = 400 \mu\text{mol g}^{-1}$. Data is based on the average value for triplicate analysis.

Note; the effect of the template extraction procedure on the binding characteristics of the polymers will be discussed further in Section 4.3.4.

The imprinted polymers had a higher capacity relative to corresponding non-imprinted polymers over the entire concentration range. This further suggests the presence of specific binding sites in the imprinted polymers.

4.3.2. The Langmuir, Freundlich and Langmuir Freundlich isotherms

Linearised forms of the LI, FI and L-FI isotherms were applied to the experimental data by plotting the various parameters listed in Table 4.4

Table 4.4. Linearised forms of LI, FI and L-FI [4].

Isotherm	Linearised Form	Plot	Parameters
LI	$1/B = (1/N_t a) + (1/F)$	1/B versus 1/F	$N_t = 1/\text{intercept}$, a = intercept/slope
FI	$m \log F = \log A$	log B versus log F	a = y intercept, m = slope
L-FI	Solver function *	log B versus log F	Fitting coefficients- N_t , a and m.

* L-FI were fitted to the log-log plot of the experimental isotherms using Microsoft Excel by varying the fitting parameters to minimise the coefficient of determined (R^2) to 1 as described by Shimizu *et al.* [10].

Unlike LI and FI, L-FI binding constants cannot be derived through linerisation of the model [11]. Instead a curve fitting programme such as Microsoft Excel solver function must be used. Limerisation of FI is achieved by plotting the experimental isotherm in log-log format [9]. The method for linerising LI is known as Benesi-Hildebrand analysis which results in a double reciprocal equation that is obtained by linear transformation of LI.

Tables 4.5. *A*, *B* and *C* lists the binding data obtained from LI, FI and L-FI (respectively) for each composition, while Table 4.6. summarises the regression, R^2 , values obtained.

Table 4.5. A. Binding data for each polymer composition obtained using LI.

EGDMA	N_t ($\mu\text{mol g}^{-1}$)		a (mM^{-1})	
	MIP	NIP	MIP	NIP
40 (mmol)	-44.1	22.7	-1.01	1.96
30 (mmol)¹	-158.7	25.0	-0.56	1.79
30 (mmol)²	52.9	111.1	4.11	0.32
20 (mmol)	-8.1	-25.8	-6.27	-1.16
10 (mmol)	-31.9	-59.5	-4.91	-1.04

B. Binding data for each polymer composition obtained using FI.

EGDMA	a ($\mu\text{molg}^{-1}\text{mM}^{-1}$)		m		K_0 (mM^{-1})	
	MIP	NIP	MIP	NIP	MIP	NIP
40 (mmol)	37.6	17.1	0.84	0.71	74.9	54.5
30 (mmol)¹	50.2	16.7	0.74	0.62	198.7	93.4
30 (mmol)²	47.9	18.6	0.60	0.73	631.8	54.8
20 (mmol)	92.8	41.0	0.91	0.91	145.3	59.2
10 (mmol)	104.4	46.1	0.78	0.84	387.1	95.7

C. Binding data for each polymer composition obtained using L-FI.

EGDMA	N_t ($\mu\text{mol g}^{-1}$)		a (mM^{-1})		m	
	MIP	NIP	MIP	NIP	MIP	NIP
40 (mmol)	88.6	635.5	0.94	0.03	0.97	0.72
30 (mmol)¹	136.7	149.6	0.78	0.13	0.99	0.69
30 (mmol)²	66.0	42.3	3.3	0.96	1.00	1.00
20 (mmol)	259.9	170.2	0.52	0.33	1.00	1.00
10 (mmol)	281.9	134.9	0.53	0.59	0.80	1.00

C. continued. Binding data for each polymer composition obtained using L-FI.

EGDMA	$K_o(\text{mM}^{-1})$ **		Limits of affinity distribution (mM^{-1}) ***	
	MIP	NIP	MIP	NIP
40 (mmol)	0.94	0.008	0.32 - 28.3	0.29 – 6.99
30 (mmol) ¹	0.78	0.13	0.30 - 35.7	0.28 – 6.98
30 (mmol) ²	3.3	0.96	0.29 -106.4	0.28 – 45.6
20 (mmol)	0.52	0.33	0.39 – 52.9	0.71 – 25.7
10 (mmol)	0.46	0.59	0.40 – 84.0	0.33 – 65.0

**The average association constant $K_o = a^{1/m}$.

*** Limits of affinity distribution were calculated from the maximum and minimum values of F by the

relationships $K_{\min} = \frac{1}{F_{\max}}$ and $K_{\max} = \frac{1}{F_{\min}}$, [10,12].

Table 4.6. Regression (R^2) values for each polymer composition obtained from LI, FI and L-FI.

EGDMA	LI		FI		L-FI	
	MIP	NIP	MIP	NIP	MIP	NIP
40 (mmol)	0.936	0.698	0.921	0.847	0.892	0.843
30 (mmol) ¹	0.921	0.789	0.927	0.909	0.968	0.905
30 (mmol) ²	0.977	0.993	0.926	0.943	0.977	0.985
20 (mmol)	0.578	0.816	0.851	0.827	0.868	0.846
10 (mmol)	0.754	0.989	0.919	0.932	0.921	0.954

4.3.2.1. LI results

The negative results obtained for fitting the LI to the experimental isotherm are due to the fact that a negative intercept was obtained for the respective plots. This implied that the LI alone was not suitable for assessment of the polymers. The regression values (R^2) for the polymers were poorer when LI was used as opposed to FI and L-FI. This also indicates that LI was unsuitable for polymer analysis.

4.3.2.2. FI results

The suitability of FI in assessing the binding characteristics of the imprinted polymers was determined by plotting the experimental isotherm in log B versus log F format. As all plots (MIPs and NIPs) were curved over the entire concentration range the suitability of the FI is diminished (refer to Figure 4.3.). The curvature of the log B-log F plots implies polymer saturation [10], which means the use of the FI in modelling the binding behaviour of the polymers will yield inaccurate binding parameters. This is an important limitation of the FI which should not be overlooked. Deviations from the FI occur at the higher concentration region of the experimental isotherm and as a result it is unable to model the saturation / binding behaviour.

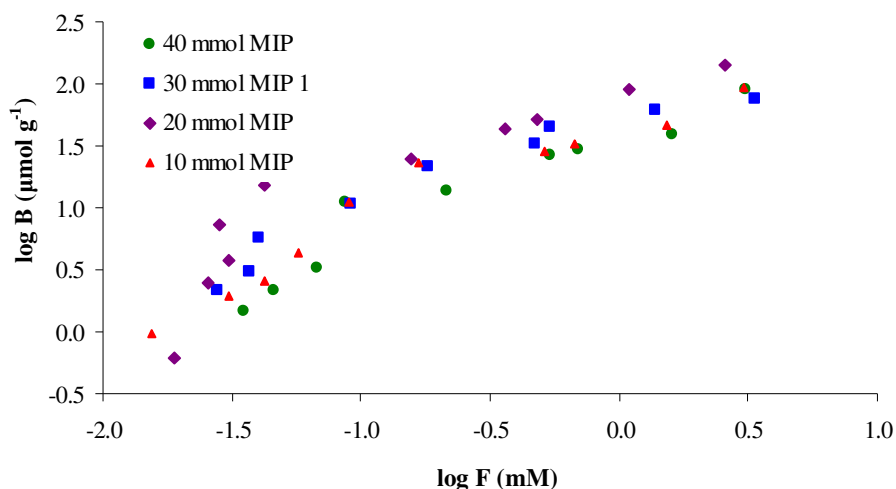


Figure 4.3. log –log plots for imprinted polymers. Data is based on the average value for triplicate analysis.

In all cases, with the exception of the 40 mmol MIP, the FI was deemed to fit the experimental isotherm more accurately than the LI. This is based on analysis of the R^2 values for the respective polymers (refer to Table 4.6.). There is no apparent trend in the heterogeneity indices, m , obtained by varying the crosslinking monomer concentration. The 20 mmol MIP gave the highest m value (0.91) which indicates that the system is approaching homogeneity. However, because the linear regression values show poor fits (0.837 – 0.921) to the FI, it is suggested that the values obtained through use of the FI are inaccurate. Poor R^2 values may arise from the wide concentration range in which the isotherm was generated as it is unable to accurately model the binding behaviour at high analyte concentrations.

At the higher concentrations of EGDMA the m values were lower for NIP than MIP while the reverse was true at the lower concentrations (10 mmol). This implies that the NIP was more heterogeneous at the lower concentrations of EGDMA. This was in agreement with previous findings where NIP polymers were found to be more heterogeneous than corresponding imprinted polymers [13]. It should be noted that for the 40 and 30 mmol NIP leeching occurred at the lower analyte concentrations (Table 4.2.). As a result the NIP polymers contained fewer experimental data points than the MIPs and so caution must be taken when comparing these results.

4.3.2.3. L-FI results

By fitting the experimental data to L-FI the R^2 values were improved in relation to the individual R^2 values obtained for LI and FI, which indicate a better fit to L-FI. The L-FI plots for the 10 mmol MIP is shown in Figure 4.4. The fitting coefficients N_t , a and m can be easily determined by applying the L-FI to the experimental isotherm. For these values to be accurately obtained K_o (average association constant) must fall within the limits $\frac{1}{F_{\min}}$ and $\frac{1}{F_{\max}}$ (the limits of affinity distribution). This is a pre-requisite in determining the suitability of L-FI. These values were determined by the relationships $K_{\min} = \frac{1}{F_{\max}}$ and $K_{\max} = \frac{1}{F_{\min}}$, where F is the concentration of free analyte in solution. As the K_o value for all of the polymers falls within these limits (coupled with the

improved R^2 values) the information obtained on the binding characteristics are deemed appropriate for polymer study. The general trend observed for the average association constant, K_o , was that it decreased with decreasing EGDMA content. The reduction in K_o may be attributed to the presence of less defined binding sites as a result of lower amounts of crosslinking monomer.

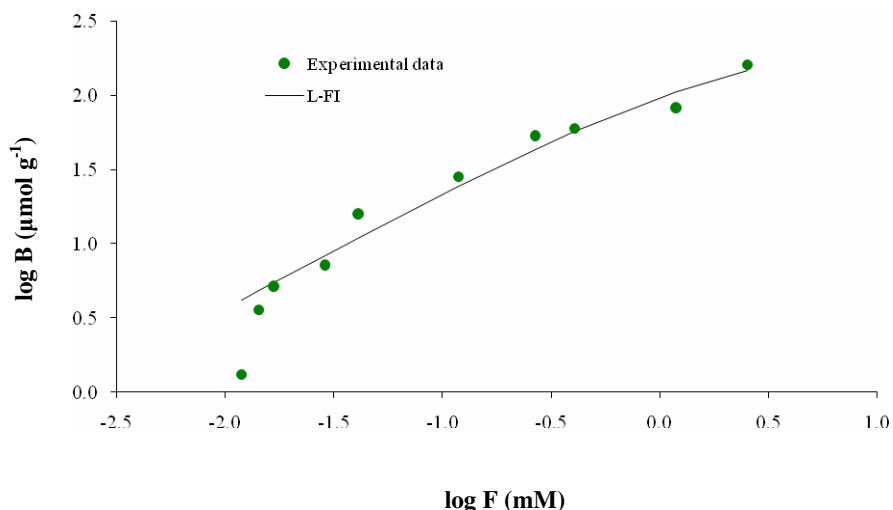


Figure 4.4. The L-FI plot for imprinted polymer formed with 10 mmol EGDMA.

The total number of binding sites, N_t , was found to increase with decreasing EGDMA content. This trend was expected due to the increased flexibility which permitted the intrinsic sites of the polymer to become occupied, resulting in the observed overall higher capacity of the polymers. As the initial concentration of template to monomer remained constant for all polymers there should, in theory, be an equal number of binding sites present in all of the polymers. However, applying the L-FI to the polymers indicated that this was not the case. The flexibility, various porous structures and the particle size distributions of the polymers combined with the swelling in chloroform may have resulted in greater access within the polymer matrix (all of which have been discussed in Chapters 2 and 3). This then resulted in a higher degree of binding, which may have been both specific and non-specific in nature, as shown in Section 3.3. Therefore, while the number of sites was shown to increase with decreasing EGDMA content the values given do not account for potential non-specific binding. The relationship between N_t and swelling ratio in chloroform is depicted in Figure 4.5.

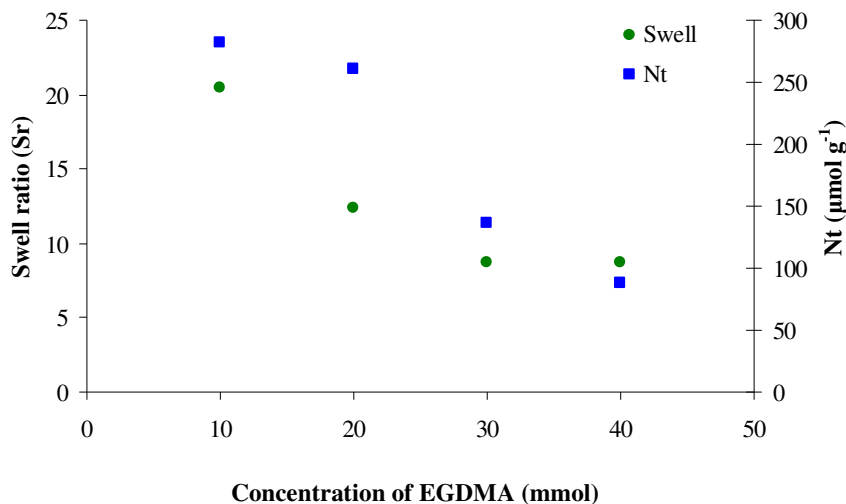


Figure 4.5. Relationship between swell ratio and the total number of binding sites.

The total number of binding sites for the NIP polymers can be used as a measurement of non-specific binding. N_t for the 40 and 30 mmol NIPs must be taken with caution as they had a lower number of data points present in the experimental isotherm, as discussed earlier. As the data points that were measured were predominately in the higher concentration region the L-FI may not have reduced to the FI. This may have contributed to the anomalous results obtained. The N_t for the remaining NIP polymers were all lower than corresponding MIPs. This is an indication of a lower capacity for the NIPs, which was consistent with the rebinding studies carried out in Chapter 3. The difference in the number of binding sites between MIP and NIP polymers may be used as an indication of the number of specific sites present in the imprinted polymers.

The heterogeneity indices, m , for all polymers are high indicating that the polymers are approaching homogeneity. This result was unexpected as the polymers were imprinted non-covalently which typically results in heterogeneity due to the instability of the template-monomer complexes pre-polymerisation. A value of m equal to one results in the L-FI reducing to the LI. The FI is inaccurate at very low concentrations of analyte [4], as a result the L-FI is also inaccurate at very low analyte amounts. The heterogeneity index values obtained may be due to the inability of the L-FI to accurately reduce to the FI at very low concentrations, as is evident in Figure 4.4.

4.3.3. Affinity distribution spectra

From the parameters obtained from L-FI an affinity distribution (AD) spectrum can be generated for the polymer species. An AD displays the population of binding sites, N , having a particular association constant, K . For the affinity distribution spectra to be deemed accurate the K_0 value, determined from the L-FI fitting parameters, must fall within the limits of affinity distribution. As was seen in Table 4.5 all polymers fell within these limits with the exception of the 40 and 30 mmol NIPs. The area under the curve corresponds to the total number of binding sites.

The AD spectra for MIPs and NIPs are shown in Figure 4.6 and 4.7, respectively, and are plotted in semi-log format. The exponentially decaying region correlates with re-loading in the lower concentration region and assesses the high affinity sites. As the AD spectra shown are unimodal distributions, as opposed to only displaying the exponentially decaying region, it indicates that the polymers have been assessed in a broad concentration region and that the polymers have reached saturation. As a result more information can be gained on the type and number of binding sites. The narrow shape of the distributions indicates that the imprinted polymers are relatively homogeneous in nature, which was determined by fitting the data to L-FI. The heterogeneity index determines the shape of the distribution where the shape broadens when m is reduced from 1 to 0. The AD spectra were clearly able to distinguish between each polymer composition.

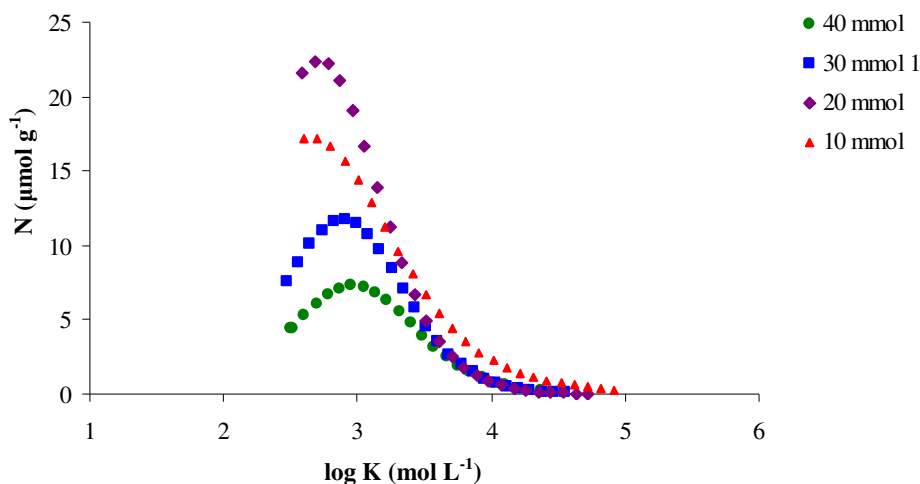


Figure 4.6. Affinity distribution spectra for imprinted polymers.

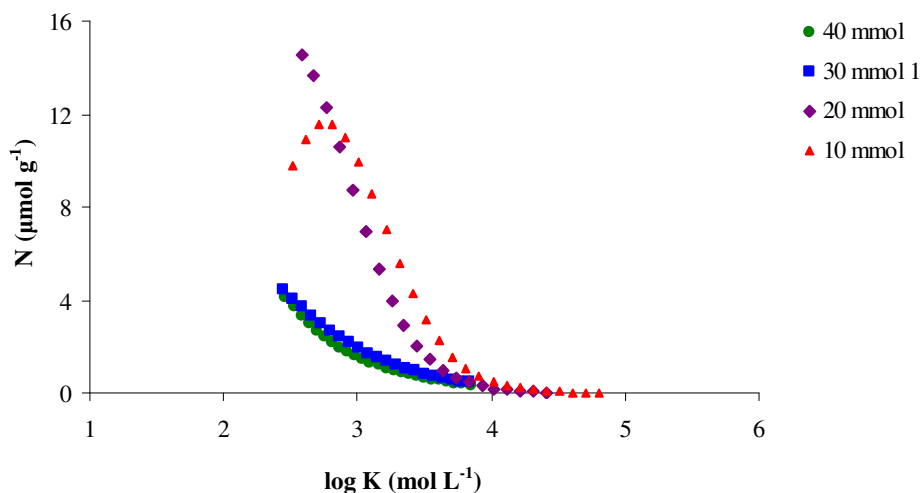


Figure 4.7. Affinity distribution spectra for non-imprinted polymers.

For the imprinted polymers, the number of binding sites increased with decreasing EGDMA concentration, with the exception of the 10 and 20 mmol compositions. A change in the K value for the maximum number of binding sites (N_{\max}) with composition change was also identified. N_{\max} shifted to a lower K value with decreased EGDMA concentration, again suggesting the presence of less defined binding sites due to the potential destabilisation of the template-monomer complexes in the early stages

of polymerisation. Aside from N_t , the fitting parameters a and m , as well as K_i , (refer to Equation 4.4.) should be considered when determining the binding sites *via* AD. As these parameters are different between the two compositions different AD spectra were expected.

The shape of the NIP polymers distribution were also dictated by the fitting parameters generated from the binding isotherm. The 40 and 30 mmol polymer produced a different shape to the other compositions. However, as the K_o values fell outside the limits of affinity distributions the resultant spectra are said to contain considerable errors. In general, MIPs and corresponding NIPs have a similar broad unimodal distribution. The shape or broadness of the peaks are similar due to their similar m values. The differences lie in the N_{max} , which were less for the NIPs. The K_o value was also less for NIPs (with the exception of the 10 mmol composition), all of which suggested stronger binding capability of the MIPs which varied with composition. These results correlate with the binding studies carried out in Chapter 3 where increased capacity was accompanied by a loss in specificity which was attributed to the presence of less defined binding sites

4.3.4. The effect of the template extraction procedure on binding characteristics

The template and residual bleed from the polymers appeared to be removed using the procedure described in Section 2.2.3. But, as was indicated in Table 4.2., there was evidence of bleed from some of the polymers during reloading at lower analyte concentrations. Leeching from polymer materials is often reported as a restriction to their usage, particularly in solid phase extraction procedures when an analyte is being pre-concentrated from very low levels. Imprinting a structural analogue of the analyte of interest is viewed as a method to circumvent this problem [14].

The bleed that was observed from the NIP data can be attributed to the presence of unreacted monomer units, presumably due to a different degree of crosslinking or polymerisation. The swelling effect of methanol on the polymers was highlighted in Chapter 2. Although it did swell the polymers, it was not to the same extent as chloroform. Thus, it is recommended that washing in a solvent that swells (or a “good

solvent”) the polymer to a large extent and that is capable of solvating un-reacted monomers, *i.e.* the porogen, to treat the polymers prior to use.

The results relating to the effect of the template extraction procedure are listed in Table 4.5. A general observation based in the regression values was that the accuracy of the isotherms for the polymers extracted using a Soxhlet apparatus was improved relative to those that were not. N_t for 30 mmol MIP 2 was much lower than MIP 1, implying that this extraction technique resulted in the destruction of binding sites. This finding is in agreement with earlier studies [15].

The template extraction procedure was found to have a dramatic effect on the affinity distributions obtained, Figure 4.8. Whilst the more rigorous extraction procedure using a Soxhlet apparatus did reduce the total number of binding sites, those sites that did remain had higher binding energies. This was also true for the non-imprinted polymer, but relative to the corresponding MIP extracted using a Soxhlet apparatus it had a lower average binding strength. This highlights the presence of specific binding sites within the imprinted polymers.

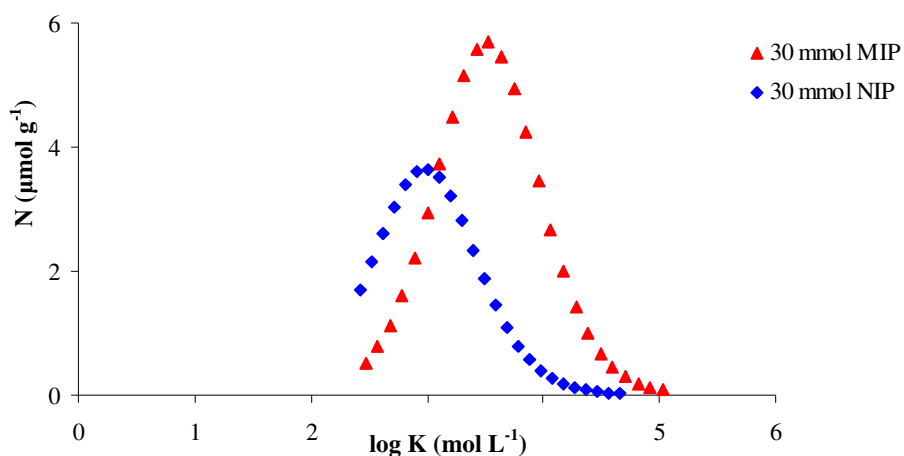


Figure 4.8. Affinity distribution spectra for 30 mmol MIP and NIP that were extracted using a Soxhlet apparatus.

4.4. Conclusions

The binding characteristics of MAA imprinted polymers selective towards 2-aminopyridine were assessed using three different binding models, each with their different requirements for use. The L-FI was identified as the most appropriate model for use, for the concentration range under study. A complementary relationship between polymer morphology and the total number of binding sites was identified. The binding behaviour of the polymers as quantified by L-FI was found to be dependant on polymer composition. It has also been shown how L-FI may be used to give an approximation of the number of specific binding sites in imprinted polymers by analysis of MIP and NIP data. The results for the NIP polymers, particularly the 40 and 30 mmol compositions, highlighted the importance of polymer preparation prior to use. The bleed that was encountered resulted in a lower number of experimental data points and so a direct comparison could not be made.

Findings using L-FI correlated with results obtained using AD spectra. While AD spectra have found use in assessing the binding behaviour of imprinted polymers, their use to study the effect of crosslinking monomer concentration on N_t and K_o , and their dependency on polymer morphology has been limited. They are particularly useful in visually displaying the relationship between the number of binding sites and their respective energy. A range of binding sites with different affinities were identified using AD and L-FI. These ranges were dependant on polymer composition. This data correlated with porosity data, affinity and specificity result trends (Chapters 2 and 3). A decrease in association constant with decreased amounts of crosslinking monomer, as demonstrated by both L-FI and AD spectra, implied the presence of less defined binding sites. Again a correlation with affinity data was made, where the presence of increased non-specific binding was attributed to increased access to binding sites with less shape integrity.

The heterogeneity indices, m , as determined from L-FI were unexpected as they were calculated as being homogeneous or near homogeneous. The m values as determined from the FI had a greater distribution and were less homogeneous. Although these values were inaccurate due to deviations from FI, analysis using both FI and L-FI in a

narrower concentration range would be useful in an attempt to gain a greater insight in to the heterogeneity index, and to determine with more certainty the most suitable isotherm and the appropriate concentration range for examining polymer binding behaviour, particularly since all of the binding models used have limitations in terms of concentration range.

References

1. B. Sellergren and K. J. Shea, *Journal of Chromatography A* **690**, 29-39 (1995).
2. C. J. Allender, K. R. Brian, and C. M. Heard, *Chirality* **9**, 233-237 (1997).
3. K. J. Shea and D. Sasaki, *Journal of the American Chemical Society* **113**, 4109-4120 (1991).
4. J. A. Garcia-Calzon and M. E. Diaz-Garcia, *Sensors and Actuators B: Chemical* **123**, 1180-1194 (2006).
5. A. Katz and M. Davies, *Macromolecules* **32**, 4113-4121 (1999).
6. G. Wulff, T. Gross, R. Schonfeld, T. Schrader, and C. Kirsten, *Molecular and Ionic Recognition with Imprinted Polymers*, R. A. Bartsch and M. Maeda, eds., (American Chemical Society, Washington DC, 1998), 10-28.
7. G. Wulff, R. Grobe-Einsler, W. Vesper, and A. Sarhan, *Makromolekular Chemistry* **178**, 2817-2825 (1977).
8. E. Yilmaz, K. Mosbach, and K. Haupt, *Analytical Communications* **36**, 167-170 (1999).
9. R. J. Umpleby, S. C. Baxter, M. Bode, J. Berch Jr., R. Shah, and K. D. Shimizu, *Analytica Chimica Acta* **435**, 35-47 (2001).
10. R. J. Umpleby, S. C. Baxter, Y. Chen, R. Shah, and K. D. Shimizu, *Analytical Chemistry* **73**, 4584-4591 (2001).
11. K. D. Shimizu, "Binding Isotherms," *Molecularly Imprinted Materials: Science and Technology*, Y. A. Ramstrom, ed., (Marcel Dekker, New York, 2005), 419-434.
12. R. J. Umpleby II, S. C. Baxter, Y. Chen, R. N. Shah, and K. D. Shimizu, *Analytical Chemistry* **73**, 4584-4591 (2001).
13. J. L. Urraca, M. D. Marazuela, E. R. Merino, G. Orellana, and M. C. Moreno-Bondi, *Journal of Chromatography A* **1116**, 127-134 (2006).
14. B. A. Rashid, R. S. Briggs, J. N. Hay, and D. Stevenson, *Analytical Communications* **34**, 303-305 (1997).
15. C. Cacho, E. Turiel, A. Martin-Esteban, C. Preze-Conde, and C. Camara, *Journal of Chromatography B* **802**, 347-353 (2004).

Chapter 5

Characterisation of polymers using thermal desorption GC-MS

5.1. Introduction

Whilst the affinity of imprinted polymers is influenced by the interaction of template with functional monomer pre- and post polymerisation on a molecular level, it is also dictated by the physical make up of the polymer at the macro level, which has been demonstrated in the previous chapters of work.

Imprinted polymers have generated great interest due to their ability to act as selective phases similar to those of a biological nature. They afford numerous advantages over their biological counterparts, such as their resistance to extreme pH levels as well as their stability at elevated temperatures. Svenson and Nicholls [1] demonstrated that imprinted polymers, prepared from methacrylic acid (MAA) and ethylene glycol dimethacrylate (EGDMA) retained affinity when exposed for 24 h to solutions with a broad pH range and also when exposed to temperatures (24 h) of up to 150 °C. Other studies of polymers with similar compositions have exhibited thermal stability at temperatures up to 250 °C without significant degradation [2,3].

Characterisation of polymers (including everyday polymeric products such as paints, plastics and adhesives) are carried out using a variety of techniques which include optical microscopy (*e.g.* scanning electron microscopy (SEM), transmission electron microscopy (TEM) and scanning probe microscopy (SPM) [4,5]), gas sorption measurements (*e.g.* nitrogen or mercury sorption [6]), FTIR and NMR analysis [7,8]. Thermal properties of polymers are evaluated using techniques such as differential scanning calorimetry (DSC) and thermogravimetric analysis (TGA). This can provide information about physical properties such as glass transition temperature (T_g), crystallisation temperature (T_c), melt temperature (T_m), the degradation or decomposition temperature (T_D) and crosslink density [2,9-11]. The molecular weight distributions can be determined using techniques such as gel permeation chromatography (GPC) [12] and size exclusion chromatography (SEC) [13]. The molecular recognition behaviour of imprinted polymers is typically assessed by equilibrium rebinding experiments or through HPLC analysis [14].

Utilizing the thermal stability of imprinted polymers, the use of a thermal desorption GC-MS methodology for the pre-treatment, characterisation and analysis of molecularly imprinted polymers has previously been presented [15]. The technique involved the use of a direct probe device (Chromatoprobe) (Figure 5.1.) attached to a GC-MS. The use of pre-determined temperature programmes enabled the removal of volatile materials, such as template and un-reacted monomers. The power of MS permitted the identification of co-desorbing components. Result data suggested that a morphological difference between imprinted and non-imprinted species existed. The technique also demonstrated the potential to identify polymer specificity and selectivity for the composition under investigation.

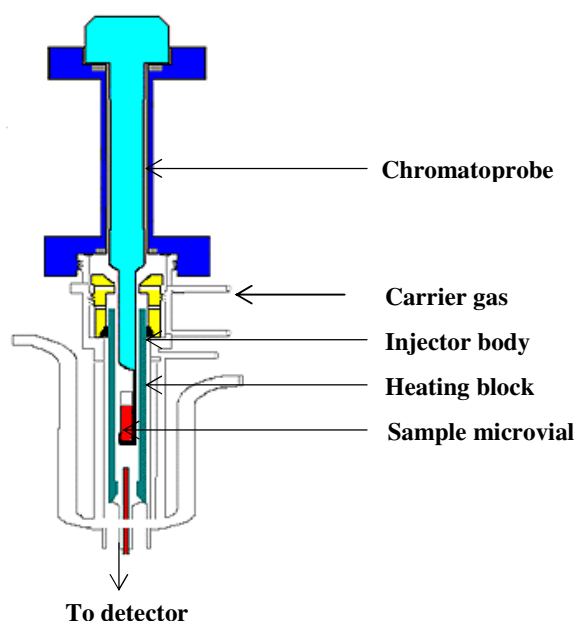


Figure 5.1. Varian direct probe device (Chromatoprobe) [16].

Based on the findings presented above, the work described herein was carried out in an attempt to further probe the suitability of this powerful MS-based technique for the characterisation of molecularly imprinted polymers, with a view to potentially developing a solid phase microextraction (SPME) fibre. Of particular interest is the sensitivity of the system in characterising polymers with fundamental differences in their porous structure. To further validate this novel technique, comparisons in the affinity obtained by thermal desorption GC-MS and by solution phase binding studies

will be made. The polymers used for this study had been synthesised and characterised (in terms of both physical and chemical properties) in previous chapters. Thus, they were deemed suitable for assessing the scope of thermal desorption GC-MS for the characterisation of imprinted polymers as direct correlations could be made.

5.2. Experimental

5.2.1. Materials and instrumentation

Table 5.1. The materials used.

Reagent	Supplier	Assay
Chloroform	Lennox (Ireland)	99.0-99.4 %
Acetonitrile	Lennox (Ireland)	99.9 %
Methanol	Lennox (Ireland)	99.8 %
2-Aminopyridine	Sigma-Aldrich (Ireland)	99 + %

Polymers used were those prepared as described in Section 2.2.1., particle size < 25 μm .

Instrumentation

- A Varian CP-3800 gas chromatograph coupled with a Varian Saturn 2000 GC/MS/MS detector was utilised for this study. A Varian Chromatoprobe (Figure 5.1.) was attached to one of the temperature programmable injection ports of the GC which was connected *via* a programmable switching valve to the MS detector through a 1 m uncoated capillary column (i.d. 100 μm) housed in the GC column oven. The flow gas was CP-grade helium at 0.5 mL min^{-1} . The programmable switching valve was used to select fractions for MS analysis or to vent fractions to waste in order to protect the MS detector from excessive exposure in the early part of the thermal treatment.

5.2.2. Thermal desorption analysis

1 mg quantities of polymeric species were accurately weighed out. The polymers were subjected to a pre-treatment temperature programme, Figure 5.2., to desorb any unreacted, volatile components. The temperature was initially maintained at 80 $^{\circ}\text{C}$ for 1 min to allow removal of water and other volatile materials. After 1 min the detector was activated, and the temperature increased to 250 $^{\circ}\text{C}$ at a rate of 15 $^{\circ}\text{C min}^{-1}$. It was then held at 250 $^{\circ}\text{C}$ for 11 min. A split ratio of 40:1 was used. Ion generation was

achieved by Electron Impact Ionisation (EI) and spectra with a mass to charge ratio (m/z) ranging from 40 to 350 were collected. Both NIP and MIP polymers were pre-treated in this manner. The column oven, which was used to control the temperature of the transfer column, was held at 80 °C for 1 min and then raised to 170 °C at 15 °C min⁻¹.

Following pre-treatment, polymers were then reloaded with 5 µL of 4 mg mL⁻¹ solution of 2-apy in chloroform, acetonitrile and methanol, and, were thermally desorbed under a second controlled temperature programme (Figure 5.2.). This programme employed two separate temperature ramps. The detector was inactive for the first 8 min to facilitate the removal of the loading solvent (at 80 °C). After 8 min the detector was turned on and the temperature ramped to 200 °C at 20 °C min⁻¹. This temperature was maintained for 6 min followed by a second temperature ramp to 250 °C at 50 °C min⁻¹. The temperature at 250 °C was held for a further 6.5 min. A split ratio of 200:1 was employed. The column oven was held at 50 °C for 8 min and then raised to 250 °C at 100 °C min⁻¹.

The pre-treatment and subsequent reloading temperature programmes, illustrated in Figure 5.2. were obtained after extensive development and optimisation [15,17].

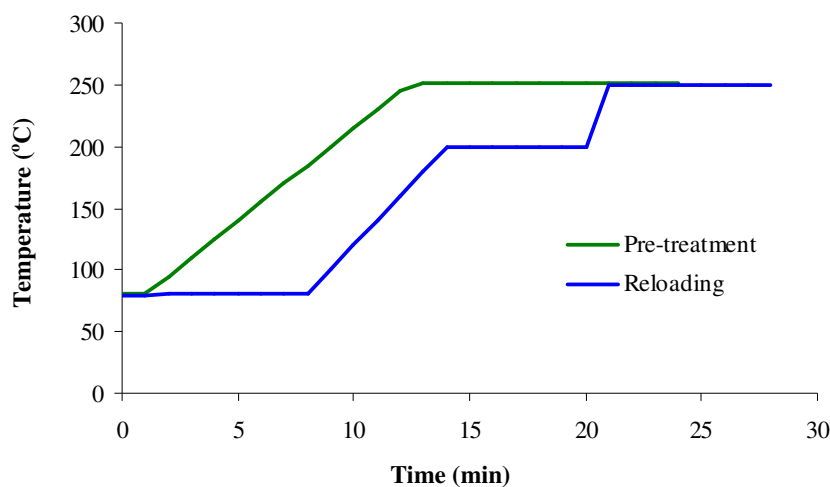


Figure 5.2. Thermal desorption pre-treatment and reloading temperature programmes employed.

5.3. Results and discussion

5.3.1. Mass spectra of polymer components

Figure 5.3. *A*, *B*, *C*, *D* and *E* show the mass spectra of 2-aminopyridine (2-apy), 4-vinylpyridine (4-VP), methacrylic acid (MAA), methyl methacrylate (MMA), and ethyleneglycol dimethacrylate (EGDMA) respectively. All spectra were obtained from the NIST mass spectral search programme (version 1.6d).

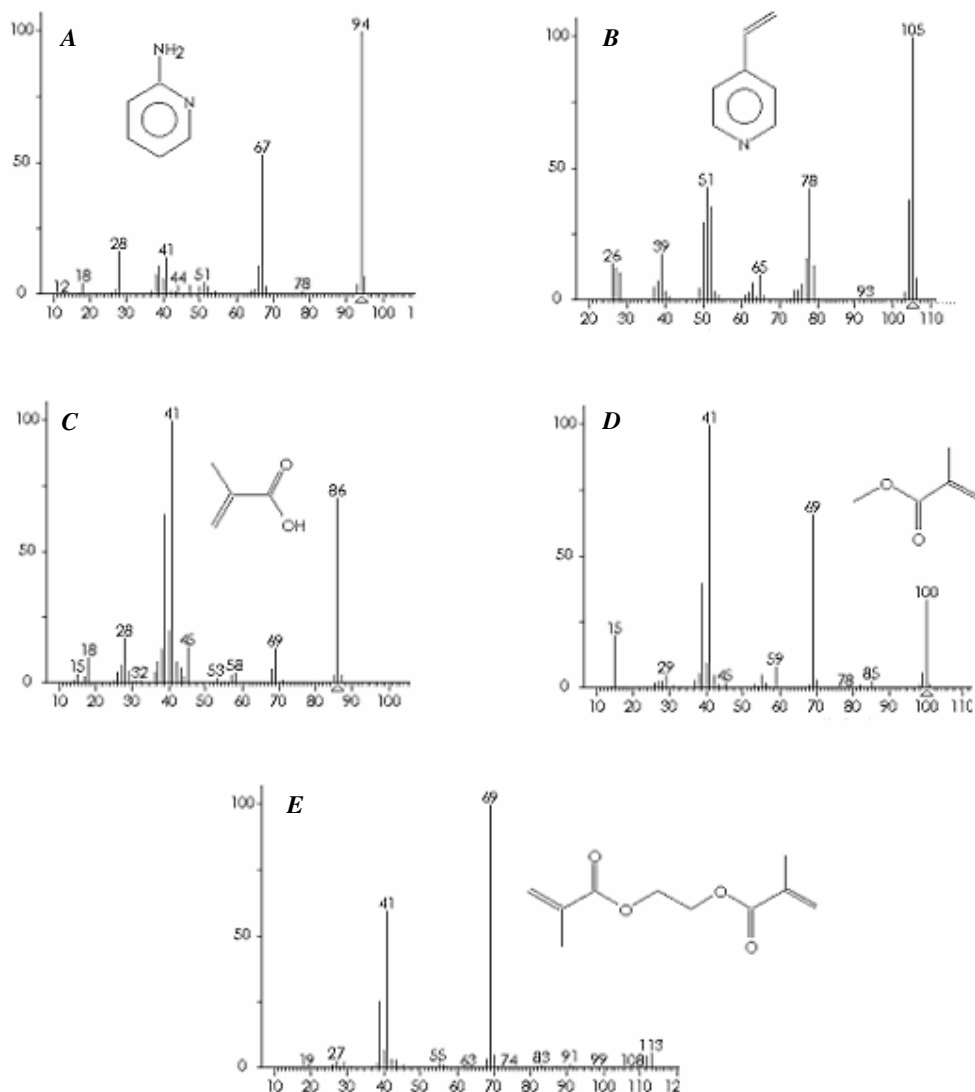


Figure 5.3. Mass spectra of *A*; 2-aminopyridine, *B*; 4-vinylpyridine, *C*; methacrylic acid, *D*; methyl methacrylate and *E*; ethyleneglycol dimethacrylate.

An advantage of mass spectral (MS) analysis is its ability to identify a compound in a mixture of co-eluting components. However, this is provided that the compound of interest produces a unique ion of sufficient abundance. The base ion (ion with 100 % abundance) is typically used so as to give maximum sensitivity. If this ion is not unique to the particular analyte a second ion of high abundance is instead used. This is the case for MAA where its base ion, m/z 41, is also found as a fragment ion in EGDMA.

5.3.2. Polymer pre-treatment

5.3.2.1. Bleed composition analysis

In non-covalent imprinting the interactions between template and functional monomer are weak in nature and are governed by thermodynamic factors. Addition of heat to the pre-polymerisation mixture has been shown to weaken these interactions, particularly hydrogen bonds [18,19]. Whilst this is a disadvantage when attempting to form highly selective imprinted polymers, it can be used in an advantageous capacity post-polymerisation to facilitate template removal through weakening of the interactions. Thus, the thermal desorption technique used in these studies is based on this phenomenon.

Figures 5.4. illustrates the RIC profiles obtained for MIP and NIP species for the three different monomeric systems containing 40 mmol of EGDMA. It is apparent from the reconstructed ion chromatograms (RIC which is the total ion count of all the ions detected (m/z 40 - 350)) that NIP species produced more bleed than corresponding MIP species. This was consistently observed across all compositions, which suggests that there was potentially a lower rate of polymerisation in the NIP species which may have resulted in fundamental differences in the polymer backbone. This also correlated with results reported in Chapter 4 where the NIP polymers also displayed higher levels of bleed relative to corresponding imprinted polymers during low levels of analyte reloading.

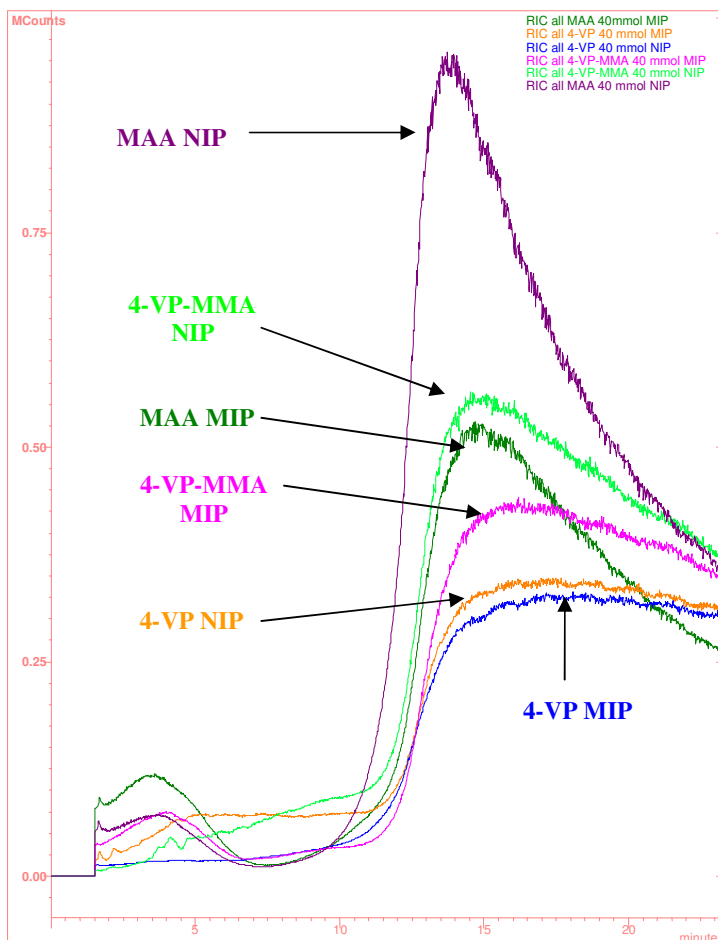


Figure 5.4. Reconstructed Ion Chromatograms (RIC) for MAA, 4-VP and 4-VP-MMA MIP and NIP species formed with 40 mmol EGDMA.

It is interesting to note that a difference exists in the shapes of the RIC profiles between the three monomer compositions. The MAA profiles have a moderately sharp peak with the maximum level of bleed corresponding to the maximum temperature (250 °C) reached in the temperature programme employed. This then declines relatively fast while the temperature is maintained at 250 °C.

For the 4-VP containing polymers the distinction between MIP and NIP bleed is less than that observed for MAA polymers. Again the bleed reaches a maximum at 250 °C, and for those polymers containing 4-VP only it plateaus off whilst for the co-monomer system it gradually decreases, albeit at a lesser rate than MAA. This implies that a

difference in the degree of crosslinking may exist between each monomeric composition, with the MAA polymers being crosslinked to a lesser extent.

Figure 5.5. illustrates the RIC profile, m/z 69 (EGDMA), m/z 94 (2-apy) and m/z 86 (MAA) for the 10 mmol MIP formed using MAA as the functional monomer, and it demonstrates how each polymeric component of interest can be monitored without interference. The high level of bleed relative to each of the components would suggest the presence of partly polymerised monomer.

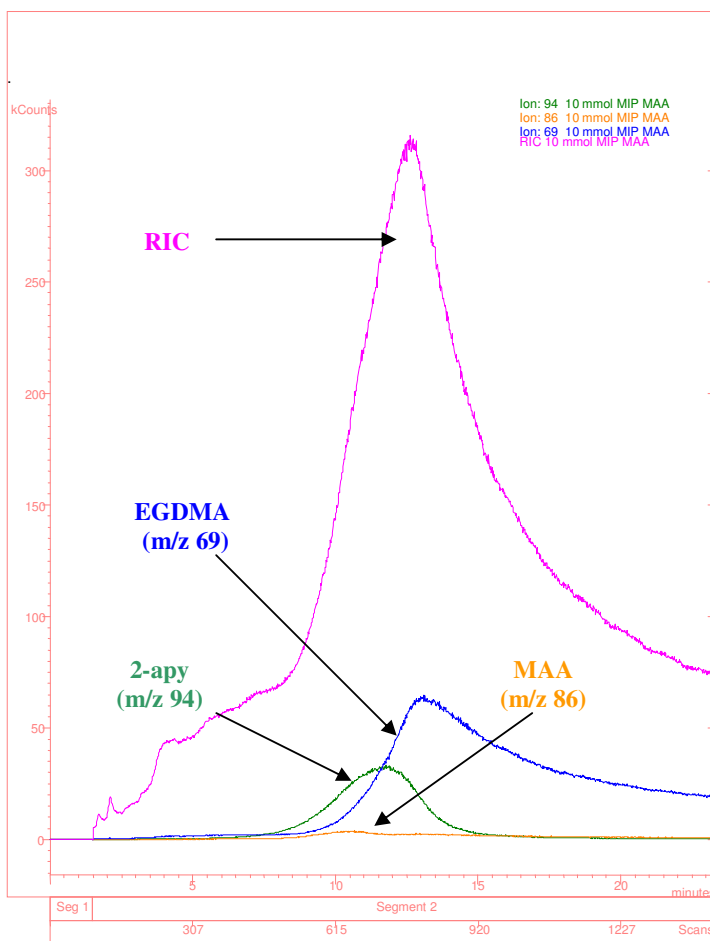


Figure 5.5. Overlay of RIC, m/z 94, m/z 69 and m/z 86 for 10 mmol MIP formed with MAA.

The bleed consisted mainly of EGDMA (m/z 69). As can be seen in Figure 5.6, the bleed for the MAA polymers increased with increasing amount of EGDMA used in the polymer formulation. This higher level of bleed was expected as there was a larger concentration of EGDMA present in the polymer composition and it suggests that the entire quantity of EGDMA was not involved in polymer formation. As the polymerisation proceeds and the onset of gelation occurs the excess double bonds will become less accessible within the highly crosslinked domains of the polymer [20].

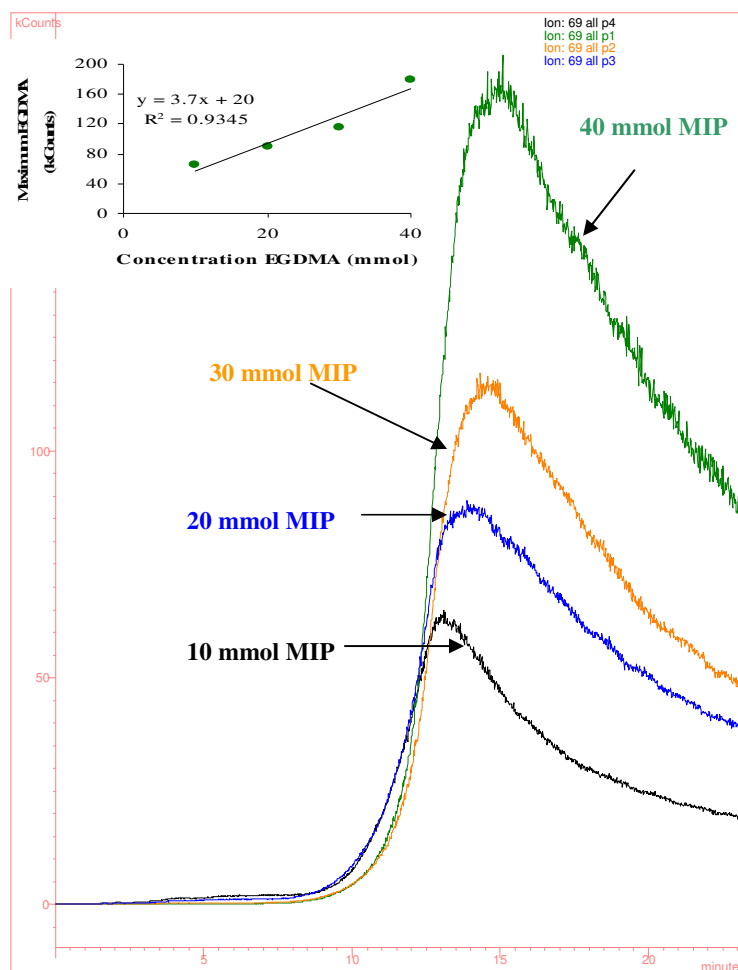


Figure 5.6. Bleed due to EGDMA from MAA polymers. Bleed increases in the order 10 mmol < 20 mmol < 30 mmol < 40 mmol. The insert shows the maximum EGDMA bleed for each composition.

Figure 5.7. illustrates the bleed for 40 mmol MIP and NIP formed using MAA as the functional monomer. The bleed attributed to EGDMA was higher for NIP than

corresponding MIP species. This result is significant as it suggests that the NIP and MIP species are not crosslinked to the same degree, and therefore, a difference in the degree of crosslinking may exist.

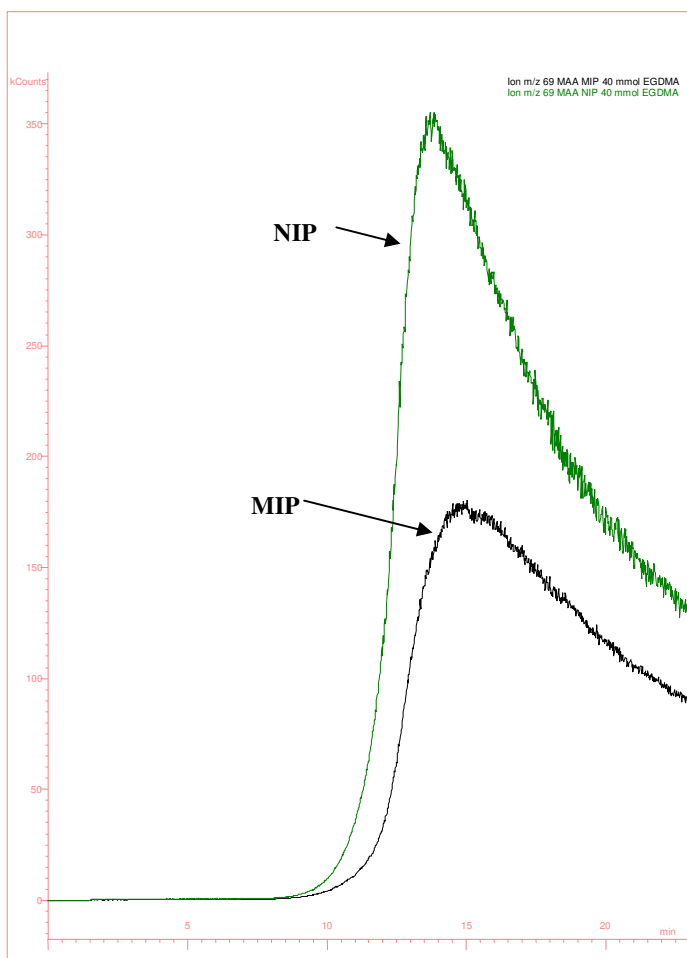


Figure 5.7. Mass spectra EGDMA (m/z 69), (crosslinking monomer), desorbed from MAA MIP and NIP prepared with 40 mmol EGDMA.

This trend was observed in multiple analyses, for all MIP and corresponding NIP species across the monomeric systems formed with different concentrations of EGDMA. However, what is more significant is that the differences in bleed between the MIP and NIP species was greater for MAA polymers than for the 4-VP and 4-VP-MMA polymers, Figure 5.8. This again would suggest a difference in polymeric structure due to the type and nature of the functional monomer employed in polymer formation, and correlates with results obtained in the nitrogen sorption experiments where MAA

polymers displayed fundamentally different adsorption/desorption isotherms and overall had larger BET surface areas, pore volume and pore sizes. While definite differences in the morphology of the polymers have been established, a technique such as Differential Scanning Calorimetry (DSC) could be used to identify differences in the degree of crosslinking.

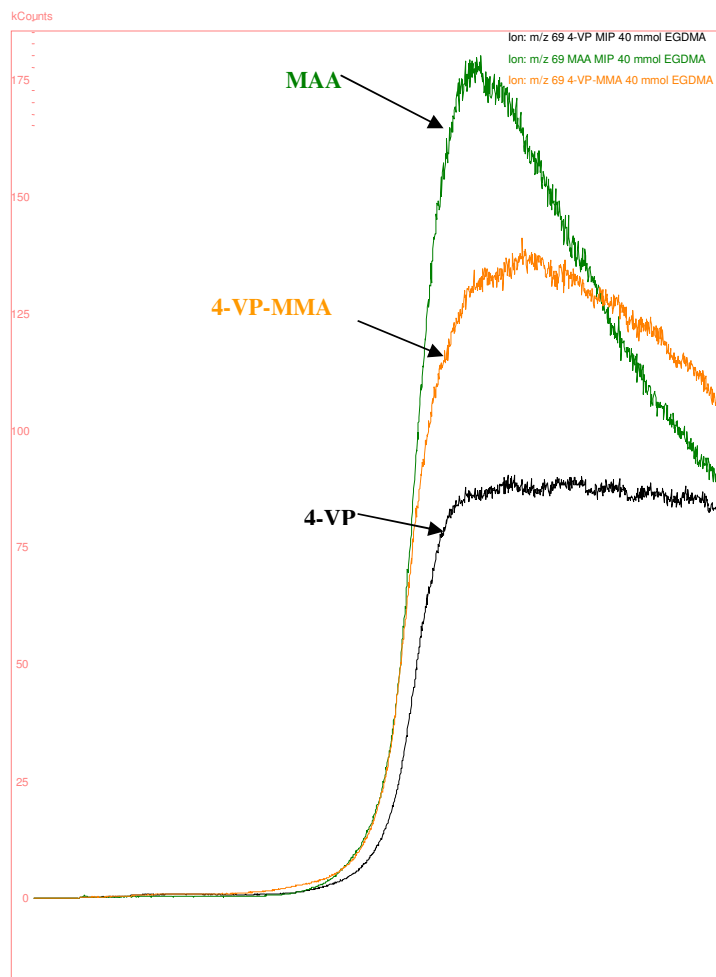


Figure 5.8. Bleed due to EGDMA for MAA, 4-VP and 4-VP-MMA polymers formed from 40 mmol EGDMA.

A comparison for the pre-treatments for the 40 mmol MIPs formed with and without functional monomer showed that the RIC was higher when the polymer was formed with no functional monomer (the comparison was made to the polymer formed using MAA as the functional monomer. The profiles are not shown). This was not expected as the RIC is the total ions generated in the pre-selected selected mass range (m/z 40 – 350 in this case) and as no functional monomer was used in the formulation there were

potentially less volatile components available for desorption. When higher amounts of EGDMA were used in polymer formulation, the mole ratio of MAA to EGDMA decreased, and the resultant polymers formed were more rigid. Lower amounts of crosslinking monomer, and hence higher mole ratios of MAA to EGDMA, produced more flexible polymers. Therefore, with the addition of no functional monomer it might be expected that polymers with a higher crosslink density would form (Refer to Table 2.3. for nominal crosslink ratio values).

Successive pre-treatments were carried out on the polymers and the RIC was found to decrease with each pre-treatment. Figure 5.9. displays a plot of the bleed due to EGDMA for each pre-treatment. Each data point was taken as the maximum level of bleed in the respective profiles.

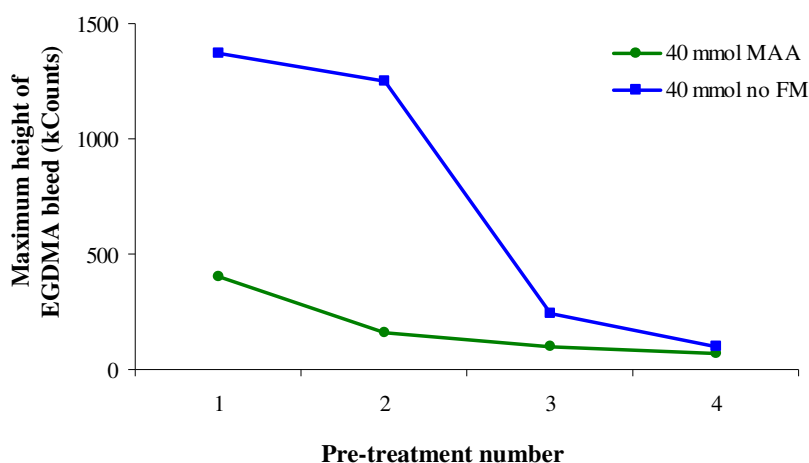


Figure 5.9. EGDMA bleed for successive pre-treatments of 40 mmol MIP formed with and without functional monomer.

The graph shows evidence of desorption of EGDMA from both polymers with prolonged exposure to evaluated temperatures, which may have been due to residual EGDMA or possible degradation. Evidence for degradation was supported in earlier studies by a reduction in the area of peak 2 relative to peak one by consecutive reloadings on the same polymer sample [15]. The significance of peak one and two will be discussed at a later stage. The EGDMA bleed was much higher for the polymer formed in the absence of functional monomer. The bleed decreased rapidly going from

pre-treatment 2 to 3. By pre-treatment 4 it had reached levels similar to that of the MAA polymer.

Overall the polymer formed using no functional monomer was more susceptible to thermal degradation. This was despite the claim (above) that, in theory, it should have been more crosslinked. It is therefore proposed that while lower mole ratios of functional monomer to crosslinking monomer form rigid polymers, a minimum amount is required to prevent the formation of a flexible backbone. The addition of functional monomer should provide an extra point (*i.e.* double bond) for crosslinking to take place. Thus, the polymers that did not contain functional monomer had a lower degree of crosslinking.

Selection of the ions specific to MAA and 4-VP (m/z 86 and 105 respectively) showed that there was slight desorption of the functional monomers (profiles not shown). The level of bleed was small relative to the respective RIC profiles. As the composition of crosslinking monomer decreased the bleed due to the functional monomer remained relatively consistent. This was expected as the concentration of functional monomer in each composition remained constant. The bleed from MIP and corresponding NIP polymers was also similar in all cases. The level of bleed observed between MAA and 4-VP containing polymers was similar at each EGDMA composition. Although MAA and 4-VP were present in smaller quantities than EGDMA, the consistently low levels of bleed imply that it was better incorporated into the polymer network.

5.3.2.2. Template removal

Template removal was carried using the pre-treatment method as shown in Figure 5.2. Particles of less than 25 μm diameter were used for thermal desorption studies and as they had not been subjected to a template extraction procedure and had remnants of the original template present. Selection of the ion m/z 94 allowed the template removal to be followed during the pre-treatment stage. Selection of the same ion for the NIP species showed that its intensity was not above that of the low intensity background and so its detection was possible without significant interference, Figure 5.10.

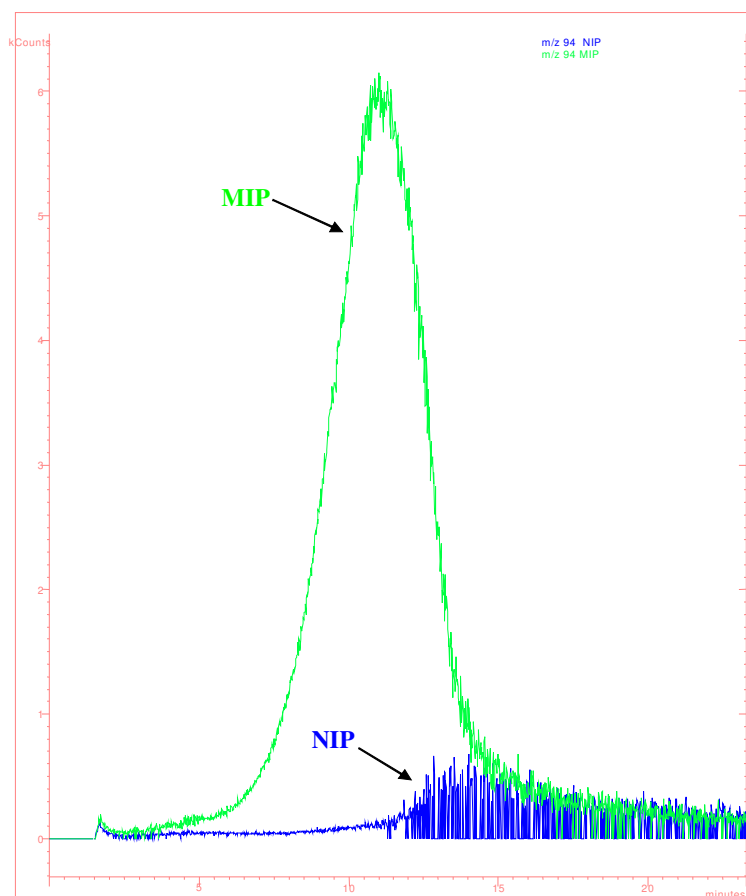


Figure 5.10. Mass spectra for 2-apy (m/z 94) for MIP and corresponding NIP species, MAA polymers prepared with 30 mmol EGDMA.

Integration of the profiles showed that for the MAA polymers there was an increase in response (counts) for the 2-apy ion (m/z 94) as the concentration of EGDMA in each polymer decreased, Figure 5.11. A minimum amount of crosslinking monomer is required to maintain the integrity of the binding sites. Therefore, a reduction in crosslinker (EGDMA) may lead to a higher degree of flexibility, which would increase the rate of egress of the template from the polymer as the template is not tightly retained. It is suggested that this is the case for the polymers under study. The amount of 2-apy used remained constant for all compositions while the amount of EGDMA was varied. The amount of 2-apy displaced was dependant on the quantity of EGDMA employed in polymer synthesis, as a higher amount of crosslinker resulted in a higher degree of template retention. Two successive pre-treatments for the same sample of MIP showed that the maximum amount of 2-apy was displaced from the polymer with one pre-treatment (Figure 5.11). As different levels of template were displaced for the various polymers it is suggested that the template was irreversibly retained within the polymers formed from higher amounts of EGDMA.

A correlation with porosity data (Section 2.3.4.) is also identified. Larger average pore diameters and a wider pore distribution, as seen in those polymers formed from lower amounts of EGDMA, would facilitate the release of template from the polymers. This combined with the flexibility of the polymers may have contributed to the increased response. A higher quantity of displaced template would imply that there were more unoccupied binding sites within the polymer network available for subsequent rebinding.

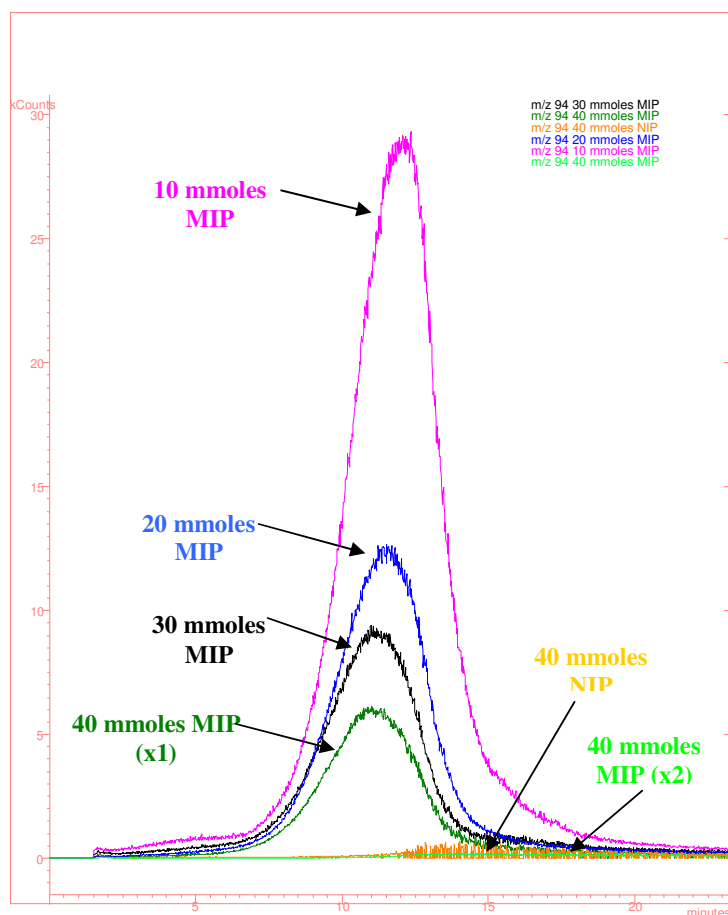
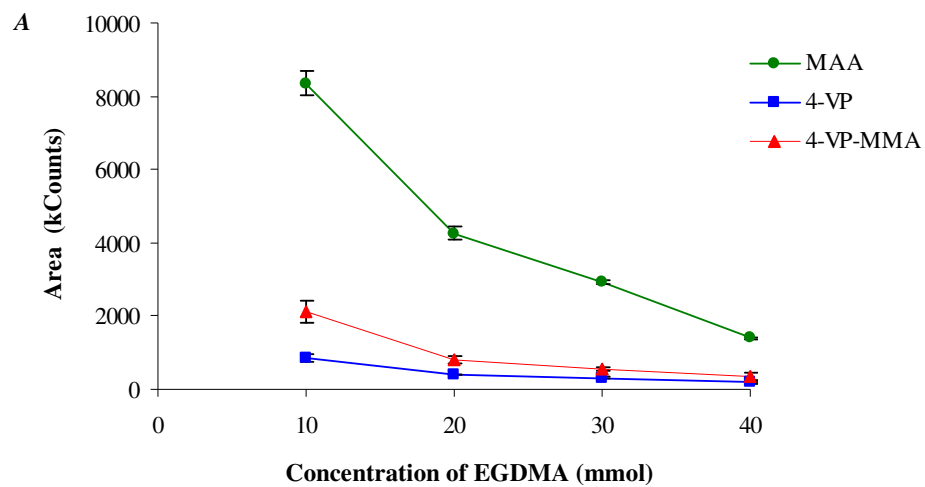


Figure 5.11. 2-Apy ion (m/z 94) desorbed from MIP species prepared with 40 - 10 mmol EGDMA. Two successive pre-treatments for 40 mmoles MIP and the desorption profile for 40 mmol NIP are also shown.

The template displaced from MAA polymers was greater than that displaced from 4-VP polymers and the co-monomer system, Figure 5.12 A and B. There was no 2-apy displaced from the polymers prepared with no functional monomer. As the template could not be thermally removed to the same degree from the 4-VP containing polymers it is proposed that 2-apy was more tightly retained within polymers containing 4-VP. This hypothesis also correlates with the solution phase extraction profiles, where initial template removal was difficult to achieve. Again correlations with nitrogen sorption data exists. Overall the 4-VP containing polymers were less porous than the MAA polymers. The 10 mmol 4-VP polymers were suggested as having a very small level of

porosity. The flexibility due to lower amounts of EGDMA being present in the polymer formulation must also be accounted for when analysing the amount of template displacement. The amount of 2-apy displaced from each polymer composition was consistently reproducible across triplicate analysis.



Continued on the next page

B

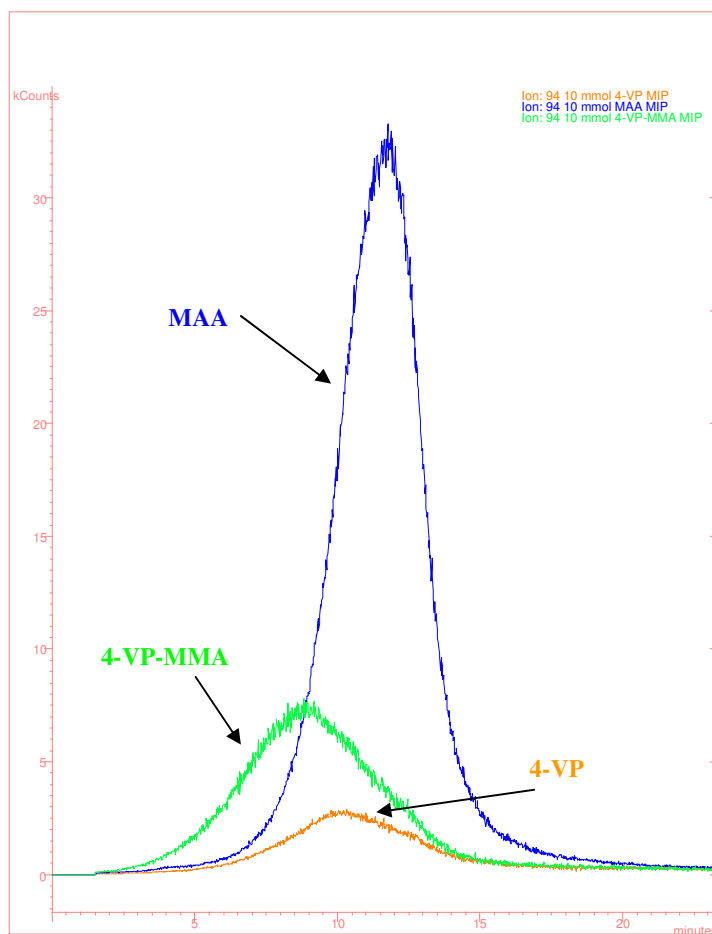


Figure 5.12. A; 2-apy displaced from MAA, 4-VP and 4-VP-MMA 40 – 10 mmol EGDMA imprinted polymers. Errors bars are based on standard deviation of +/-1 for n = 3. **B;** 2-apy desorption profiles from MAA, 4-VP and 4-VP-MMA 10 mmol EGDMA imprinted polymers.

5.3.4. Examination of polymer specificity utilising thermal desorption studies

The affinity of the thermally pre-treated polymers (MAA and 4-VP only) was assessed by reloading 5 μL of 4 mg mL^{-1} solution of 2-apy in chloroform, which was subsequently desorbed using a second temperature programme (Figure 5.2.). This temperature programme was chosen after extensive method development and it ensured that 2-apy was retained in the polymer until the MS detector was activated [15,17].

Figure 5.13 illustrates the RIC for 40 and 10 mmol MAA MIPs and the profiles for 2-apy, EGDMA, MAA and chloroform (m/z 83) for the 10 mmol MAA imprinted polymer. The RIC profile, more specifically the high level of bleed relative to the other components, would suggest possible degradation coinciding with the ramps of the temperature programme employed. There was less bleed for the 40 mmol polymer than for the 10 mmol suggesting a higher level of degradation for the latter composition. This was also observed for the 4-VP polymers although the shape (not shown) was slightly different suggesting a different rate of degradation. This correlated with results obtained in the preliminary investigations into the suitability of this technique [15]. Consecutive reloadings on the same polymer sample resulted in a reduction of the polymers ability to selectively retain the analyte, as expressed in terms of the area of peak 2 (the significance of peak 2 will be discussed in detail at a later stage). This was attributed to polymer degradation. However, it was not substantial enough to prevent identification of a specific response of MIP over NIP after seven consecutive reloadings.

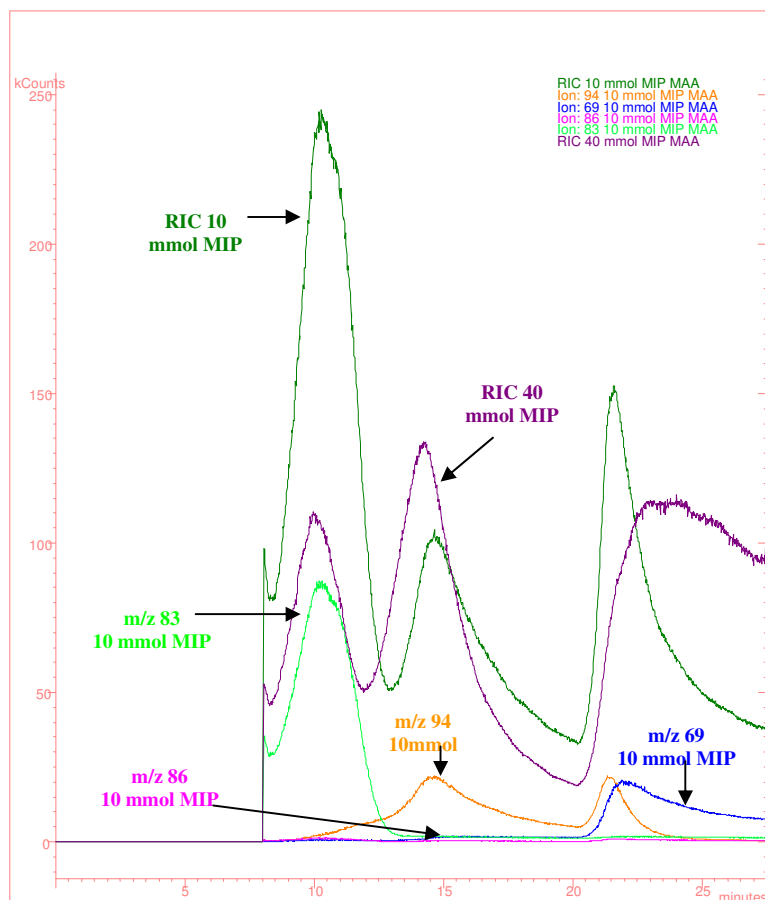


Figure 5.13. RIC and the profiles for 2-apy, EGDMA and chloroform for the 10 mmol MAA imprinted polymer.

Bleed due to EGDMA was identified during the template reloading stage, again, suggesting possible degradation. Analysis of the EGDMA bleed for 10 mmol MIP (MAA) during the pre-treatment and reloading stages are shown in Figure 5.15. (4-VP results were similar). The maximum temperature reached during both the pre-treatment and reloading was 250 °C. It is evident from Figure 5.14, that a larger amount of EGDMA was displaced during the pre-treatment stage. It is presumed that the bleed in the pre-treatment stage was due to residual un-reacted crosslinking monomer. As the binding capability of the polymers was shown to diminish with prolonged exposure to evaluated temperatures [15], suggesting possible destruction of binding sites, it is suggested that the bleed during reloading was due to degradation as opposed to removal

of residual EGDMA. A combination of techniques such as thermogravimetric analysis (TGA), DSC and nitrogen sorption porosimetry would give a better insight to potential degradation.

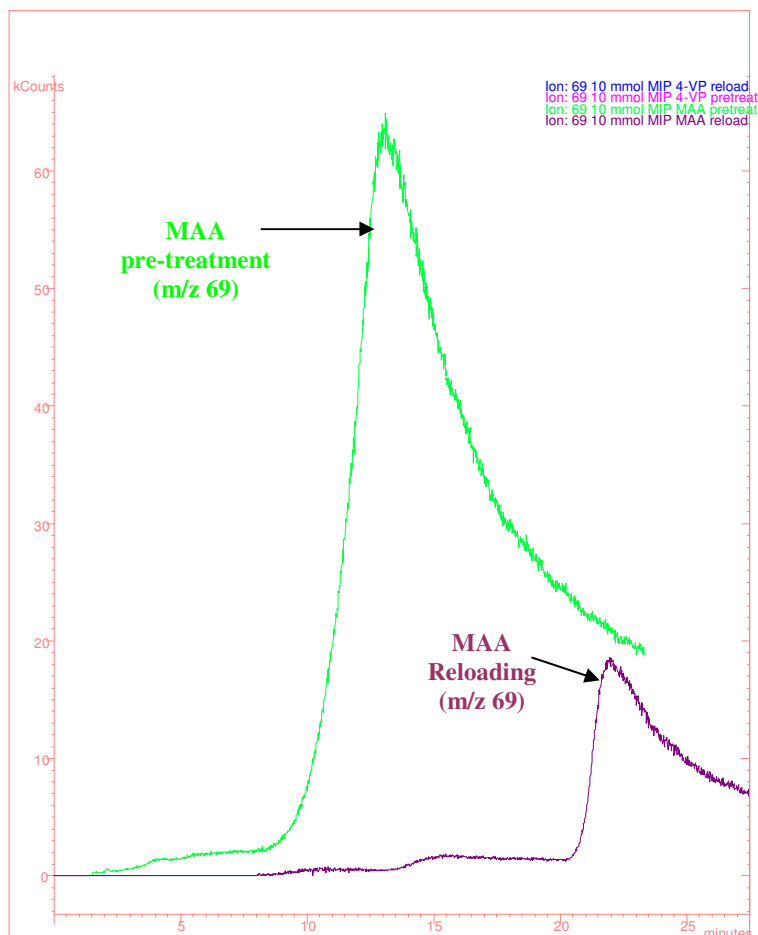


Figure 5.14. Bleed attributed to EGDMA for 10 mmol imprinted polymer (MAA) for pre-treatment and reloading.

Another interesting result arising from comparison of the RIC profiles is that in the pre-treatment stage the RIC for the 40 mmol polymers was higher than that for the 10 mmol polymers. The opposite effect was observed for reloading of the polymers, Figure 5.15. As can be seen the EGDMA bleed was less for the 10 mmol than the 40 mmol polymer. It is suggested that the 10 mmol polymers may have degraded faster due to a less crosslinked polymer network.

The RIC profiles for reloading in chloroform, acetonitrile and methanol were similar in terms of the actual levels of bleed. Figure 5.16. Chloroform was shown to swell the polymers to a larger extent than acetonitrile or methanol (Chapter 2), which may have had the potential to facilitate migration of un-reacted monomers to the surface of the polymers, thereby increasing the level of bleed. As the level of bleed observed in the RIC profiles for each solvent were essentially similar, although the shapes may have differed slightly, it is suggested that the increased bleed was due to degradation as opposed to un-reacted or partly polymerised low molecular weight monomers.

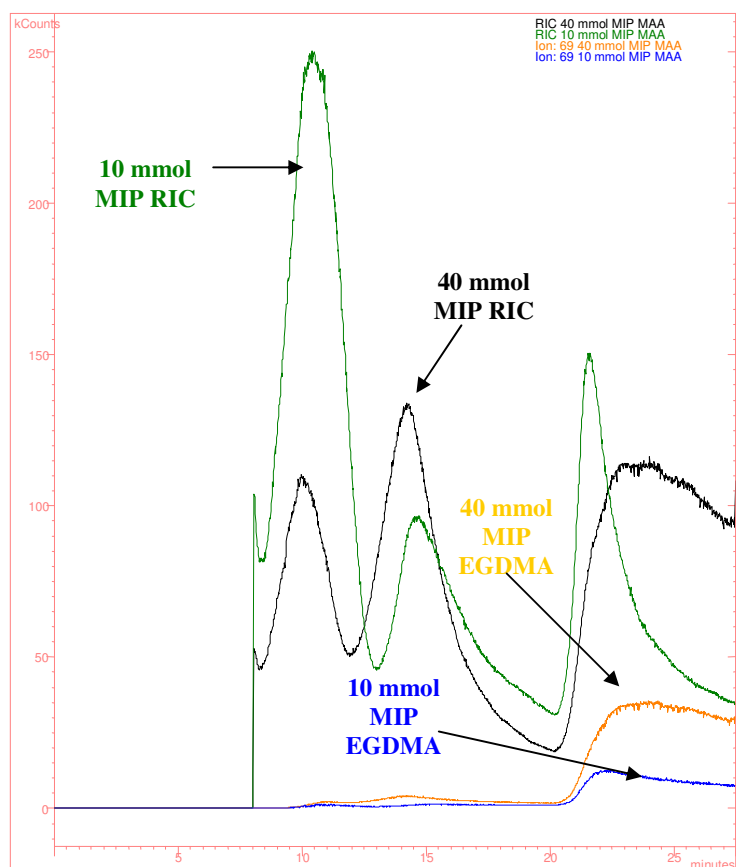


Figure 5.15. RIC and EGDMA profiles (reloading 2-apy in chloroform) for 40 and 10 mmol MAA imprinted polymer

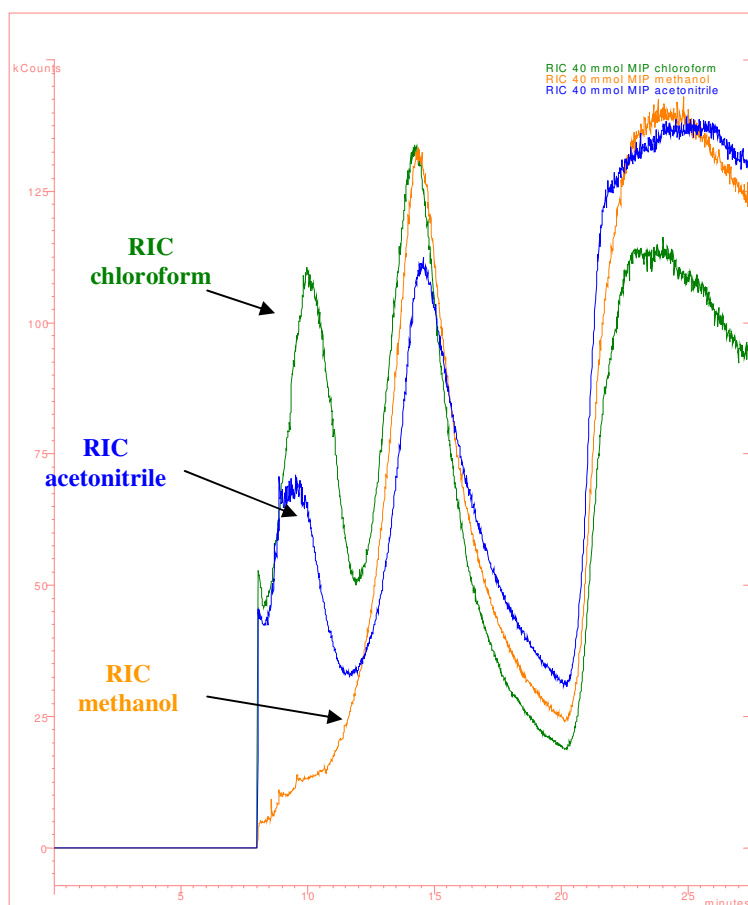


Figure 5.16. RIC profiles for reloading 2-apy in chloroform, acetonitrile and methanol onto MAA 40 mmol EGDMA imprinted polymer.

The displacement of 2-apy was again followed by selection of m/z 94. The MAA polymers will be discussed first.

For 2-apy reloading in chloroform, the profiles consisted of two peaks, which corresponded to the second ramp in the temperature programme. The area under each peak represents the amount of reloaded material desorbed. The area of peak 2 (given as a percentage) in relation to the total area for 2-apy for MAA polymers is given in Table 5.2. It is apparent that the area attributed to peak 2 changed with polymer composition (this is also shown for 40 – 10 mmol MIPs in Figure 5.17). A reduction of EGDMA was

accompanied by an increase in area of peak 2. Expressed as a percentage of the total area, the percentage increase was from 2.79 (+/- 0.11) % to 26.90 (+/- 1.93) %, when going from the 40 to 10 mmol (MIPs). As a higher temperature, and therefore greater energy, was required to displace all of the 2-apy (represented by peak 2), it is suggested that the reloaded analyte had greater access to the internal binding sites and functionality of the polymer when lower amounts of EGDMA were used to form the polymers. The higher degree of displacement observed at the lower temperatures for the polymers with a higher concentration of EGDMA imply that 2-apy was bound only to the surface of the polymer (due to rigidity, thus preventing access). Similar trends were observed for non-imprinted polymers where the percentage area for peak 2 for non-imprinted polymers increased from 1.18 (+/- 0.22) % to 28.85 (+/- 1.25) % when going from high to low amounts of EGDMA.

Table 5.2. Thermal desorption data for 2-apy (m/z 94) for MAA polymers. %RSD for total area MIPs = 5.66% and %RSD for total area NIPs = 7.81%

EGDMA (mmol)	Total area (kCounts (+/- SD))		Area pk 2 (kCounts (+/- SD))		% Area pk 2 (kCounts (+/- SD))	
	MIP	NIP	MIP	NIP	MIP	NIP
40	5730 (+/- 38)	5345 (+/- 519)	160 (+/- 7)	63 (+/- 13)	2.79 (+/- 0.11)	1.18 (+/- 0.22)
30	5097 (+/- 50)	6096 (+/- 338)	491 (+/- 22)	244 (+/- 26)	9.63 (+/- 0.37)	4.01 (+/- 0.49)
20	5769 (+/- 193)	5749 (+/- 197)	1266 (+/-289)	829 (+/- 38)	21.86 (+/- 5.08)	14.42 (+/- 0.22)
10	5494 (+/- 160)	5096 (+/- 160)	1477 (+/-101)	1470 (+/- 18)	26.90 (+/- 1.93)	28.85 (+/- 1.25)

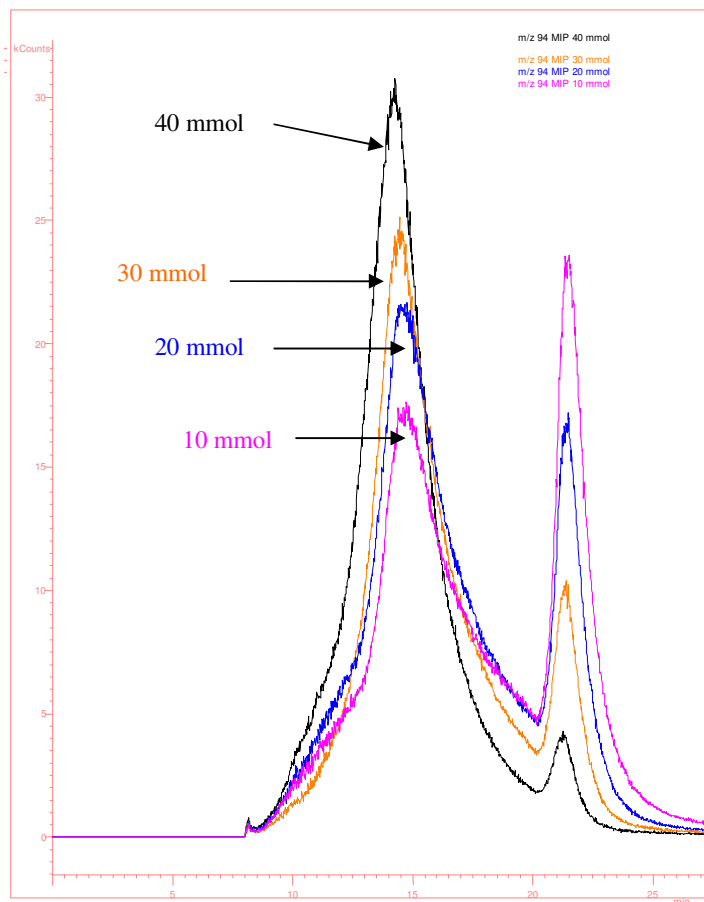
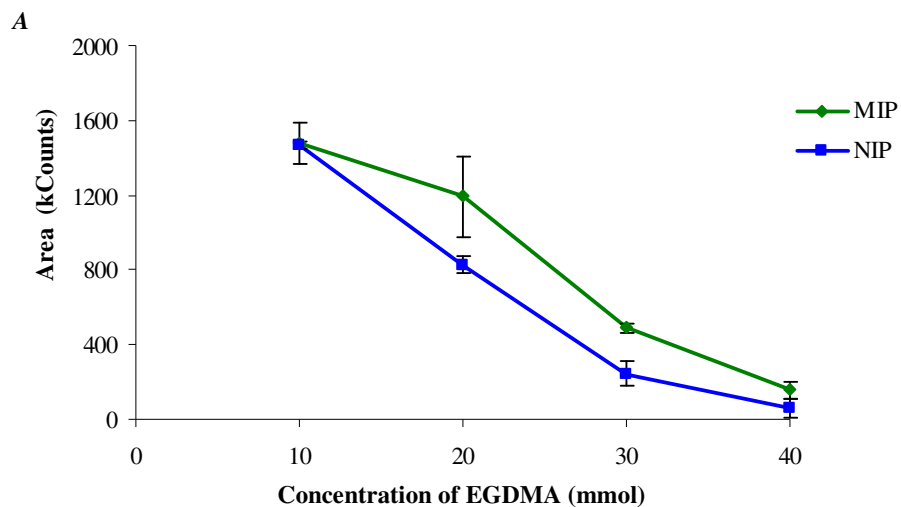


Figure 5.17. Desorption profiles for MAA MIP species prepared with 40 - 10 mmol EGDMA.

The area of peak 2 for NIP polymers was consistently smaller than that obtained for peak 2 of the corresponding MIP species. This implied that MIP species had the ability to selectively retain 2-apy to a higher degree than NIP species. As the concentration of EGDMA decreased, the discrimination between MIP and NIP profiles also decreased, Figure 5.18 A and B, which suggested a loss of specificity.



B

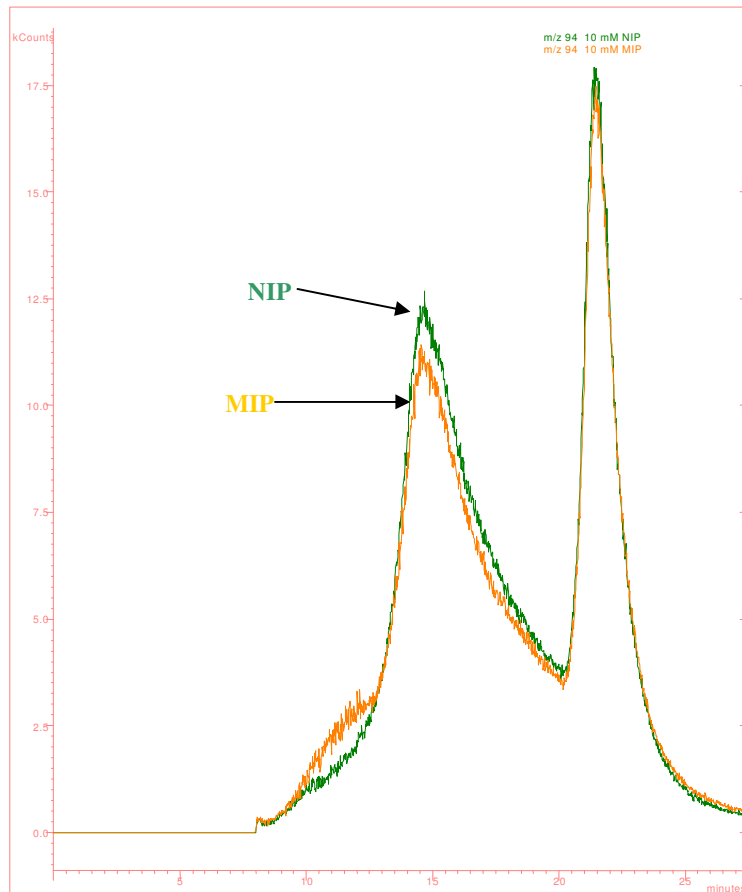


Figure 5.18. Desorption of 2-apy from MAA polymers A; Area of peak 2 for MIP and NIP polymers and B; MIP and NIP desorption profiles prepared with 10 mmol EGDMA. Errors bars are based on standard deviation of +/-1 for n = 3.

It has been proposed [15] that the percentage area for peak 2 MIP/ percentage area for peak 2 NIP is a measure of a specific response of the MIP compared to its reference NIP . The variation in this ratio with varying EGDMA concentration (Table 5.3.) provides an interesting insight into polymer morphology. Where the amount of EGDMA in the polymer composition is highest (40 and 30 mmol MIP and NIP) the ratio of percentage peak 2 MIP/ percentage peak 2 NIP is also highest indicating the presence of relatively inflexible imprinted sites in these polymers. When the amount of EGDMA is lowest MIP and NIP displayed a very similar response. This is consistent with a more flexible polymer which is able to conformationally adapt and bind the reloaded template.

Table 5.3. % Area peak 2 MIP/ % Area peak 2 NIP polymers. Errors are based on +/- 1 standard deviation for n= 3

EGDMA (mmol) (MIP/NIP)	% Area peak2 MIP/ % Area peak2 NIP
40	2.36 (+/- 0.54)
30	2.40 (+/- 0.39)
20	1.52 (+/- 0.44)
10	0.93 (+/- 0.11)

In the rebinding experiment a fixed amount of polymer (≈ 1 mg) was used in combination with a fixed volume, 5 μ L, of 4 mg mL⁻¹ solution of 2-apy. Thus, the number of free carboxyl groups increased as the percentage of EGDMA in the polymer composition decreased. As the binding of 2-apy is attributed to hydrogen bonding interactions with carboxyl groups [21] it is expected that 2-apy should bind more strongly to the polymer (both MIP and NIP) as the concentration of EGDMA is reduced.

The total area count of 2-apy desorbed from MIP and NIP species, with the various crosslinker concentrations are shown in Figure 5.19. The results demonstrate not only the reproducibility of the desorption technique, but also the accuracy of manually injecting 5 μL of the analyte onto the polymers (the % RSD values are reported in Table 5.2.).

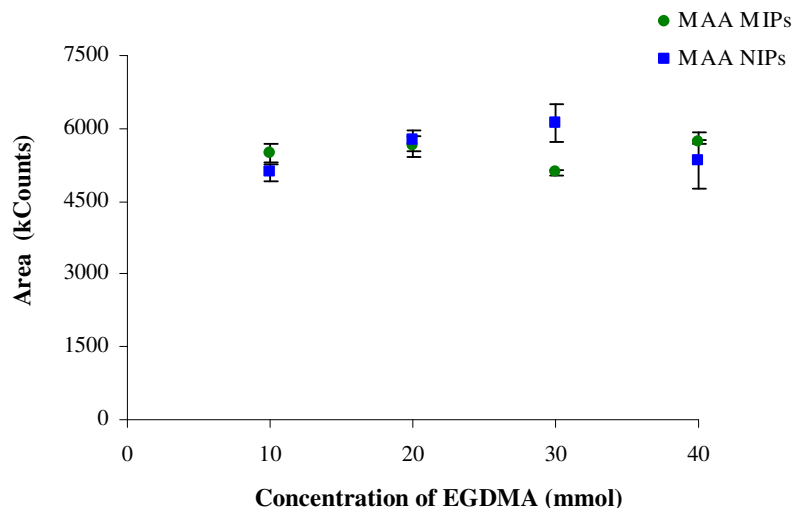


Figure 5.19. Total area count for desorption profiles of 2-apy desorbed from MAA MIP and NIP polymers. Error bars are based on +/-1 standard deviation for n=3

The investigation of specificity of the polymers containing only 4-VP was carried out as described for the MAA polymers. Desorption profiles obtained for 4-VP imprinted polymers are illustrated in Figure 5.20. Unlike the results obtained for the MAA polymers, the bulk of the 2-apy was displaced at lower temperatures. This implies that the 2-apy was bound only to the surface of the polymers and was not retained within the polymer matrix, due to low porosity. It was only with the polymer formed from 10 mmol EGDMA that a higher temperature was required for 2-apy displacement. As these polymers were found to be very non-porous materials (Chapter 2) it is suggested that the phenomenon observed here was due to surface functionality as opposed to porosity features.

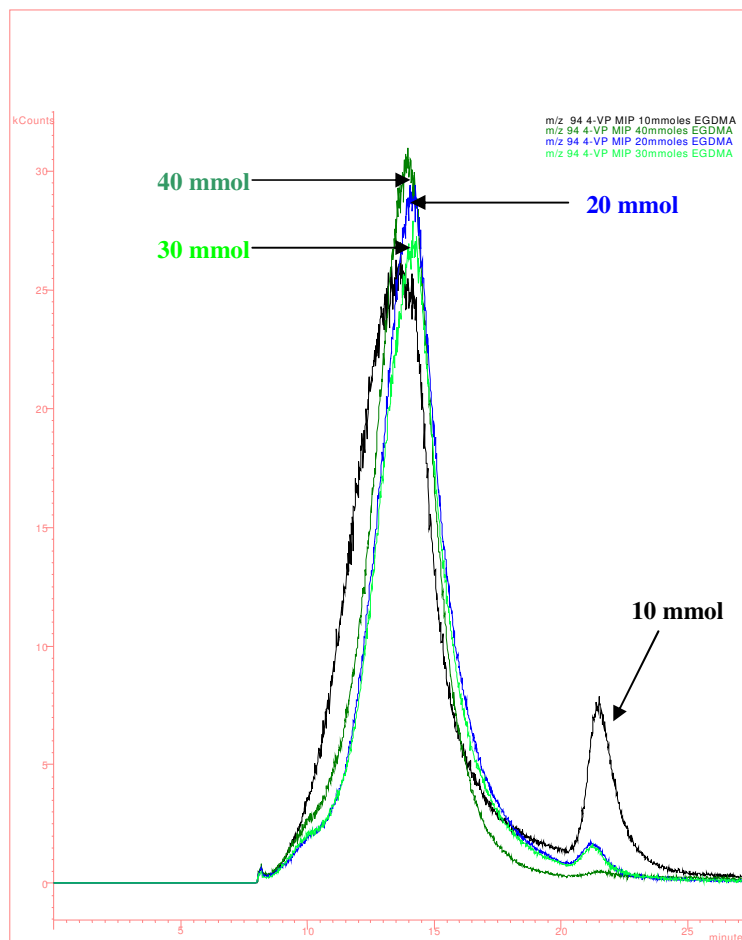


Figure 5.20. Desorption profiles obtained for reloading 2-apy onto 4-VP MIP species prepared with 40 – 10 mmol EGDMA.

A higher temperature was also required to displace 2-apy from the 10 mmol NIP species, which suggested some degree of retention at lower concentrations of EGDMA. However, as can be seen from Figure 5.21., statistically there was no difference between MIP and NIP, and no specificity of MIP over NIP could be identified.

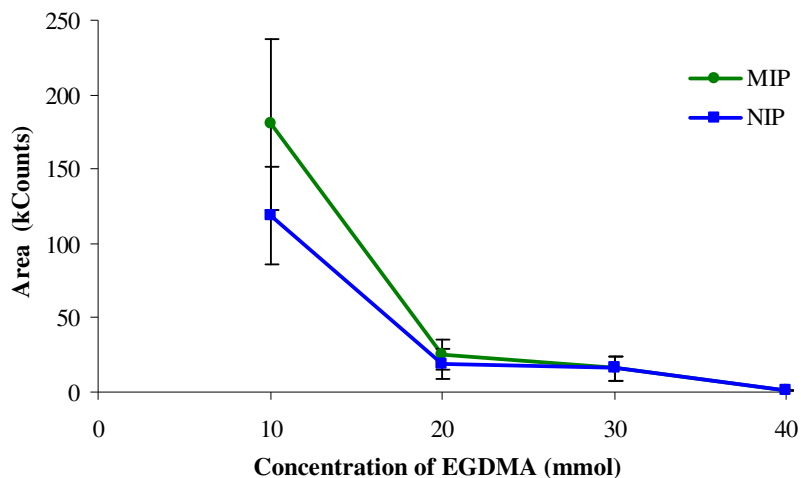


Figure 5.21. MIP and NIP desorption profiles 4-VP polymers prepared with 40 -10 mmol EGDMA. Error bars are based on +/-1 standard deviation for n=3.

Overall the binding onto 4-VP polymers was less than for MAA counterparts, as illustrated by the elution of 2-apy at lower temperatures. It is suggested that the difference in the degree of binding is due to a difference in the morphology of the polymers *i.e.* that 4-VP polymers have a more rigid structure and a less porous structure than MAA polymers.

5.3.5. Comparison of binding results obtained using thermal desorption GC-MS and UV-based solution phase analysis

To further validate the thermal desorption method in the characterisation of imprinted polymers a comparison was made between affinity results obtained *via* desorption studies utilising GC-MS and those obtained in a solution phase as assessed by UV/VIS spectroscopy (Chapter 3). This comparison was made for the MAA polymers.

When the binding behaviour of the polymers was assessed in a solution phase (Chapter 3) using chloroform the overall affinity of the polymers, both specific and non-specific in nature, was found to increase with decreasing EGDMA content. This phenomenon was attributed to the higher number of free carboxyl groups found in the polymers as the concentration of EGDMA in the composition was reduced which increased the capacity of the polymers. The loss of specificity which was observed between the MIP and NIP polymers provides support for the flexible nature of the polymer, combined with its increased porosity, with change in polymer composition. A correlation is identified between this trend and that seen using thermal desorption. The degree of non-specific binding, when assessed in the solution phase by UV/VIS spectroscopy and in the solid phase by thermal desorption, was found to significantly increase with decreasing EGDMA content.

A second correlation was identified through analysis of the specificity of the polymers obtained by both systems. Specificity is generally expressed in terms of imprinting factor (IF) which is defined as follows [22]:

$$\text{IF} = B_{\text{MIP}} / B_{\text{NIP}} \quad \text{(Equation 5.1.)}$$

Where B is concentration of substrate bound to the polymer.

In the thermal desorption analysis, the area of peak 2 was cited as an indication of polymer specificity and so the ratio of % area due to peak 2 for MIP and NIP was taken

as an equivalent to IF. Table 5.4. lists these ratios and the IF values obtained in the solution phase for the different polymer compositions. Within experimental error, the IF and ratio of % area peak 2 MIP and NIP was found to be proportional to the amount of EGDMA in the polymer composition. A decrease in both of these ratios signifies a reduction in discrimination between MIP and NIP species due to an increase in non-specific binding.

Table 5.4. Imprinting factor (IF) values and % Area peak 2 MIP/ % Area peak 2 NIP polymers.

EGDMA (mmol) (MIP/NIP)	Imprinting Factor (IF) (Chloroform)	% Area peak2 MIP/ % Area peak2 NIP (Thermal Desorption)
40	1.97 (+/- 0.05)	2.36 (+/- 0.54)
30	1.64 (+/- 0.08)	2.40 (+/- 0.39)
20	1.5 (+/- 0.05)	1.52 (+/- 0.44)
10	1.09 (+/- 0.03)	0.93 (+/- 0.11)

When reloading in the solution phase was carried out in acetonitrile and methanol, the trends in affinity in terms of amount of crosslinking monomer were similar. However, the differences in the overall affinity of the polymers between the solvents was due to their respective polarities and hydrogen bonding capabilities, with increased hydrogen binding capability resulting in decreased affinity. The effect of solvent swelling on the polymers also affects the affinity. As discussed in Chapter 2 acetonitrile and methanol swelled the polymers to a smaller extent than chloroform. Therefore, they were unable to open the polymer network to the same extent and so the amount of template ingress into the crosslinked media was reduced. This combined with the polarity contributed to the lower affinity, which was both specific and non-specific in nature.

Reloading in methanol and acetonitrile had no effect on the GC-MS desorption profiles obtained *i.e.* the relationship between the bleed and 2-apy desorption was similar to that observed in chloroform. This is because the volatile solvents were evaporated off during the first 8 min when the temperature was maintained at 80 °C. This is in contrast to data obtained in the solvent phase where affinity across the different polymers was found to

decrease with increasing hydrogen bonding capability (chloroform < acetonitrile < methanol). This clear difference in rebinding results, obtained in the three solvents, between the GC-MS and solution phase illustrates the importance of the solvent, and its influence on polymers, in the solution phase work. It also demonstrates the significance of morphology on affinity. It should be noted that most of the solvent was evaporated in the initial 8 min at 80 °C while the analyte was retained [15]. Thus, observed affinity of MIP over NIP (for those polymers formed with high amounts of EGDMA) may be attributed to varying morphology between the polymers.

5.4. Conclusions

The sensitivity of direct probe thermal desorption GC-MS in examining the relationship between composition, morphology and imprint media performance has been demonstrated. In the pre-treatment stage analysis of reconstructed ion chromatograms (RIC) and selection of appropriate ions specific to the various polymer components, including the template, illustrates how this technique can give an insight into morphological properties of polymers of various compositions. In all cases the results obtained by thermal desorption GC-MS were supported by earlier nitrogen sorption studies (Chapter 2) which determined various physical parameters including porosity and surface area.

The technique is novel in terms of analysing the thermal stability/degradation properties of polymers. Whilst other techniques such as TGA can offer a similar insight into the thermal properties of polymers, this technique is more specific as it allows identification of the various degradents. It is suggested that the technique is not applicable solely to the characterisation of imprinted polymers and that it may be used for the assessment of other polymeric materials.

Although the bleed could not be directly quantified, a qualitative analysis of the bleed for each polymer identified a potential fundamental difference in structure of the polymer backbone for each imprinted and corresponding non-imprinted polymers (aside from the presence of binding sites in imprinted polymers). This was true for each crosslinking monomer concentration within each functional monomer system (including those formed using no-functional monomer). Some material may have been lost during the grinding and sieving process but the consistent and reproducible trends between MIP and corresponding NIP materials suggests that a difference in crosslinking and degree of polymerisation may exist. This claim should be investigated further using an array of techniques.

The technique also demonstrated the ability to facilitate template removal, the extent of which was directly related to not only the amount of crosslinking monomer but also the type of functional monomer used in polymer formulation. Again, correlations with

morphology data and template extraction in solution phase were identified which further highlights the potential of this thermal desorption technique.

The ability of thermal desorption GC-MS to identify differences in polymer performance based on composition was established and correlations were identified between data obtained by thermal desorption GC-MS and by nitrogen sorption analysis of the polymers. Analysis of the reloading profiles suggested polymer degradation at prolonged exposure to evaluated temperatures, which should be investigated further. This apparent degradation was shown to be dependant on composition.

To validate the technique, polymer performance, in terms of re-binding, was also assessed in a solution phase and direct correlations in the specific response of the polymers and their relationship to polymer composition using both techniques was identified. As solvent had no effect on the thermal desorption behaviour of the polymers studied it implies that this technique can analyse the interactions occurring purely between polymer and template in the absence of solvent effects, as observed when using UV/VIS spectroscopy

Overall, it can be concluded that thermal desorption GC-MS has the ability to characterise molecularly imprinted polymers that have fundamental differences in their polymer structures. Some level of polymer degradation has been identified. However, it is felt that it is insufficient to prevent the future development of a MISPME fibre for analysis by this technique, particularly since the initial investigations into this technique have shown that the degradation does not prevent a specific response of MIP over NIP [15]. A methacrylic acid 20 or 30 mmol EGDMA composition would appear to be an ideal starting point for the development of such a MISPME fibre, as both compositions offer a compromise between the amount of template displaced during pre-treatment, the specific response of MIP over NIP during reloading and the level of bleed due to potential degradation also observed during analyte reloading.

References

1. J. Svenson and I. A. Nicholls, *Analytica Chimica Acta* **435**, 19-24 (2001).
2. G. F. Levchik, K. Si, S. V. Levchik, G. Camino, and C. A. Wilkie, *Polymer Degradation and Stability* **65**, 395-403 (1995).
3. F. M. Uhl, S. V. Levchik, G. F. Levchik, C. Dick, J. J. Liggat, C. E. Snape, and C. A. Wilkie, *Polymer Degradation and Stability* **71**, 317-325 (2001).
4. L. C. Sawyer and D. T. Grubb, *Polymer Microscopy*, 2nd (Chapman and Hall, Oxford, 1996).
5. C. Cristallini, G. Ciardelli, N. Barbani, and P. Giusti, *Macromolecular Bioscience* **4**, 31-38 (2004).
6. S. Lowell, J. Shields, M. Thomas, and M. Thommes, *Characterization of Porous Solids and Powders: Surface Area, Pore Size and Density.*, (Kluwer Academic Publishers., Dordrecht, The Netherlands., 2004).
7. S. R. Sandler, W. Koro, J.-A. Bonested, and E. M. Pearce, *Polymer Synthesis and Characterization. A laboratory manual*, (Academic Press, San- Diego, 1998).
8. K. Sirisinha and S. Chimdist, *Polymer Testing* **25**, 518-526 (2006).
9. F. M. Uhl, S. V. Levchik, G. F. Levchik, C. Dick, J. J. Liggat, C. E. Snape, and C. A. Wilkie, *Polymer Degradation and Stability* **71**, 317-325 (2001).
10. H. Varghese, S. S. Bhagawan, and S. Thomas, *Journal of Thermal Analysis and Calorimetry* **63**, 749-763 (2001).
11. R. Rutkaite, G. Buika, N. Kreiveniene, and J. V. Grazulevicius, *Polymer Degradation and Stability* **78**, 143-147 (2002).
12. P. Munk, *Introduction to macromolecular science*, 1st edition (Wiley Interscience, 1989).
13. H. G. Elias, *An introduction to polymer science*, 1st edition (VCH Publishers Inc., 1997).
14. J. A. Garcia-Calzon and M. E. Diaz-Garcia, *Sensors and Actuators B: Chemical* **123**, 1180-1194 (2006).
15. W. Cummins, P. Duggan, and P. McLoughlin, *Analytical and Bioanalytical Chemistry* **391**, 1237-1244 (2008).
16. www.varianinc.com, (2007).
17. W. Cummins, PhD Thesis (Waterford Institute of Technology, Ireland, 2006).
18. B. Sellergren, *Makromolekulare Chemie* **190**, 2703-2711 (1989).

19. B. Sellergren, *Chirality* **1**, 63-68 (1989).
20. B. Sellergren and A. Hall, "Fundamental aspects of the synthesis and characterisation of imprinted network polymers," *Molecularly imprinted polymers. Man-made mimics of antibodies and their applications in analytical chemistry.*, B. Sellergren, ed., (Elsevier, Amsterdam, 2001), 21-55.
21. Z. Jie and H. Xiwen, *Analytica Chimica Acta* **381**, 85-91 (1999).
22. T. Pap and G. Horvai, *Journal of Chromatography A* **1034**, 99-107 (2004).

Chapter 6

Development of photosensitive PVA for use as Molecularly Imprinted Polymers

6.1. Introduction

Polyvinyl alcohol (PVA) is a highly water soluble resin containing pendant hydroxyl groups which allow the introduction of a wide range of functional groups by simple chemical reactions. PVA can be modified with a number of chromophores to render it photosensitive, upon exposure to UV/ VIS light of an appropriate wavelength. Typical chromophores with which PVA has been derivatized include:

- Cinnamate compounds *e.g.* reaction with cinnamoyl chloride to give polyvinyl cinnamate [1],
- Styrylpyridinium compounds [2] and
- Conjugated heterocyclic compounds *e.g.* furan or thiophene compounds [3].

All of the chromophores mentioned above contain double bonds through which a photocrosslinking reaction occurs, typically a [2+2] cycloaddition reaction. PVA has excellent film characteristics and the introduction of photosensitivity to the backbone has resulted in its use as commercial negative photoresists [4] or for the immobilisation of enzymes [5].

Given these properties modified PVA has great potential for use as sensors or drug delivery devices, as described in Section 1.11. This study carries out a preliminary investigation into the use of modified PVA for the preparation of molecularly imprinted polymers. PVA is typically used in molecular imprinting to act as a stabiliser for suspension polymerisation techniques [6]. Thus, this is the first attempt to use it as an imprint medium. Apart from its excellent film control characteristics, modified PVA has potential for use as MIPs as it has several advantages over thermally initiated acrylic based systems, such as no need for additional crosslinker or initiator and excellent control over the degree of crosslinking which does not have to be carried out in an inert atmosphere. The [2+2]-cycloaddition reaction, which is the crosslinking mechanism that the chromophores listed above undergo, can be reversed if desired which adds more control over the photosensitivity. Development of PVA as an imprint medium may be particularly advantageous for the potential use as molecularly imprinted membranes

(MIMs), as sensor devices or as drug delivery systems as molecular imprinting can be superior than conventional techniques.

The overall aims of the preliminary investigations were to;

- Introduce photosensitivity to PVA by reaction with a suitable chromophore,
- Develop a stable and reproducible crosslinked film,
- To integrate the film to an analytical technology (Attenuated Total Reflectance-Fourier Transform Infrared (ATR-FTIR) spectroscopy,
- To study the impact of the template on the polymer,
- Make recommendations for the further development of modified PVA for use as MIPs.

6.2. Experimental

6.2.1. Materials, equipment and instrumentation

Table 6.1. The materials used.

Reagent	Supplier	Assay
4-Methyl pyridine	Sigma-Aldrich (Ireland)	99 +%
Terephthaldehyde	Sigma-Aldrich (Ireland)	99 +%
Dimethyl sulphate	Sigma-Aldrich(Ireland)	99 +%
Piperidine	Sigma-Aldrich(Ireland)	99 %
Polyvinyl alcohol	Sigma-Aldrich (Ireland)	87-89 %
		Hydrolysed
Cinnamaldehyde	Sigma-Aldrich (Ireland)	99 +%
<i>o</i> -Phosphoric acid	Sigma-Aldrich (Ireland)	85 %
Dimethyl sulphoxide	Sigma-Aldrich (Ireland)	99 +%
2-Aminopyridine	Sigma-Aldrich (Ireland)	99 +%
Chloroform	Lennox (Ireland)	99.0-99.4 %
Methanol	Lennox (Ireland)	99.8 %
Ethanol	Sigma-Aldrich (Ireland)	96 %
Acetonitrile	Lennox (Ireland)	99.9 %
Acetone	Lennox (Ireland)	99 %

Equipment and instrumentation

- Mechanical stirrer- Stuart Scientific Stirrer SS2.
- UV lamp: medium pressure mercury lamp which emitted across the spectral range 220-600 nm (Griffin and George).
- UV/Vis spectrometer: UV-2401PC Shimadzu (JVA Ireland Ltd)
- FTIR: Excalibur Series Digilab FTIR spectrometer with a cryogenic MCT (mercury-cadmium-telluride) detector (JVA Ireland Ltd) coupled with a Shimadzu LC-10 ATvp solvent delivery system (HPLC pump).
- Zinc selenide (ZnSe) crystals: Dimensions 72 mm x 10 mm x 6 mm. The angle of incidence was 45° which gave 6 internal reflections with the contact measuring surface. MicroOptica Ltd, Moscow, Russia.

6.2.2. Preparation of photosensitive PVA

6.2.2.1. Synthesis of styrylpyridinium salt (4-SbQ)

4-SbQ (1-methyl-4-[2-(formylphenyl)ethenyl]pyridinium methosulphate) (Figure 6.1.) was synthesised using the following method described by Ichimura and Watanabe [7]; 0.1 mol (9.14 g) of 4-methylpyridine were added to 25 mL of methanol in a round bottom flask. This mixture was then placed in an ice-bath to facilitate cooling, followed by the drop wise addition of 0.1 mol (12.61 g) of dimethyl sulphate. The resultant mixture was left to stand at ambient temperature for one hour. 0.3 mol (40.2 g) of terphthalaldehyde were subsequently added and dissolved by heating. 1.4 mL (0.01 mol) of piperidine was added and the reaction mixture was heated under reflux for five hours. The hot mixture was filtered while hot to collect the by-product, bispyridinium salt. 150 mL of ethanol followed by 50 mL of acetone were added to the hot filtrate, which was then left to stand overnight. Yellow crystals of 4-SbQ were collected by filtration and washed with ethanol and acetone. Electronic absorption spectra were obtained in deionised water and IR spectra taken using a single reflectance ATR solid sample attachment. UV/VIS; $\lambda_{\text{max}} = 345 \text{ nm}$, extinction coefficient = $38,7808 \text{ L mol}^{-1} \text{ cm}^{-3}$. IR; 3048 cm^{-1} (vinyl C-H), 2833 cm^{-1} (aldehydic C-H), 2740 cm^{-1} (aldehydic C-H), 1697 cm^{-1} (C=O), 1646 cm^{-1} (vinyl C=C), 1623 cm^{-1} (aromatic C=C), 1567 cm^{-1} (C=N), 1523 cm^{-1} (aromatic C-C), 1215 cm^{-1} (S=O), 987 cm^{-1} (trans C-H out of plane bending), 728 cm^{-1} (aromatic C-H out of plane bending), MP. 225-230 °C

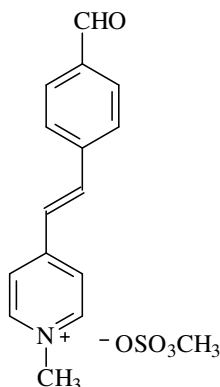


Figure 6.1. Structure of 4-SbQ.

6.2.2.2. Reaction of 4-SbQ and cinnamaldehyde with PVA and preparation of the imprinted polymers.

10 g of PVA partly hydrolysed PVA (87-89 % hydrolysis) were slowly dissolved in 90 g deionised water using a mechanical stirrer. The solution was then heated up to facilitate complete dissolution. Heat and stirring were required for the dissolution of the modified PVA as its solubility is greatly impeded by its hydroxyl groups, which cause the PVA to have a high affinity for water, with strong hydrogen bonding between the intra- and intermolecular hydroxyl groups [8]. The mass equivalent to the desired mol % of chromophore grafted to the PVA backbone was determined using Equation 6.1.

$$\left[\frac{(X / Mr)}{10 / 49} \right] * 100 = Y \text{ mole } \% \quad \text{(Equation 6.1.)}$$

Where X = the mass of chromophore,

Mr = the molecular weight of the chromophore,

10 = mass of PVA to be modified (g),

49 = molecular weight of PVA/ degree of polymerisation.

(M_w of PVA = 205,000 g mol⁻¹ (data supplied by the manufacturer))

The mass equivalent of 1 mole % 4-SbQ and 35 mol % cinnamaldehyde (Figure 6.2.) were added to the PVA aqueous solution (separately). 1 mL of *o*-phosphoric acid was added to both solutions which were left to stir for 24 h. The PVA-4-SbQ was precipitated out of solution using acetone, collected by Buchner filtration and washed with methanol to removed un-reacted components. A known mass of product was redissolved and the % grafting was determined by UV spectroscopy (approximately 1 mol % in all cases). The λ_{max} value for the 4-SbQ displayed a bathochromic shift (typically 15 nm) when it was appended to the PVA backbone. This correlated with earlier studies where the phenomenon was attributed to the association of the SbQ groups [9]. IR spectroscopy was not used to investigate the extent of grafting as it was not sensitive enough to detect the low levels of 4-SbQ attached to the polymer backbone. The PVA-cinnamaldehyde (PVA-cinn) precipitated out of the aqueous solution as the

reaction proceeded. The product was collected by Buchner filtration and washed with water and methanol.

Both PVA-4-SbQ and PVA-cinn were dissolved in DMSO to prepare a 7.5 % w/w solution. The template species, 2-apy, was added in a 2:1 ratio of hydroxyl groups:2-apy (2.4 g 2-apy per 30 g PVA-4-SbQ solution and 0.75 g 2-apy per 30 g PVA-cinn solution). An amount of the polymer solutions were retained for use as the non-imprinted polymers. The polymer solutions were spin coated onto ATR crystals (PVA-SbQ 2000 rpm 15 sec, PVA-cinn 1000 rpm for 15 sec), dried in the oven at 80 °C to remove the excess DMSO and crosslinked under a UV lamp (approximately 3 cm from the lamp) for 10 h.

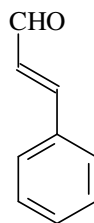


Figure 6.2. Structure of cinnamaldehyde.

6.2.3. ATR-FTIR analysis of the polymer films

The crystals were placed in a Specac Thermostabilised Flow Cell (110 μ L) and the template was removed by passing methanol (in the case of the SbQ films) or water (cinnamaldehyde) at a flow rate of 2.5 mL min⁻¹ over the surface of the films, which were housed in the flow cell, using a HPLC pump for 2 h (7200 s) intervals. Template removal was monitored during the 2 h intervals by an IR kinetics run (resolution of 4 cm⁻³, sensitivity 1, time resolution 20 s). The waste stream was also monitored *via* UV spectroscopy for template removal. Figure 6.3. illustrates a schematic diagram of the IR system.

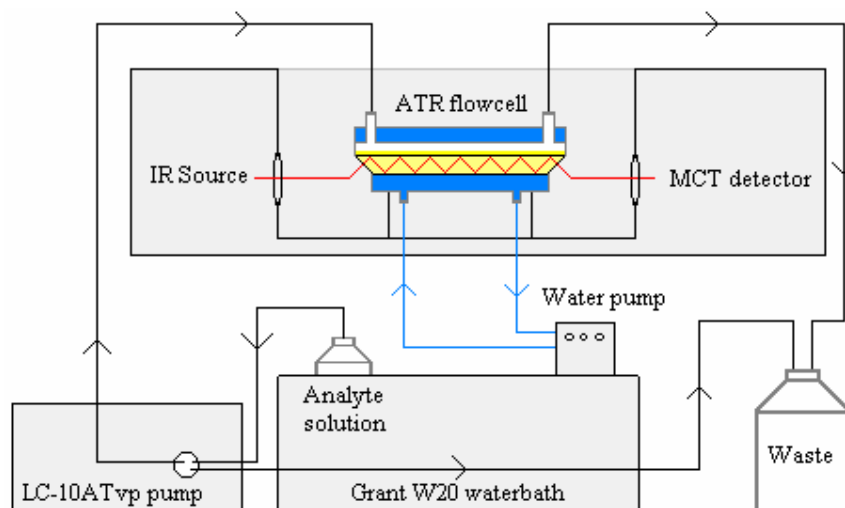


Figure 6.3. Schematic diagram of the system employed [10].

Various solutions of 2-apy in water or chloroform were reloaded onto the polymer films. Non-imprinted polymers were treated in an identical manner. All analyses were carried out at 25 °C.

6.3. Results and discussion

6.3.1. Initial investigations using PVA-4-SbQ

The initial investigations of this novel study involved the use of PVA that was modified with 4-SbQ. This derivatized polymer was chosen because when exposed to UV irradiation, undergoes a [2+2]-cycloaddition reaction leaving a crosslinked polymer which is insoluble in water. The styryl pyridinium groups exhibit extremely high photosensitivity even if the content of these groups attached to the chain is quite low [11], thus maintaining the bulk properties of the PVA, leaving the hydroxyl groups available for interaction with the template species 2-apy, as seen in Figure 6.4. Although potential hydrogen bonding interactions have been identified with the template and the hydroxyl groups, possible π -cation interactions between the template and the chromophore are more likely to occur, as shown.

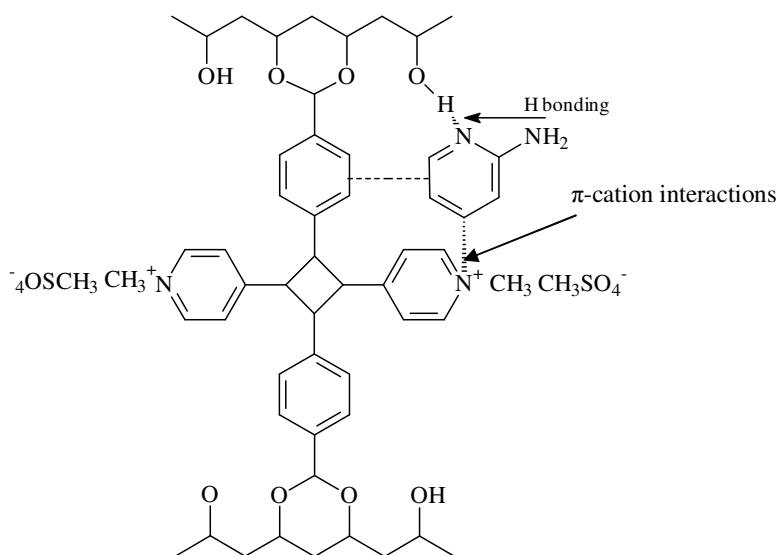


Figure 6.4. Potential interactions between 2-apy and PVA modified with 4-SbQ.

The SbQ chromophore was readily synthesised *via* a two step reaction, quaternisation followed by condensation. The 4-SbQ was attached to the PVA through an acid catalysed acetalisation reaction with the aldehyde group to yield a six-membered acetal ring between adjacent hydroxyl groups (intramolecular acetalisation), as was shown in Figure 6.4. The photofunctional group was attached to the PVA on a mole percent basis. Approximately 1 mole % of SbQ was grafted to the PVA in all cases. There is a limitation to the amount of 4-SbQ that can be attached as the PVA particles aggregate and cause the solution to become viscous and it eventually gels. As a result it becomes difficult to work with. The presence of the counter ion is said to contribute to the increased association [4,12]. As the content increases to greater than 2 mol % the solution becomes a gel like material [7]. This increase in viscosity is attributed to the association of the styrylpyridinium groups, causing the linear polymeric chains to interact, thereby increasing the viscosity [9]. However, an advantage of this system is that it is extremely photosensitive, and can impart water insolubility. The increased level of photosensitivity was viewed as an extremely advantageous property and was one of the main contributing factors when identifying this novel approach for the formation of imprinted polymers.

Due to the limited solubility of modified PVA in common organic solvents, DMSO was chosen as the solvent to cast the PVA films. The extent of modification of PVA with the

chromophore was so low that the bulk properties of the PVA (in terms of solubility (discussed in detail in Section 1.9.)), remained unchanged. The DMSO also acted as the medium in which the pre-polymerisation complexes were formed. DMSO is a polar solvent (dielectric constant 49) and it may potentially have interrupted the proposed H-bonding interactions with the template. On the other hand it may have promoted possible π - π interactions. However, as it was less polar than water it was chosen based on the possibility of potential H-bond interactions.

The initial investigations found that while a reproducible film was prepared using PVA-4-SbQ, the level of crosslinking was insufficient to maintain a stable film. The level of insolubility imparted with such low levels of 4-SbQ are sufficient for use as negative photoresists, as durability due to prolonged or multiple usage is not an issue, *i.e.* the films are used only once. Analysis of the waste stream from the ATR-FTIR system (Figure 6.3.) for the NIP polymers indicated the presence of PVA, suggesting that the film was being removed from the surface of the crystal when being washed with methanol, and so it was not further analysed. Whilst the PVA is rendered water insoluble with low amounts of SbQ, it is felt that polar solvents such as methanol may swell it and the constant flow of solvent over the surface may eventually cause it to lift from the smooth surface of the ATR crystal and wash it away. Thus, the low levels of crosslinker were deemed unsuitable for this particular system.

Similar results were obtained when the films were cast onto a glass slide, the surface of which had been abraded in an attempt to increase adhesion. Abrasion was carried out using fine sandpaper (coated aluminium oxide) as opposed to chemical etching of the glass.

6.3.2. ATR-FTIR analysis

The initial investigations described above indicated that a higher level of crosslinking was required for the films, and so cinnamaldehyde was chosen. The cinnamaldehyde groups do not associate in solution to the same extent as 4-SbQ and so the extent of modification can be increased. The groups are capable of association due to the hydrophobic nature of the cinnamate groups. The cinnamoylated PVA can also undergo

a cyclodimerisation reaction, as depicted in Figure 6.5. The interactions between 2-apy and the cinnamoylated-PVA (PVA-cinn) are similar to those described for PVA-4-SbQ (refer to Figure 6.4.)

The percentage of modification for the PVA-cinn polymers was not determined due to its very limited solubility in most common organic solvents, with the exception of DMSO which absorbs in the same UV region as cinnamaldehyde. As the polymer precipitated out of aqueous solution it indicated a high level of grafting to the polymer backbone

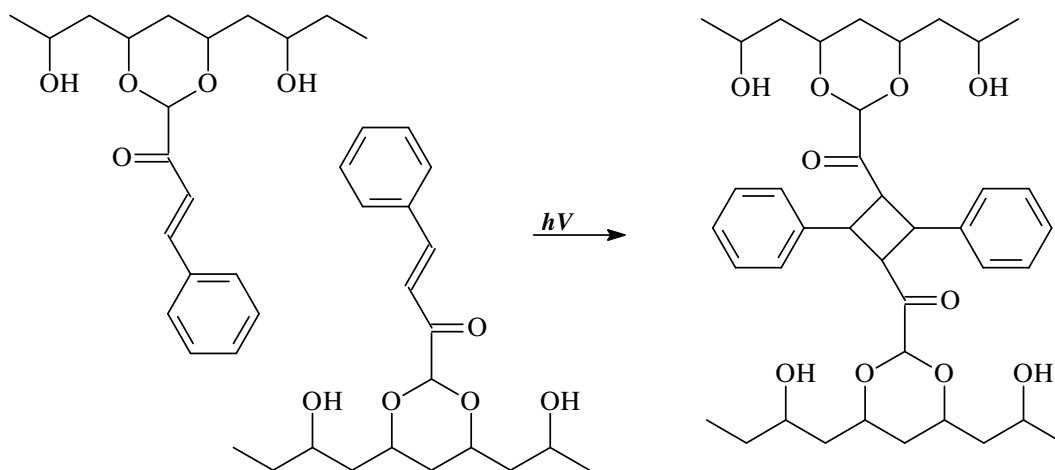


Figure 6.5. Photoinduced bimolecular crosslinking reaction of poly(vinyl cinnamate).

ATR spectroscopy utilises the phenomenon of total internal reflection (Figure 6.6). Reflection occurs when a beam of radiation passes from a denser to a less dense medium. The fraction of beam that is reflected increases as the angle of incidence increases. The depth of penetration of the beam into the membrane on the surface of the waveguide (the ATR crystal in this case) is dependent on the wavelength of radiation (λ), the refractive index of the crystal, n_c , the refractive index of the sample, n_w , and the angle of incidence of the beam at the surface of the crystal, θ . The depth of penetration is smallest for materials with high refractive indices. The evanescent field energy, E , is a function of the distance from the ATR surface and at approximately three times the depth of penetration it decreases to approximately 5 % of its initial magnitude [10].

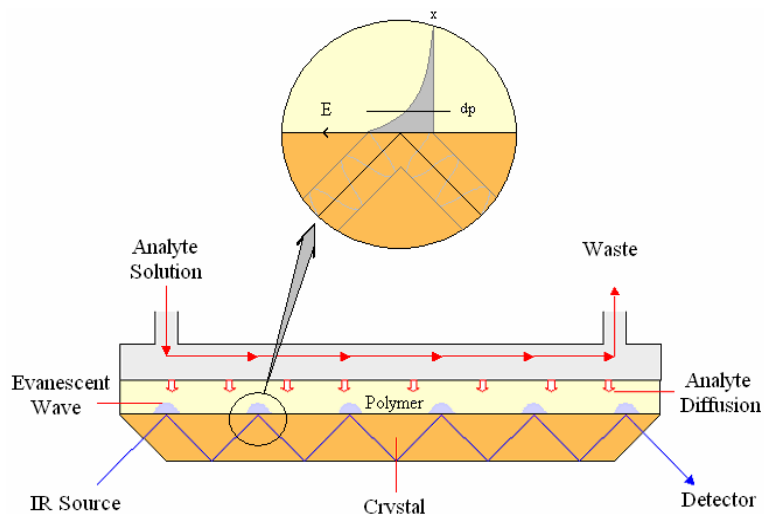


Figure 6.6. Schematic representation of ATR in a multi reflection polymer clad waveguide [10].

There is evidence of the presence of the cinnamate group in the PVA by the appearance of a C=C band at 1666 cm^{-1} , which was not present in the spectrum of un-modified PVA (spectrum not shown). As this band was low in intensity (Figure 6.7.), it is suggested that the level of modification is low. The bands at 1735 , 1244 and 1125 cm^{-1} are attributed to C=O, C-O-C asymmetric and C-O-C symmetric stretches of the residual acetate of the PVA, respectively.

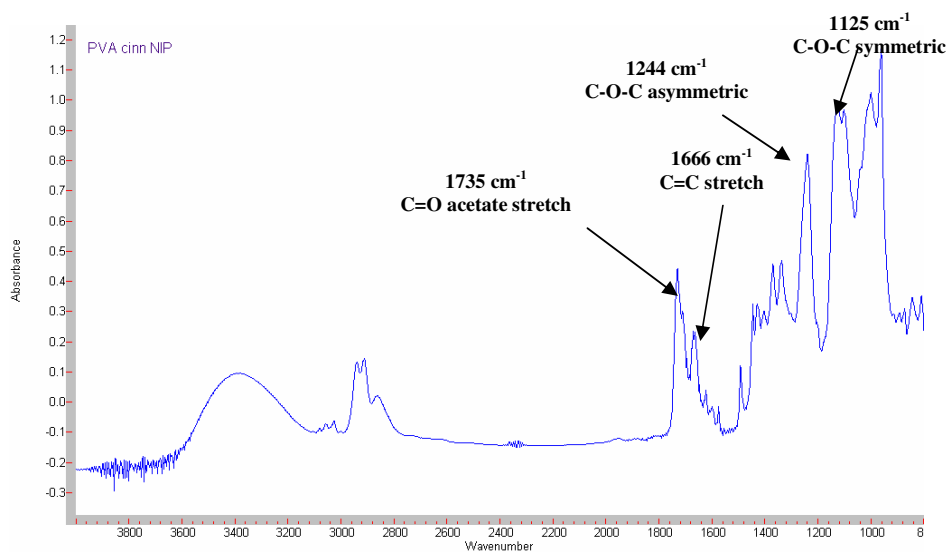


Figure 6.7. IR spectrum of PVA-cinn.

The key IR bands of 2-apy are depicted in Figure 6.8.

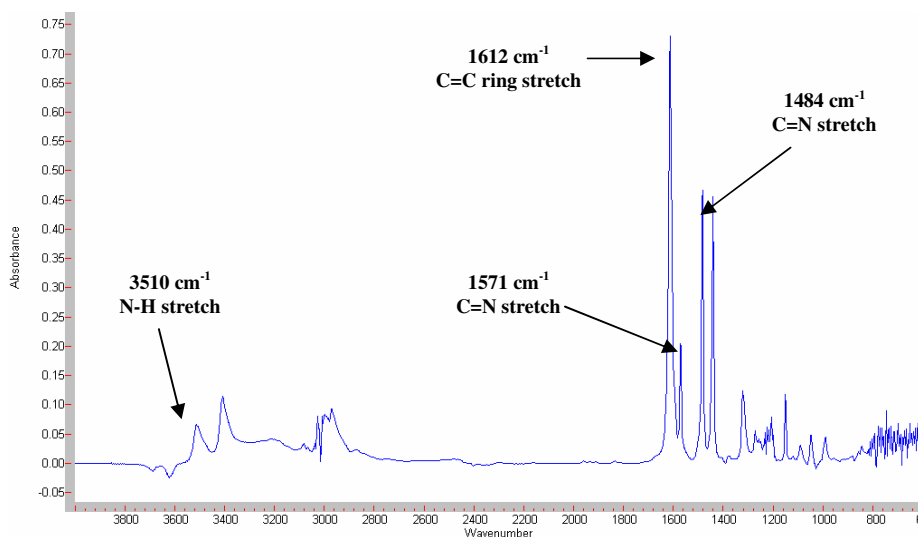


Figure 6.8. IR spectrum of 2-apy.

The IR spectrum of the PVA-cinn MIP (Figure 6.9.) is weak in the 1800-1400 cm⁻¹ region. There is the addition of a peak at 1580 cm⁻¹ which may possibly suggest the presence of template and as the band is shifted it implied interactions of 2-apy with the polymer backbone. As the 1580 cm⁻¹ band was relatively weak, the template removal was qualitatively monitored by UV/VIS spectroscopic analysis of the waste line (Figure 6.3.). The template was visible in the MIP washings for the first 6 h after which it was no longer detected.

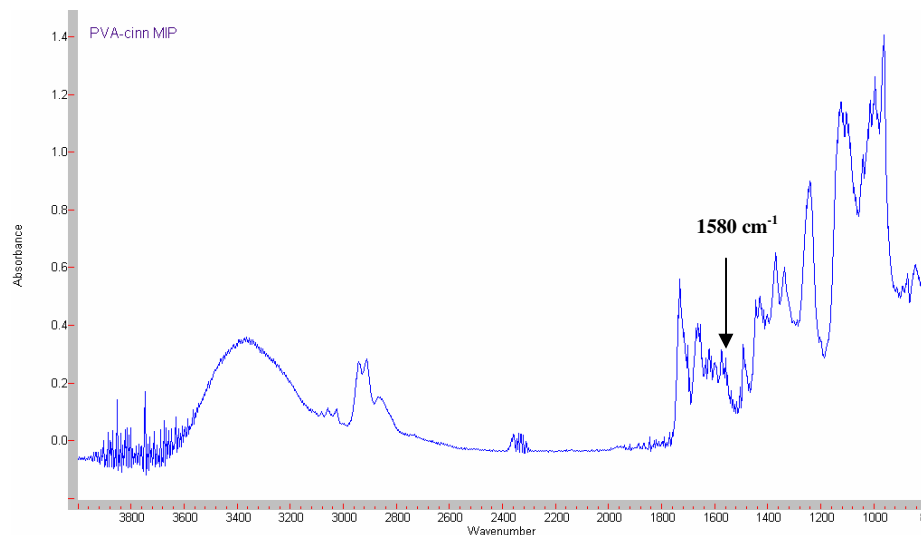


Figure 6.9. IR spectrum of PVA-cinn MIP.

6.3.2.1. Water ingress

The rate of water ingress into the PVA-cinn films was analysed by monitoring the OH stretch (3320 cm^{-3}). Water ingress can be used as measure of polymer polarity, and so the effect of the template on the film, if any, can be monitored. Figure 6.10 illustrates the sum of the spectra taken during the kinetics run. Plasticisation or swelling of the polymers occurred, which caused negative bands to occur between $1800\text{ to }800\text{ cm}^{-1}$ as they moved outside the sensing region.

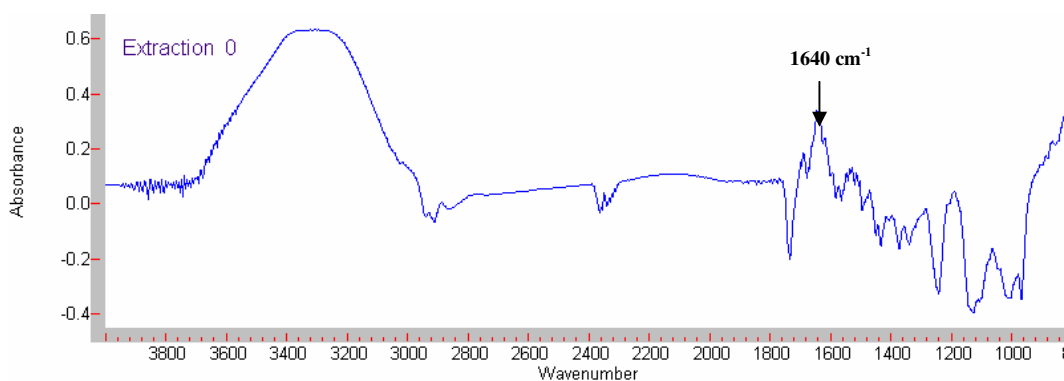


Figure 6.10. Water ingress into a PVA-cinn MIP as monitored *via* a 2 h (7200 s) kinetics run.

The kinetics profile of the water ingress for MIP and NIP are shown in Figure 6.11.

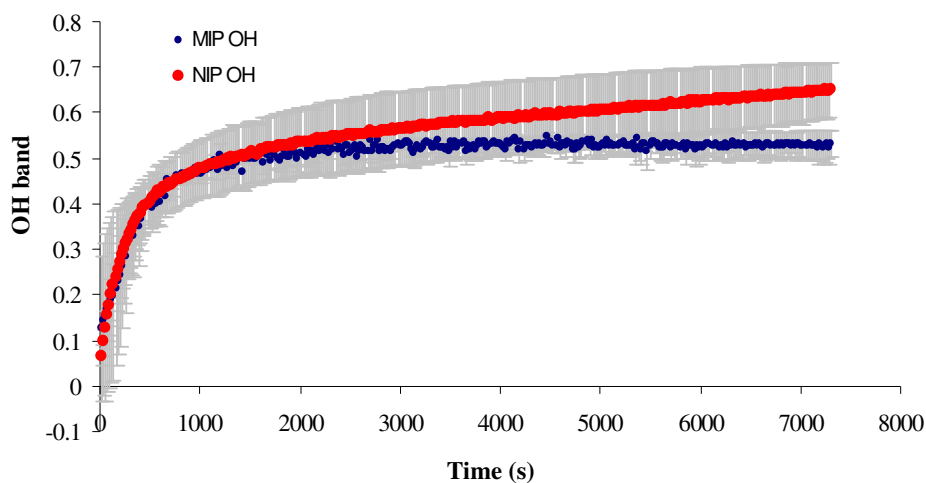


Figure 6.11. Diffusion of water (OH) stretch into PVA-cinn MIP and NIP. Data is based on the average value for triplicate analysis.

The initial rate of ingress was the same for both polymers. As the kinetics run neared completion the NIP was slightly higher than the MIP, indicating that it was slightly more hydrophilic than the MIP. The presence of the positive band at 1640 cm^{-1} suggested water interaction with the polymer. It is proposed that this interaction occurred with the C=O of the acetate group, and that a band shift from 1735 cm^{-1} also occurred. As the water ingressed into the film plasticisation also occurred, which also caused the negative band observed at 1735 cm^{-1} .

The kinetic profiles for the band at 1640 cm^{-1} are shown in Figure 6.12. The higher level of ingress for NIP over MIP also indicates that the NIP is more hydrophilic than the MIP.

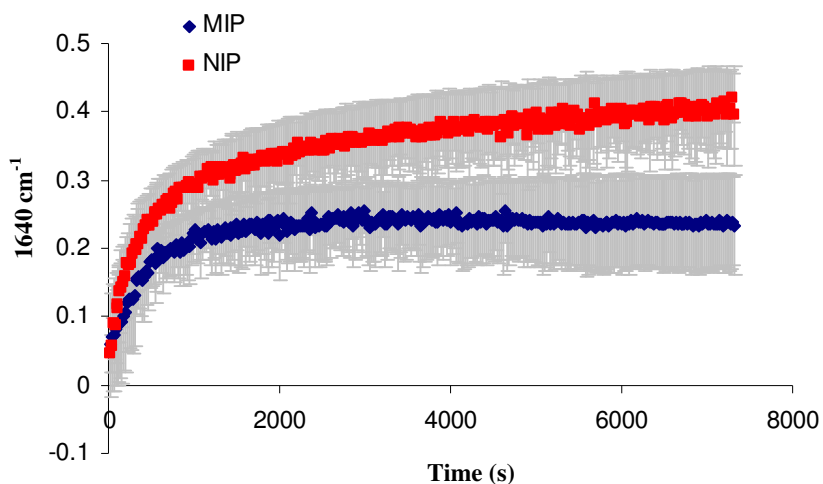


Figure 6.12. Kinetics profile for 1640 cm^{-1} during of diffusion of water into PVA-cinn MIP and NIP.

6.3.2.2. 2-aminopyridine reloading

After the template removal the polymers were reloaded with 2-apy in either chloroform or water. Prior to the chloroform analysis the system (and film) was washed with acetonitrile for 30 min to prevent immiscibility between it and water. Potential chloroform ingress to the polymer was monitored by passing chloroform over the film for a total of 3 h. As can be seen in Figure 6.13, there was a small level of ingress as indicative by the band at 1215 cm^{-1} .

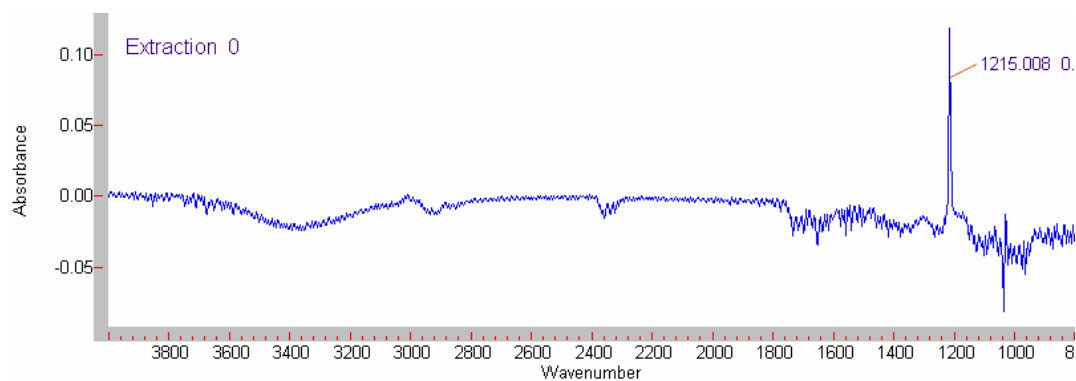


Figure 6.13. Analysis of chloroform ingress into a PVA-cinn MIP.

The MIP and NIP kinetics profile for chloroform ingress (Figure 6.14.) shows a higher rate for the MIP over NIP suggesting that the MIP is more hydrophobic than the NIP.

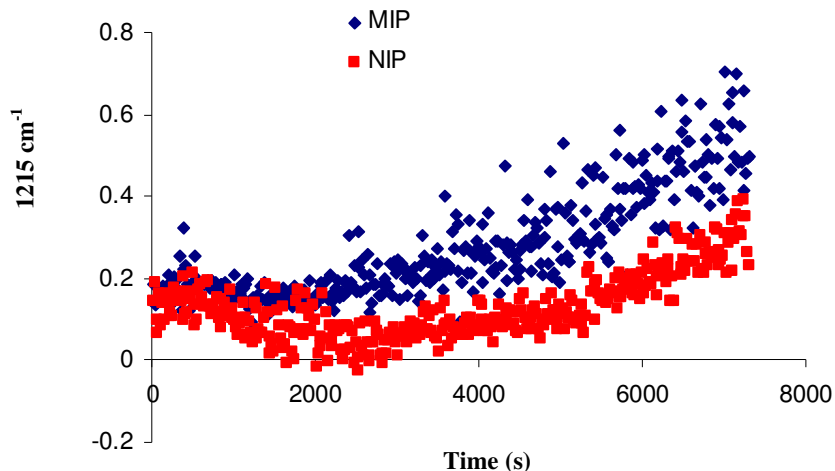


Figure 6.14. Kinetics of chloroform ingress into a PVA-cinn MIP.

A blank was then taken of the polymer after it had been exposed to the chloroform to eliminate matrix effects during analyte reloading. A 0.37 mM solution of 2-apy in chloroform was passed over the film at a rate of 1 mL⁻¹. After 10 h of equilibration, there was no evidence of 2-apy ingress into the film. As chloroform is hydrophobic, it was expected that the 2-apy would adsorb into the predominately hydrophilic polymer, possibly forming hydrogen bonds with the polymer backbone, without the adsorption of chloroform. Although it was stated earlier that the PVA-cinn was hydrophobic as it precipitated out of solution during the grafting procedure, it was thought that the bulk of the system was hydrophilic. Assuming all of the cinnamaldehyde grafted to the PVA that still left approximately 53 mole % of hydroxyl groups remaining (the PVA used was 87-89 % hydrolysed prior to grafting). A low flow rate was used to facilitate the adsorption of 2-apy. If the coated film was too thick then 2-apy may not have reached the sensing region, and thus the associated bands for 2-apy were not observed. Another possibility was that the 2-apy may have adsorbed onto the surface of the polymer. A possible low degree of crosslinking combined with the non swelling effect of chloroform may have prevented migration into the sensing region.

Reloading in water may seem contradictory as it was the medium in which the template was initially extracted with. As water was shown to swell the polymer it was thought that the template might ingress with the water into the film. As 2-apy was not observed

after a 12 h period it was suggested that the template did not reach the sensing region, again, due possibly to the thickness of the film or that it was not crosslinked enough and the increased plasticisation would have prevented pre-concentration of the analyte into the sensing region. The high concentration of solution used may have been sufficient for hydrophobic interactions to occur with the chromophore, which if they had occurred on the surface of the polymer it may not have reached the sensing region.

6.4. Conclusions

A preliminary investigation into the use of modified polyvinyl alcohol (PVA) for use as molecularly imprinted polymers has been carried out. The method of analysis that was used, ATR-FTIR, was chosen as it is widely used as a sensing device. For example, it has been shown to be a suitable methodology for the pre-concentration of analytes typically found in industrial waste process streams by diffusion into appropriate polymeric films, such as Teflon [13]. As PVA has excellent film properties, this technique was chosen as the most appropriate method of analysis.

The results indicated that for a stable and durable film to be formed the PVA must be highly crosslinked, and so PVA that was modified with cinnamaldehyde was pursued for further use. Initial investigations based on the water ingress suggested that the MIP was slightly more non-polar than the NIP. This would imply that the level of crosslinking was higher for the MIP as it had a slightly lower affinity for water.

In the subsequent reloading stage, the ATR-FTIR technique was incapable of detecting 2-apy diffusion into the polymer films. It is felt that for both the water and the chloroform reloading that the concentration of 2-apy reloaded and the exposure time was sufficiently high for potential ingress, as the system has previously been shown to sense analytes at a concentration as low as 100 ppm in a 2 h analysis time [10]. The following reasons are suggested for non-detection of the analyte:-

- If the films were too thick then the analyte may not have reached the sensing region, which is three times the depth of penetration, as shown in Figure 6.5.
- If the film was not highly crosslinked and had an open porous structure due to the plasticisation effect of water, the analyte may possibly have migrated through the film in the direction of the solvent flow as opposed to migrating into the sensing region, which would be expected with a rigid structure.

As template removal was achieved with the initial washing step, it is suggested the results obtained may be due to a combination of surface binding, film thickness and

insufficient levels of crosslinking. Further work based on the reasons identified above should be carried out. Optimisation of the polymer coating procedure to achieve optimum film thickness, which is typically three times the depth of penetration, should be carried out in the future to ensure that sensing was not the issue. This requires knowledge of the refractive index of the polymer. Investigations into the degree of crosslinking should also be carried out in an attempt to achieve analyte diffusion.

References

1. B. Duncalf and A. S. Dunn, "Photosensitized Reactions of Polyvinyl Alcohol used in Printing Technology and Other Applications," *Properties and Applications of Polyvinyl Alcohol*, C. A. Finch, ed., (Weiley and Sons, Chichester, 1977), 461-490.
2. K. Ichimura and S. Watanabe, *Journal of Polymer Science: Polymer Letters Edition* **18**, 617 (1980).
3. S. W. Fang, J. H. Timpe, and A. Gandini, *Polymer* **43**, 3505-3510 (2002).
4. K. Ichimura, *Journal of Polymer Science: Polymer Chemistry Edition*. **20**, 1411-1417 (1982).
5. T. Uhlich, M. Ulbricht, and G. Tomaschewski, *Enzyme and Microbiology Technology* **19**, 124-131 (1996).
6. H. Khan and J. K. Park, *Biotechnology and Bioprocess Engineering* **11**, 503-509 (2006).
7. K. Ichimura and S. Watanabe, *Journal of Polymer Science: Polymer Chemistry*. **20**, 1419-1432 (1982).
8. C. A. Finch, "Chemical Properties of Polyvinyl Alcohol," *Properties and Applications of Polyvinyl Alcohol*, C. A. Finch, ed., (Weiley and Sons, Chichester, 1977), 183-197.
9. E. S. Cockburn, R. S. Davidson, and J. E. Pratt, *Journal of Photochemistry and Photobiology A: Chemistry* **94**, 83-88 (1996).
10. K. Flavin, *PhD Thesis, Waterford Institute of Technology, Ireland*. (2006).
11. K. Ichimura and S. Watanabe, *Journal of polymer Science: Polymer Letters Edition*. **18**, 617 (1980).
12. K. Ichimura and S. Watanabe, *Journal of Polymer Science: Polymer Chemistry Edition* **20**, 1419-1432 (1982).
13. K. Flavin, H. Hughes, V. Dobbin, P. Kirwan, K. Murphy, H. Steiner, B. Mizaikoff, and P. McLoughlin, *International Journal of Environmental Analytical Chemistry*. **86**, 401-415 (2006).

Chapter 7

Conclusions and future work

7.1. Conclusions

The overall aim of this research work was to carry out a detailed investigation into the role of polymer morphology on imprint medium performance, with a view to identifying the key parameters responsible for optimum polymer performance for non-covalent imprinting. The further development of a novel thermal desorption GC-MS methodology for the characterisation of MIPs was also investigated. Recent interest in the area of molecular imprinting has expanded and much of the work focuses on the development of MIPs for a wider variety of applications, and so the exact role of the physical properties of the polymers is often overlooked. The nature of the work presented was carried out in a systematic manner so as to contribute to a greater understanding of the molecular imprinting process.

In terms of non-covalent imprinting, the typical investigations in relation to polymer composition include the ratio of template to functional monomer [1,2], porogen type [3-6] and the types and amount of crosslinker [7,8]. However, the effect of compositional change is usually assessed in terms of performance or chromatographic behaviour. It is only in a relatively small number of cases that the performance of the polymers resulting from compositional changes is linked directly to the physical characteristics of the polymers [5,9-12]. Other factors such as the polymerisation conditions (the temperature [13] and pressure [14] of initiation, initiator concentration [15] and length of initiation [16]) on the physical properties of imprinted polymers have also been studied, however, a systematic investigation of simultaneously varying the amount of crosslinking monomer and the type of functional monomer on the performance of polymers and a subsequent link to the physical parameters has not been previously carried out.

As the role of the template has been studied in detail [17-20], the main body of this work involved a detailed characterisation of a number of polymeric phases which were synthesised by varying the amount and type of crosslinking (ethyleneglycol dimethacrylate (EGDMA)) and functional monomer (methacrylic acid (MAA), 4-vinylpyridine (4-VP) and methyl methacrylate (MMA)), respectively. Twenty four different compositions (12 MIPs and 12 NIPs) were synthesised and the impact of

polymer composition on the physical parameters of the polymers was determined using a number of techniques, including nitrogen sorption, solvent swell, particle size and SEM analysis. This was a novel and detailed examination of the role of polymer composition on morphology. The results obtained from the physical characterisation were linked directly to the affinity of the polymers. The impact of polymer composition on the binding parameters of the MAA polymers were further analysed by the novel application of three binding models (Langmuir (LI), Freundlich (FI) and Langmuir-Freundlich (L-FI) isotherms) and by generating affinity distribution (AD) spectra. A novel methodology for the characterisation of molecularly imprinted polymers containing fundamental differences in the polymer structure by the use of thermal desorption GC-MS was also presented.

The template used in the synthesis of the polymers was 2-aminopyridine and although it was previously imprinted, [17,21-23] it was chosen because of its small size and uncomplicated functionality and chemical properties. This permitted a detailed examination of the exact role of polymer composition on the physical parameters, which in turn could be linked directly to polymer performance, without the added complication of a complex template to consider. The functional monomers were chosen based on the potential for interactions with 2-apy. Within each functional monomer system the concentration of crosslinking monomer was changed while keeping the remaining polymer components constant. This resulted in a variation of the percentage of each of the remaining components in each of the compositions.

The nature of the functional monomer employed was found to produce polymers of differing morphology. This was apparent at the template extraction stage, where a low level of 2-apy was removed from the 4-VP polymers relative to the MAA polymers. While all polymers were mesoporous, the nitrogen sorption results also indicated that the 4-VP containing polymers were found to be less porous than the corresponding MAA polymers. This was attributed to a potentially higher degree of crosslinking which in turn would have resulted in the polymer chains being densely packed, thus leading to the lower pore volume. The swelling studies also suggested that the 4-VP polymers were less porous and had a higher degree of crosslinking than corresponding MAA polymers, as the swell ratio was consistently higher for the MAA polymers relative to

the 4-VP polymers, in all solvents. The higher degree of crosslinking would have maintained the position of the chains in the polymer network [24], thereby reducing the swelling effect of the solvents on the closely packed polymer chains.

Assessment of the polymer performance showed that the MAA polymers displayed affinity for 2-apy and two structural analogues (3- and 4-apy), whilst the 4-VP containing polymers did not. The affinity and selectivity results for the MAA polymers were directly correlated to their physical parameters. Polymer affinity, specificity and selectivity demonstrated sensitivity to parameters such as the chemical nature of the solvent and pKa of binding analyte. The level of sensitivity demonstrated by these parameters was in turn found to be directly related to the differences in polymer morphology. The effect of solvent swelling on the polymers had a limited impact on the imprinting factors obtained when going from high to low amounts of EGDMA. However, when comparing results obtained in chloroform and acetonitrile, the swelling effect (as well as the nature of the solvent) was thought to contribute to the results obtained. A decrease in pore size (diameter) found with increasing EGDMA resulted in a lower capacity, which suggested a greater sieving capability of those polymers. An inverse relationship between the cumulative pore volume and the affinity of the polymers was identified, which suggested that the flexibility or the swelling of the polymer in the various solvents contributed to the binding results. The increased number of free carboxyl groups associated with a decrease in EGDMA concentration was also a contributing factor to the higher capacity and the non-specific binding observed in the polymers. In the case of the 4-VP polymers the lower free volume, due to the proposed increased level of crosslinking, was thought to inhibit diffusion into the polymers, resulting in no affinity for the binding analyte.

Although the porosity of the MAA polymers formed with lower amounts of EGDMA was smaller, in terms of the surface area and volume, relative to those formed from higher amounts, the wider diameter, distribution, increased flexibility and smaller particle diameter all contributed to the increased capacity. It was concluded by analysis of the MAA polymers that maximum specificity is not always achieved in the porogenic solvent. Acetonitrile in general displayed better results relative to chloroform. This was attributed to the fact that it did not swell the polymers to the same extent, particularly

for the lower concentrations of EGDMA where the integrity of the binding sites was retained. It also resulted from a reduction in non-specific binding, which is always an issue in imprinting, due to the stronger hydrogen bonding capability. While maximum or improved specificity is always desired, there is a trade off between it and capacity.

The LI, FI and L-FI were used to examine the binding behaviour of the MAA polymers in detail. Earlier studies that utilised all three isotherms for polymer characterisation compared covalent and non-covalent polymers, all of which were taken from the literature [25]. The FI has been used previously to examine the binding behaviour of polymers formed using different compositions [26]. The use of the individual isotherms, or as a combination, have typically been used to identify the most appropriate model for a given template using only one polymer composition [27], a comparison of bulk and precipitation polymers [28], assessment of binding to films [29], by varying the type of functional monomer and the template used [30] or used for the assessment of the cross reactivity of an imprinted polymer [31]. Thus, this is the first report of the use of the LI, FI and L-FI isotherms in an attempt to link the effects of polymer composition and morphology to the subsequent performance of polymer systems.

In terms of the overall capacity of the polymers obtained for the experimental binding isotherms, the increased concentration of analyte bound to the polymers formed using lower amounts of EGDMA was attributed directly to its lower level of crosslinking, which in the presence of solvent would have permitted greater template ingress into the polymer network. The L-FI was deemed the most appropriate isotherm for analysis in the concentration range used. This was based on the improved linear regression values obtained when it was fit to the experimental data. The L-FI was sufficiently sensitive to identify changes in binding site energies with change in composition and correlations were identified between the physical properties of the polymers and the results obtained, where the total number of binding sites increased with increasing flexibility. The average binding energy of the sites decreased with decreasing EGDMA amounts. This highlights the importance of the crosslinking monomer in maintaining the fidelity of the binding sites during polymerisation. The AD spectra were a useful tool in displaying the relationship between the number of binding sites and their associated energy. This was

also the first use of AD spectra based on the L-FI fitting parameters in the examination of composition on polymer performance.

The NIP data could not be directly correlated to the MIP binding parameters as the NIP polymers exhibited bleed or un-reacted monomer/polymer components at low levels of analyte concentration. This highlighted the importance of a complete and efficient template extraction and polymer washing procedure prior to use. A batch of polymer that was subject to extraction *via* a Soxhlet apparatus was found to have a lower number of binding sites relative to the corresponding polymer that was extracted using an alternative method, but it had a higher average binding site energy. This would imply the destruction of lower affinity binding sites using the more rigorous extraction procedure.

Thermal desorption GC-MS has been identified as a novel technique that is suitable for the characterisation of molecularly imprinted polymers. Through the use of temperature programmes, an initial polymer pre-treatment stage permitted the removal of residual/un-reacted monomeric/ polymeric components. The power of MS enabled a qualitative analysis of the types of bleed. The bleed for the polymers that were under study was found to consist mainly of EGDMA, and it was consistently higher for NIPs relative to corresponding MIPs. This suggested that a difference in the degree of crosslinking existed. Imprinted and corresponding non-imprinted polymers were found to swell to the same extent (within error) in the various solvents and, there was also no overall correlation in the MIP and NIP porosity data, both of which highlighted the sensitivity of the GC-MS technique in identifying differences in the degree of crosslinking.

The sensitivity of the GC-MS technique was further exemplified in its ability to characterise polymers that had different physical structures arising from differences in their polymer compositions. The level of bleed from the MAA polymers was higher than that from corresponding 4-VP or 4-VP-MMA polymers. This correlated with the suggestion in Chapter 2 that the 4-VP polymers were crosslinked to a higher degree than the corresponding MAA polymers. The lower pore volume or free space of the 4-VP polymers limited diffusion of the thermally desorbed materials from the polymers. Selection of the ion specific to the template species for each of the monomeric systems

also showed that less (template) was desorbed from the 4-VP polymers. This also correlated with the template extraction procedure which was carried out in a solution phase.

Thermal desorption GC-MS was shown to be capable of assessing polymer affinity, and the results were comparative to those obtained in the solution phase binding studies. There was no appreciable level of affinity for the 4-VP polymers as determined by thermal desorption GC-MS. The affinity of the MAA polymers was determined and a loss of specificity was demonstrated with decreasing EGDMA amounts. Similar trends were observed when binding was assessed in solution phase. The higher degree of analyte retention observed with decreasing EGDMA concentration suggests a higher number of binding sites, as shown in Chapter 4.

As direct correlations (as described above) with the results obtained from the thermal desorption GC-MS technique were identified with the results obtained in Chapters 2-4 the suitability of this novel technique in the characterisation of MIPs is demonstrated. Therefore, this technique could be used as rapid means of assessment of polymer performance, without the need for solvents, prior to subsequent use. As the loading solvent had no effect on the affinity results obtained *via* thermal desorption analysis it is suggested that the technique is capable of analysing pure polymer-template interactions in the absence of solvent effects.

A second area of this research focused on the preliminary investigation into the use of modified polyvinyl alcohol (PVA) as molecularly imprinted polymers. This system was identified for investigation due to its previous applications as sensors [32] and hydrogels in drug delivery systems [33]. The chemical structure of PVA allows it to undergo numerous reactions to alter its properties. The relative simplicity and control of modification is also an attractive feature.

Photosensitivity was easily introduced to the PVA backbone by reaction with a suitable chromophore. The initial investigations of the work involved the use of PVA that was modified with a styrylpyridinium salt, 4-SbQ. The advantage of this system was that it exhibits extremely high levels of photosensitivity when present in low concentrations

[34]. This results in the bulk properties of the PVA remaining unchanged, thus leaving the hydroxyl groups available for interactions with the template, 2-apy. However, a disadvantage to this technique is that the extent of modification is limited as the SbQ groups associate and the polymeric solution increases in viscosity and gels.

This phenomenon also proved to be a disadvantage when preparing the PVA-4-SbQ films. The polymers were cast onto ATR crystals and subsequently analysed using ATR-FTIR spectroscopy. Whilst a reproducible film could be coated, the level of crosslinking was insufficient to produce a stable film that could withstand the template removal procedure. Based on this finding, it was decided to form a film with a higher level of crosslinking.

Cinnamaldehyde was chosen as an alternative chromophore to 4-SbQ as the percentage of modification could be substantially increased. The resultant films were sufficiently stable and durable to remain adhered to the surface of the crystal for the subsequent analysis. A comparison of the level of water and chloroform ingress into the polymers suggested that the NIP was slightly more hydrophobic than the MIP. As the analyte was not detected in the subsequent reloading it is suggested that further method development in terms of the degree of crosslinking or film thickness is required.

7.2. Future work

The physical characterisation suggested that the 4-VP polymers produced less porous polymers than corresponding MAA counterparts. This was attributed to increased packing of the polymer chains, resulting in a lower free volume of the polymers. Further thermal analysis of the polymers by techniques such as differential scanning calorimetry (DSC) or thermogravimetric analysis (TGA) would provide a greater insight into the degree of crosslinking and the glass transition temperatures, respectively. The use of these methodologies could also be used to further investigate the findings obtained using thermal desorption GC-MS, where it is proposed that the NIP polymers are less crosslinked than corresponding MIP polymers.

Determination of the polymer structures in the swollen state would give a better indication of the relationship between pore structure and the binding results obtained and would also provide a link to the degree of crosslinking. Inverse size exclusion chromatography is a methodology that can be used to determine the porous structures in the swollen state. Typically the polymer to be determined is packed into a column and used as the stationary phase while standards with different molecular weights are injected onto the column [35]. The rate and order of elution of the standards can be used to gain information on the porous structure.

NMR studies on the various polymer compositions at the onset of polymerisation in combination with thermal analysis on the final polymer would provide further insight to the mechanisms of polymer formation. The polymerisation of MAA is effected by the types of complexes present [36]. If crosslinking monomer affects the integrity of the monomer-template complexes pre- and during the early stages of polymerisation, further studies on the influence of the crosslinking monomer concentration on the polymerisation would also provide information on the complex mechanism of polymer formation, and its effect on porosity and performance.

The mole ratios of functional monomer to crosslinking monomer used in this study ranged from 1:8.8 to 1:2.2. In all systems where the crosslinking concentration was varied, the amount of monomer used remained constant. The ratios of 4-VP:EGDMA

that were used were similar to ratios commonly employed in the literature [37-42]. The key difference was that the polymerisation was carried out in solvents other than chloroform (methanol/water, acetonitrile, THF, toluene). The pore properties of the polymers were not reported. Thus, in an attempt to gain further insight into the polymer forming process, the 4-VP (and MAA polymers for comparison purposes) should be synthesised in a range of solvents to determine whether or not phase separation, arising from different solubility parameters, could be used to impart porosity, and ultimately affinity.

The porosity of the polymers could be further tailored by modifying the polymerisation conditions. For example, Piletsky *et. al.* have demonstrated that decreasing the polymerisation time results in an increased polymer surface area and pore volume [16]. However, the separation factors of the polymers were poor in relation to longer polymerisation times. A further study also suggested that lowering the concentration of initiator results in lower rigidity, but lower polymerisation times resulted in poorer separation factors [15].

Combinatorial or computational imprinting could be used in an attempt to find an optimum formulation for using 4-VP for the molecular imprinting of 2-apy. However, if a further series of 4-VP (and MAA) polymers were synthesised by varying the porogen, initiator concentration and the polymerisation time, the use of thermal desorption GC-MS would offer a fast and efficient methodology for screening the polymers not only in terms of affinity but also to give an estimate of the morphology/degree of crosslinking of the polymers (relative to each other).

As the thermal desorption GC-MS was capable of analysing pure polymer-template interactions in the absence of solvent effects, the generation of an experimental isotherm and assessment of the binding parameters of the polymers, in a similar manner to the work carried out in Chapter 4, could be used as a more accurate assessment of polymer binding properties.

It is felt that the level of polymer degradation identified using the thermal desorption methodology is insufficient to prevent the future development of a MISPME fibre for analysis by this technique, particularly since the initial investigations into this technique have shown that the degradation does not prevent a specific response of MIP over NIP [43]. The 20 or 30 mmol EGDMA MAA composition has been identified as an ideal starting point for the development of such a MISPME fibre, as both compositions offer a compromise between the amount of template displaced during pre-treatment, the specific response of MIP over NIP during reloading and the level of bleed due to potential degradation also observed during analyte reloading. Further development of this a MISPME fibre coupled to the thermal desorption GC-MS methodology could potentially lead to its use for the detection of analytes of environmental significance.

In relation to the development of modified PVA for use as an imprinted phase, further investigations into the degree of crosslinking are required. While the cinnamaldehyde modified PVA was sufficient to form stable and durable films, the level of plasticisation of the films was too high to allow analyte pre-concentration. This was attributed directly to an insufficient level of crosslinking. The use of cinnamaldehydes with electron donating and withdrawing groups could be used to increase the level of sensitivity in the films [44], which might contribute to a more crosslinked polymer. Alternative chromophores, which can be attached to the PVA in higher quantities, may also be used including the example given in Figure 7.1.

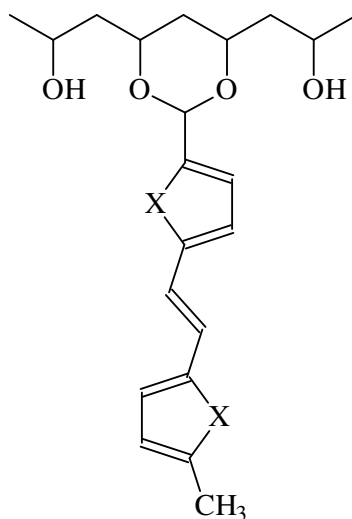


Figure 7.1. PVA modified with a furan or thiophene based chromophore [45].

Optimisation studies on the film thickness should also be carried out to ensure that the analyte is reaching the sensing region.

In conclusion, it is felt that this body of work highlights the importance of a fundamental understanding of the physical parameters of imprinted polymers which are attributable to subsequent performance. While the success of imprinted polymers is usually reported as the level of interaction with the template species, this work emphasises the fact that the physical properties of the polymer are equally important, and must also be considered when analysing the binding characteristics of imprinted polymers.

References

1. E. Yilmaz, K. Mosbach, and K. Haupt, *Analytical Communications* **36**, 167-170 (1999).
2. H. S. Andersson, J. G. Karlsson, S. A. Piletsky, A. C. Koch-Schmidt, K. Mosbach, and I. A. Nicholls, *Journal of Chromatography A* **848**, 39-49 (1999).
3. W. Dong, M. Yan, Z. Liu, G. Wu, and Y. Li, *Separation and Purification Technology* **53**, 183-188 (2007).
4. R. J. Ansell and K. Mosbach, *Journal of Chromatography A* **787**, 55-66 (1997).
5. B. Sellergren and K. J. Shea, *Journal of Chromatography* **635**, 31-45 (1993).
6. R. H. Schmidt, A. S. Belmont, and K. Haupt, *Analytica Chimica Acta* **542**, 118-124 (2005).
7. Z. Zhang, H. Li, H. Lia, L. Nie, and S. Yao, *Sensors and Actuators B* **105**, 176-182 (2005).
8. C. Yu and K. Mosbach, *Journal of Chromatography A* **888**, 63-72 (2000).
9. X. Dong, H. Sun, X. Lu, H. Wang, S. Liu, and N. Wang, *Analyst* **127**, 1427-1432 (2002).
10. S. Song, A. Wu, X. Shi, R. Li, Z. Lin, and D. Zhang, *Analytical and Bioanalytical Chemistry* **390**, 2141-2150 (2008).
11. M. Glad, P. Reinholdssen, and K. Mosbach, *Reactive Polymers* **25**, 47-54 (1995).
12. J. Haginaka, H. Tabo, and C. Kagawa, *Journal of Pharmaceutical and Biomedical Analysis* **46**, 877-881 (2008).
13. Y. Lu, C. Li, X. Wang, P. Sun, and X. Xing, *Journal of Chromatography B* **804**, 53-59 (2004).
14. S. A. Piletsky, E. V. Piletska, A. Guerreiro, I. Chianella, K. Karim, and A. P. F. Turner, *Macromolecules* **37**, 5018-5022 (2004).
15. I. Mijangos, F. Navarro-Villoslada, A. Guerreiro, E. Piletska, I. Chianella, K. Karim, A. Turner, and S. Piletsky, *Biosensors and Bioelectronics* **22**, 381-387 (2006).
16. S. A. Piletsky, I. Mijangos, A. Guerreiro, E. V. Piletska, I. Chianella, K. Karim, and A. Turner, *Macromolecules* **38**, 1410-1414 (2005).
17. W. Cummins, P. Duggan, and P. McLoughlin, *Biosensors and Bioelectronics* **22**, 372-380 (2006).
18. D. Spivak, R. Simon, and J. Campbell, *Analytica Chimica Acta* **504**, 23-30 (2004).

19. D. Spivak, "Selectivity in molecularly imprinted polymers," *Molecularly imprinted materials: science and technology*, Y. A. Ramstrom, ed., (Marcel Dekker, New York, 2005), 395-417.
20. T. Zhang, F. Liu, W. Chen, J. Wang, and L. Kean, *Analytica Chimica Acta* **450**, 53-61 (2001).
21. W. Cummins, P. Duggan, and P. McLoughlin, *Analytica Chimica Acta* **542**, 52-60 (2005).
22. Z. Jie and H. Xiwen, *Analytica Chimica Acta* **381**, 85-91 (1999).
23. W. M. Mullett, M. F. Dirie, E. P. C. Lai, H. Guo, and X. He, *Analytica Chimica Acta* **414**, 123-131 (2000).
24. J. M. G. Cowie, *Polymers: Chemistry And Physics Of Modern Materials*, 1st edition (International textbook company limited, 1973).
25. R. J. Umpleby, S. C. Baxter, Y. Chen, R. Shah, and K. D. Shimizu, *Analytical Chemistry*. **73**, 4584-4591 (2001).
26. R. J. Umpleby, S. C. Baxter, M. Bode, J. Berch Jr., R. Shah, and K. D. Shimizu, *Analytica Chimica Acta* **435**, 35-47 (2001).
27. M. Lehmann, M. Dettling, H. Brunner, and G. E. M. Tovar, *Journal of Chromatography B* **808**, 43-50 (2004).
28. C. Cacho, E. Turiel, A. Martin-Esteban, C. Preze-Conde, and C. Camara, *Journal of Chromatography B* **802**, 347-353 (2004).
29. X. Li and S. M. Husson, *Biosensors and Bioelectronics* **22**, 336-348 (2006).
30. F. G. Tamayo, J. L. Casillas, and A. Martin-Esteban, *Journal of Chromatography A* **1069**, 173-181 (2005).
31. E. Turiel, C. Preze-Conde, and A. Martin-Esteban, *Analyst* **128**, 137-141 (2003).
32. B. Leca, R. M. Morelis, and P. R. Coulet, *Sensors and Actuators B* **26-27**, 436-439 (1995).
33. K. Morimoto, S. Fukanoki, K. Morisaka, S. H. Hyon, and Y. Ikada, *Chemical and Pharmaceutical Bulletins* **37**, 2491 (1989).
34. K. Ichimura and S. Watanabe, *Journal of Polymer Science: Polymer Letters Edition* **18**, 617 (1980).
35. Y. deMiguel, T. Rohr, and D. Sherrington, "Structure, morphology, physical formats and characterisation of polymer supports," *Polymeric materials in organic synthesis and catalysis*, M. R. Buchmeiser, ed., (Wiley-VCH, Weinheim, 2003), 1-52.

36. F. D. Kuchta, A. M. van Herk, and A. L. German, *Macromolecules* **33**, 3641-3649 (2000).
37. C. Baggiani, G. Giraudi, C. Giovannoli, C. Tozzi, and L. Anfossi, *Analytica Chimica Acta* **504**, 43-52 (2004).
38. M. Kempe and K. Mosbach, *Journal of Chromatography A* **664**, 276-279 (1994).
39. M. Kempe, L. Fischer, and K. Mosbach, *Journal of Molecular Recognition* **6**, 25-29 (1993).
40. K. Haupt, A. Dzgoev, and K. Mosbach, *Analytical Chemistry* **70**, 628-631 (1998).
41. M. Jonatta, R. Weiss, B. Mizaikoff, O. Bruggemann, L. Ye, and K. Mosbach, *International Journal of Environmental Analytical Chemistry*. **80**, 75-86 (2001).
42. F. G. Tamayo, J. L. Casillas, and A. Martin-Esteben, *Analytica Chimica Acta* **482**, 165-173 (2003).
43. W. Cummins, P. Duggan, and P. McLoughlin, *Analytical and Bioanalytical Chemistry* **391**, 1237-1244 (2008).
44. A. E. Mathai, R. P. Singh, and S. Thomas, *Journal of Membrane Science* **202**, 34-54 (2002).
45. S. W. Fang, J. H. Timpe, and A. Gandini, *Polymer* **43**, 3505-3510 (2002).

Appendix